Delaunay Configuration B-Splines

Florian Schlenker

April 2022

UNIVERSITÄT PASSAU

Delaunay Configuration B-Splines

Florian Schlenker

Dissertation zur Erlangung des Doktorgrades
der Naturwissenschaften (Dr. rer. nat.)
eingereicht an der Fakultät für Informatik und Mathematik
der Universität Passau

Dissertation submitted to the
Faculty of Computer Science and Mathematics
at the University of Passau
in partial fulfillment of the requirements for the
degree of a Doctor of Natural Sciences (Dr. rer. nat.)

Betreuer / Supervisor: Prof. Dr. Tomas Sauer
Faculty of Computer Science and Mathematics
University of Passau

Externer Gutachter / External Examiner: Prof. Dr. Hendrik Speleers
Department of Mathematics
Università degli Studi di Roma “Tor Vergata”

Passau, April 2022

Florian Schlenker

Delaunay Configuration B-Splines

Dissertation

Passau, April 2022

Abstract

The generalization of univariate splines to higher dimensions is not straightforward. There are different approaches, each with its own advantages and drawbacks. A promising approach using Delaunay configurations and simplex splines is due to Neamtu.

After recalling fundamentals of univariate splines, simplex splines, and the well-known, multivariate DMS-splines, we address Neamtu's DCB-splines. He defined two variants that we refer to as the nonpooled and the pooled approach, respectively. Regarding these spline spaces, we contribute the following results.

We prove that, under suitable assumptions on the knot set, both variants exhibit the *local finiteness property*, i.e., these spline spaces are locally finite-dimensional and at each point only a finite number of basis candidate functions have a nonzero value. Additionally, we establish a criterion guaranteeing these properties within a compact region under mitigated assumptions.

Moreover, we show that the knot insertion process known from univariate splines does *not* work for DCB-splines and reason why this behavior is inherent to these spline spaces. Furthermore, we provide a necessary criterion for the knot insertion property to hold true for a specific inserted knot. This criterion is also sufficient for bivariate, nonpooled DCB-splines of degrees zero and one. Numerical experiments suggest that the sufficiency also holds true for arbitrary spline degrees.

Univariate functions can be approximated in terms of splines using the Schoenberg operator, where the approximation error decreases quadratically as the maximum distance between consecutive knots is reduced. We show that the Schoenberg operator can be defined analogously for both variants of DCB-splines with a similar error bound.

Additionally, we provide a counterexample showing that the basis candidate functions of nonpooled DCB-splines are not necessarily linearly independent, contrary to earlier statements in the literature. In particular, this implies that the corresponding functions are *not* a basis for the space of nonpooled DCB-splines.

Zusammenfassung

Univariate Splines können nicht unmittelbar auf mehrere Dimensionen verallgemeinert werden. Jedoch gibt es verschiedene Ansätze mit jeweils unterschiedlichen Vor- und Nachteilen. Eine vielversprechende Herangehensweise, die Delaunay-Konfigurationen und Simplex-Splines verwendet, stammt von Neamtu.

Nachdem wir die Grundlagen von univariaten Splines, Simplex-Splines und den bekannten multivariaten DMS-Splines wiederholt haben, beschäftigen wir uns mit Neamtus DCB-Splines. Er führte zwei verschiedene Varianten ein, die als nicht-aggregierter beziehungsweise aggregierter Ansatz bezeichnet werden. In Bezug auf diese Splineräume präsentieren wir die folgenden Ergebnisse.

Wir zeigen zum einen, dass beide Varianten unter geeigneten Voraussetzungen an die Knotenmenge die sogenannte Lokale-Endlichkeits-Eigenschaft besitzen. Dies bedeutet, dass die Splineräume lokal endlichdimensional sind und dass an jedem Punkt nur eine endliche Anzahl der Kandidaten an Basisfunktionen einen von null verschiedenen Wert aufweist. Zusätzlich ermitteln wir ein Kriterium, welches diese Eigenschaften auf einem kompakten Gebiet auch unter schwächeren Voraussetzungen garantiert.

Darüber hinaus zeigen wir, dass der von den univariaten Splines her bekannte Prozess des Knoteneinfügens für DCB-Splines *nicht* funktioniert, und begründen, warum dieses Verhalten in der Natur dieser Splineräume liegt. Außerdem geben wir ein notwendiges Kriterium dafür an, dass die Knoteneinfüge-Eigenschaft für einen bestimmten einzufügenden Knoten gegeben sein kann. Für bivariate nicht-aggregierte DCB-Splines von Grad null und eins ist dieses Kriterium auch hinreichend. Numerische Experimente legen ferner die Vermutung nahe, dass dies unabhängig vom Splinegrad der Fall ist.

Univariate Funktionen können mithilfe des Schoenberg-Operators durch Splines approximiert werden. Dabei hat eine Verringerung des maximalen Abstands zweier aufeinanderfolgender Knoten eine quadratische Verringerung des Approximationsfehlers zur Folge. Wir zeigen, dass der Schoenberg-Operator für beide Variaten von DCB-Splines auf analoge Art und Weise und mit einer ähnlichen Fehlerschranke definiert werden kann.

Zusätzlich geben wir ein Gegenbeispiel an, das zeigt, dass die Basisfunktions-Kandidaten der nicht-aggregierten DCB-Splines nicht notwendigerweise linear unabhängig sind, was einen Gegensatz zu früheren Behauptungen in der Literatur darstellt. Dies impliziert insbesondere, dass die entsprechenden Funktionen *keine* Basis für den Raum der nicht-aggregierten DCB-Splines bilden.

Acknowledgments

First of all, I would like to thank my supervisor, Prof. Dr. Tomas Sauer, not only for his support and guidance throughout my whole time at the University of Passau but also for encouraging me to write this dissertation. He advised me in the process of finding suitable research topics, supported me in gaining research results with fruitful and affirmative discussions, and proofread the final outcome.

Secondly, I want to thank Prof. Dr. Hendrik Speleers from the *Università degli Studi di Roma "Tor Vergata"*, who showed genuine interest in my work since the early stages, for his counsel and for writing a report on this thesis.

I also would like to thank my (partly former) colleagues at the *FORWISS* institute and the *Chair of Digital Image Processing* at the *University of Passau*, in particular the members of the *Fraunhofer-Forschergruppe für Wissensbasierte Bildverarbeitung*, for their advice, many interesting talks both of a scientific and nonscientific nature, as well as all the social events strengthening our team spirit. Especially, I want to thank Dr. Erich Fuchs for supporting me with his organizational talents and for being our shield against bureaucracy.

Special thanks go to Benedikt, Martina, Michael, and Thomas, who spent their precious leisure time to proofread (parts of) this dissertation, for their valuable remarks.

Furthermore, I express my gratitude to two kinds of friends of mine: to those who believed in me writing this thesis, for the motivation to prove them right; and to those who (at least) told me that they do *not* believe in me writing this thesis, for the motivation to prove them wrong.

This thesis would probably not exist without my parents, who constantly supported all aspects of my education and development. They have a considerable share in sparking my interest in sciences from the early days of childhood.

Finally, I want to express my deepest gratitude to Christina, who also had to endure me in times of stress and despair during the last years. Without her support, distraction and reassurance, this thesis would not have been possible.

Thank you all!

Contents

List of Figures

List of Tables

List of Abbreviations

CAGD	Computer Aided Geometric Design
DCB-Splines	Delaunay Configuration B-Splines
DMS-Splines	Dahmen-Micchelli-Seidel-Splines
FEM	Finite Element Method
IgA	Isogeometric Analysis
NURBS	Non-Uniform Rational B-Splines
PDE	Partial Differential Equation
PLI	Piecewise Linear Interpolation

Symbols and Notation

Symbol	Description	First use / Definition
$\mathbb{N}_0$	Natural numbers including zero: $\{0, 1, 2, \dots\}$	p. 7
$\mathbb{N}_+$	Natural numbers without zero: $\{1, 2, 3, \dots\}$	p. 9
$\mathbb{Z}$	Integers: $\{\dots, -1, 0, 1, \dots\}$	p. 22
$\mathbb{R}$	Real numbers	p. 7
$\mathbb{R}_+$	Positive real numbers	p. 73
$\mathbb{R}_{\geq 0}$	Nonnegative real numbers	p. 35
Δ_d	d-dimensional standard simplex	Def. 3.6
$\mathbb{S}_{d-1}$	$(d-1)$-sphere in the d-dimensional Euclidean space	p. 108
$\lvert A \rvert$	Cardinality of the set A	p. 17
A^c	Complement of the set A	p. 107
$\mathfrak{P}(A)$	Power set of the set A	p. 54
$A \,/\, \sim$	Set of equivalence classes of A by equivalence relation $\sim$	p. 85
$[a]_\sim$	Equivalence class of a with respect to equivalence relation $\sim$	p. 85
$\operatorname{span}(A)$	Linear span of the set A	p. 58
$\operatorname{aff}(A)$	Affine hull of the set A	Def. 3.1
$\operatorname{conv}(A)$	Convex hull of the set A	Def. 3.4
$\operatorname{vol}_d(A)$	d-dimensional volume of the set A	p. 37
$\dim U$	Dimension of the linear or affine (sub)space U	p. 34
∂A	Topological boundary of the set A	p. 73
A°	Topological interior of the set A	p. 64
$\overline{A}$	Topological closure of the set A	p. 100
$B_r(c)$	Open ball with center c and radius r	p. 73
$B_r^A(c)$	Open ball with center c and radius r restricted to an affine subspace A	p. 123
$B(A)$	Circumcircle generated by the $d+1$ points in A	Def. 4.7
$\operatorname{cen}(A)$	Center of circumcircle generated by the points in A	p. 106
$\operatorname{rad}(A)$	Radius of circumcircle generated by the points in A	p. 119

$C_a(\theta)$	Open cone with aperture a and axis θ with apex in the origin	Def. 5.6
$C_a(t,\theta)$	Open cone with aperture a and axis θ with apex in t	p. 138
$a_n(\theta)$	Maximum aperture a such that $C_a(\theta)$ contains less than n knots	p. 111
$H(t,\theta)$	Half space generated by the hyperplane passing through t with normal vector θ such that $\langle \cdot - t, \theta \rangle > 0$	p. 137
a_j	j-th component of the vector a	p. 34
$a_{i,j}$	j-th component of the vector a_i	p. 34
$\mathbf{0}$	Zero vector in the considered vector space	p. 35
$\mathbf{e}_i$	i-th unit vector in the considered vector space	p. 35
$\|v\|$	Euclidean norm of the vector v	p. 108
$\|v\|_\infty$	Supremum norm of the vector v	p. 9
$\|A\|_\mathrm{F}$	Frobenius norm of the matrix A	p. 199
$\langle \cdot, \cdot \rangle$	Standard scalar product	p. 108
$\|\alpha\|$	Length of the multiindex α	Def. 3.9
ϵ_j	j-th unit multiindex	Def. 3.9
$\Gamma_{l,d}$	Set of multiindices of length l with d components	Def. 3.9
$\Gamma_{\leq l,d}$	Set of multiindices of length at most l with d components	Def. 3.9
$\delta_{i,j}$	Kronecker delta: 1 if $i = j$ and 0 otherwise	p. 12
$\deg p$	Degree of the polynomial p	Def. 2.1
f'	First derivative of the univariate function f	p. 14
f''	Second derivative of the univariate function f	p. 14
$f^{(k)}$	k-th derivative of the univariate function f, $k \in \mathbb{N}_0$	p. 17
$\frac{\mathrm{d}}{\mathrm{d}t}$	Differential operator	p. 24
D_y	Directional differential operator	p. 45
$\nabla f(z)$	Gradient of the function f at z	p. 200
$H_f(z)$	Hessian matrix of the function f at z	p. 199
$f\|_I$	Restriction of the function f to the interval I	p. 10
$f \equiv a$	The function f has value a on its whole domain	p. 39
supp f	Support of the given function f	p. 13
$L_m f$	Polynomial of order m interpolating f at m given sample positions	p. 9
$I_2 f$	Continuous piecewise linear function interpolating f at given knots	p. 12
$S_{m,X}$	Univariate Schoenberg operator for splines of degree m with respect to knots X	Def. 2.23

$S_{m,X}$	Multivariate Schoenberg operator for DCB-splines of degree m with respect to knots X	Def. 7.2
$[x_0, \ldots, x_n]f$	Divided difference of f with respect to $x_0, \ldots, x_n$	Def. 2.7
$g_{j,m,X}$	j-th univariate Greville site for splines of degree m with respect to knot sequence X	Def. 2.23
$g_{K,m,X}$	Greville site with respect to Delaunay configuration K for DCB-splines of degree m with respect to knot set X	Def. 7.1
$u_j(t \mid X)$	j-th barycentric coordinate of t with respect to the reference points X	Def. 3.2
$d(X)$	Determinant of $d+1$ vectors given as X, where 1 is added as first component to each vector	p. 37
$d_j(t \mid X)$	Determinant of $d+1$ vectors given as X, where the j-th vector has been replaced by the vector t and 1 is added as first component to each vector	p. 37
$\mathbb{1}_A$	Indicator function of the set A	p. 41
sgn	Signum function	p. 125
H_i	i-th hat function with respect to a given set of knots	Def. 2.6
$(\cdot - x)_+^k$	Truncated power function with respect to $x \in \mathbb{R}$, $k \in \mathbb{N}_0$	Def. 2.10
$B_{j,m,X}$	j-th univariate B-spline of degree m with respect to knot sequence X	Def. 2.11
$M(\cdot \mid x_0, \ldots, x_n)$	Normalized (univariate) B-spline with respect to knots $x_0, \ldots, x_n$	p. 40
$M(\cdot \mid x_0, \ldots, x_n)$	Simplex spline with respect to knots $x_0, \ldots, x_n$	Def. 3.15
$M^{\mathrm{DMS}}(\cdot \mid X)$	Simplex spline with respect to knots X rescaled for DMS-splines	p. 64
$N(\cdot \mid K)$	Normalized simplex spline with respect to Delaunay configuration K	Def. 4.14
$W_\alpha(\cdot)$	Normalized B-weight with respect to multiindex α and a given collection of knots	p. 63
Π	Space of univariate polynomials	Def. 2.1
Π_m	Space of univariate polynomials of degree at most m	Def. 2.1
$\Pi(\mathbb{R}^d)$	Space of d-variate polynomials	Def. 3.10
$\Pi_m(\mathbb{R}^d)$	Space of d-variate polynomials of degree at most m	Def. 3.10
$\Pi_{m,X}$	Space of piecewise polynomials of degree at most m with respect to breakpoints X	Def. 2.4

$\Pi_{m,X,R}$	Space of piecewise polynomials of degree at most m with respect to breakpoints X and continuity constraints R	p. 17
$\mathcal{C}(I)$	Space of continuous functions with domain I	p. 9
$\mathcal{C}^k(I)$	Space of k-times continuously differentiable functions with domain I, $k \in \mathbb{N}_0$	p. 17
$\mathcal{S}_{m,X}$	Space of univariate splines of degree m with knot sequence X	Def. 2.13
$\mathcal{S}_{d,m,X}$	Generic space of d-variate splines of degree m with knot set X	p. 54
$\mathcal{S}^{\mathrm{DMS}}_{m,\mathcal{T},X}$	Space of DMS-splines of degree m with respect to triangulation $\mathcal{T}$ and knot set X	Def. 4.2
$\mathcal{S}_{m,X}$	Space of nonpooled DCB-splines of degree m with knot set X	Def. 4.20
$\mathcal{S}'_{m,X}$	Space of pooled DCB-splines of degree m with knot set X	Def. 4.21
$\mathcal{B}_{m,X}$	Basis candidate for the space of nonpooled DCB-splines of degree m with knot set X	Def. 4.20
$\mathcal{B}'_{m,X}$	Basis candidate for the space of pooled DCB-splines of degree m with knot set X	Def. 4.21
$\sim$	Relation identifying Delaunay configurations for nonpooled DCB-splines	Def. 4.20
$\simeq$	Relation identifying Delaunay configurations for pooled DCB-splines	p. 86
$V_X(x)$	Voronoi region of $x \in X$ with respect to knot set X	Def. 4.6
$V_X(Y)$	Voronoi region of $Y \subseteq X$ with respect to knot set X	Def. 4.12
$\mathcal{E}(X)$	Set of adjacent knots in the Voronoi diagram with respect to knot set X	Def. 4.6
$\mathcal{V}(X)$	Voronoi diagram with respect to knot set X	Def. 4.6
$\mathcal{K}(X)$	Delaunay triangulation of the knot set X	Def. 4.9
$\mathcal{K}_m(X)$	Set of Delaunay configurations of degree m with respect to knot set X	Def. 4.13
$\mathcal{K}_{I,m}(X)$	Set of Delaunay configurations of degree m with respect to knot set X and interior knots given by $I \subseteq X$	Def. 4.21
$\mathcal{I}_m(X)$	Set of all collections of interior knots occurring in Delaunay configurations of degree m with respect to the knot set X	Def. 4.21
$\mathfrak{B}(K)$	Set of boundary knots of Delaunay configuration K	Def. 4.13

$\mathfrak{I}(K)$	Set of interior knots of Delaunay configuration K	Def. 4.13
$\mathfrak{U}(K)$	Unoriented Delaunay configuration corresponding to Delaunay configuration K	Def. 4.13
$\mathcal{O}(\cdot)$	Big O in the Bachmann–Landau notation	p. 13

Note that tuples and sets are different concepts since tuples allow duplicate entries and respect the order of the elements, which is not the case for sets. However, during the course of the thesis, there are situations in which we consider a tuple as set without further comment. In these cases, the order of the elements as well as potential duplicates do not play a role. For example, we use the $\in$-symbol for tuples. Conversely, there are also situations in which a set is considered as tuple, which is again only possible if the order of elements is irrelevant. This, for example, is the case when we use a set of d elements as input to a d-variate, symmetric function.

Throughout the thesis, we use the symbol $\subseteq$ in expressions like $A \subseteq B$ for two sets A, B to indicate that A is a subset of B or A is equal to B. Conversely, the expression $A \subset B$ indicates that A is a *proper* subset of B and, in particular, that A is not equal to B. The symbols $\supseteq$ and $\supset$ are defined analogously.

1 Introduction

> *All exact science is dominated by the idea of approximation.*
>
> — **Bertrand Russell**

1.1 Motivation

The quote cited above is the very first sentence in the introduction of Steffen's book on the history of approximation theory [Ste06, p. vii] and indicates the vast importance of approximation theory in mathematics. Approximation theory addresses the *"approximative determination of a given quantity"* [Ste06, p. vii] using a set of well-understood objects.

These quantities can be numbers or functions, for example. The Babylonian mathematicians found a procedure to approximate the mostly irrational square roots of numbers using well-understood rational numbers, which is today known as Heron's method [ZZZ16, p. 55ff]. Another example for approximation problems are regression problems, where one tries to approximate *"an unknown function based on some finite amount of data (often measurements)"* [Sch07, p. 1].

However, computers only have limited accuracy, and therefore, numerical computations are almost never exact [Ste06, p. vii]. It is not possible to express every real world quantity in digital terms using a computer. On the other hand, also the inaccuracies of sensors causing noise in the measurements indicate that, with real world data, it is often more reasonable to refrain from exact reproduction of the measurements and be content with approximating them instead.

The approach to find an approximation for some unknown function f can usually be separated into two stages [Sch07, p. 2]:

1. Choosing an appropriate class of candidate functions: Like the Babylonians used the class of rational numbers to approximate certain irrational numbers, one has to choose a set of functions that will be used to approximate f.

2. Contriving a selection scheme which chooses a specific function from the class as approximant to f. To be able to decide which function is the *best* approximant to f, it is necessary to choose a metric which determines the difference between two functions.

Since the choice of the class of candidate functions has a huge influence on the quality of the resulting approximation, this stage is very important. Schumaker gives the following properties, which are typically desired from such a class $\mathcal{F}$ of functions [Sch07, p. 2]:

1. All functions in $\mathcal{F}$ should exhibit a certain amount of smoothness: Usually, the functions under consideration arise from real world scenarios and describe a physical process, which can often be modeled by (partial) differential equations. Solutions to these equations naturally feature a smooth behavior.

2. The flexibility of the class of functions $\mathcal{F}$ should be large enough to provide a good approximation of arbitrary sufficiently smooth functions.

3. For all functions in $\mathcal{F}$, it has to be possible to manipulate and store them easily on a computer: Since computers only have a finite amount of memory, a finite set of numbers has to be sufficient to describe the function uniquely.

4. The functions in $\mathcal{F}$ are required to enable efficient evaluation on a computer with sufficient accuracy. Since many computations are based on derivatives or integrals of functions, it should be possible to compute and evaluate these quantities, too.

Although the last two points have been of minor interest in theoretical considerations, they are crucial in modern applications, which almost exclusively make use of computers [Sch07, p. 2].

One possible choice of candidate functions are polynomials up to a certain degree as this class of functions is well understood and has a relatively simple structure. However, we will see in the next chapter that the global nature of polynomials entails a lack of flexibility, which renders them inappropriate for many types of data.

In order to overcome this limitation, one moves to considering *piecewise* polynomials, which are also known as *splines* nowadays. For the construction of a spline, one has to choose the positions (called *knots*) at which the polynomial pieces are glued together, the smoothness constraints at these positions, and the degree of the polynomial pieces.

We motivate the use of splines in approximation problems exemplarily by the following two applications:

1. *Computer Aided Geometric Design (CAGD):* The field of CAGD *"is concerned with the design, computation, and representation of curved objects on a computer"* [BHS94, p. 106]. This primarily involves (univariate) curves, which have a one-dimensional parameter space, as well as surfaces, whose parameter space is two-dimensional and which, therefore, require multivariate concepts. The advantage of using splines instead of polynomials is easy to see for this application: Assume that a user designing some model desires to change the object in a certain region. The global behavior of polynomials immediately yields a propagation of this change to every position of the model. On the contrary, the local nature of splines restricts all changes to a bounded region, which presumably meets the user's expectation.

2. *Finite Element Method (FEM):* FEM is a technique for the numerical solution of differential equations, which is widely used in applied mathematics and engineering applications, such as fluid flow, continuum mechanics and thermodynamics [Höl03, p. 1]. It is based on the idea of discretizing the continuous domain by splitting it into partitions like triangles or tetrahedra, for example [Höl03, p. 9]. In order to find an approximate solution to the continuous problem, one then uses a basis of functions, each of which is defined with respect to several vertices of the partitioning. These functions are called *finite elements* and are often piecewise polynomials [Höl03, p. 8] with support on few neighboring cells [Höl03, p. 12]. Together with the continuity constraints imposed on the boundaries of adjacent cells, this reveals a close connection between FEM and splines. The approximation error can be made arbitrarily small by refining the partitioning of the domain.

Splines have been studied thoroughly in literature, and the univariate case, where the resulting spline is a one-dimensional object, is well understood. However, the generalization of splines to the multivariate case is not straightforward. Despite the huge variety of available approaches, *"there does not seem to exist a generalization that is commonly agreed to be the 'right' one"* [Nea01b, p. 355]. One proposal, which is very promising due to its geometric motivation and elegance, has been introduced by Neamtu in [Nea01a] and [Nea01b]. Although it has been shown that this spline space exhibits many appealing properties, there are still open questions regarding both theoretical and practical issues. The goal of this thesis is to provide proofs and answers to a few of these questions.

1.2 Contributions

Throughout the thesis, we will refer to Neamtu's multivariate spline space as *Delaunay Configuration B-splines (DCB-splines)*. His method, which will be defined in Section 4.3, comes in two different variants: One of them will be called *pooled DCB-splines*, whereas we will refer to the second one as *nonpooled DCB-splines*. Although the focus of this thesis is on the nonpooled approach, it will turn out that many of our results will also be applicable to the pooled variant.

Neamtu formulated the most important properties desired from a multivariate spline space in his *Fundamental Problem* [Nea01b] and constructed DCB-splines in order to provide a solution to that problem. In fact, it has been claimed that both the pooled and the nonpooled approach satisfy all the properties listed in the Fundamental Problem [Nea01b]. However, to the best of our knowledge, for some of these properties, there has not been given a proof in literature so far. Therefore, our aim is to prove these properties by answering the following questions:

1. *Local finiteness*: Under which conditions do pooled and nonpooled DCB-splines have the properties that

   a) each point is in the support of only a finite number of basis candidate functions and

   b) the restriction of the spline space to any compact region has finite dimensions?

2. *Linear independence*: Are the basis candidate functions of the nonpooled DCB-splines linearly independent, and do they, therefore, really constitute a basis?

In addition to these questions arising from the Fundamental Problem, we consider another two properties, which hold true for univariate splines and are important for both theoretical and practical considerations:

3. *Approximation*: Are nonpooled and pooled DCB-splines suitable for approximation tasks? Can we define an operator yielding an approximation of reasonable quality of a given function in terms of DCB-splines?

4. *Knot insertion*: It is known from the univariate case that the spline space generated by a refined knot sequence is a superset of the spline space generated by the original knot set. Does this property also apply to nonpooled DCB-splines in general? Otherwise, is it possible to formulate necessary or sufficient criteria for this property?

As it will turn out, we are able to confirm that the *local finiteness property* (Question 1) holds true for both pooled and nonpooled DCB-splines under suitable assumptions and that both spline spaces are well-suited for approximation (Question 3). However, we will provide a counterexample to Question 2 by specifying a knot set yielding linear dependent basis candidate functions. Note that this result does *not* apply to the pooled approach, where the question is still open. Furthermore, we will prove by another negative example that the knot insertion property (Question 4) does not hold true for DCB-splines in general. We will extend this by providing a necessary criterion for knot insertion which applies to the nonpooled spline space. Moreover, we will show that this criterion is also sufficient for bivariate, nonpooled DCB-splines of degrees zero and one. Numerical evidence suggests that the sufficiency holds true independently of the spline degree, which we will formulate as a conjecture.

1.3 Structure

The thesis is organized as follows: After this introductory chapter, we will recall univariate splines in Chapter 2. As we will focus on similarities and differences of univariate and multivariate spline spaces, a thorough understanding of univariate splines is important. Therefore, the introduction to these splines will be rather detailed.

Next, we will consider simplex splines in Chapter 3 as a first step towards multivariate spline spaces. These simplex splines are a natural generalization of B-splines, which act as basis functions in univariate spline spaces. Hence, simplex splines are a promising concept for multivariate basis functions.

In Chapter 4, we will come to multivariate spline spaces. After showing the difficulties that arise when switching to higher dimensions, we will use Neamtu's formulation of the Fundamental Problem [Nea01b] to specify the desired properties for multivariate spline spaces. Then, we will introduce different approaches, which finally culminate in the well-known DMS-splines. Since none of these methods is a solution to the Fundamental Problem, Neamtu defined another approach, which is based on a generalization of the Delaunay triangulation. We will present his ideas and close the chapter with a list of further methods towards multivariate splines.

After that, we will investigate the properties of Neamtu's spline spaces by providing answers to the questions that we have formulated before. We consider local finiteness in Chapter 5 and start by motivating certain assumptions on the set of knots. We will show subsequently that, under these assumptions, the local finiteness property

indeed holds true. Afterwards, we will conclude the chapter by presenting corollaries following from this property and by showing a way how to mitigate the assumptions on the knot set.

Chapter 6 is dedicated to the knot insertion property. We will present an example showing that this property cannot be expected to hold true for DCB-splines in general. Then, we will make this insight more precise by formulating a criterion that is necessary for the knot insertion property to be fulfilled. The remainder of the chapter investigates the sufficiency of this criterion. To that end, we will introduce Micchelli's knot insertion formula for simplex splines and give an alternative proof which shows that this formula is practically equivalent to Micchelli's recursion formula for simplex splines. Using the knot insertion formula, we will show that, at least in the nonpooled, bivariate case and for degrees zero and one, the criterion is indeed sufficient.

Using DCB-splines for approximation tasks is considered in the first section of Chapter 7. To that end, we will introduce a multivariate analogue of the Schoenberg operator and show that it offers quadratic convergence with respect to the maximum radius of circumcircles of Delaunay configurations. Afterwards, we will investigate the condition of the basis candidate. Here, it will turn out that at least nonpooled DCB-splines can in fact contain linearly dependent basis candidate functions, which in turn shows that this variant is not a solution to the Fundamental Problem.

In the final chapter of the thesis, we will summarize our results regarding DCB-splines, consider some practical issues, and finally give a perspective for potential future research.

2 Univariate Splines

> *It's the job that's never started as takes longest to finish.*
>
> **— J. R. R. Tolkien**
> The Lord of the Rings

Before we turn to multivariate splines, we consider the univariate case in this chapter. A thorough introduction to these well-understood concepts is especially important as we are going to discuss similarities and differences between univariate and multivariate spline spaces later.

2.1 From Polynomials to Splines

In this section, we introduce *polynomials* and show that they are not always a good choice for approximation. After that, we use *piecewise polynomials* for *piecewise linear interpolation (PLI)* and *cubic spline interpolation*. As a generalization of these two special cases, we will then define *splines* and state that the *B-splines* form a basis. We close the chapter by listing important properties of splines, which we will try to generalize to the multivariate case over the course of this thesis.

2.1.1 Polynomials

We start with the well-known definition of polynomials:

Definition 2.1. (Polynomial) Let $p : \mathbb{R} \to \mathbb{R}$. If we can find an $m \in \mathbb{N}_0$ and *coefficients* $a_0, \dots, a_m \in \mathbb{R}$ such that

$$p(t) = \sum_{k=0}^{m} a_k t^k \quad \text{for all } t \in \mathbb{R},$$

then p is called *polynomial* of order $m+1$. Its *degree* is defined as

$$\deg p := \begin{cases} -\infty & \text{if } a_k = 0 \text{ for all } k \in \{0,\dots,m\}, \\ \max\{k \in \{0,\dots,m\} \mid a_k \neq 0\} & \text{otherwise.} \end{cases}$$

The set of all polynomials is denoted by Π. For $m \in \mathbb{N}_0$, the set Π_m of all polynomials of degree at most m is defined as

$$\Pi_m := \{p \in \Pi \mid \deg p \leq m\}.$$

◀

Together with coefficientwise addition and scalar multiplication, the sets Π and Π_m, $m \in \mathbb{N}_0$, form a vector space.

Note that there is a difference between the degree and the order of a polynomial. A polynomial of order $m+1$, $m \in \mathbb{N}_0$, always has degree at most m. The order equals the dimension of the corresponding vector space Π_m, whereas the degree describes the highest power present in a polynomial. As we use both definitions simultaneously, special caution should be exercised when working with these terms.

A polynomial is uniquely identified by its coefficients. Since, for each polynomial, only a finite number of coefficients differ from zero, a polynomial can be represented by a finite set of numbers.

To evaluate a polynomial at some position $t \in \mathbb{R}$, we just perform additions and multiplications of the coefficients and the number t. This can be done efficiently using the Horner scheme. Moreover, derivatives and integrals of polynomials are again polynomials and can be constructed by a simple modification of the coefficients. Therefore, the last two conditions on Schumaker's list in Section 1.1 regarding the suitability of function classes for approximation are fulfilled for polynomials.

In addition, polynomials are infinitely differentiable and, hence, have maximum smoothness, which ensures the first condition. This follows directly from the fact that derivatives of polynomials are again polynomials.

It remains to be shown that polynomials can approximate arbitrary sufficiently smooth functions. One of the most important theorems on this topic is due to Weierstrass:

Theorem 2.2 (Weierstrass approximation theorem)**.** Let $I \subseteq \mathbb{R}$ be a compact interval and $f \in \mathcal{C}(I)$. For each $\epsilon > 0$, there exists a polynomial $p \in \Pi$ satisfying $\|f - p\|_\infty < \epsilon$. ◀

Hence, any continuous function can be approximated by polynomials within a compact interval, which ensures the second condition on Schumaker's list. However, the theorem does not give any information about the degree of this polynomial.

In the following example, which is due to Runge and can be found in [Sch07, p. 101f], we consider the following problem: Approximate a particular continuous function f by a polynomial of some degree that interpolates f at certain positions.

Example 2.3. Let $f : \mathbb{R} \to \mathbb{R},\ t \mapsto 1/(t^2 + 1)$ and $m \in \mathbb{N}_+$ with $m > 1$. We take m equally spaced samples of f in the interval $[-5, 5]$ at the positions

$$x_i = -5 + 10\frac{i-1}{m-1} \quad \text{for all } i \in \{1, \ldots, m\}.$$

These samples uniquely determine a polynomial $L_m f$ of order m that interpolates f at these positions [Tim06, p. 58f]. The graphs of f, $L_5 f$, $L_{15} f$ are depicted in Figures 2.1a and 2.1b. As one can see, $L_{15} f$ is a much better approximation of f compared to $L_5 f$ near the center of the interval $[-5, 5]$. However, $L_{15} f$ oscillates in the boundary regions of the interval and, therefore, massively deviates from f, even though f is optimally smooth. ◀

For the function f in the previous example, Runge proved in [Run01] (see also [IK94, p. 275ff]) that the maximum approximation error in the interval $[-5, 5]$ will get even larger when the polynomial degree is increased further.

In [Boo01, p. 24], switching from interpolation to approximation is investigated, as presented in Figure 2.1c. However, at least for reasonable sample positions and polynomial degrees, the error is reduced by a factor of four at most, independently of the approximation scheme.

This nonconvergence-behavior of interpolating polynomials reveals that polynomials lack flexibility and, therefore, are of limited suitability for approximation tasks. One of the reasons is

> *"deeply rooted in one of their most conspicuous properties, heralded earlier as a virtue: polynomials are smooth. In fact, polynomials are too smooth."* [Sch07, p. 103]

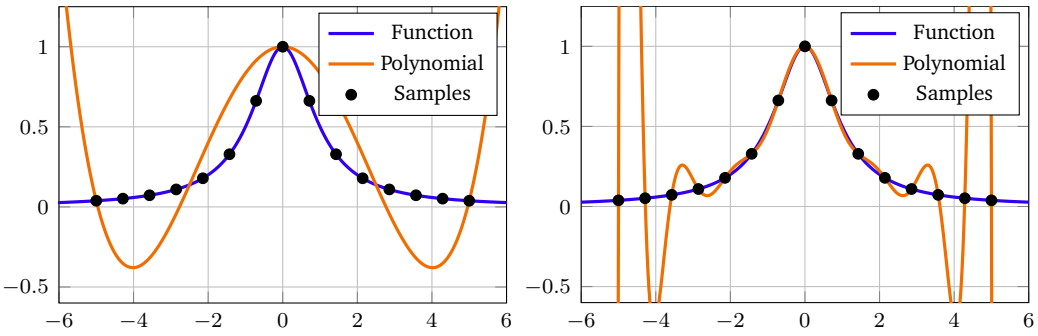

(a) Interpolating polynomial of order 5

(b) Interpolating polynomial of order 15

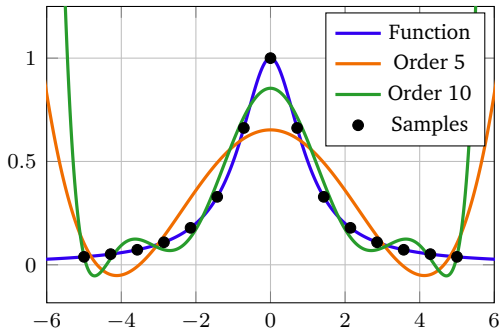

(c) Approximation using polynomials

Fig. 2.1: Using polynomials to approximate or interpolate the function $t \mapsto 1/(t^2+1)$ *(blue)* at the given samples *(black)*. The results *(orange and green)* exhibit an oscillating behavior independently of the method.

This is due to the fact that each polynomial is uniquely determined by its values in any nonempty open set since we can choose a sufficiently large number of distinct samples in this open set [Sch07, p. 103]. In the next subsection, we will try to overcome this global nature of polynomials by considering *piecewise* polynomials.

2.1.2 Piecewise Polynomials

We give a formal definition of the term *piecewise polynomial* now, which is essentially the one given in [Sch07, p. 4].

Definition 2.4 (Piecewise polynomial)**.** Let $m \in \mathbb{N}_0$, $n \in \mathbb{N}_+$, and $x_0, \ldots, x_n \in \mathbb{R}$ with $x_0 < \ldots < x_n$. For all $i \in \{0, \ldots, n-2\}$, define $I_i := [x_i, x_{i+1})$, and let $I_{n-1} := [x_{n-1}, x_n]$. A function $f : [x_0, x_n] \to \mathbb{R}$ satisfying

$$f|_{I_i} \in \Pi_m \quad \text{for all } i \in \{0, \ldots, n-1\}$$

is called *piecewise (univariate) polynomial of degree at most* m *with breakpoints* $x_0, \ldots, x_n$. If $m = 1$, we call f a *piecewise linear function*. Using $X := (x_0, \ldots, x_n)$, we refer to the set of all piecewise polynomials of degree at most m with breakpoints at X as $\Pi_{m,X}$. ◀

Note that we placed no constraints on the junctions between two adjacent polynomial pieces. In particular, f may not even be continuous.

2.1.3 Piecewise Linear Interpolation

We will first look at *Piecewise Linear Interpolation (PLI)*, which, in some sense, is the opposite of polynomial interpolation: While polynomials are infinitely differentiable and, therefore, have maximum smoothness, we will require the functions under consideration in this subsection to be continuous, but they will not be differentiable at the breakpoints between pieces in general. On the other hand, a polynomial has a global nature since its values on any nonempty, open set determine the whole polynomial uniquely, whereas values of a continuous piecewise linear function in an interval between two breakpoints influence the function only in that interval and the two neighboring ones. The simple structure of such continuous piecewise linear functions can be seen in the following proposition.

Proposition 2.5. Let f be a continuous piecewise linear function with breakpoints $x_0, \ldots, x_n \in \mathbb{R}$ satisfying $x_0 < \ldots < x_n$. Then, for each $i \in \{0, \ldots, n-1\}$, one has

$$f(t) = \frac{x_{i+1} - t}{x_{i+1} - x_i} f(x_i) + \frac{t - x_i}{x_{i+1} - x_i} f(x_{i+1}) \quad \text{for all } t \in [x_i, x_{i+1}].$$

◀

We consider the locality of continuous piecewise linear functions in more detail and, to that end, define *hat functions* in accordance with [Boo01, p. 32f]:

Definition 2.6 (Hat function)**.** Let $[a, b] \subseteq \mathbb{R}$ and $a = x_0 < \cdots < x_n = b$ for some $n \in \mathbb{N}_+$. Furthermore, define $x_{-1} := a$ and $x_{n+1} := b$. For $i \in \{0, \ldots, n\}$, the i-th *hat function* with respect to the *knot sequence* $X := (x_{-1}, \ldots, x_{n+1})$ is defined as

$$H_i : \mathbb{R} \to \mathbb{R}, \quad t \mapsto \begin{cases} \frac{t - x_{i-1}}{x_i - x_{i-1}} & \text{if } x_{i-1} < t \leq x_i, \\ \frac{x_{i+1} - t}{x_{i+1} - x_i} & \text{if } x_i \leq t < x_{i+1}, \\ 0 & \text{otherwise.} \end{cases}$$

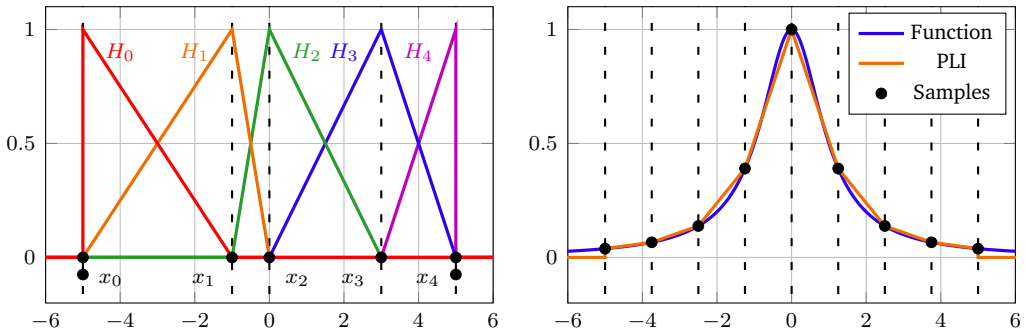

(a) Hat functions with respect to the given knot sequence *(black dots)*

(b) Interpolating the function $t \mapsto 1/(t^2+1)$ using PLI with knots at the sample sites

Fig. 2.2: Hat functions and piecewise linear interpolation. Breakpoints are indicated by *black, dashed* lines.

For H_0 and $t = x_0$ as well as for H_n and $t = x_n$, we use the expression with a nonzero denominator as definition. ◀

The collection of all hat functions with respect to a certain knot sequence is depicted in Figure 2.2a. Hat functions are continuous piecewise linear functions. Additionally, it is easy to see that

$$H_i(x_j) = \delta_{i,j} \quad \text{for all } i, j \in \{0, \dots, n\}, \tag{2.1}$$

as stated in [Boo01, p. 33]. In particular, the hat functions are linearly independent. For an arbitrary function $f : [a, b] \to \mathbb{R}$, we define

$$I_2 f := \sum_{i=0}^{n} f(x_i) H_i. \tag{2.2}$$

Since all hat functions are continuous piecewise linear functions with breakpoints at X, it is clear that $I_2 f$ is also a continuous piecewise linear function with breakpoints at X. From Equation (2.1), it follows that $I_2 f$ interpolates f at all sites in X [Boo01, p. 33], as shown in Figure 2.2b. The segments of a piecewise linear function can be regarded as polynomials of order two, which is also the justification for the subscript in the operator I_2.

Assume now that f is also a continuous piecewise linear function with breakpoints at X and domain $[a, b]$. Let $t \in [a, b]$, and choose $i \in \{0, \dots, n-1\}$ such that $x_i \le t \le x_{i+1}$. Proposition 2.5 then yields

$$I_2 f(t) = \sum_{j=0}^{n} f(x_j) H_j(t) = f(x_i) H_i(t) + f(x_{i+1}) H_{i+1}(t) = f(t).$$

As this equation is valid for all $t \in [a, b]$, it follows that $I_2 f = f$. In particular, every continuous piecewise linear function with breakpoints at X and domain $[a, b]$ can be represented in this way as linear combination of hat functions, with coefficients given by the function values $f(x)$ at the breakpoints $x \in X$. Together with the linear independence ensured by Equation (2.1), this observation shows that the hat functions are a basis for the space of continuous piecewise linear functions with domain $[a, b]$ and breakpoints exactly at the sites in X, which have been used for the construction of the hat functions [Boo01, p. 33].

Piecewise linear functions can also be used to interpolate or approximate given data, like samples of a certain function, for example. For details on this topic, we refer to [Boo01, p. 33ff]. In particular, for a twice continuously differentiable function f and n equidistant interpolation sites, which also act as breakpoints, the error $\|f - I_2 f\|_\infty$ is of order $\mathcal{O}(n^{-2})$ [Boo01, p. 35].

The hat functions feature a pleasantly small support: For $i \in \{0, \ldots, n\}$, one has supp $H_i = [x_{i-1}, x_{i+1}]$. Hence, also the function value $f(x_i)$, which is used as coefficient for H_i in the hat function representation (2.2), only influences $I_2 f$ on this interval, which shows the local nature of (continuous) piecewise linear functions.

We may mention here that the pieces of such piecewise linear functions are not *linear* in an algebraic sense. In fact, the correct term would be *affine*. Nevertheless, it is common to call this type of functions *linear*, which is why we stick to this term for that purpose.

2.1.4 Cubic Spline Interpolation

In the previous subsections, we have seen the extreme cases: Polynomials have a global nature, while continuous piecewise linear functions have a very good localization. Conversely, the latter type of functions is not differentiable in general, whereas polynomials are infinitely differentiable and, thus, feature maximum smoothness.

The following question naturally arises from these facts: Is there a way to combine the best of these two extreme cases? Starting from continuous piecewise linear functions, the following two modifications are necessary for this purpose:

1. The linear pieces between two breakpoints are polynomials and, therefore, are infinitely differentiable. The problem is with the breakpoints. Hence, we have to place additional differentiability constraints at the breakpoints in order to

obtain a higher degree of differentiability of the overall function. This can be achieved by requiring that derivatives of adjoining pieces coincide.

2. Since these linear pieces are uniquely determined by the value of the function and its derivative at a certain site within the corresponding interval, enforcing these two values to coincide for adjoining pieces would imply that these two pieces are segments of the same polynomial. By applying this argument at all breakpoints, we see that the whole function is a single affine-linear function in this case. Therefore, we have to use polynomial pieces of a higher degree between each pair of adjacent breakpoints.

Let $m \in \mathbb{N}_0$ be the maximum degree of the polynomial pieces between two neighboring breakpoints, which will be called the *degree* of the resulting spline later. We consider the special case of degree $m = 3$, which is a very common choice [Boo01, p. 39]. Furthermore, assume that we have a function $f : \mathbb{R} \to \mathbb{R}$ and interpolation sites $x_0 < \cdots < x_n$ for some $n \in \mathbb{N}_+$ which are again real numbers. We will use the interior knots $x_1, \ldots, x_{n-1}$ as the breakpoints of the piecewise polynomial. Hence, the resulting piecewise polynomial consists of n pieces $p_0, \ldots, p_{n-1} \in \Pi_3$, each one being a polynomial of degree at most three and, therefore, having order four [Boo01, p. 39]. This results in $4n$ degrees of freedom in total. We require each polynomial piece to interpolate the value of f at the two bounding interpolation sites, i.e.,

$$p_i(x_i) = f(x_i), \quad p_i(x_{i+1}) = f(x_{i+1}) \quad \text{for all } i \in \{0, \ldots, n-1\}, \tag{2.3}$$

so that there remain two degrees of freedom per piece. In order to obtain a smooth function, we place constraints on the junctions between two adjacent pieces now. We seek the values of the first and second order derivative to coincide, which can be expressed via the following equations [Boo01, pp. 39, 43]:

$$p_i'(x_{i+1}) = p_{i+1}'(x_{i+1}), \quad p_i''(x_{i+1}) = p_{i+1}''(x_{i+1}) \quad \text{for all } i \in \{0, \ldots, n-2\}.$$

By subtracting the number of equations from the total degrees of freedom, we obtain $4n - 2n - 2(n-1) = 2$. Therefore, we still have two degrees of freedom left, which refer to the slopes at the beginning and the end of the interval $[x_0, x_n]$ under consideration [Boo01, p. 43]. Figure 2.3 depicts some of the most common methods to choose these two values [Boo01, p. 43ff], namely:

1. If $f'(x_0)$ and $f'(x_n)$ are known, one can choose the slopes $p_0'(x_0)$ and $p_{n-1}'(x_n)$ accordingly.

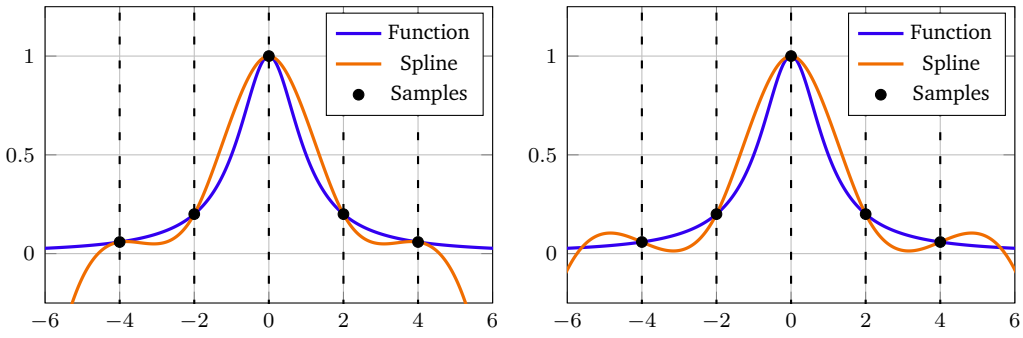

(a) Interpolating slopes at the boundary

(b) Natural spline interpolation

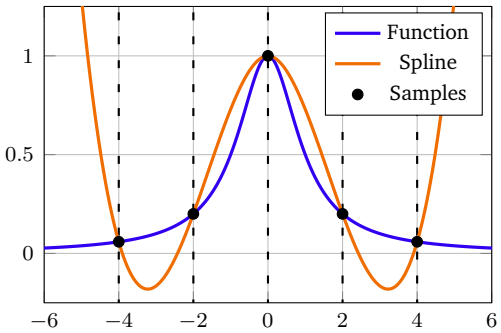

(c) Not-a-knot boundary condition

Fig. 2.3: Cubic spline interpolation *(orange)* of the function $t \mapsto 1/(t^2+1)$ *(blue)* at the given samples *(black)*. Each plot presents a different approach of choosing the boundary conditions.

2. If $f''(x_0)$ and $f''(x_n)$ are known instead, one can force the first and the last polynomial piece and, hence, the overall piecewise polynomial function to interpolate the curvature of f at x_0 and x_n, respectively.

3. By setting the second derivatives $p_0''(x_0)$ and $p_{n-1}''(x_n)$ to zero, one obtains the method called *natural spline interpolation*.

4. If $n \geq 3$, it is also possible to enforce the third derivatives of the polynomial pieces to coincide at the breakpoints x_1 and x_{n-1}. Since polynomial pieces of degree three satisfying this condition are in fact the same polynomial, the breakpoints x_1 and x_{n-1} disappear, which is why this method is called *not-a-knot* condition.

After choosing one of these strategies, all equations can be written as linear system with a unique solution, which can be solved efficiently [Boo01, p. 43].

Hence, we get a function that is twice continuously differentiable and a polynomial of degree three between adjacent breakpoints. Furthermore, it interpolates the

function f at the breakpoints. The construction of a piecewise polynomial function with exactly these properties is called *cubic spline interpolation* [Boo01, p. 43].

If we do not wish to interpolate some given function, we lose $n+1$ equations in (2.3) and, therefore, have $n+3$ degrees of freedom in total to control the shape of the resulting function. Note that we have to keep $n-1$ equations in (2.3) to enforce continuity of the overall function.

In this subsection, we only investigated one particular example of splines. One of the restrictions, of course, was the arbitrary choice of the degree m of the polynomial pieces. However, it could also be possible that we are content with a piecewise polynomial function with only one continuous derivative and instead want to spend more degrees of freedom on interpolation. In *cubic Hermite interpolation*, for example, one not only interpolates the values of f at the breakpoints but also its slopes [Boo01, p. 40]. Are these tasks still in the scope of splines, though? So far, we did not give a rigid definition for the term *spline*. We will make up for this in the next section by defining the spline space and giving a convenient basis.

2.2 Definition of Univariate Splines

It follows directly from Definition 2.1 of polynomials of degree at most m, $m \in \mathbb{N}_0$, and the linear independence of the monomials $1, t, t^2, \ldots, t^m$ that these monomials are a basis for the vector space Π_m. On the other hand, we have seen in Subsection 2.1.3 that the hat functions are a basis for the space of continuous piecewise linear functions. Naturally arising from these observations is the question whether such a basis can be constructed for the functions we dealt with in Subsection 2.1.4, i.e., piecewise polynomials of a higher degree with continuity constraints.

2.2.1 The Spline Space

Let $m \in \mathbb{N}_0$ denote the degree of the polynomial pieces, and choose a strictly increasing sequence of breakpoints $X = (x_0, \ldots, x_n) \in \mathbb{R}^{n+1}$, $n \in \mathbb{N}_+$. In Subsection 2.1.4, we considered the particular case $m = 3$ and three continuity constraints at each interior breakpoint $x_1, \ldots, x_{n-1}$, i.e., continuity of the piecewise polynomial function and its first and second order derivative. However, we want to restrict ourselves neither to a specific spline degree nor to a specific number of continuity constraints. In fact, we aim to assign an individual number of constraints to each interior breakpoint.

We can express the desired number of continuity constraints by specifying a tuple $R = (r_1, \dots, r_{n-1}) \in \mathbb{N}_0^{n-1}$ [Boo01, p. 82] and requiring the following to hold true for a piecewise polynomial function g of degree m with breakpoints at X: For each $i \in \{1, \dots, n-1\}$, we can find an open neighborhood $U(x_i) \subseteq [x_0, x_n]$ around x_i such that $g|_{U(x_i)} \in \mathcal{C}^{r_i}(U(x_i))$. Similarly to the notation in [Boo01, p. 82], we summarize all functions satisfying these conditions in the space $\Pi_{m,X,R}$.

As it turns out, a basis for the space $\Pi_{m,X,R}$ is given by the *B-splines*, which we will define in the next subsections, following [Boo01, p. 87].

2.2.2 Divided Differences

For the definition of B-splines, we have to recall the concept of *divided differences* first. In this work, we will only give a definition and present a formula for their computation. For a more comprehensive introduction to divided differences, we refer to [Boo01, p. 3ff] and [Sch07, p. 45ff].

Definition 2.7 (Divided difference)**.** Let $k \in \mathbb{N}_0$, and choose not necessarily distinct sites $x_0, \dots, x_k \in [a, b] \subseteq \mathbb{R}$. Let $X := (x_0, \dots, x_k)$. Define X' as the set of *distinct* sites in X, and let

$$\mu(x') := \left| \left\{ i \in \{0, \dots, k\} \;\middle|\; x_i = x' \right\} \right| \quad \text{for all } x' \in X'$$

denote the multiplicity of a site in X. The *divided difference*

$$[x_0, \dots, x_k] f$$

for some function $f : [a, b] \to \mathbb{R}$ is defined as the leading coefficient of the unique polynomial $p \in \Pi_k$ satisfying

$$p^{(r)}(x') = f^{(r)}(x') \quad \text{for all } r \in \{0, \dots, \mu(x') - 1\},\ x' \in X'. \tag{2.4}$$

Clearly, the existence of the corresponding derivatives of f is required. ◀

Note that this definition, which is an adapted version of the one given in [Boo01, p. 3], is well-defined as the corresponding Hermite problem has a unique solution. In particular, we have exactly $k + 1$ equations in (2.4) and likewise $k + 1$ degrees of freedom to construct a polynomial of order $k + 1$.

Divided differences can be computed easily using the following recursive formula [Boo01, p. 6].

Proposition 2.8 (Recursive formula for divided differences)**.** Let $[a, b] \subseteq \mathbb{R}$ be a nonempty interval, $k \in \mathbb{N}_0$, and $f \in \mathcal{C}^k([a, b])$. One has

$$[x]f = f(x) \quad \text{for all } x \in [a, b]. \tag{2.5}$$

Moreover, for $x_0, \ldots, x_k \in [a, b]$ and arbitrary $i, j \in \{0, \ldots, k\}$ with $x_i \neq x_j$, the equality

$$[x_0, \ldots, x_k]f = \frac{[x_0, \ldots, x_{i-1}, x_{i+1}, \ldots, x_k]f - [x_0, \ldots, x_{j-1}, x_{j+1}, \ldots, x_k]f}{x_j - x_i} \tag{2.6}$$

holds true, whereas one has

$$[x_0, \ldots, x_k]f = \frac{f^{(k)}(x_0)}{k!} \tag{2.7}$$

for $x_0 = \cdots = x_k$. ◀

According to this proposition, one can compute the value of any divided difference by reducing it to divided differences with fewer arguments using the recursion formula in (2.6) until in each divided difference only one *distinct* site is left.

The remaining values can then be obtained using Formulas (2.5) and (2.7), respectively, depending on the number of arguments left. In fact, when looking at these formulas more closely, it turns out that (2.5) is just the particular case $k = 0$ of the more general Formula (2.7).

Furthermore, from the free choice of sites in (2.6), it follows that divided differences are symmetric in their arguments [Boo01, p. 6]. This also seems reasonable when looking at Definition 2.7 [Boo01, p. 4].

We close the subsection with the following example regarding different ways to compute a divided difference:

Example 2.9. Consider the interval $[0, 2]$ and the interpolation sites $x_0 = 1$ and $x_1 = 2$. Let

$$f : [0, 2] \to \mathbb{R}, \quad t \mapsto t^2 - 2.$$

The results in this subsection enable the computation of the divided difference $[x_0, x_1]f$ in two different ways:

1. *Using Definition 2.7*: To obtain the value of $[x_0, x_1]f$ using the divided difference definition, we have to find the unique polynomial of degree one interpolating f at $x_0 = 1$ and $x_1 = 2$, which can be calculated to be

$$p : [0, 2] \to \mathbb{R}, \quad t \mapsto 3t - 4.$$

The divided difference $[x_0, x_1]f$ is by definition the leading coefficient of p, and consequently, $[x_0, x_1]f = 3$.

2. *Using Proposition 2.8*: The computation can also be performed using Formulas (2.5) and (2.6):

$$[x_0, x_1]f = \frac{[x_1]f - [x_0]f}{x_1 - x_0} = \frac{f(x_1) - f(x_0)}{x_1 - x_0} = 3.$$

◀

2.2.3 B-Splines

Before being able to define B-splines, we still have to introduce *truncated power functions* in accordance with [Boo01, p. 82f] first:

Definition 2.10 (Truncated power function)**.** Let $x \in \mathbb{R}$ and $k \in \mathbb{N}_0$. Using

$$(\cdot - x)_+ : \mathbb{R} \to \mathbb{R}, \quad t \mapsto \max\{t - x, 0\},$$

one can define the *truncated power function* as

$$(\cdot - x)_+^k : \mathbb{R} \to \mathbb{R}, \quad t \mapsto \Big((t - x)_+\Big)^k,$$

where we make the assignment $0^0 := 0$ for $k = 0$. ◀

Some plots of truncated power functions are depicted in Figure 2.4. Clearly, $(\cdot - x)_+^k$ is a piecewise polynomial of degree k with a breakpoint at x. It is continous if and only if $k \geq 1$ and, in this case, has $k - 1$ continuous derivatives [Boo01, p. 82].

These properties motivate the consideration of using truncated power functions as basis for the spline space $\Pi_{m,X,R}$. In fact, when choosing breakpoints and degrees appropriately, these functions constitute a basis [Boo01, p. 83f]. However, truncated power functions feature some unpleasant properties [Boo01, p. 84]: Firstly, since these functions have a very large support, the evaluation of a spline at a certain site

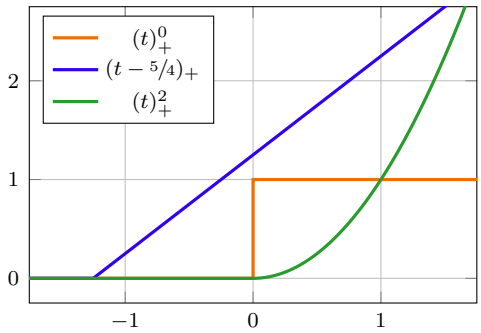

Fig. 2.4: Truncated power functions of different degrees

would involve many basis functions. Secondly, if two breakpoints are chosen very close to each other, the condition of the basis can be very bad, resulting in numerical issues. Therefore, in particular for computational purposes, it is more reasonable to use a basis formed by *B-splines*, which are obtained as rescaled divided differences of truncated power functions [Boo01, p. 87]:

Definition 2.11 (B-spline)**.** Let $n \in \mathbb{N}_+$, $m \in \mathbb{N}_0$, and let $x_0, \dots, x_{n+m} \in \mathbb{R}$ be a nondecreasing sequence of *knots*. The *j-th (normalized) B-spline of degree m with respect to the knot sequence* $X := (x_0 \dots, x_{n+m})$ is for $j \in \{0, \dots, n-1\}$ defined as

$$B_{j,m,X} : \mathbb{R} \to \mathbb{R}, \quad t \mapsto (x_{j+m+1} - x_j)\, [x_j, \dots, x_{j+m+1}](\cdot - t)_+^m.$$

◀

Examples of B-splines are presented in Figure 2.5a. The connection between B-splines and the space $\Pi_{m,X,R}$ is established by the following theorem, which is due to Curry and Schoenberg [CS66]. Both the theorem and its proof can be found in [Boo01, p. 97f].

Theorem 2.12 (Curry-Schoenberg)**.** Let $m \in \mathbb{N}_0$ and $k \in \mathbb{N}_+$. Furthermore, let $Y := (y_0, \dots, y_k) \in \mathbb{R}^{k+1}$ be a strictly increasing sequence of breakpoints, and set $R := (r_1, \dots, r_{k-1})$, where $r_1, \dots, r_{k-1} \in \{0, \dots, m\}$ specify the number of continuity constraints at the interior breakpoints. For

$$n := k(m+1) - \sum_{i=1}^{k-1} r_i,$$

let $X := (x_0, \dots, x_{m+n}) \in \mathbb{R}^{m+n+1}$ be a nondecreasing sequence of knots that is connected to the breakpoints Y via the following two conditions:

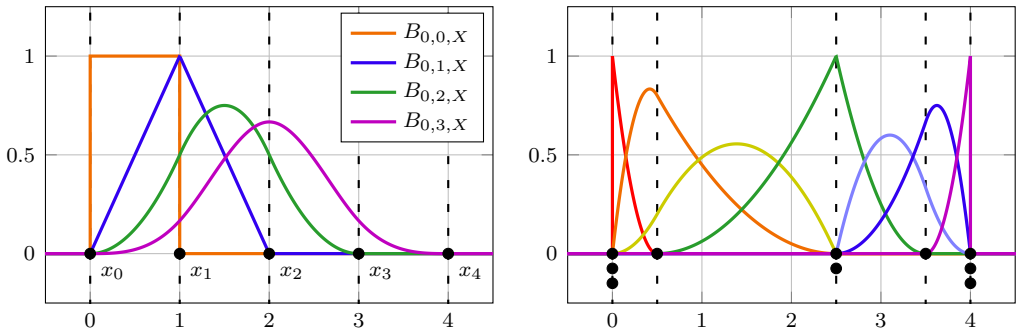

(a) Examples of B-splines with degrees ranging from zero to three

(b) Collection of B-splines of degree two, generated by the depicted sequence of knots

Fig. 2.5: B-splines of various degrees and the collection of B-spline basis functions generated by some knot sequence. Knots are indicated by black dots and the corresponding breakpoints as black, dashed lines. The multiplicity of a knot is expressed in the number of dots at a certain position.

(i) The site y_i occurs exactly $(m+1-r_i)$-times in X:

$$\left|\left\{j \in \{0,\dots,m+n\} \,\middle|\, x_j = y_i\right\}\right| = m+1-r_i \quad \text{for all } i \in \{1,\dots,k-1\}.$$

(ii) $x_0 \le \cdots \le x_m \le y_0$ and $y_k \le x_n \le \cdots \le x_{m+n}$.

The set $\{B_{j,m,X} \mid j \in \{0,\dots,n-1\}\}$ of B-splines is a basis for $\Pi_{m,Y,R}$ on the interval $[x_m, x_n]$. ◀

In this theorem, we constructed the knot sequence X from the sequence of breakpoints Y and the continuity constraints R. Naturally, it is possible to skip that step and start directly with the knot sequence. This finally motivates the following definition of the spline space $\mathcal{S}_{m,X}$ in accordance with [Boo01, p. 93]:

Definition 2.13 (Spline space)**.** Let $m \in \mathbb{N}_0$ and $n \in \mathbb{N}_+$. For a nondecreasing sequence of knots $X = (x_0,\dots,x_{m+n}) \in \mathbb{R}^{m+n+1}$, we define the *spline space* $\mathcal{S}_{m,X}$ *of degree* m as

$$\mathcal{S}_{m,X} := \left\{ \sum_{j=0}^{n-1} a_j B_{j,m,X} \,\middle|\, a_0,\dots,a_{n-1} \in \mathbb{R} \right\}.$$

◀

If the knot sequence X satisfies the two conditions established in Theorem 2.12, the B-splines are a basis for $\Pi_{m,Y,R}$, and consequently, $\mathcal{S}_{m,X} = \Pi_{m,Y,R}$. Figure 2.5b depicts the basis functions generated by a certain sequence of knots.

Note that, for simplicity, we only considered finite sequences of knots and breakpoints in the previous subsections. The underlying concepts, however, work more generally: When considering biinfinite knot sequences $(x_i)_{i\in\mathbb{Z}}$, the sum in the previous definition has to be taken pointwise. We will see in Proposition 2.15 that, due to the locality of B-splines, each point is in the support of only a finite set of B-splines. Hence, there are no convergence issues even for infinite knot sequences [Boo01, p. 93].

Both B-splines and the corresponding spline space have many appealing properties. We will list some of them in the next section.

2.3 Properties of Univariate Splines

Throughout this section, let $m \in \mathbb{N}_0$ denote the spline degree, and let $X = (x_j)_{j\in\mathbb{Z}}$ be a nondecreasing, biinfinite knot sequence, which covers the whole real line, i.e.,

$$\lim_{j\to-\infty} x_j = -\infty \quad \text{and} \quad \lim_{j\to\infty} x_j = \infty.$$

Following [Boo01, p. 87ff], we list important properties of B-splines and the spline space generated by them. Like in the previous sections, we omit all proofs and instead refer to the book by de Boor [Boo01] for more details.

2.3.1 Properties of B-Splines

We begin with some basic properties of B-splines: It follows from Definition 2.11 that B-splines of degree zero are characteristic functions of intervals between adjacent knots. In particular, $B_{j,0,X} \equiv 0$ if $x_j = x_{j+1}$. For B-splines of a higher degree, one can establish a recurrence relation using B-splines of a lower degree. The results are summarized in the following proposition [Boo01, p. 89f]:

Proposition 2.14 (B-spline recurrence relation)**.** For all $j \in \mathbb{Z}$ and $t \in \mathbb{R}$, the following equations hold true:

(i) If $m = 0$, one has

$$B_{j,0,X}(t) = \begin{cases} 1 & \text{if } x_j \le t < x_{j+1}, \\ 0 & \text{otherwise.} \end{cases} \tag{2.8}$$

(ii) If $m \geq 1$, one can apply the recurrence relation

$$B_{j,m,X}(t) = w_{j,m}(t)B_{j,m-1,X}(t) + \Big(1 - w_{j+1,m}(t)\Big)B_{j+1,m-1,X}(t), \qquad (2.9)$$

where

$$w_{j,m}(t) = \frac{t - x_j}{x_{j+m} - x_j}.$$

◀

Note that the weights $w_{j,m}$ are undefined if $x_j = x_{j+m}$. As the corresponding B-splines are constant zero-functions in that case, it is not necessary to evaluate these weights, though.

Since characteristic functions are nonnegative, the same holds true for B-splines of degree zero. It follows by induction that B-splines of arbitrary degree are nonnegative as the coefficients used in the recurrence relation in (2.9) are nonnegative on the support of the corresponding lower degree B-splines [Boo01, p. 91]. Furthermore, when we trace the support of degree zero B-splines through m applications of the recurrence relation, it turns out that the support of B-splines is the span of $m + 2$ consecutive knots. Thus, one can formulate the following proposition [Boo01, p. 91].

Proposition 2.15 (B-spline support and positivity)**.** For all $j \in \mathbb{Z}$, one has

$$\begin{aligned} B_{j,m,X}(t) &> 0 \quad \text{for all } t \in (x_j, x_{j+m+1}), \\ B_{j,m,X}(t) &= 0 \quad \text{for all } t \notin [x_j, x_{j+m+1}). \end{aligned}$$

In particular, $B_{j,m,X} \equiv 0$ if $x_j = x_{j+m+1}$. ◀

When looking at this result from a slightly different point of view, it turns out that only $m + 1$ B-splines are nonzero at a certain site. Hence, the value at each site is only influenced by $m + 1$ coefficients, which emphasizes the local nature of splines and is also an important property for efficient algorithms.

2.3.2 Continuity and Derivatives

The Curry-Schoenberg Theorem ensures that the B-splines span the space of piecewise polynomials $\Pi_{m,Y,R}$. Hence, each linear combination of B-splines has to be a piecewise polynomial of degree m with breakpoints at Y and continuity constraints

between adjacent polynomial pieces specified by R. These constraints are controlled by the knot multiplicity, which leads to the following insights [Boo01, pp. 90f, 99]:

Proposition 2.16. Let $g \in \mathcal{S}_{m,X}$. For each $j \in \mathbb{Z}$, the following holds true:

(i) The pieces between two knots are polynomials of degree at most m:

$$g|_{[x_j, x_{j+1})} \in \Pi_m.$$

(ii) If x_j has multiplicity $k \in \mathbb{N}_+$, i.e., x_j appears exactly k-times in the sequence X, then g has $m - k$ continuous derivatives at x_j. ◀

In [Boo01, p. 99], the latter property is expressed as follows:

$$\text{number of continuity constraints at } x_j \; + \; \text{number of knots at } x_j \; = m + 1.$$

This rule even works for a site $t \in \mathbb{R}$ with no associated knots: As it has multiplicity zero, we have $m + 1$ continuity constraints there. Hence, the function value and the first m derivatives of the polynomial pieces at both sides of t coincide. Since a polynomial of degree m is uniquely determined by these values, it follows that both polynomial pieces are in fact pieces of the same polynomial, which is exactly the expected behavior at sites without a knot [Boo01, p. 99].

Now that we know about the differentiability of spline functions, we are also interested in a formula for the computation of derivatives. It has been shown in [Boo01, p. 115f] that the derivative of a spline function is a spline of a lower degree whose coefficients are normalized differences of the original coefficients:

Proposition 2.17. Let $g \in \mathcal{S}_{m,X}$ with coefficients $(a_j)_{j\in\mathbb{Z}}$, and let $m \geq 1$. For all $t \in \mathbb{R}$ at which g is differentiable, the first derivative of g at t is given by

$$\frac{\mathrm{d}g}{\mathrm{d}t}(t) = \frac{\mathrm{d}}{\mathrm{d}t}\left(\sum_{j\in\mathbb{Z}} a_j B_{j,m,X}\right)(t) = m \sum_{j\in\mathbb{Z}} \frac{a_j - a_{j-1}}{x_{j+m} - x_j} B_{j,m-1,X}(t).$$

◀

Similar to Proposition 2.14, the denominator on the right hand side is undefined if a knot has a multiplicity of at least $m + 1$. But also in this case, the corresponding B-splines are zero-functions and, therefore, can be ignored.

2.3.3 Polynomial Reproduction

The spline space $\mathcal{S}_{m,X}$ contains all piecewise polynomials of degree at most m satisfying certain continuity constraints at the knots specified by X. Since polynomials fulfill all continuity constraints, we can expect that each polynomial of degree at most m is contained in $\mathcal{S}_{m,X}$. In this subsection, we consider the coefficients leading to a particular polynomial.

The relation between splines and polynomials is established by *Marsden's identity* (see [Mar70] and [Boo01, p. 95]), for which there is an elegant formulation using *polar forms*. As we will make use of this concept later, we already recall it here in accordance with [Ram89, p. 326] and [Ram87]:

Theorem 2.18 (Blossoming principle)**.** Let $p \in \Pi_m$. There is a uniquely defined *polar form* $P : \mathbb{R}^m \to \mathbb{R}$ of p satisfying the following properties.

(i) P is symmetric in all arguments: For all $z_1, \dots, z_m \in \mathbb{R}$ and $i, j \in \{1, \dots, m\}$ with $i < j$, one has

$$\begin{aligned} &P(z_1, \dots, z_{i-1}, z_i, z_{i+1}, \dots, z_{j-1}, z_j, z_{j+1}, \dots, z_m) \\ &= P(z_1, \dots, z_{i-1}, z_j, z_{i+1}, \dots, z_{j-1}, z_i, z_{j+1}, \dots, z_m). \end{aligned} \tag{2.10}$$

(ii) P is multiaffine: Let $i \in \{1, \dots, m\}$ and $z_1, \dots, z_m \in \mathbb{R}$. Furthermore, let $n \in \mathbb{N}_+$, $a_0, \dots, a_n \in \mathbb{R}$, and $\widetilde{z}_0, \dots, \widetilde{z}_n \in \mathbb{R}$ such that

$$\sum_{j=0}^{n} a_j \widetilde{z}_j = z_i \quad \text{and} \quad \sum_{j=0}^{n} a_j = 1.$$

Then, it follows that

$$\sum_{j=0}^{n} a_j P(z_0, \dots, z_{i-1}, \widetilde{z}_j, z_{i+1}, \dots, z_m) = P(z_0, \dots, z_m).$$

(iii) The polynomial p is the diagonal of the polar form P: For each $z \in \mathbb{R}$, one has

$$P(z, \dots, z) = p(z). \tag{2.11}$$

Conversely, each symmetric and multiaffine $P : \mathbb{R}^m \to \mathbb{R}$ uniquely defines a polynomial of degree at most m as its diagonal. ◀

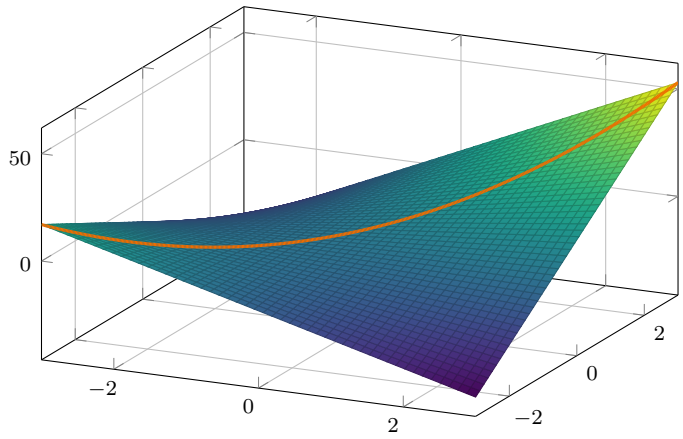

Fig. 2.6: Blossoming principle. We display the polar form P of Example 2.19 and its associated polynomial p *(orange)* on the diagonal.

Multiaffinity demands that the polar form is an affine function (i.e., a polynomial of degree at most one) with respect to all arguments. Hence, the essence of the preceding theorem is *"that we can trade one parameter of degree [...][m] for [...][m] symmetric parameters, each of degree* 1*"* [Ram89, p. 325]. We demonstrate the concept of polar forms in the following example.

Example 2.19. We consider the polynomial

$$p : \mathbb{R} \to \mathbb{R}, \quad z \mapsto 4z^2 + 6z - 1$$

and derive its polar form P. Since p is of degree two and P is multiaffine, it has the shape

$$P : \mathbb{R}^2 \to \mathbb{R}, \quad (u, v) \mapsto a_3uv + a_2u + a_1v + a_0,$$

with coefficients $a_0, \dots, a_3 \in \mathbb{R}$. The symmetry of P enforces that $a_1 = a_2$. When using the same value $z \in \mathbb{R}$ for both arguments and applying the diagonal property (2.11), we obtain

$$P(z, z) = a_3z^2 + (a_1 + a_2)z + a_0 = p(z).$$

A comparison of coefficients immediately yields $a_0 = -1$, $a_3 = 4$, and $a_1 = a_2 = 3$. Hence, the polar form of p is uniquely determined as

$$P : \mathbb{R}^2 \to \mathbb{R}, \quad (u, v) \mapsto 4uv + 3u + 3v - 1.$$

The polynomial p and its polar form P are displayed in Figure 2.6. ◀

As a special case of a formula given in [Ram87, p. 101], Marsden's identity can be formulated as follows by employing the blossoming principle:

Theorem 2.20 (Marsden's identity)**.** For each polynomial $p \in \Pi_m$ with polar form P, one can represent p in terms of B-splines as

$$p(t) = \sum_{j \in \mathbb{Z}} P(x_{j+1}, \ldots, x_{j+m}) B_{j,m,X}(t) \quad \text{for all } t \in \mathbb{R}.$$

◀

Hence, the coefficient for a specific B-spline when representing a polynomial with respect to the B-spline basis is determined by evaluating its polar form at m successive knots inside the support of the B-spline.

Here, we used the assumptions on the knot sequence X that we have stated at the beginning of the section: According to Proposition 2.15, each B-spline is supported on the closed interval bounded by its outermost knots. Consequently, all spline functions with respect to a knot sequence that does not cover the whole real line $\mathbb{R}$ have compact support. As the only polynomial with compact support is the zero-function, Marsden's identity would only hold true on a certain interval in that case.

Moreover, for infinite knot sequences, the previous theorem also motivates the admission of infinite sums in Definition 2.13 since it would be impossible to represent polynomials in terms of B-splines if only a finite set of coefficients could differ from zero.

A constant function can be considered as polynomial of degree at most m for all $m \in \mathbb{N}_0$ and, thus, has an associated polar form in m variables, which is also a constant function. Using the constant one-function as input to Marsden's identity yields the following corollary [MS88, p. 252]:

Corollary 2.21 (Partition of unity)**.** For all $t \in \mathbb{R}$, one has

$$\sum_{j \in \mathbb{Z}} B_{j,m,X}(t) = 1.$$

◀

There is also a well-known generalization of Marsden's identity to *piecewise* polynomials, which provides the coefficients of an arbitrary spline function [Ram87, p. 101]:

Theorem 2.22. Let $(a_j)_{j\in\mathbb{Z}}$ be a sequence in $\mathbb{R}$. For all $k \in \mathbb{Z}$, define the polynomial

$$p_k := \left(\sum_{j\in\mathbb{Z}} a_j B_{j,m,X}\right)\Big|_{[x_k,x_{k+1})} \in \Pi_m,$$

and let P_k be the polar form of p_k. Then, one has

$$a_j = P_k(x_{j+1},\ldots,x_{j+m}) \quad \text{for all } k \in \{j,\ldots,j+m\},\ j \in \mathbb{Z}.$$

◀

In particular, the evaluation of the polar form yields the same value independently of the choice of k.

2.3.4 Approximation

Assume that we have a certain function $f : \mathbb{R} \to \mathbb{R}$ and aim at an approximation of f in terms of B-splines. In Section 1.1, we recalled the two stages of an approximation process: The class of candidate functions in this case is the spline space $\mathcal{S}_{m,X}$, whereas the selection scheme choosing a specific approximant will be the *Schoenberg operator*, which can be defined as follows [Boo01, pp. 96, 141]:

Definition 2.23 (Greville sites, Schoenberg operator)**.** Let $f : \mathbb{R} \to \mathbb{R}$ and $m \geq 1$.

(i) For $j \in \mathbb{Z}$, the *j-th Greville site* is defined as

$$g_{j,m,X} := \frac{1}{m}\sum_{k=1}^{m} x_{j+k}.$$

(ii) The *Schoenberg operator* of degree m with respect to the knot sequence X is defined as

$$S_{m,X}f := \sum_{j\in\mathbb{Z}} f(g_{j,m,X})B_{j,m,X} \quad \in \mathcal{S}_{m,X}.$$

◀

For an example regarding the application of the Schoenberg operator, we refer to Figure 2.7. Without further assumptions on the function f, we cannot expect this approximation to be good in an L^∞-sense as f can behave arbitrarily between two Greville sites. However, if we restrict f to the simple class of polynomials of degree at most one, we can prove the following [Boo01, pp. 96, 141]:

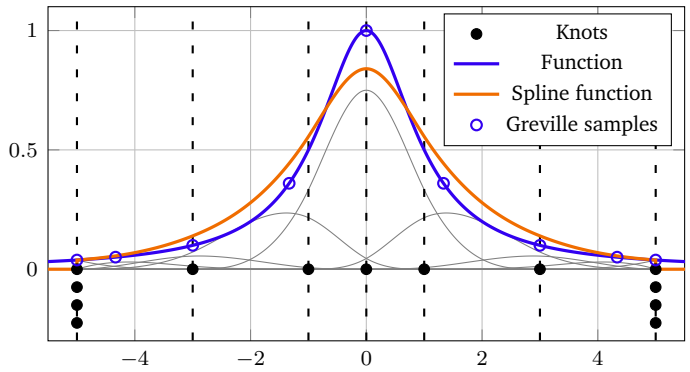

Fig. 2.7: Application of the Schoenberg operator. We approximate the function $f : t \mapsto 1/(t^2+1)$ *(blue)* by splines of degree three with respect to the given sequence of knots *(black dots)* using the Schoenberg operator. To that end, we evaluate f at the Greville sites and use these samples *(blue dots)* as coefficients for the corresponding B-splines *(gray)*. The resulting spline function is displayed in *orange*.

Proposition 2.24 (Linear exactness)**.** Let $p \in \Pi_1$. If $m \geq 1$, one has $S_{m,X}\, p = p$. ◀

Although the restriction to Π_1 is quite strong, one can use the previous proposition to get a much more general result regarding the approximation quality for arbitrary $\mathcal{C}^2$-functions [Boo01, p. 142]:

Theorem 2.25 (Approximation order)**.** Let $f \in \mathcal{C}^2(\mathbb{R})$ and $m \geq 1$. The difference between f and its Schoenberg approximant $S_{m,X} f$ is bounded by

$$\|f - S_{m,X} f\|_\infty \leq m^2 \|f''\|_\infty h^2, \tag{2.12}$$

where $h := \sup_{i\in\mathbb{Z}} |x_{i+1} - x_i|$. ◀

For a proof of the exact bound in (2.12), we refer to [Sau12, p. 44f]. The essence of the theorem is that, for a given function and a given knot sequence, one can make the approximation error *arbitrarily small* by refining the knot sequence. The bound can also be considered locally, which shows that a dense knot sequence is especially important in regions of large curvature since the absolute value of the second derivative appearing in the bound in (2.12) is large there [Sau12, p. 44]. In other words, the spline functions are more flexible in regions with a high density of knots.

According to (2.12), the approximation error when applying the Schoenberg operator is in $\mathcal{O}(h^2)$. Whereas this approximation order is even sharp, a better approximation can be achieved by using a more sophisticated approximation procedure [Boo01, p. 142].

2.3.5 Knot Insertion

In the previous subsection, we learned that, when approximating a given function, a dense knot sequence is especially important in areas of large curvature. One question arising from this fact is the following:

Consider a spline function $g \in \mathcal{S}_{m,X}$ of degree m with respect to some knot sequence X, and assume that we desire more flexibility in a certain region. Hence, we insert a finite number of knots in that region in order to enhance the flexibility. But are we still able to represent g in terms of the spline space with respect to the refined knot sequence? That is indeed the case, as shown by following theorem, which is due to Boehm [Boe80] and can be found in [Boo01, p. 137]. Clearly, it is sufficient to consider the insertion of one knot at a time since any (finite) refinement can be achieved by adding single knots iteratively [Boo01, p. 135].

Theorem 2.26 (Knot insertion)**.** Let $x^* \in \mathbb{R}$, and choose the index $i \in \mathbb{Z}$ such that $x_{i-1} \leq x^* < x_i$. Through the assignment

$$x_j^* := \begin{cases} x_j & \text{if } j < i, \\ x^* & \text{if } j = i, \\ x_{j-1} & \text{if } j > i, \end{cases} \quad \text{for all } j \in \mathbb{Z},$$

one can define the refined knot sequence $X^* := (x_j^*)_{j\in\mathbb{Z}}$, which is again nondecreasing. Let $(a_j)_{j\in\mathbb{Z}}$ be any sequence of coefficients in $\mathbb{R}$, and define

$$a_j^* := (1 - w_j)a_{j-1} + w_j a_j, \quad \text{where } w_j = \begin{cases} 0 & \text{if } x^* \leq x_j, \\ \frac{x^* - x_j}{x_{j+m} - x_j} & \text{if } x_j < x^* < x_{j+m}, \\ 1 & \text{if } x_{j+m} \leq x^*, \end{cases}$$

for all $j \in \mathbb{Z}$ to obtain another sequence $(a_j^*)_{j\in\mathbb{Z}}$ of coefficients in $\mathbb{R}$. Then, the identity

$$\sum_{j\in\mathbb{Z}} a_j B_{j,m,X} = \sum_{j\in\mathbb{Z}} a_j^* B_{j,m,X^*}$$

holds true. In particular, $\mathcal{S}_{m,X} \subseteq \mathcal{S}_{m,X^*}$. ◀

2.3.6 Condition of the B-Spline Basis

The following property reveals the relation between spline coefficients and spline value, as shown in [Boo01, p. 131].

Proposition 2.27 (Convex hull property)**.** Let $t \in \mathbb{R}$, and choose $i \in \mathbb{Z}$ such that $x_i \leq t < x_{i+1}$. Choose real-valued coefficients $(a_j)_{j\in\mathbb{Z}}$, and let

$$g := \sum_{j\in\mathbb{Z}} a_j B_{j,m,X} \qquad \in \mathcal{S}_{m,X}$$

denote the associated spline function. Then, $g(t) \in \operatorname{conv}(a_{i-m}, \ldots, a_i)$, where conv denotes the convex hull of the given coefficients, as will be specified in Definition 3.4 later. In particular,

$$\min\{a_{i-m}, \ldots, a_i\} \leq g(t) \leq \max\{a_{i-m}, \ldots, a_i\}.$$

◀

These properties directly follow from the nonnegativity of B-splines (see Proposition 2.15) and the partition of unity (see Corollary 2.21). Furthermore, one can show that a similar inequality also holds for the converse [Boo01, p. 132]:

Proposition 2.28 (Condition)**.** Let $(a_i)_{i\in\mathbb{Z}}$ be a coefficient sequence in $\mathbb{R}$. There exists a constant $C(m) \in \mathbb{R}_+$, which only depends on m, such that, for all $i \in \mathbb{Z}$, one has

$$|a_i| \leq C(m) \sup_{t\in[x_{i+1},x_{i+m}]} \left| \sum_{j\in\mathbb{Z}} a_j B_{j,m,X}(t) \right|.$$

◀

By combining Propositions 2.27 and 2.28, one obtains the following relation [Boo01, p. 133]:

$$C(m)^{-1}\|a\|_\infty \leq \left\| \sum_{j\in\mathbb{Z}} a_j B_{j,m,X} \right\|_\infty \leq \|a\|_\infty.$$

Hence, the B-splines constitute a relatively well-conditioned basis for $\mathcal{S}_{m,X}$. This close relation between spline coefficients and spline values also motivates the term *control points* for the coefficients $(a_i)_{i\in\mathbb{Z}}$ [Boo01, p. 133].

There are many more interesting properties regarding B-splines, such as the locally linear independence or the variation diminishing property. However, we will close our introduction to univariate splines here and focus on another topic instead: The generalization of the concepts presented in this chapter to higher dimensions. For more details on univariate splines, we again refer to the books by Carl de Boor [Boo01] and Larry Schumaker [Sch07].

3 Simplex Splines

> *Real change, enduring change, happens one step at a time.*
>
> **— Ruth Bader Ginsburg**

In the previous chapter, we constructed spline functions $g : \mathbb{R} \to \mathbb{R}$ with both a one-dimensional domain and a one-dimensional value range. The generalization to vector-valued function spaces can be achieved easily by using vectors in $\mathbb{R}^d$ for some $d \in \mathbb{N}_+$ instead of scalars as control points and employing componentwise operations. The resulting object is a curve in $\mathbb{R}^d$ [Boo01, p. 133]. However, the curve itself is still a one-dimensional object. In order to overcome this limitation and obtain surfaces, we have to increase the dimension of its domain. As a first step to that end, we will recall *simplex splines*, which can act as basis functions for multivariate spline spaces, as one possible generalization of B-splines in this chapter.

After defining simplices, barycentric coordinates, and multivariate polynomials in the following section, we will recall a certain geometric interpretation of univariate B-splines, which will be used as motivation for the subsequent definition of simplex splines. Afterwards, we will list important properties of simplex splines and close the chapter with some examples.

3.1 General Multivariate Concepts

We recall essential multivariate concepts now, such as barycentric coordinates, simplices, and multivariate polynomials, which are employed throughout the thesis.

3.1.1 Simplices and Barycentric Coordinates

The most common type of coordinate systems are Cartesian coordinate systems. This choice is reasonable if one has a canonical origin and associated coordinate axes.

However, in some situations, these requirements are not fulfilled and one desires to express points with respect to a given set of reference points instead. In this case, *barycentric coordinates*, which employ affine instead of Euclidean geometry, are a handy tool.

Definition 3.1 (Affine combination, affine hull)**.** Let $d \in \mathbb{N}_+$, $n \in \mathbb{N}_0$, and choose reference points $x_0, \dots, x_n \in \mathbb{R}^d$. An *affine combination* of these reference points is an expression

$$\sum_{k=0}^{n} \lambda_k x_k, \quad \text{where } \lambda_0, \dots, \lambda_n \in \mathbb{R}, \ \sum_{k=0}^{n} \lambda_k = 1. \tag{3.1}$$

The set of all affine combinations of $x_0, \dots, x_n$ is called the *affine hull (of $x_0, \dots, x_n$)* and is denoted by

$$\operatorname{aff}(x_0, \dots, x_n) := \left\{ \sum_{k=0}^{n} \lambda_k x_k \;\middle|\; \lambda_0, \dots, \lambda_n \in \mathbb{R}, \ \sum_{k=0}^{n} \lambda_k = 1 \right\}.$$

The reference points are called *affinely independent* if

$$\operatorname{aff}(x_0, \dots, x_{i-1}, x_{i+1}, \dots, x_n) \subset \operatorname{aff}(x_0, \dots, x_n) \quad \text{for all } i \in \{0, \dots, n\}.$$

◀

The affine hull of a given set of reference points is an affine subspace of $\mathbb{R}^d$, i.e., a shifted linear subspace, as displayed in Figure 3.1a. We define the dimension

$$\dim \operatorname{aff}(x_0, \dots, x_n)$$

of an affine hull as the dimension of the corresponding linear subspace.

The expressions in (3.1) can be combined into the following system of linear equations:

$$\begin{pmatrix} 1 \\ t_1 \\ \vdots \\ t_d \end{pmatrix} = \begin{pmatrix} 1 & \cdots & 1 \\ x_{0,1} & \cdots & x_{n,1} \\ \vdots & \ddots & \vdots \\ x_{0,d} & \cdots & x_{n,d} \end{pmatrix} \begin{pmatrix} \lambda_0 \\ \vdots \\ \lambda_n \end{pmatrix}. \tag{3.2}$$

This system is solvable for any $t \in \mathbb{R}^d$ if and only if the matrix is nonsingular, which is exactly the case if $\operatorname{aff}(x_0, \dots, x_n) = \mathbb{R}^d$, i.e., $\dim \operatorname{aff}(x_0, \dots, x_n) = d$. Reference points satisfying this condition are usually called *in general position* (see Definition 3.18 below). With the additional assumption that $d = n$, the system is solvable *uniquely* and the numbers $\lambda_0, \dots, \lambda_n$ are called *barycentric coordinates* [LS07a, p. 18]:

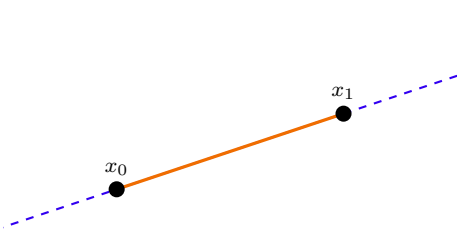

(a) Affine hull *(blue, dashed)* and convex hull *(orange)* of the given points x_0 and x_1. The convex hull is formed by all affine combinations with nonnegative coefficients.

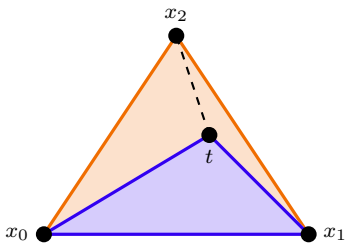

(b) Geometric interpretation of barycentric coordinates. The coordinate $u_2(t \mid x_0, x_1, x_2)$ equals the ratio of the area of the *blue* triangle and the area of the *orange* triangle.

Fig. 3.1: Affine and convex hulls are closely related to barycentric coordinates.

Definition 3.2 (Barycentric coordinates)**.** Let $d \in \mathbb{N}_+$, $t \in \mathbb{R}^d$, and choose reference points $x_0, \ldots, x_d \in \mathbb{R}^d$ with $\dim \operatorname{aff}(x_0, \ldots, x_d) = d$. For each $k \in \{0, \ldots, d\}$, the k-th coefficient λ_k of the uniquely determined solution of Equation (3.2) is called *k-th barycentric coordinate*

$$u_k(t \mid X) := \lambda_k$$

of t with respect to $X := (x_0, \ldots, x_d)$. ◀

Example 3.3. Let $d \in \mathbb{N}_+$ and $X = (\mathbf{0}, \mathbf{e}_1, \ldots, \mathbf{e}_d)$, where $\mathbf{e}_i$ denotes the i-th unit vector in $\mathbb{R}^d$ for $i \in \{1, \ldots, d\}$. Then, $\dim \operatorname{aff}(X) = d$, and the barycentric coordinates of $t = (t_1, \ldots, t_d) \in \mathbb{R}^d$ with respect to X are given as

$$\left(1 - \sum_{k=1}^{d} t_k,\, t_1, \ldots, t_d\right),$$

which yields a conversion formula from Cartesian to barycentric coordinates. ◀

A particular kind of affine combinations are those with nonnegative coefficients:

Definition 3.4 (Convex combination, convex hull)**.** Let $d \in \mathbb{N}_+$, $n \in \mathbb{N}_0$, and choose reference points $x_0, \ldots, x_n \in \mathbb{R}^d$. A *convex combination* of these reference points is an expression

$$\sum_{k=0}^{n} \lambda_k x_k, \quad \text{where } \lambda_0, \ldots, \lambda_n \in \mathbb{R}_{\geq 0},\ \sum_{k=0}^{n} \lambda_k = 1.$$

The set of all convex combinations

$$\operatorname{conv}(x_0, \ldots, x_n) := \left\{ \sum_{k=0}^{n} \lambda_k x_k \;\middle|\; \lambda_0, \ldots, \lambda_n \in \mathbb{R}_{\geq 0},\ \sum_{k=0}^{n} \lambda_k = 1 \right\}$$

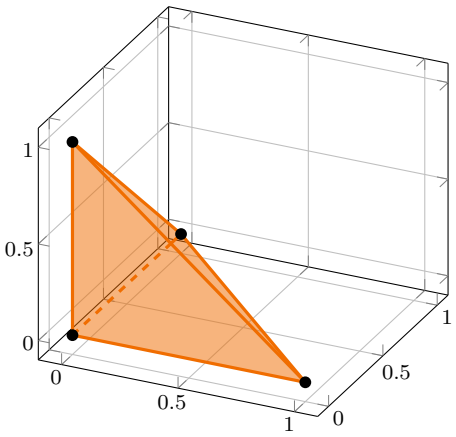

Fig. 3.2: The standard simplex in three dimensions

of the given reference points is called *convex hull (of* $x_0, \dots, x_n$*)*. ◀

For an example, we again refer to Figure 3.1a. The convex hull of a reference system of affinely independent points is also known as *simplex*:

Definition 3.5 (Simplex)**.** Let $d \in \mathbb{N}_+$ and $n \in \mathbb{N}_0$ with $n \leq d$. Furthermore, choose $x_0, \dots, x_n \in \mathbb{R}^d$. If $\dim \operatorname{aff}(x_0, \dots, x_n) = n$, then $\operatorname{conv}(x_0, \dots, x_n)$ is called *(nondegenerate* n*-)simplex*. If $\dim \operatorname{aff}(x_0, \dots, x_n) < n$, then $\operatorname{conv}(x_0, \dots, x_n)$ is called *degenerate (*n*-)simplex*. ◀

If, for instance, $n = 1$, a simplex is a line segment, and if $n = 2$, it is a triangle. The most common simplex is the *standard simplex*, which is displayed in Figure 3.2 and can be defined as follows in accordance with [Mic79]:

Definition 3.6 (Standard simplex)**.** For $d \in \mathbb{N}_+$, we define the *(*d*-dimensional) standard simplex* Δ_d as

$$\Delta_d := \left\{ (a_0, \dots, a_d) \in \mathbb{R}^{d+1}_{\geq 0} \;\middle|\; \sum_{k=0}^{d} a_k = 1 \right\}.$$

For any integrable function $f : \Delta_d \to \mathbb{R}$, we define the integral over the standard simplex Δ_d as

$$\int_{\Delta_d} f(a)\,\mathrm{d}a := \int_0^1 \int_0^{1-a_1} \cdots \int_0^{1-a_1-\cdots-a_{d-1}} f\left(1 - \sum_{k=1}^{d} a_k, a_1, \dots, a_d\right) \mathrm{d}a_d \cdots \mathrm{d}a_1.$$

◀

We can use the notion of simplices to obtain the following geometric interpretation of barycentric coordinates [LS07a, p. 19].

Remark 3.7. When solving Equation (3.2) using Cramer's rule with the same prerequisites as in Definition 3.2, one obtains the following equations for the barycentric coordinates:

$$u_k(t \mid X) = \frac{d_k(t \mid X)}{d(X)} \quad \text{for all } k \in \{0, \dots, d\}, \tag{3.3}$$

where

$$d(X) := \det \begin{pmatrix} 1 & \cdots & 1 \\ x_{0,1} & \cdots & x_{d,1} \\ \vdots & \ddots & \vdots \\ x_{0,d} & \cdots & x_{d,d} \end{pmatrix},$$

$$d_k(t \mid X) := \det \begin{pmatrix} 1 & \cdots & 1 & 1 & 1 & \cdots & 1 \\ x_{0,1} & \cdots & x_{k-1,1} & t_1 & x_{k+1,1} & \cdots & x_{d,1} \\ \vdots & \ddots & \vdots & \vdots & \vdots & \ddots & \vdots \\ x_{0,d} & \cdots & x_{k-1,d} & t_d & x_{k+1,d} & \cdots & x_{d,d} \end{pmatrix}.$$

Since the absolute value of the determinant $d(X)$ equals the volume of the simplex $\operatorname{conv}(X)$ up to a factor of $1/d!$, the fraction in (3.3) can be interpreted as ratio between the volume of a subsimplex $\operatorname{conv}(X_k^t)$ and the volume of $\operatorname{conv}(X)$ itself, where $X_k^t := (x_0, \dots, x_{k-1}, t, x_{k+1}, \dots, x_d)$. The simplex $\operatorname{conv}(X_k^t)$ equals the simplex $\operatorname{conv}(X)$ except that the k-th vertex has been replaced by t. If, for instance, $d = 2$ and $k = 1$, one has

$$u_1(t \mid X) = \frac{\operatorname{vol}_2(\operatorname{conv}(x_0, t, x_2))}{\operatorname{vol}_2(\operatorname{conv}(x_0, x_1, x_2))},$$

where $\operatorname{vol}_n(A)$ for any $n \in \{1, \dots, d\}$ and for any $A \subseteq \mathbb{R}^d$ such that $\dim \operatorname{aff}(A) \leq n$ denotes the n-dimensional Lebesgue measure in an n-dimensional affine subspace containing A. This geometric interpretation is depicted in Figure 3.1b. The specific point $t \in \mathbb{R}^2$ with barycentric coordinates

$$u_k(t \mid X) = \frac{1}{d+1} \quad \text{for all } k \in \{0, \dots, d\},$$

i.e., for which all subsimplices have the same volume, is the barycenter of the simplex $\operatorname{conv}(X)$. This fact also motivates the term *barycentric coordinates*. ◀

Remark 3.8. The barycentric coordinates of a point sum up to one by definition. A *direction* is usually considered as a difference of two points, which is also valid for

their Cartesian coordinates. When representing the points in barycentric coordinates, however, the components of the difference vector sum up to zero instead. Therefore, if the component sum of a vector is zero, the vector is often referred to as *barycentric direction*. Hence, barycentric coordinates allow a distinction between points and directions. ◀

In the current chapter, barycentric coordinates will appear only implicitly (in Propositions 3.19 and 3.24). However, they will also be used explicitly over the course of the thesis.

3.1.2 Multivariate Polynomials

We have seen that univariate splines are piecewise polynomials. Hence, it will be desirable that simplex splines, as a generalization of univariate splines, are piecewise *multivariate polynomials*. Before defining multivariate polynomials, we recall *multiindices*, which are a handy notational tool for working with multivariate objects:

Definition 3.9 (Multiindex)**.** Let $n \in \mathbb{N}_+$. Then, $\alpha := (\alpha_1, \dots, \alpha_n) \in \mathbb{N}_0^n$ is called *multiindex*, and its *length* is denoted by

$$|\alpha| := \sum_{i=1}^{n} \alpha_i \quad \in \mathbb{N}_0.$$

For a given $\ell \in \mathbb{N}_0$, we summarize all multiindices of length ℓ and all multiindices of length at most ℓ in the sets

$$\Gamma_{\ell,n} := \left\{ \alpha \in \mathbb{N}_0^n \;\middle|\; |\alpha| = \ell \right\} \quad \text{and} \quad \Gamma_{\leq \ell,n} := \left\{ \alpha \in \mathbb{N}_0^n \;\middle|\; |\alpha| \leq \ell \right\},$$

respectively. For $i \in \{1, \dots, n\}$, the *unit-multiindex* is given as $\epsilon_i := (\delta_{i,1}, \dots, \delta_{i,n})$. ◀

Sometimes it is more convenient to use a zero-based indexing scheme for multiindices, especially when working with barycentric coordinates. It will be clear from the context which indexing scheme is being employed.

Using multiindices, one can define the space of multivariate polynomials as follows:

Definition 3.10 (Multivariate polynomial)**.** Let $d \in \mathbb{N}_+$ and $m \in \mathbb{N}_0$. If one chooses coefficients $p_\alpha \in \mathbb{R}$ for each $\alpha \in \Gamma_{\leq m,d}$, the function

$$p : \mathbb{R}^d \to \mathbb{R}, \quad x \mapsto \sum_{\alpha \in \Gamma_{\leq m,d}} p_\alpha x^\alpha, \quad \text{where } x^\alpha := \prod_{k=1}^{d} x_k^{\alpha_k},$$

is called *d-variate polynomial of (total) degree at most m*. The *(total) degree* of p is defined as

$$\deg p := \begin{cases} -\infty & \text{if } p \equiv 0, \\ \max\Big\{ |\alpha| \;\Big|\; \alpha \in \Gamma_{\leq m,d},\ p_\alpha \neq 0 \Big\} & \text{otherwise.} \end{cases}$$

The set of all d-variate polynomials is denoted by $\Pi(\mathbb{R}^d)$. All d-variate polynomials of total degree at most m are summarized in the set

$$\Pi_m(\mathbb{R}^d) := \Big\{ p \in \Pi(\mathbb{R}^d) \;\Big|\; \deg p \leq m \Big\}.$$

◀

3.2 Definition of Simplex Splines

In the following subsection, we will recall an interesting geometric interpretation of B-splines. Subsequently, we will use a multivariate generalization of this interpretation for the definition of simplex splines.

3.2.1 Univariate Geometric Interpretation

The idea of simplex splines is based on a certain geometric interpretation of univariate B-splines, which has already been discovered by Curry and Schoenberg in [CS66]. It is established by two different representations of divided differences. The first one is given by the Hermite-Genocchi formula, which [Mic79] relies on:

Theorem 3.11 (Hermite-Genocchi formula)**.** Let $n \in \mathbb{N}_+$, $x_0, \ldots, x_n \in \mathbb{R}$, and set $x := (x_0, \ldots, x_n)^\intercal$. For each $f \in \mathcal{C}^n(\mathbb{R})$, one has the identity

$$[x_0, \ldots, x_n] f = \int_{\Delta_n} f^{(n)}(a^\intercal x) \mathrm{d}a. \tag{3.4}$$

◀

Note that the integrability of the integrand in the Hermite-Genocchi formula is ensured by the continuity of $f^{(n)}$ and the compactness of Δ_n.

Another identity for divided differences, which can also be found in [Mic79], incorporates rescaled versions of B-splines. B-splines have been introduced in Definition 2.11 using divided differences, and by expanding f in terms of a Taylor polynomial with integral remainder, one obtains the following equation (see also [Boo76] and [Boo05, p. 62] for more details).

Proposition 3.12. Let $n \in \mathbb{N}_+$. Choose $x_0, \dots, x_n \in \mathbb{R}$ such that $x_0 \leq \cdots \leq x_n$ and $x_0 < x_n$. Define $X := (x_0, \dots, x_n)$. For $f \in \mathcal{C}^n([x_0, x_n])$, one has

$$[x_0, \dots, x_n]f = \int_{x_0}^{x_n} M(t \mid x_0, \dots, x_n) f^{(n)}(t) \, \mathrm{d}t, \tag{3.5}$$

where the *normalized B-spline* is defined as

$$M(t \mid x_0, \dots, x_n) := \frac{1}{(n-1)!} [x_0, \dots, x_n](\cdot - t)_+^{n-1} = \frac{1}{(n-1)!} \frac{B_{0,n-1,X}(t)}{x_n - x_0}.$$

◀

We combine Identities (3.4) and (3.5) now. Since $M(\cdot \mid x_0, \dots x_n)$ is supported on $[x_0, x_n]$, we can expand the integral in (3.5) to the whole real line. Furthermore, we substitute $g := f^{(n)}$ in both formulas [Mic95, p. 151], which yields the following corollary [Mic79].

Corollary 3.13. Let $n \in \mathbb{N}_+$. Choose $x_0, \dots, x_n \in \mathbb{R}$ such that $x_0 \leq \cdots \leq x_n$ and $x_0 < x_n$. Define $x := (x_0, \dots, x_n)^\intercal$. For all integrable functions $g : \mathbb{R} \to \mathbb{R}$, one has

$$\int_{\mathbb{R}} M(t \mid x_0, \dots, x_n) g(t) \, \mathrm{d}t = \int_{\Delta_n} g(a^\intercal x) \mathrm{d}a. \tag{3.6}$$

◀

Hence, the value of $M(t \mid x_0, \dots, x_n)$ equals the *"number of ways per unit volume"* [Mic80] a given $t \in \operatorname{conv}(x_0, \dots x_n)$ can be represented as convex combination of the knots $x_0, \dots, x_n$.

The importance of that corollary becomes clear when considering the integration variables in (3.4) as barycentric coordinates with respect to the vertices of some

n-dimensional simplex V. To that end, we lift the real numbers $x_0, \dots, x_n$ to $\mathbb{R}^n$ by choosing $y_0, \dots, y_n \in \mathbb{R}^{n-1}$ [Mic79] and defining

$$\widehat{x}_0 := \begin{pmatrix} x_0 \\ y_0 \end{pmatrix}, \quad \widehat{x}_1 := \begin{pmatrix} x_1 \\ y_1 \end{pmatrix}, \quad \dots, \quad \widehat{x}_n := \begin{pmatrix} x_n \\ y_n \end{pmatrix} \quad \in \mathbb{R}^n.$$

One can show that the actual way of lifting the points does not matter as long as the first component is preserved and the resulting simplex $V := \operatorname{conv}(\widehat{x}_0, \dots, \widehat{x}_n)$ is nondegenerate [Mic95, p. 151f], i.e., as long as $\dim \operatorname{aff}(\widehat{x}_0, \dots, \widehat{x}_n) = n$. In particular, it follows from $x_0 < x_n$ that there are at least two distinct values and, thus, an appropriate lifting is possible. According to [Mic95, p. 152] and [Mic79], one can rewrite the right-hand side of Identity (3.6) as

$$\int_{\Delta_n} g(a^\intercal x) \mathrm{d}a = \frac{1}{n! \operatorname{vol}_n(V)} \int_{\mathbb{R}^n} \mathbb{1}_V(t_1, \dots, t_n) g(t_1) \, \mathrm{d}t_n \cdots \mathrm{d}t_1 \tag{3.7}$$

since we have encoded the values $x_0, \dots, x_n$ in the first component of the vertices $\widehat{x}_0, \dots, \widehat{x}_n$ of V and the indicator function $\mathbb{1}_V(t)$, which has the value 1 if $t \in V$ and 0 otherwise, ensures that we integrate over each argument of g exactly as often as in the convex combinations of the original expression.

By combining (3.6) and (3.7) and considering the integrands, we obtain

$$M(\cdot \mid x_0, \dots, x_n) = \frac{1}{n! \operatorname{vol}_n(V)} \int_{\mathbb{R}^{n-1}} \mathbb{1}_V(\cdot, t_2, \dots, t_n) \mathrm{d}t_n \cdots \mathrm{d}t_2,$$

according to [Mic79]. Note that we have an $(n-1)$-fold integral on the right-hand side now instead of the n-fold integral in Identity (3.7). We summarize this insight in the following theorem [Mic95, p. 152].

Theorem 3.14. Let $n \in \mathbb{N}_+$, and let $x_0, \dots, x_n \in \mathbb{R}$ with at least two distinct values. Choose a lifting $\widehat{x}_0, \dots, \widehat{x}_n \in \mathbb{R}^n$ of these values such that $\dim \operatorname{aff}(\widehat{x}_0, \dots, \widehat{x}_n) = n$ and

$$\widehat{x}_{0,1} = x_0, \quad \dots, \quad \widehat{x}_{n,1} = x_n.$$

Let $V = \operatorname{conv}(\widehat{x}_0, \dots, \widehat{x}_n)$. Then, for all $t \in \mathbb{R}$, one has

$$M(t \mid x_0, \dots, x_n) = \begin{cases} \dfrac{\operatorname{vol}_{n-1}(\{v \in V \mid v_1 = t\})}{n! \operatorname{vol}_n(V)} & \text{if } n \geq 2, \\ \dfrac{\mathbb{1}_V(t)}{\operatorname{vol}_1(V)} & \text{if } n = 1. \end{cases} \tag{3.8}$$

◀

This fraction between two different volumes is illustrated in Figure 3.3.

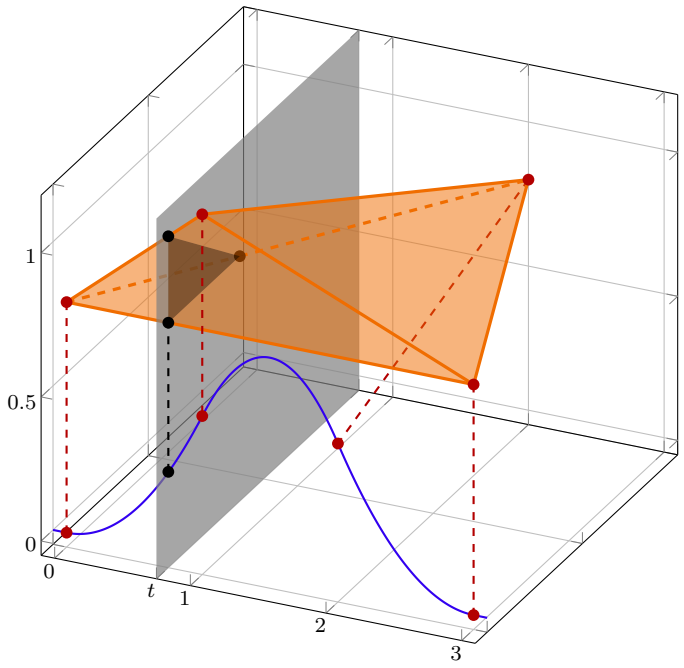

Fig. 3.3: Geometric interpretation of univariate B-splines of degree two. The value of a B-spline at a certain position t *(black dot)* corresponds to the volume of the intersection of the simplex V *(orange)* and the hyperplane $\{v \in \mathbb{R}^n \mid v_1 = t\}$ *(gray)*, normalized according to the volume of V. The corresponding knots and (lifted) vertices are depicted in *red*. Based on Figure 1 in [Nea01a].

3.2.2 Multivariate Generalization

As it turns out, the geometric interpretation of univariate B-splines contains the key to a multivariate analogue, as discovered by de Boor [Boo76] (and earlier by Schoenberg in the complex plane). Assume that we constrain not only one but $d \in \mathbb{N}_+$ coordinates of the point $v \in V$ in Equation (3.8), so that we obtain a d-variate function, which is called *simplex spline* and is displayed in Figure 3.4. We define it in accordance with [Mic79; Mic80]:

Definition 3.15 (Simplex spline)**.** Let $m \in \mathbb{N}_0$, $d \in \mathbb{N}_+$, and let $x_0, \ldots, x_{m+d} \in \mathbb{R}^d$ with $\dim \operatorname{aff}(x_0, \ldots, x_{m+d}) = d$. Furthermore, let $\widehat{x}_0, \ldots, \widehat{x}_{m+d} \in \mathbb{R}^{m+d}$ be lifted points, i.e., there are $y_0, \ldots, y_{m+d} \in \mathbb{R}^m$ satisfying

$$\widehat{x}_0 = \begin{pmatrix} x_0 \\ y_0 \end{pmatrix}, \quad \widehat{x}_1 = \begin{pmatrix} x_1 \\ y_1 \end{pmatrix}, \quad \ldots, \quad \widehat{x}_{m+d} = \begin{pmatrix} x_{m+d} \\ y_{m+d} \end{pmatrix},$$

and

$$\dim \operatorname{aff}(\widehat{x}_0, \ldots, \widehat{x}_{m+d}) = m + d.$$

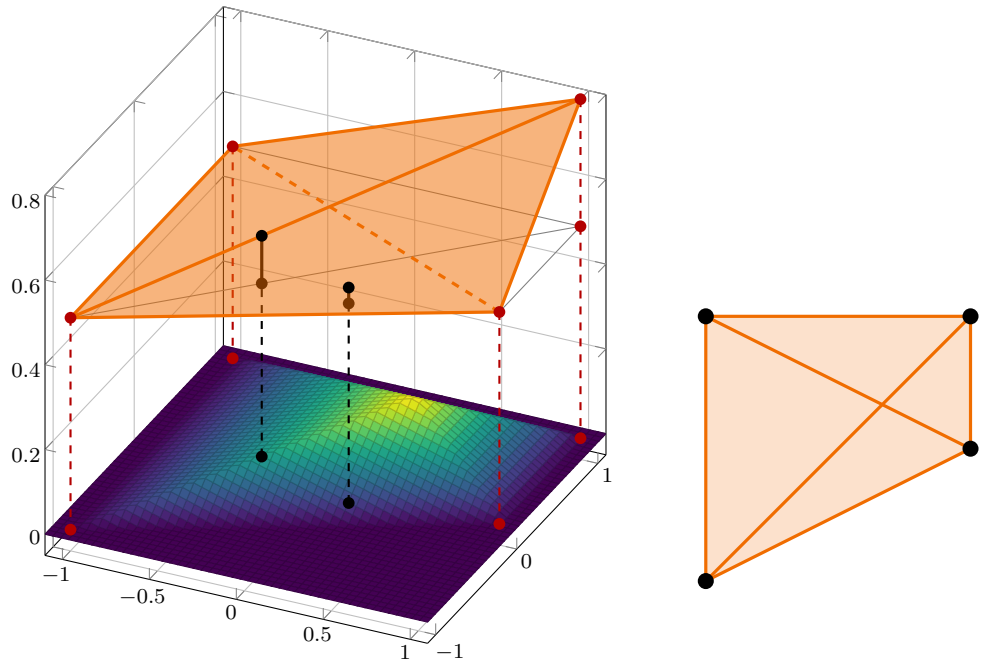

(a) Geometric interpretation and resulting function

(b) Knot set and support

Fig. 3.4: Simplex splines as volumetric projections of higher-dimensional simplices for $d = 2$ and $m = 1$. The values of the simplex spline on the left-hand side at certain positions *(black dots)* are determined by the volumes of the intersections *(black lines)* of the $(m + d)$-dimensional simplex *(orange)* and (one-dimensional) affine subspaces, normalized according to the volume of the simplex. The support and the knots of the resulting simplex spline are depicted on the right-hand side. Based on Figures 2 and 4 in [Nea01a].

Let $V = \operatorname{conv}(\widehat{x}_0, \ldots, \widehat{x}_{m+d})$. The *(d-variate) simplex spline (of degree m with respect to the knots $x_0, \ldots, x_{m+d}$)* is defined for $t = (t_1, \ldots, t_d) \in \mathbb{R}^d$ as

$$M(t \mid x_0, \ldots, x_{m+d}) := \begin{cases} \dfrac{\operatorname{vol}_m(\{v \in V \mid v_1 = t_1, \ldots, v_d = t_d\})}{(m+d)! \operatorname{vol}_{m+d}(V)} & \text{if } m \geq 1, \\ \dfrac{\mathbb{1}_V(t_1, \ldots, t_d)}{d! \operatorname{vol}_d(V)} & \text{if } m = 0. \end{cases} \tag{3.9}$$

◀

Note that the requirement $\dim \operatorname{aff}(x_0, \ldots, x_{m+d}) = d$ is necessary for the construction of a suitable lifting. Under the assumption that $\dim \operatorname{aff}(x_0, x_{m+1}, \ldots, x_{m+d}) = d$ (which can be met in any case by reordering the points), one obtains a canonical lifting, which is a multivariate analogue of the univariate one given in [Mic95, p. 152], by choosing

$$y_0 = y_{m+1} = \cdots = y_{m+d} = \mathbf{0} \quad \text{and} \quad y_i = \mathbf{e}_i \quad \text{for all } i \in \{1, \ldots, m\}.$$

However, also in this case, the specific way of lifting the points does not matter. This fact in particular follows from the multivariate analogue of Corollary 3.13, which is formulated in the following Proposition and is due to Micchelli [Mic79; Mic80].

Proposition 3.16. Let $m \in \mathbb{N}_0$, $d \in \mathbb{N}_+$, and choose $x_0, \ldots, x_{m+d} \in \mathbb{R}^d$ such that $\dim \operatorname{aff}(x_0, \ldots, x_{m+d}) = d$. Define $X := (x_0, \ldots, x_{m+d}) \in \mathbb{R}^{d \times (m+d+1)}$. For any integrable function $g : \mathbb{R}^d \to \mathbb{R}$, the following identity holds true:

$$\int_{\mathbb{R}^d} g(t) M(t \mid x_0, \ldots, x_{m+d}) \mathrm{d}t = \int_{\Delta_{m+d}} g(Xa) \mathrm{d}a.$$

◀

As this identity determines a simplex spline for almost every $t \in \mathbb{R}^d$ and since, according to [Mic79], Equation (3.9) implies that simplex splines are continuous for $m > 0$, Proposition 3.16 may also be used as definition of a simplex spline [Mic80]. For $m = 0$, however, the simplex spline is discontinuous at the boundary of the simplex $\operatorname{conv}(x_0, \ldots, x_d)$, and therefore, its value at that boundary is not defined by Proposition 3.16. As Definition 3.15 reduces to (3.8) for $d = 1$, it follows that 1-variate simplex splines are just renormalized B-splines.

3.3 Properties of Simplex Splines

We will recall some of the most important properties of simplex splines now. The first result follows directly from the definition of simplex splines [Boo76]:

Proposition 3.17. Let $d \in \mathbb{N}_+$, $m \in \mathbb{N}_0$, and choose $x_0, \ldots, x_{m+d} \in \mathbb{R}^d$ such that $\dim \operatorname{aff}(x_0, \ldots, x_{m+d}) = d$. Then, $M(t \mid x_0, \ldots, x_{m+d}) \geq 0$ for all $t \in \mathbb{R}^d$ and

$$\operatorname{supp} M(\cdot \mid x_0, \ldots, x_{m+d}) = \operatorname{conv}(x_0, \ldots, x_{m+d}).$$

◀

For simplicity, we primarily consider nondegenerate situations in the following. Hence, we assume the knots to be in *general position* [Mic95, p. 156]:

Definition 3.18 (General position)**.** Let $d \in \mathbb{N}_+$, and choose a knot set $X \subseteq \mathbb{R}^d$ with $|X| > d$. Then, X is said to be in *general position* if $\dim \operatorname{aff}(Y) = d$ for all subsets $Y \subseteq X$ with $|Y| = d + 1$. ◀

One of the most important formulas concerning simplex splines is a differentiation identity, which is due to Micchelli [Mic80; Mic79] and can be used to derive further properties of simplex splines:

Proposition 3.19. Let $m \in \mathbb{N}_0$, $d \in \mathbb{N}_+$, and let $x_0, \ldots, x_{m+d} \in \mathbb{R}^d$ be in general position. If $m \geq 2$, then $M(\cdot \mid x_0, \ldots, x_{m+d})$ is continuously differentiable on $\mathbb{R}^d$, and one has directional derivatives

$$D_y M(t \mid x_0, \ldots, x_{m+d}) = \sum_{k=0}^{m+d} \mu_k M(t \mid x_0, \ldots, x_{k-1}, x_{k+1}, \ldots, x_{m+d}) \tag{3.10}$$

for all $t \in \mathbb{R}^d$ and for each direction $y \in \mathbb{R}^d$, where $\mu_0, \ldots, \mu_{m+d} \in \mathbb{R}$ are chosen such that

$$\sum_{k=0}^{m+d} \mu_k x_k = y \quad \text{and} \quad \sum_{k=0}^{m+d} \mu_k = 0,$$

i.e., $(\mu_0, \ldots, \mu_{m+d})$ is a barycentric direction associated to y. ◀

Since the first publication of this result, many alternative proofs have been given by different authors, for example in [Höl81] using the Fourier transform, in [Dah80] using certain fundamental solutions of differential equations which are similar to the univariate truncated power functions, in [BH82b] for the more general polyhedral splines, and also in [Hak82].

Due to the recursive structure in Proposition 3.19, repeated application yields

$$M(\cdot \mid x_0, \ldots, x_{d+m}) \in \mathcal{C}^{m-1}(\mathbb{R}^d),$$

which is also valid for $m = 1$ as M is continuous in that case [Mic79].

Similar considerations of derivatives for $m = 1$ in [Mic79] lead to the conclusion that a simplex spline of degree one is continuously differentiable almost everywhere, in which case one can also apply Proposition 3.19. Hence, the derivative is a linear combination of simplex splines of degree zero, which are by definition characteristic functions, each being supported on the convex hull of $d+1$ knots. As a consequence, this linear combination is constant on every region Ω that does not intersect a convex hull generated by any set of d knots since these convex hulls bound the support of the characteristic functions and, therefore, precisely describe the discontinuous areas. Consequently, $M(\cdot \mid x_0, \ldots, x_{d+1})$ is an affine function on every region Ω. Repeated application of this argument yields that a simplex spline of degree m is a polynomial of degree at most m on Ω. These results are summarized in the following theorem [Mic79].

Theorem 3.20. Let $m \in \mathbb{N}_0$, $d \in \mathbb{N}_+$, and choose $x_0, \dots, x_{m+d} \in \mathbb{R}^d$ in general position. Set $X := \{x_0, \dots, x_{m+d}\}$, and let

$$A := \bigcup_{\substack{Y \subseteq X \\ |Y|=d}} \operatorname{conv}(Y).$$

Furthermore, denote by $\mathcal{R}$ the set of connected components of $\mathbb{R}^d \backslash A$. Then,

(i) $M(\cdot \mid x_0, \dots, x_{m+d}) \in \mathcal{C}^{m-1}(\mathbb{R}^d)$ and

(ii) $M(\cdot \mid x_0, \dots, x_{m+d})|_R \in \Pi_m(R)$ for all $R \in \mathcal{R}$. ◀

Remark 3.21. If the knots in the preceding theorem are not in general position, i.e., $\dim \operatorname{aff}(X) = d$ but

$$\ell := \min_{k \in \{0,\dots,m\}} \left\{ \left(\min_{\substack{Y \subseteq X \\ |Y|=k+d+1}} \dim \operatorname{aff}(Y) \right) = d \right\} > 0,$$

the overall smoothness is reduced to

$$M(\cdot \mid x_0, \dots, x_{m+d}) \in \mathcal{C}^{m-\ell-1}(\mathbb{R}^d).$$

We refer to [Mic80] and [Mic79] for more details. ◀

The preceding theorem ensures that simplex splines are indeed piecewise polynomials, which also justifies the term *spline*. In particular, one-dimensional simplex splines are simply (rescaled) B-splines. Another interesting relationship is the following geometric consequence of Theorem 3.20, which again has been discovered by Micchelli [Mic79]:

Remark 3.22. Let $y, z \in \mathbb{R}^d$, and choose m and X as in Theorem 3.20. Then, $M(y + \lambda z \mid X)$ as function in $\lambda \in \mathbb{R}$ is a univariate spline function of degree m. ◀

Further useful properties of simplex splines have been established in [Mic79] and are collected in the following proposition:

Proposition 3.23. Let $m \in \mathbb{N}_0$, $d \in \mathbb{N}_+$, and choose $x_0, \dots, x_{m+d} \in \mathbb{R}^d$ such that $\dim \operatorname{aff}(x_1, \dots, x_{m+d}) = d$.

(i) For all permutations σ of the set $\{0, \dots, m+d\}$, one has

$$M(\cdot \mid x_{\sigma(0)}, \dots, x_{\sigma(m+d)}) = M(\cdot \mid x_0, \dots, x_{m+d}).$$

(ii) For all $y \in \mathbb{R}^d$, one has

$$M(\cdot \mid x_0 + y, \ldots, x_{m+d} + y) = M(\cdot - y \mid x_0, \ldots, x_{m+d}).$$

(iii) For all nonsingular $A \in \mathbb{R}^{d\times d}$ and for any $t \in \mathbb{R}^d$, one has

$$M(t \mid Ax_0, \ldots, Ax_{m+d}) = \frac{1}{|\det A|} M(A^{-1}t \mid x_0, \ldots, x_{m+d}).$$

◀

We close the section with a useful recursion formula [Mic80] for the evaluation of simplex splines, which is due to Micchelli and is the multivariate analogue of Identity (2.9). As the knots in the affine combination therein can be chosen arbitrarily, however, this formula is even more general [Mic79].

Proposition 3.24 (Micchelli's recursion formula)**.** Let $d \in \mathbb{N}_+$, $m \in \mathbb{N}_+$ with $m \geq 2$, and choose $x_0, \ldots, x_{m+d} \in \mathbb{R}^d$ in general position. Let $t \in \mathbb{R}^d$, and choose an arbitrary affine combination of t, i.e.,

$$\lambda_0, \ldots, \lambda_{m+d} \in \mathbb{R}, \quad \sum_{k=0}^{m+d} \lambda_i x_i = t, \quad \sum_{k=0}^{m+d} \lambda_i = 1.$$

Then, the identity

$$M(t \mid x_0, \ldots, x_{m+d}) = \frac{1}{m} \sum_{k=0}^{m+d} \lambda_k M(t \mid x_0, \ldots, x_{k-1}, x_{k+1}, \ldots, x_{m+d}) \tag{3.11}$$

holds true. ◀

Hence, simplex splines can be evaluated by computing simplex splines of lower degrees recursively. The restriction to degrees of at least two is necessary since problems arise in Identity (3.11) when evaluating simplex splines at discontinuities, which are present in simplex splines of degree zero at the boundary of their support. Aside from numerical issues, the definition of simplex splines of degree zero would have to be more sophisticated in order to enable the application of Identity (3.11) for $m = 1$. These discontinuities will be excluded in several results of the thesis and are the reason why some identities only hold *almost* everywhere. We will mention this fact in most situations but not on every occurrence throughout the thesis. Hence, one should always be aware of this difficulty when considering simplex splines of

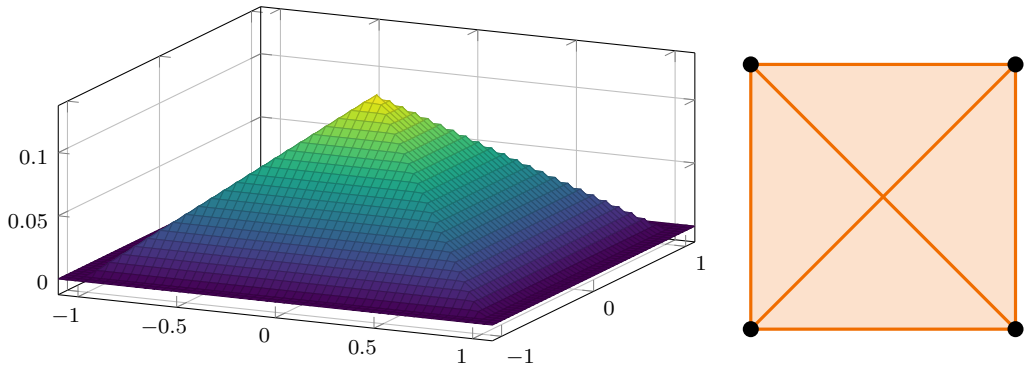

(a) Simplex spline (b) Knot set

Fig. 3.5: Example of a simplex spline of degree one with knots arranged in a square

degree zero. We refer to [Mic79] and Subsection 8.2.1 for more details on this topic.

Remark 3.25. Consider an arbitrary evaluation site $t \in \operatorname{conv}(x_0, \ldots, x_{m+d})$. Due to Carathéodory's theorem, $d+1$ nonzero summands are always sufficient in Identity (3.11). Furthermore, the corresponding knots can be chosen in a way that t can be represented as convex combination of these knots. Then, one has $\lambda_k \geq 0$ for all $k \in \{0, \ldots, m+d\}$. Hence, the value of a simplex spline at a site t in its support is always a nonnegative convex combination of $d+1$ simplex splines of degree $m-1$ evaluated at t. The specific choice of knots depends on t, however [Mic79]. ◀

3.4 Examples of Simplex Splines

In this section, we give some examples of bivariate simplex splines in order to facilitate a better understanding of these functions and to demonstrate the properties that we have derived in the previous section. We present different simplex splines of degree one in Figures 3.5, 3.6, and 3.7. On the contrary, *quadratic* simplex splines (i.e., of degree two) are displayed in Figures 3.8, 3.9, 3.10, and 3.11 with a focus on highlighting the effects of degenerate knot sets. A *cubic* simplex spline is depicted in Figure 3.12. The lines connecting two knots indicate where polynomial pieces touch each other, whereas the shaded areas correspond to the support of the resulting simplex splines.

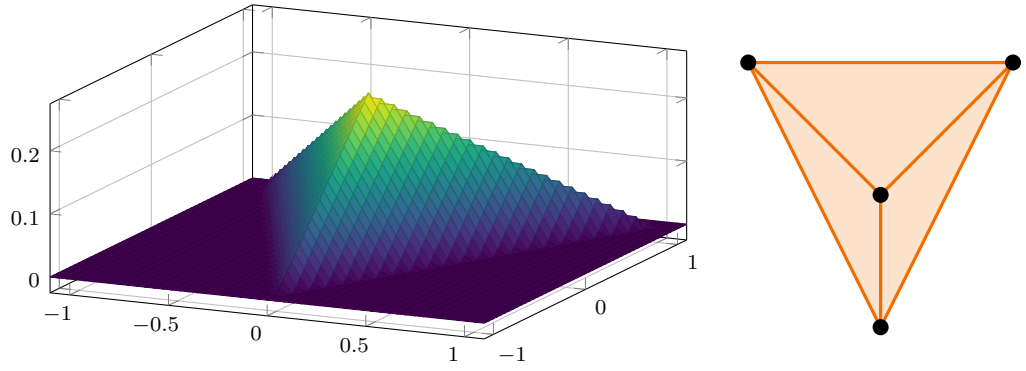

(a) Simplex spline (b) Knot set

Fig. 3.6: Example of a simplex spline of degree one, where one knot is in the convex hull of the other three knots

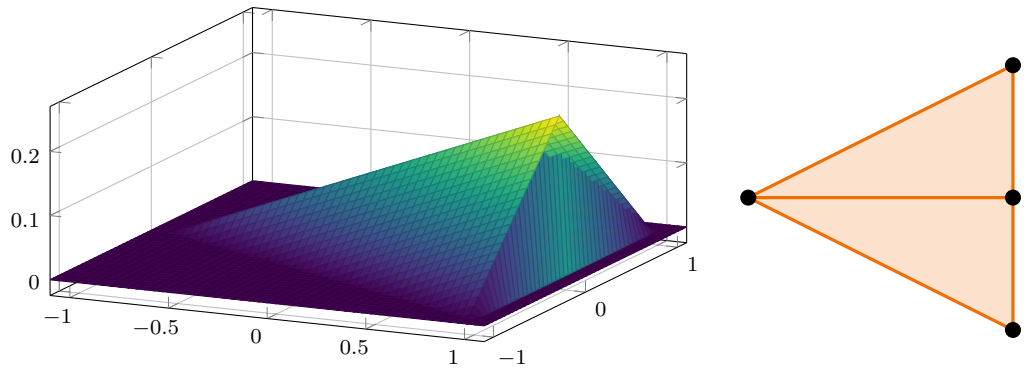

(a) Simplex spline (b) Knot set

Fig. 3.7: Example of a simplex spline of degree one with a discontinuity, which is caused by three knots being arranged in a line

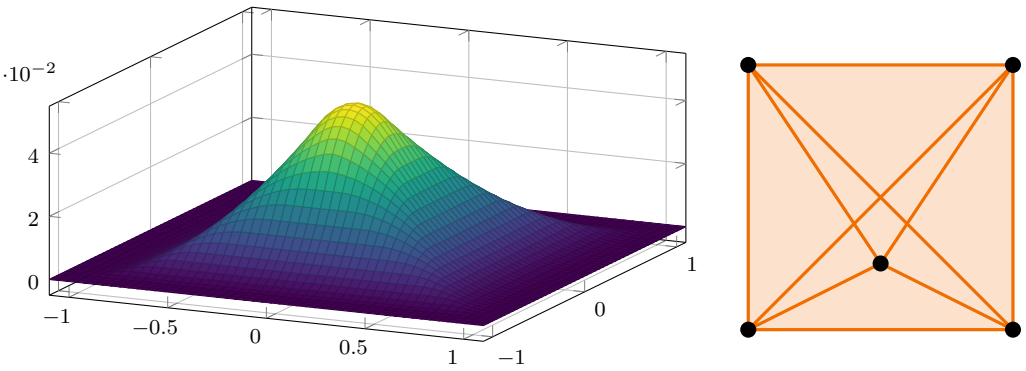

(a) Simplex spline (b) Knot set

Fig. 3.8: Example of a quadratic simplex spline with respect to knots in general position

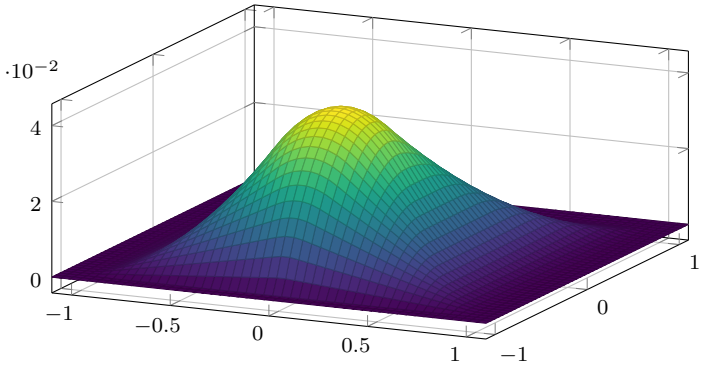

(a) Simplex spline

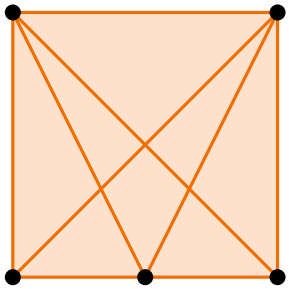

(b) Knot set

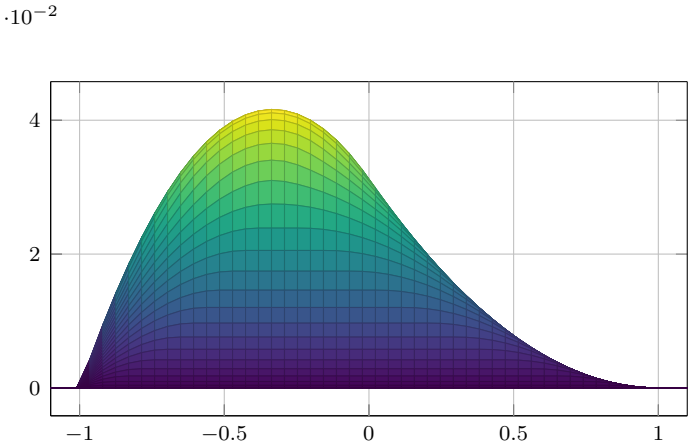

(c) Cross section at coordinate zero

Fig. 3.9: Example of a quadratic simplex spline with respect to a degenerate knot set causing a nondifferentiable edge at the boundary of the support, as can be seen in the cross section

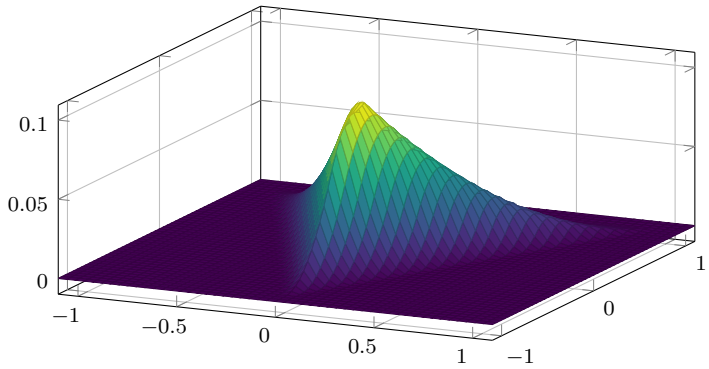

(a) Simplex spline

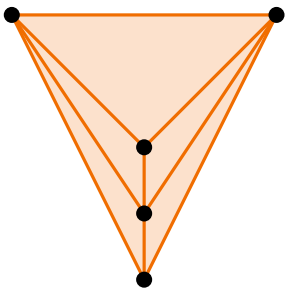

(b) Knot set

Fig. 3.10: Example of a quadratic simplex spline with respect to a degenerate knot set leading to a nondifferentiable ridge in the interior of the support

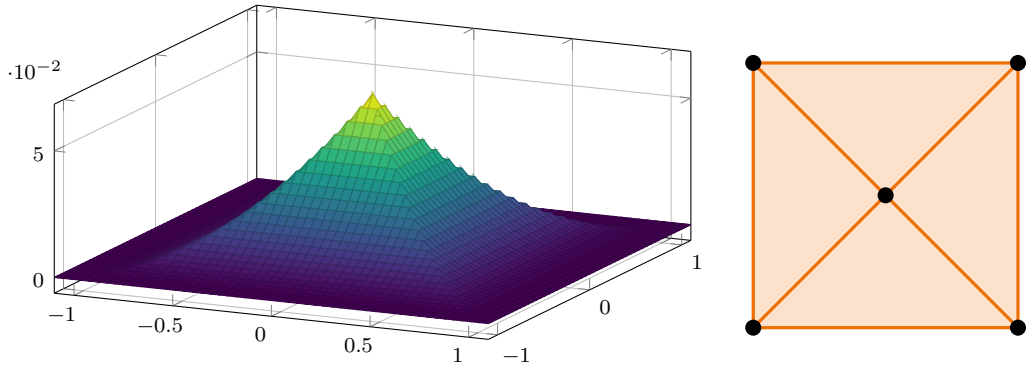

(a) Simplex spline (b) Knot set

Fig. 3.11: Example of a quadratic simplex spline with respect to a degenerate knot set causing nondifferentiable edges and a peak in the resulting function

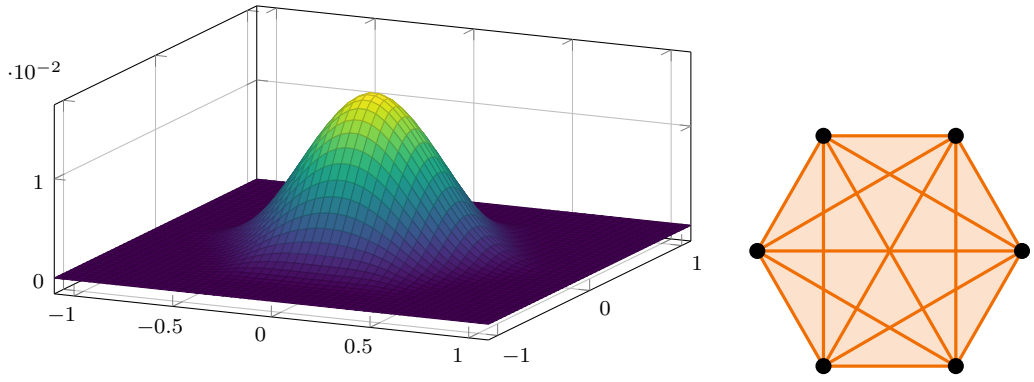

(a) Simplex spline (b) Knot set

Fig. 3.12: Example of a cubic simplex spline, where all knots are arranged in a regular hexagon

4 Multivariate Spline Spaces

> *Mathematics is like love; a simple idea, but it can get complicated.*
>
> **— George Pólya**

In the previous chapter, we recalled a multivariate analogue of univariate B-splines. The univariate spline space was defined as linear span of the B-splines specified by a given knot sequence. In a multivariate setting, however, a problem arises in this step, which we will investigate in the following section. As it will turn out, there is no straightforward strategy for the definition of an appropriate multivariate spline space. Hence, we will formulate the properties that we expect from a reasonable spline space. Afterwards, we will consider two different approaches towards multivariate splines.

4.1 Constructing Multivariate Spline Spaces

In the following subsection, we will identify the essential problem in the construction of a multivariate spline space. In order to be able to verify if a given solution to that problem is reasonable, we will define the desired properties for multivariate spline spaces subsequently.

4.1.1 Generalizing the B-Spline Basis

In Definition 2.13, we defined the univariate spline space as linear span of all B-splines with respect to a given knot sequence. The B-splines were constructed using all sets of $m+2$ *consecutive* knots, where $m \in \mathbb{N}_0$ was the spline degree.

Let us consider the space $\mathbb{R}^d$ for $d \in \mathbb{N}_+$ now. We recall that $m+d+1$ points give rise to a d-variate simplex spline of degree m. This number reduces to $m+2$ (as in the univariate case) when setting d to one, which again indicates that simplex splines are (renormalized) B-splines for $d = 1$, as we have mentioned earlier.

Therefore, the task is to find subsets of knots of size $m+d+1$ that give rise to simplex splines spanning a reasonable spline space. However, the concept of *consecutive* knots in the one-dimensional setting relies on the ordering of the real numbers. As there is no natural ordering on $\mathbb{R}^d$ for $d > 1$, the issue of choosing appropriate basis candidate functions becomes relevant in the multivariate case [Nea01a].

One simple option would be to choose all knot subsets of size $m + d + 1$ for the construction of simplex splines. This, however, would yield linear dependent basis candidate functions which can have a very large support [Nea01b, p. 361f]. This suggests that a more sophisticated approach is necessary to obtain a spline space with the desired properties. These properties will be formulated in the following subsection.

4.1.2 The Fundamental Problem

As indicated, the generalization of splines to higher dimensions is not straightforward. We noted earlier that we want to construct a *reasonable* spline space. However, this term is obviously very vague. We will eradicate this shortcoming now by defining the precise properties that are desirable for a multivariate spline space, as formulated in [Nea01b, p. 356f]:

Requirements. Let $d \in \mathbb{N}_+$, $m \in \mathbb{N}_0$, and choose a knot set $X \subseteq \mathbb{R}^d$. A d-variate spline space $\mathcal{S}_{d,m,X}$ generated by a countable set $\mathcal{B} \subseteq \mathcal{S}_{d,m,X}$ of basis candidate functions should feature the following properties:

(A) The functions in $\mathcal{S}_{d,m,X}$ are piecewise polynomials of degree at most m on regions induced by X, i.e., there is a system of knot subsets $\mathcal{P} \subseteq \mathfrak{P}(X)$ such that, for all $P \in \mathcal{P}$, one has $|P| = d$, and such that

$$g|_R \in \Pi_m(R) \quad \text{for all } g \in \mathcal{S}_{d,m,X},\ R \in \mathcal{R},$$

where $\mathcal{R}$ denotes the set of connected components of the set $\mathbb{R}^d \backslash A$ and A is the union of all lower-dimensional simplices connecting the knot subsets specified by $\mathcal{P}$:

$$A := \bigcup_{P \in \mathcal{P}} \operatorname{conv}(P).$$

(B) Each spline function in $\mathcal{S}_{d,m,X}$ has optimal smoothness, i.e., is $(m-1)$-times continuously differentiable:

$$\mathcal{S}_{d,m,X} \subseteq \mathcal{C}^{m-1}(\mathbb{R}^d).$$

(C) The spline space $\mathcal{S}_{d,m,X}$ contains all polynomials of degree at most m:

$$\Pi_m(\mathbb{R}^d) \subseteq \mathcal{S}_{d,m,X}.$$

(D) The spline space $\mathcal{S}_{d,m,X}$ is locally finite-dimensional:

$$\dim \mathcal{S}_{d,m,X}|_\Omega < \infty \quad \text{for all compact } \Omega \subseteq \mathbb{R}^d.$$

(E) Each point lies in the support of only a finite number of basis candidate functions:

$$|\{B \in \mathcal{B} \mid t \in \operatorname{supp} B\}| < \infty \quad \text{for all } t \in \mathbb{R}^d.$$

(F) The basis candidate functions are compactly supported, and each spline function in $\mathcal{S}_{d,m,X}$ can be represented as a (possibly infinite) linear combination of basis candidate functions, i.e., for each $g \in \mathcal{S}_{d,m,X}$, there exist coefficients $a_B \in \mathbb{R}$, $B \in \mathcal{B}$, such that

$$g = \sum_{B \in \mathcal{B}} a_B B.$$

(G) The basis candidate functions in $\mathcal{B}$ are linearly independent, and the representation in the previous requirement is therefore unique: For all coefficient sets $a_B \in \mathbb{R}$, $B \in \mathcal{B}$, the implication

$$\sum_{B \in \mathcal{B}} a_B B \equiv 0 \quad \Rightarrow \quad a_B = 0 \text{ for all } B \in \mathcal{B}$$

holds true. In particular, this implies that $\mathcal{B}$ constitutes a basis.

(H) For $d = 1$, the basis candidate functions in $\mathcal{B}$ are B-splines, and the spline space $\mathcal{S}_{d,m,X}$ equals the univariate splines:

$$\mathcal{S}_{1,m,X} = \mathcal{S}_{m,X}.$$

◀

The search for a strategy to construct a spline space meeting these requirements for all choices of m, d and for almost every knot set $X \subseteq \mathbb{R}^d$ satisfying Assumptions (i) and (ii) below is called *Fundamental Problem* in [Nea01b, p. 356f].

(i) X covers the whole space, i.e., $\operatorname{conv}(X) = \mathbb{R}^d$,

(ii) X is locally finite and, therefore, has no accumulation points, i.e.,

$$|X \cap \Omega| < \infty \quad \text{for all compact } \Omega \subseteq \mathbb{R}^d.$$

Regarding these assumptions on X, several remarks are in order:

Usually, knot sets that are encountered in practical applications should exhibit local finiteness in the sense of Assumption (ii). Its goal is, on the one hand, to be able to work with a finite number of objects in any bounded region (as ensured by Requirements (D) and (E)) and, on the other hand, to avoid academic counterexamples.

On the contrary, Assumption (i) is a more severe restriction since most practical knot sets are finite and, therefore, have a bounded convex hull. However, at this point, we do not want to consider boundary regions but concentrate on the core region, which is not influenced by the boundary of the knot set. The easiest way to achieve this is to choose $\operatorname{conv}(X) = \mathbb{R}^d$ as, in this case, $\operatorname{conv}(X)$ has no boundary.

Furthermore, we expect Requirements (A) - (H) to hold true only for *almost every* knot set satisfying the stated assumptions. This comes from the fact that we want to ignore degenerate cases, like situations where $d+1$ points lie in the same hyperplane and, therefore, give rise to a degenerate simplex. In particular, this is the case when one has multiple knots at the same site. Whereas these configurations certainly have to be dealt with in practical applications (see Subsection 8.2.2), they are of minor interest for the task of creating an appropriate spline space [Nea01b, p. 356].

In the following sections, we will revisit two different approaches towards a reasonable multivariate spline space generated by arbitrary knot sets, both making use of the simplex spline functions that we have defined in the previous chapter.

4.2 DMS-Splines

One of the most common multivariate spline spaces is the approach introduced by Dahmen, Micchelli, and Seidel [DMS92], which is known as *Dahmen-Micchelli-Seidel-splines (DMS-splines)*. In this section, we will briefly recall the path from the

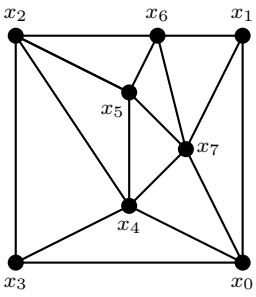

Fig. 4.1: Example of a triangulation of the knot set $\{x_0, \dots, x_7\} \subseteq \mathbb{R}^2$. Each element of the triangulation corresponds to three knots that are pairwise interconnected.

first space using simplex splines to the DMS-splines. Since this approach is based on the notion of *triangulations*, we will now define this term in a way similar to [Hußß99, p. 13] but more general:

Definition 4.1 (Triangulation)**.** Let $d \in \mathbb{N}_+$ and $\Omega \subseteq \mathbb{R}^d$. Let $X \subseteq \Omega$ be countable. Then, $\mathcal{T} \subseteq \mathfrak{P}(X)$ is a *triangulation* of Ω with respect to the vertices X if

(i) $|T| = d + 1$ for all $T \in \mathcal{T}$,

(ii) $\mathrm{vol}_d(\mathrm{conv}(T)) > 0$ for all $T \in \mathcal{T}$,

(iii) $\bigcup_{T \in \mathcal{T}} \mathrm{conv}(T) = \Omega$,

(iv) $\mathrm{conv}(T) \cap \mathrm{conv}(T') = \mathrm{conv}(T \cap T')$ for all $T, T' \in \mathcal{T}$, and if

(v) $\mathrm{conv}(T) \cap X = T$ for all $T \in \mathcal{T}$. ◀

For an example of a triangulation, we refer to Figure 4.1. If $\mathcal{T}$ is a triangulation, then, for each $T \in \mathcal{T}$, the convex hull $\mathrm{conv}(T)$ is a nondegenerate simplex. These simplices subdivide Ω, and if two simplices have a nonempty intersection, the intersection is a lower-dimensional face of both simplices. Here, a *face* denotes the convex hull of a subset of the vertices of a simplex.

4.2.1 A Geometric Approach

Directly after the definition of simplex splines as projections of higher-dimensional simplices in [Boo76], de Boor showed a possible construction of a spline space spanned by a collection of simplex splines. To that end, let $m \in \mathbb{N}_0$ denote the spline degree, and let $d \in \mathbb{N}_+$ be the dimension of the spline domain, i.e., one employs d-variate simplex splines. One considers the set $\mathbb{R}^d \times \Omega$ for an arbitrary convex $\Omega \subseteq \mathbb{R}^m$ with $\mathrm{vol}_m(\Omega) = 1$ and constructs an arbitrary triangulation $\mathcal{T}$ of $\mathbb{R}^d \times \Omega$

[Boo76], where all vertices should be contained in the boundary of $\mathbb{R}^d \times \Omega$ [Dah79]. Then, each element of $\mathcal{T}$ spans a nondegenerate $(m+d)$-dimensional simplex and, therefore, gives rise to a d-variate simplex spline of degree m, which is denoted by M_T for each $T \in \mathcal{T}$. Since $\mathcal{T}$ is a triangulation, the intersection $\operatorname{conv}(T) \cap \operatorname{conv}(T')$ for two distinct $T, T' \in \mathcal{T}$ is empty or a lower-dimensional face and, therefore, in particular a null set. As a consequence, it follows with $a_T := \operatorname{vol}_{m+d}(\operatorname{conv}(T))$ for each $T \in \mathcal{T}$ that, for $m \geq 1$ (just to avoid the improperly defined value of simplex splines of degree zero on the boundary of their support) and any $t \in \mathbb{R}^d$, one has

$$\begin{aligned}\sum_{T\in\mathcal{T}} a_T M_T(t) &= \sum_{T\in\mathcal{T}} \operatorname{vol}_m\Big(\Big\{v \in \operatorname{conv}(T) \;\Big|\; v_1 = t_1, \ldots, v_d = t_d\Big\}\Big) \\ &= \operatorname{vol}_m\left(\left\{v \in \bigcup_{T\in\mathcal{T}} \operatorname{conv}(T) \;\middle|\; v_1 = t_1, \ldots, v_d = t_d\right\}\right) \\ &= \operatorname{vol}_m\Big(\Big\{v \in \mathbb{R}^d \times \Omega \;\Big|\; v_1 = t_1, \ldots, v_d = t_d\Big\}\Big) = \operatorname{vol}_m(\Omega) = 1.\end{aligned}$$

Consequently, appropriately rescaled simplex splines generated by $\mathcal{T}$ form a partition of unity [Boo82, p. 68]. It has been shown in [Dah79; Dah81] that the spline space also contains polynomials up to degree m, i.e., $\Pi_m \subseteq \operatorname{span}\{M_T \mid T \in \mathcal{T}\}$. Here, we allow infinite linear combinations in the span in order to be able to represent polynomials, which do not have compact support in general.

Although, according to [Nea01b, p. 363], the resulting simplex splines are linearly independent if Ω is chosen to be a simplex, this does not hold true in general, according to [DM82, p. 993]. The approach is visualized in Figure 4.2 for the special case $d = 1$ and $m = 2$.

Despite some appealing properties of this spline construction, it becomes infeasible in practical applications due to the necessity of computing a high-dimensional triangulation [Nea01b, p. 363f]. Furthermore, it is undesirable that the generated simplex splines depend on the specific high-dimensional triangulation in $\mathbb{R}^{m+d}$. Instead, it would be beneficial if one could derive the splines directly from some triangulation of $\mathbb{R}^d$ [Boo82, p. 69]. We will see in the next subsection how this can be achieved using a combinatorial approach.

4.2.2 A Combinatorial Approach

We will now recall an approach for the construction of a d-variate spline space which uses a triangulation of $\mathbb{R}^d$ and combinatorial methods. It has been introduced by Dahmen and Micchelli [DM82], whereas a similar method has been proposed

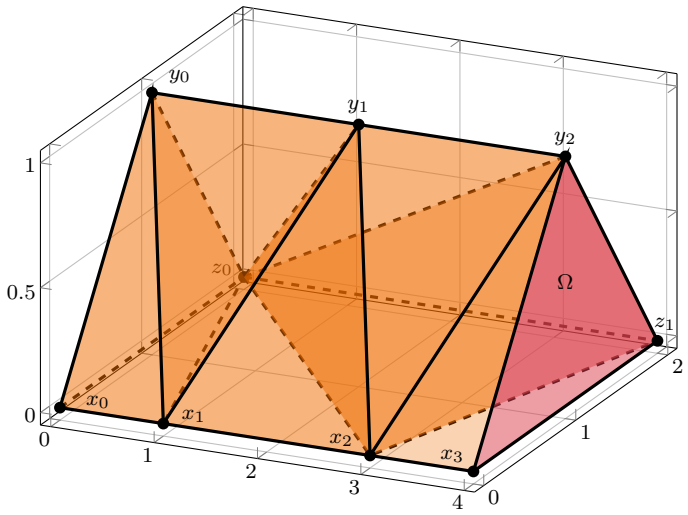

(a) Arbitrary triangulation of $[0, 4] \times \Omega$

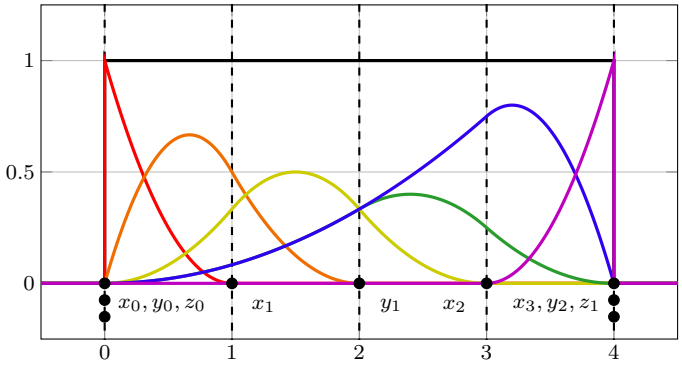

(b) Simplex splines generated by the triangulation

Fig. 4.2: Geometric approach to a multivariate spline space for $d = 1$ and $m = 2$. The triangulation presented at the top gives rise to the basis functions plotted at the bottom. Note that these functions differ from the B-splines that would have been generated by the given knot sequence.

independently by Höllig [Höl82]. Summaries can be found in [Nea01b] and [Boo82], where the latter has been used primarily for this subsection.

To that end, let us assume that $\mathcal{T}$ is a triangulation of $\mathbb{R}^d$ with respect to a vertex set $X \subseteq \mathbb{R}^d$, and let $m \in \mathbb{N}_0$ be the spline degree. The Cartesian product of two simplices is named *simploid* in [DM82]. Hence, $\operatorname{conv}(T) \times \Delta_m \subseteq \mathbb{R}^{m+d}$ is a simploid for each $T \in \mathcal{T}$.

[DM82] gives a generic way to triangulate such simploids, which is based on Kuhn's triangulation of the unit cube. Let $\widehat{T}$ denote this generic triangulation of the simploid $\operatorname{conv}(T) \times \Delta_m$ for each $T \in \mathcal{T}$. If $T \in \mathcal{T}$, there are $x_0, \ldots, x_d \in X$ such

that $T = \{x_0, \dots, x_d\}$. Then, the vertex set of the simploid $\operatorname{conv}(T) \times \Delta_m$ is given by

$$\Big\{(x_i, \mathbf{e}_j) \in \mathbb{R}^{d+m} \;\Big|\; i \in \{0, \dots, d\},\ j \in \{0, \dots, m\}\Big\}, \tag{4.1}$$

where $\mathbf{e}_0 := \mathbf{0} \in \mathbb{R}^m$. The combinatorial notion of the triangulation $\widehat{T}$ of a simploid can be seen in Figure 4.3c, which is based on [Boo82, p. 71]: Each nondecreasing path from $(0, 0)$ to (d, m) is assigned to a simplex spanned by the vertices on the path.

Furthermore, Dahmen and Micchelli proved in [DM82] that

$$\mathcal{T}^* := \bigcup_{T \in \mathcal{T}} \widehat{T}$$

constitutes a triangulation of $\mathbb{R}^d \times \Delta_m$ as long as the vertices in X are enumerated consistently. Therefore, $\mathcal{T}^*$ is a triangulation of $\mathbb{R}^d \times \Omega$ in terms of the previous subsection, and one can conclude that

$$\Pi_m \subseteq \operatorname{span}\{M_T \mid T \in \mathcal{T}^*\}, \tag{4.2}$$

where M_T denotes the simplex spline generated by the projections of all vertices of $T \in \mathcal{T}^*$ on the first d components [Boo82, p. 71]. The situation is exemplified in Figure 4.3 for $d = 1$ and $m = 2$.

Since the triangulation of every simploid $\operatorname{conv}(T) \times \Delta_m$ consists of exactly $\binom{m+d}{d}$ simplices for any $T \in \mathcal{T}$, there are exactly $\binom{m+d}{d}$ different simplex splines with support in $\operatorname{conv}(T)$, which equals the dimension of the space of d-variate polynomials of degree at most m. Hence, it follows from (4.2) that the simplex splines are linearly independent and, therefore, form a basis for the space of d-variate piecewise polynomials of degree at most m on the triangulation $\mathcal{T}$ [Boo82, p. 71].

However, as one can easily see in the vertex set (4.1) of a simploid, the $m + 1$ vertices $(x, \mathbf{e}_0), \dots, (x, \mathbf{e}_m)$ correspond to the same projected vertex $x \in \mathbb{R}^d$ for each $x \in X$, which, thus, has multiplicity $m + 1$. According to Remark 3.21, the resulting simplex splines do not have maximum smoothness [DM82, p. 1001]. In particular, the triangulation $\mathcal{T}^*$ gives rise to discontinuous simplex splines. To overcome this flaw, [DM82] proposes to *pull the knots apart*, so that, on the one hand, the linear independence and the polynomial reproduction property in (4.2) are retained and, on the other hand, all resulting simplex splines are in $\mathcal{C}^{m-1}(\mathbb{R}^d)$. We are content with showing the resulting basis functions in Figure 4.4 and refer to [DM82], [Höl82], and [Boo82] for details on this topic.

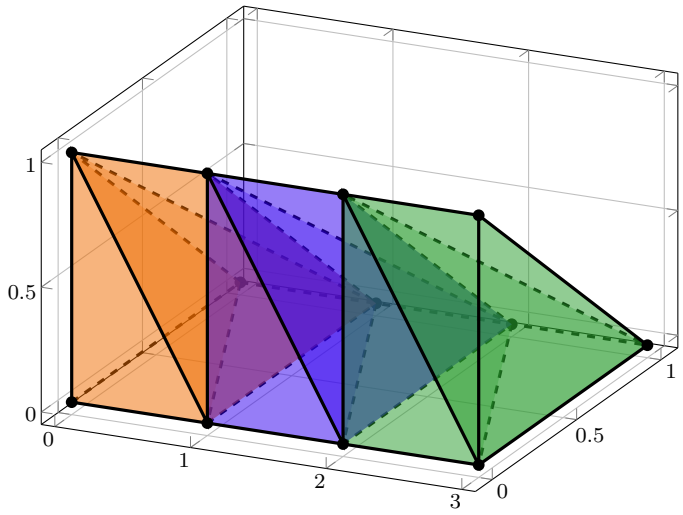

(a) The given triangulation of the interval $[0, 3]$ with knot set $\{0, 1, 2, 3\}$ is extended to a triangulation of $[0, 3] \times \Delta_m$.

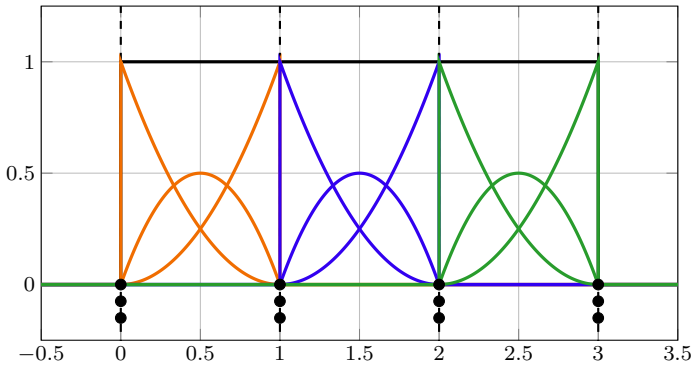

(b) The simplex splines generated by the triangulation shown above. Note that these functions feature discontinuities at the breakpoints.

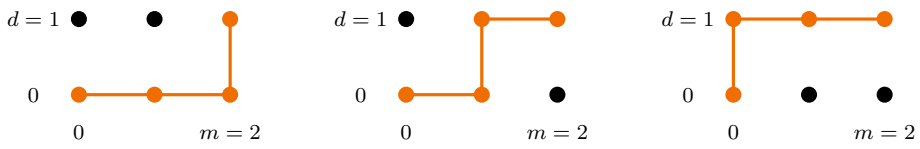

(c) The nondecreasing paths from $(0, 0)$ to (d, m) used to triangulate the simploids $T \times \Delta_m$ for all $T \in \mathcal{T}$ in the original triangulation of the interval $[0, 3]$. Based on [Boo82, p. 71].

Fig. 4.3: Combinatorial approach to a multivariate spline space for $d = 1$ and $m = 2$. The simplices shown in the figure at the top give rise to the depicted basis functions.

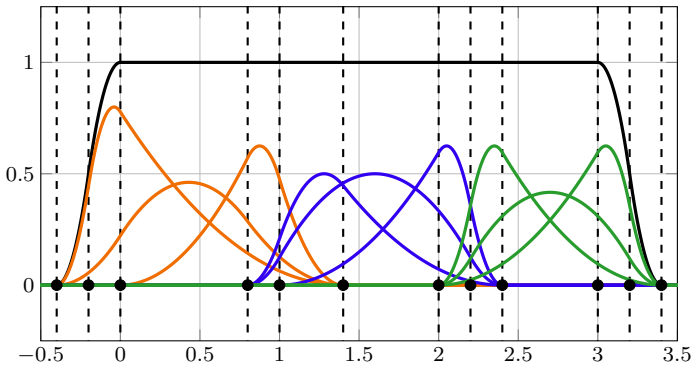

Fig. 4.4: Combinatorial approach with knots pulled apart. In contrast to Figure 4.3b, the basis functions feature optimal smoothness now.

4.2.3 B-Patches and B-Weights

Whereas the two approaches recalled in the previous subsections marked important steps towards DMS-splines, the motivation for the latter is neither based on geometric nor combinatorial concepts but is motivated by symmetric simplicial algorithms and their connection to simplex splines [DMS92].

Symmetric simplicial algorithms have been used heavily for univariate splines, especially for computational purposes. For the sake of brevity, we could not cover them in Chapter 2 and will only scratch the surface in this section. We refer to [Sei91] and [DMS92] for more details.

Assume that, for $d \in \mathbb{N}_+$ and $m \in \mathbb{N}_0$, one has a knot set

$$X := \{x_{i,j} \in \mathbb{R}^d \mid 0 \le i \le d,\ 0 \le j \le m\}$$

such that, for each $\alpha \in \Gamma_{\le m,d+1}$, one has

$$\dim \operatorname{aff}(X_\alpha) = d, \quad \text{where } X_\alpha := (x_{0,\alpha_0}, \ldots, x_{d,\alpha_d}). \tag{4.3}$$

Here, we assume from now on that the multiindices use a zero-based indexing scheme. Furthermore, let $a_\alpha \in \mathbb{R}$ for each $\alpha \in \Gamma_{m,d+1}$.

A symmetric simplicial algorithm is defined by the following recursion for each $\ell \in \{0, \ldots, m\}$, for each $\alpha \in \Gamma_{m-\ell,d+1}$, and for all $t \in \mathbb{R}^d$:

$$\begin{aligned} c_\alpha^0(t) &:= a_\alpha && \text{if } \ell = 0, \\ c_\alpha^\ell(t) &:= \sum_{i=0}^{d} u_i(t \mid X_\alpha)\, c_{\alpha+\epsilon_i}^{\ell-1}(t) && \text{if } \ell \in \{1, \ldots, m\}. \end{aligned} \tag{4.4}$$

Every c_α^ℓ is a d-variate polynomial of degree at most ℓ. Moreover, $c_{(0,\dots,0)}^m$ is called *B-patch*. All symmetric simplicial algorithms have their *associated multiaffine version* [DMS92], which, for each $\ell \in \{0,\dots,m\}$, for all $\alpha \in \Gamma_{m-\ell,d+1}$, and for any $t_1,\dots,t_m \in \mathbb{R}^d$, is defined as

$$\begin{aligned} C_\alpha^0() &:= a_\alpha && \text{if } \ell = 0, \\ C_\alpha^\ell(t_1,\dots,t_\ell) &:= \sum_{i=0}^{d} u_i(t_\ell \mid X_\alpha)\, C_{\alpha+\epsilon_i}^{\ell-1}(t_1,\dots,t_{\ell-1}) && \text{if } \ell \in \{1,\dots,m\}. \end{aligned}$$

Each C_α^ℓ is multiaffine and symmetric. Furthermore, it follows directly from the definition of the algorithm that

$$c_\alpha^\ell(t) = C_\alpha^\ell(t,\dots,t) \quad \text{for all } t \in \mathbb{R}^d,\ \ell \in \{0,\dots,m\},\ \alpha \in \Gamma_{m-\ell,d+1}.$$

Hence, C_α^ℓ is the uniquely defined polar form of the polynomial c_α^ℓ (see Theorem 2.18).

The given symmetric simplicial algorithm also has a dual correspondent, which, according to [DMS92], is given for all $t \in \mathbb{R}^d$ and $\alpha \in \Gamma_{\le m,d+1}$ by

$$W_\alpha(t) := \begin{cases} 1 & \text{if } |\alpha| = 0, \\ \sum_{i=0}^{d} u_i(t \mid X_{\alpha-\epsilon_i})\, W_{\alpha-\epsilon_i}(t) & \text{otherwise}, \end{cases}$$

so that, for all $\ell \in \{0,\dots,m\}$, one has

$$c_{(0,\dots,0)}^m(t) = \sum_{\alpha \in \Gamma_{m-\ell,d+1}} W_\alpha(t)\, c_\alpha^\ell(t).$$

If $\alpha_i = 0$ and, therefore, $\alpha - \epsilon_i \notin \Gamma_{\le m,d+1}$, we assume $u_i(\cdot \mid X_{\alpha-\epsilon_i})$ and $W_{\alpha-\epsilon_i}$ to be zero. The functions W_α are called *normalized B-weights* [DMS92].

As shown in [DMS92], the B-weights $\{W_\alpha \mid \alpha \in \Gamma_{m,d+1}\}$ are a basis of $\Pi_m(\mathbb{R}^d)$ as, on the one hand, one can show that they are linearly independent and, on the other hand, $|\Gamma_{m,d+1}| = \binom{m+d}{d} = \dim \Pi_m(\mathbb{R}^d)$. Moreover, the unique representation of a polynomial $p \in \Pi_m(\mathbb{R}^d)$ with polar form P is for all $t \in \mathbb{R}^d$ given by

$$p(t) = \sum_{\alpha \in \Gamma_{m,d+1}} P(x_{0,0},\dots,x_{0,\alpha_0-1},\dots,x_{d,0},\dots,x_{d,\alpha_d-1})\, W_\alpha(t), \tag{4.5}$$

which can be interpreted as a multivariate analogue of Marsden's identity (see Theorem 2.20). In the next subsection, we will see how one can relate these concepts to simplex splines.

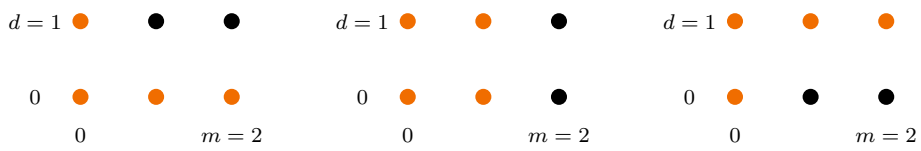

Fig. 4.5: Knot selection scheme for DMS-splines ($d = 1, m = 2$). The selected knots are depicted in *orange*. Based on Figure 23 in [Sei92a].

4.2.4 B-Weights and Simplex Splines

The setting for the simplicial algorithm in the previous subsection is quite similar to the one used in the combinatorial approach: In the simplicial algorithm, we used the knot set X containing the knots $x_{0,0}, \dots, x_{d,0}$, which, due to (4.3), are the vertices of a nondegenerate simplex. In the combinatorial approach, we had a knot with multiplicity $m+1$ at each vertex of a simplex. We pulled these $m+1$ knots apart to obtain simplex splines with maximum smoothness and, thus, had $m+1$ distinct knots at each vertex, which correspond to the knots $x_{i,0}, \dots, x_{i,m} \in X$ for each $i \in \{0, \dots, d\}$. Hence, X can be regarded as the knot set associated to one specific simplex of the triangulation $\mathcal{T}$ in the combinatorial approach.

The important relationship between B-weights and simplex splines has been discovered in [DMS92]: Let

$$\Omega := \left(\bigcap_{\alpha \in \Gamma_{\leq m, d+1}} \operatorname{conv}(X_\alpha) \right)^\circ .$$

If $\operatorname{vol}_d(\Omega) > 0$, the following identity holds true for all $\alpha \in \Gamma_{m,d+1}$:

$$W_\alpha(t) = m! \, |d(X_\alpha)| \, M(t \mid V_\alpha) \quad \text{for all } t \in \Omega,$$

where

$$V_\alpha := (x_{0,0}, \dots, x_{0,\alpha_0}, \dots, x_{d,0}, \dots, x_{d,\alpha_d}).$$

Hence, an equivalent of Formula (4.5), which only holds true on Ω and uses the collection $\{M(\cdot \mid V_\alpha) \mid \alpha \in \Gamma_{m,d+1}\}$ of simplex splines instead of B-weights, can be formulated easily. In particular, appropriately rescaled versions of these simplex splines,

$$M^{\mathrm{DMS}}(\cdot \mid V_\alpha) := m! \, |d(X_\alpha)| \, M(\cdot \mid V_\alpha) \quad \text{for all } \alpha \in \Gamma_{m,d+1},$$

constitute a partition of unity on Ω. Furthermore, the collection of simplex splines is locally linearly independent on Ω [DMS92].

The similarities between B-weights and the combinatorial approach raise the question of the differences between both concepts. According to [Nea01b, p. 366f],

it lies in the selection of the $\binom{m+d}{d}$ subsets of knots used to generate the simplex splines: The knot sets used for B-weights expose a symmetric structure, contrary to the nondecreasing paths in the combinatorial approach, as one can see when comparing Figures 4.3c and 4.5. In particular, the choice of knot sets for B-weights is independent of the numbering of the vertices of the simplex. This symmetry enables elegant identities for the representation of polynomials [Nea01b, p. 367].

For an example of a knot set X and the selection scheme in a bivariate setting, we refer to Figure 4.6.

4.2.5 Definition and Properties of DMS-Splines

In the previous subsection, we considered the relation between B-weights and simplex splines only on one simplex. However, since we aim at the construction of a spline space not only for one simplex but for a whole collection of adjacent simplices, we again assume $\mathcal{T}$ to be a triangulation of $\mathbb{R}^d$ with respect to a vertex set $Y \subseteq \mathbb{R}^d$ and assign a collection of knots consisting of $x_{y,0} := y$ and additional $x_{y,1}, \dots, x_{y,m} \in \mathbb{R}^d$ to every vertex $y \in Y$, yielding the knot set

$$X := \{x_{y,j} \mid y \in Y,\ 0 \le j \le m\},$$

which has the same structure as the projections of the pulled-apart knots in the combinatorial approach. For the remainder of the section, we consider each $T \in \mathcal{T}$ as $(d+1)$-tuple with arbitrarily ordered elements $T_0, \dots, T_d$. For all $T \in \mathcal{T}$, we define

$$\begin{aligned} X_{\alpha,T} &:= (x_{T_0,\alpha_0}, \dots, x_{T_d,\alpha_d}) && \text{for all } \alpha \in \Gamma_{\le m,d+1}, \\ V_{\alpha,T} &:= (x_{T_0,0}, \dots, x_{T_0,\alpha_0}, \dots, x_{T_d,0}, \dots, x_{T_d,\alpha_d}) && \text{for all } \alpha \in \Gamma_{\le m,d+1}, \\ \Omega_T &:= \left(\bigcap_{\alpha \in \Gamma_{\le m,d+1}} \operatorname{conv}(X_{\alpha,T}) \right)^\circ, \end{aligned}$$

as in the previous subsections. In order to ensure that the barycentric coordinates in the simplicial algorithms are well-defined, we again have to require that

$$\dim \operatorname{aff}(X_{\alpha,T}) = d \quad \text{for all } \alpha \in \Gamma_{\le m,d+1},\ T \in \mathcal{T}.$$

Furthermore, we assume that

$$\operatorname{vol}_d(\Omega_T) > 0 \quad \text{for all } T \in \mathcal{T}$$

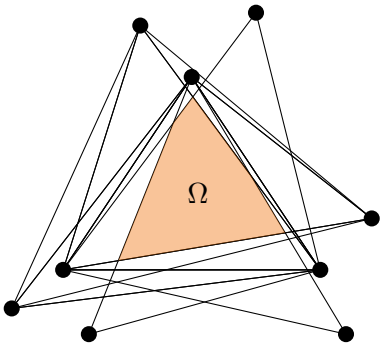

(a) The shaded region Ω *(orange)* refers to the intersection of convex hulls of collections of $d+1$ knots, on which the B-patch coincides with an appropriately normalized simplex spline. Based on Figure 2.2 in [DMS92].

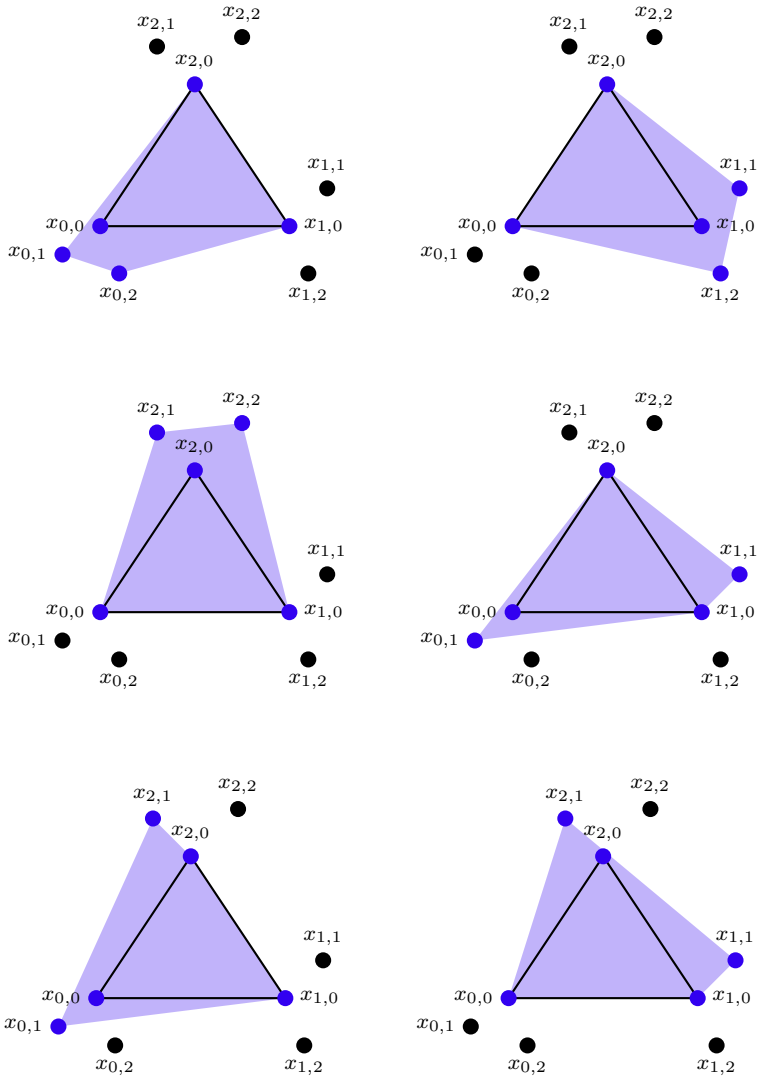

(b) The collections of knots chosen by the selection scheme for DMS-splines. The selected / active knots are depicted in *blue*, whereas the shaded regions refer to the support of the associated simplex splines. Based on Figure 11 in [Nea01b].

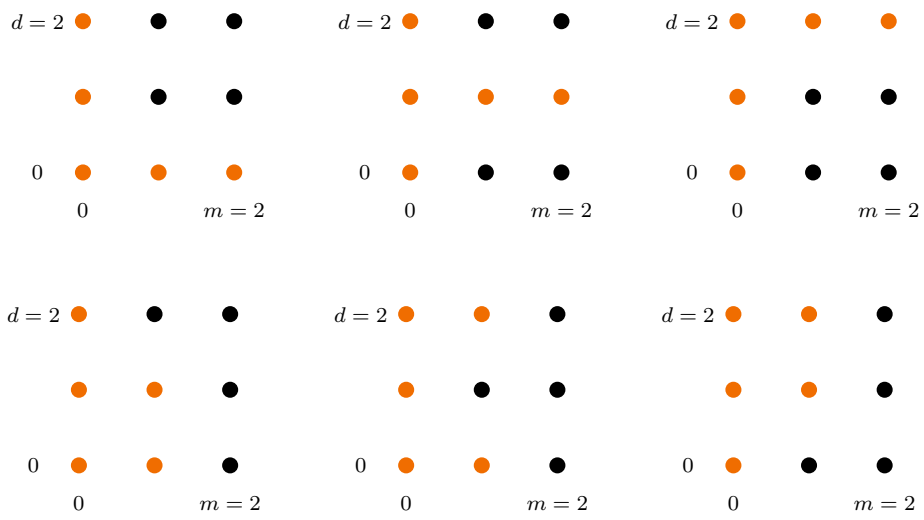

(c) The collections of knots chosen by the selection scheme for DMS-splines, illustrated in accordance with Figure 4.5. Based on Figure 23 in [Sei92a].

Fig. 4.6: Example of the knot selection scheme for DMS-splines ($d = 2$, $m = 2$). Each of the vertices of a d-dimensional simplex has $m + 1$ associated knots.

and define the space of DMS-Splines in accordance with [DMS92] as follows:

Definition 4.2 (DMS-splines)**.** With the stated prerequisites, the space of *DMS-splines* is defined as

$$\mathcal{S}^{\mathrm{DMS}}_{m,\mathcal{T},X} := \operatorname{span}\left\{ M^{\mathrm{DMS}}(\cdot \mid V_{\alpha,T}) \;\middle|\; \alpha \in \Gamma_{m,d+1},\ T \in \mathcal{T} \right\}.$$

◀

Although not explicitly mentioned in [DMS92], it is necessary to allow infinite linear combinations in the definition of DMS-splines since, otherwise, all DMS-spline functions would have compact support and, therefore, it would be impossible to describe nonzero polynomials. However, since $\mathcal{T}$ is a triangulation, each $t \in \mathbb{R}^d$ is in the support of only a finite set of basis functions, and thus, the function value is well-defined.

According to [DMS92], every element of $\mathcal{S}^{\mathrm{DMS}}_{m,\mathcal{T},X}$ associated with some collection of coefficients $(a_{\alpha,T})_{\alpha\in\Gamma_{m,d+1},T\in\mathcal{T}}$ can be reduced for all $t \in \Omega_T$, $T \in \mathcal{T}$, as follows:

$$\left(\sum_{T'\in\mathcal{T}} \sum_{\alpha\in\Gamma_{m,d+1}} a_{\alpha,T'} M^{\mathrm{DMS}}(\cdot \mid V_{\alpha,T'}) \right)(t) = \sum_{\alpha\in\Gamma_{m,d+1}} a_{\alpha,T} M^{\mathrm{DMS}}(t \mid V_{\alpha,T}).$$

Hence, DMS-splines can be evaluated efficiently on the sets Ω_T, $T \in \mathcal{T}$, by means of the recursive algorithms presented above. However, if the coefficients are chosen appropriately, a recursive evaluation is also available on the regions outside of the sets Ω_T, $T \in \mathcal{T}$, as ensured by the following lemma, which is also due to [DMS92]:

Lemma 4.3. Suppose that the set of coefficients $(a_{\alpha,T})_{\alpha \in \Gamma_{m,d+1}, T \in \mathcal{T}}$ satisfies the following property: For any two adjacent simplices corresponding to $T, T' \in \mathcal{T}$, so that the common $(d-1)$-dimensional face is

$$\begin{aligned} \operatorname{conv}(T) \cap \operatorname{conv}(T') &= \operatorname{conv}\Big(x_{T_0,0}, \dots, x_{T_{p-1},0}, x_{T_{p+1},0}, \dots, x_{T_d,0}\Big) \\ &= \operatorname{conv}\Big(x_{T'_0,0}, \dots, x_{T'_{q-1},0}, x_{T'_{q+1},0}, \dots, x_{T'_d,0}\Big) \end{aligned}$$

for appropriate $p, q \in \{0, \dots, d\}$ with $p \le q$, and for all $\alpha, \beta \in \Gamma_{m,d+1}$ such that

$$\begin{aligned} &\beta_i = \alpha_i && \text{for all } i \in \{0, \dots, p-1\} \cup \{q+1, \dots, d\}, \\ &\beta_i = \alpha_{i+1} && \text{for all } i \in \{p, \dots, q-1\}, \\ &\beta_q = \alpha_p = 0, \end{aligned}$$

one has $a_{\alpha,T} = a_{\beta,T'}$. Then, for all $t \in \mathbb{R}^d$, one has

$$\left(\sum_{T \in \mathcal{T}} \sum_{\alpha \in \Gamma_{m,d+1}} a_{\alpha,T} M^{\mathrm{DMS}}(\cdot \mid V_{\alpha,T}) \right)(t) = \sum_{T \in \mathcal{T}} \sum_{\alpha \in \Gamma_{m-1,d+1}} a^*_{\alpha,T}(t)\, M^{\mathrm{DMS}}(t \mid V_{\alpha,T}),$$

where

$$a^*_{\alpha,T}(t) := \sum_{i=0}^{d} u_i(t \mid X_{\alpha,T})\, a_{\alpha+\epsilon_i,T}, \qquad \text{for all } T \in \mathcal{T},\ \alpha \in \Gamma_{m-1,d+1}.$$

◀

Furthermore, it has been shown in [DMS92] that appropriate evaluations of the polar form associated to a polynomial satisfy the conditions of Lemma 4.3, yielding Marsden's identity for DMS-splines similar to (4.5):

Theorem 4.4. Let $\mathcal{T}$, Y, and X be defined as above. For all $p \in \Pi_m(\mathbb{R}^d)$ with polar form P, the following holds true for all $t \in \mathbb{R}^d$:

$$p(t) = \sum_{T \in \mathcal{T}} \sum_{\alpha \in \Gamma_{m,d+1}} P(x_{T_0,0}, \dots, x_{T_0,\alpha_0-1}, \dots, x_{T_d,0}, \dots, x_{T_d,\alpha_d-1})\, M^{\mathrm{DMS}}(t \mid V_{\alpha,T}).$$

◀

Hence, one has $\Pi_m \subseteq \mathcal{S}^{\mathrm{DMS}}_{m,\mathcal{T},X}$. For DMS-Splines, Seidel could prove (see [Sei92b] and [Sei92a, p. 275f]) that a similar identity even holds true for piecewise polynomials, whose univariate analogue we have recalled in Theorem 2.22:

Theorem 4.5. Let $\mathcal{T}$, Y, and X be defined as above, and choose $\ell \in \{0, \dots, m-1\}$. Let $f \in \mathcal{C}^\ell(\mathbb{R}^d)$ be a piecewise polynomial of degree at most m on the triangulation $\mathcal{T}$, i.e.,

$$f_T := f|_{\mathrm{conv}(T)} \in \Pi_m(\mathrm{conv}(T)) \quad \text{for all } T \in \mathcal{T},$$

and let F_T denote the polar form of f_T for every $T \in \mathcal{T}$. If all knots have a multiplicity of at least $m - \ell$, i.e.,

$$x_{y,0} = \cdots = x_{y,m-\ell-1} \quad \text{for all } y \in Y,$$

then one can represent f using DMS-splines for all $t \in \mathbb{R}^d$ as follows:

$$f(t) = \sum_{T \in \mathcal{T}} \sum_{\alpha \in \Gamma_{m,d+1}} a_{T,\alpha} M^{\mathrm{DMS}}(t \mid V_\alpha),$$

where $a_{T,\alpha} := F_T(x_{T_0,0}, \dots, x_{T_0,\alpha_0-1}, \dots, x_{T_d,0}, \dots, x_{T_d,\alpha_d-1})$. ◀

4.2.6 DMS-Splines and the Fundamental Problem

Despite the appealing properties and elegant formulas that have been presented in the previous subsection, DMS-splines according to [Nea01b] do not solve the Fundamental Problem formulated in Subsection 4.1.2. The same holds true for both the geometric and the combinatorial approach.

The geometric approach requires the triangulation of an $(m+d)$-dimensional set. The problems arising from this fact are twofold: Firstly, the triangulation procedure is computationally very expensive. Secondly, the resulting spline space depends on the chosen triangulation, which is undesirable and not necessarily gives the ordinary univariate splines when considering the case $d = 1$ [Nea01b, pp. 364, 368]. For an example of the discrepancy, we again refer to Figure 4.2.

Both the combinatorial approach and DMS-splines just require the triangulation of a d-dimensional set, which is mostly a feasible endeavor. However, they use clouds of knots at each vertex. On the one hand, it is not clear how to choose the auxiliary knots in the clouds reasonably. On the other hand, the resulting spline space also in this case depends on the specific choice of auxiliary knots [Nea01b, p. 368]. If the auxiliary knots are very close to the original vertex, the simplex splines tend

to be “nearly” discontinuous. On the contrary, if original and auxiliary knots are far apart, it will be hard to ensure that the sets Ω_T have positive volume for each $T \in \mathcal{T}$. Although these conditions have been relaxed in [Sau95], the freedom of choice inherent in these approaches is often an unwanted feature. In particular, they do not necessarily give rise to the common univariate spline space in the case $d = 1$. Whereas a clever selection of auxiliary knots in the combinatorial approach in fact yields the ordinary univariate splines, an equivalent selection scheme does not seem to be available for higher dimensions [Nea01b, p. 369]. Contrarily, the inherent symmetry of DMS-splines renders an appropriate choice of auxiliary knots impossible, except in the case where all auxiliary knots are placed directly at the vertex and, therefore, each knot has multiplicity $m + 1$ [Nea01b, p. 369].

In summary, one can conclude that none of the approaches presented in this section fulfills Requirement (H) of the Fundamental Problem [Nea01b, p. 369]. However, a method for the construction of a multivariate spline space satisfying this requirement by construction will be introduced in the next section.

4.3 Delaunay Configuration B-Splines

As the approaches presented in the previous section (in particular the well-known DMS-splines) do not solve the Fundamental Problem and have some further drawbacks, like the necessity of auxiliary knots, we look for another approach. A very promising proposal is due to Neamtu [Nea01a; Nea01b], which *by construction* reduces to the ordinary univariate splines when considered in one dimension. Before being able to introduce this approach, we first have to recall two basic and closely related concepts, namely Voronoi diagrams and Delaunay triangulations.

4.3.1 Voronoi Diagrams

In Subsection 4.1.1, the essential difference between univariate and multivariate spline spaces has emerged already: Whereas in one dimension, one can choose *consecutive* knots for the construction of B-splines, the concept of consecutivity is not generalizable to multiple dimensions as there is no natural ordering on the spaces $\mathbb{R}^d$ for $d \geq 2$.

However, one of the most appealing properties of univariate B-splines is their *locality*: They have a relatively small support. Hence, in order to obtain equivalent properties in higher dimensions, the knots chosen to construct a simplex spline should not

be too far apart. To be able to decide if a set of knots is "far apart", we need an appropriate notion of *neighborhood* in $\mathbb{R}^d$. One way to describe the neighborhood of a knot in $\mathbb{R}^d$ is the *Voronoi diagram*. The following definition is a higher-dimensional and extended variant of the one given in [AKL13, p. 7f]:

Definition 4.6 (Voronoi diagram)**.** Let $d \in \mathbb{N}_+$, and let $X \subseteq \mathbb{R}^d$ be a set of knots with $|X| \geq 2$ which is locally finite, i.e., $|X \cap \Omega| < \infty$ for all compact $\Omega \subseteq \mathbb{R}^d$.

(i) Let $x, x' \in X$ be distinct knots. The hyperplane

$$S(x, x') := \left\{ t \in \mathbb{R}^d \;\middle|\; \|t - x\| = \|t - x'\| \right\}$$

is called *bisector of x and x'*. The bisector separates $\mathbb{R}^d$ into two (closed) half spaces $H(x, x')$ and $H(x', x)$, where

$$H(x, x') := \left\{ t \in \mathbb{R}^d \;\middle|\; \|t - x\| \leq \|t - x'\| \right\}.$$

(ii) Let $x \in X$. The *Voronoi region of x (with respect to X)* is defined as the intersection of all half spaces generated by bisectors corresponding to x:

$$V_X(x) := \bigcap_{x' \in X \setminus \{x\}} H(x, x').$$

(iii) Let $x, x' \in X$ be distinct knots. The intersection $V_X(x) \cap V_X(x')$ of the corresponding Voronoi regions is called *Voronoi face* (or *Voronoi edge* in the case $d = 2$) if

$$\mathrm{vol}_{d-1}(V_X(x) \cap V_X(x')) \neq 0.$$

We call two knots *adjacent* if they share a Voronoi face. All adjacencies are summarized in the set

$$\mathcal{E}(X) := \left\{ \{x, x'\} \subseteq X \;\middle|\; x \neq x',\ \mathrm{vol}_{d-1}(V_X(x) \cap V_X(x')) \neq 0 \right\}.$$

(iv) The *Voronoi diagram of X* is defined as the union of all Voronoi faces corresponding to pairs of distinct, adjacent knots in X:

$$\mathcal{V}(X) := \bigcup_{\{x, x'\} \in \mathcal{E}(X)} (V_X(x) \cap V_X(x')).$$

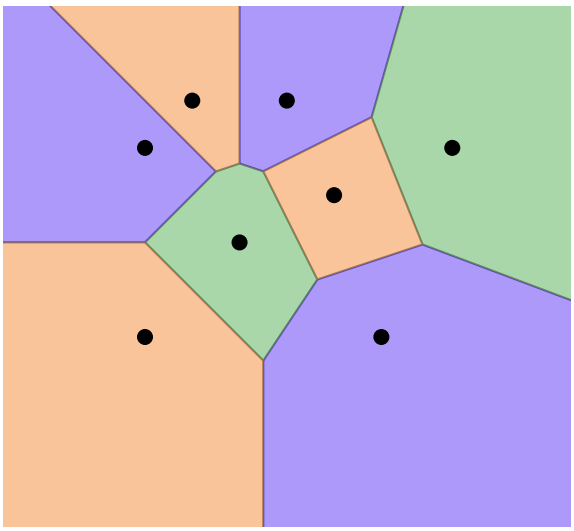

Fig. 4.7: Example of a Voronoi diagram of a given collection of knots ($d = 2$). Based on Figure 13 in [Nea01b].

An example of a Voronoi diagram is displayed in Figure 4.7. The bisector of two distinct knots $x, x' \in X$ is a hyperplane and separates the space into two half spaces: one consisting of the points closer to x than to x', and the other one containing the points closer to x' than to x. Hence, the Voronoi region $V_X(x)$ of x contains exactly the points that are closer to x than to any other knot of X.

The Voronoi region of x is a d-dimensional convex polyhedron [AKL13, p. 75], at least if X is finite. One can show that each vertex of a Voronoi region (called *Voronoi vertex*) has at least $d + 1$ incident Voronoi faces [AKL13, p. 9]. The number exceeds this minimum only if there are more than $d + 1$ knots with the same distance to the Voronoi vertex, which is the case if these vertices are cospherical, i.e., they lie on the same sphere.

Voronoi diagrams have many interesting properties. However, we refer the interested reader to [AKL13] and instead turn to Delaunay triangulations, which are closely related to Voronoi diagrams.

4.3.2 Delaunay Triangulations

When considering Delaunay triangulations, one has to exclude certain degenerate cases of the knot set $X \subseteq \mathbb{R}^d$, which refer to the *circumcircle* of subsets of knots.

Definition 4.7 (Circumcircle)**.** Let $d \in \mathbb{N}_+$, and choose $x_0, \dots, x_d \in \mathbb{R}^d$ such that $\dim \operatorname{aff}(x_0, \dots, x_d) = d$. The uniquely defined d-dimensional ball

$$B(x_0, \dots, x_d) := B_r(c), \quad r \in \mathbb{R}^+,\ c \in \mathbb{R}^d,$$

satisfying $x_0, \dots, x_d \in \partial B_r(c)$ is called *circumcircle (of $x_0, \dots, x_d$)*. As the order of the points does not matter, we write

$$B(A) := B(x_0, \dots, x_d)$$

for $A := \{x_0, \dots, x_d\}$. ◀

Definition 4.8 (General Delaunay position)**.** Let $d \in \mathbb{N}_+$ and $X \subseteq \mathbb{R}^d$ such that $|X| \geq d+1$. Then, X is said to be in *general Delaunay position* if, for all $A \subseteq X$ with $|A| = d+1$, the following two conditions hold true. Otherwise, X will be called *degenerate*.

(i) $\dim \operatorname{aff}(A) = d$,

(ii) $\partial B(A) \cap X = A$. ◀

Each knot set in general Delaunay position is clearly also in general position, according to Definition 3.18. The second condition ensures that no more than $d+1$ knots are cospherical, i.e., lie on the same sphere. Almost every locally finite knot set is in general Delaunay position, and thus, every locally finite degenerate knot set can be forced to be in general Delaunay position by applying an arbitrarily small perturbation to the concerned knots.

For a locally finite knot set in general Delaunay position, one can define the Delaunay triangulation as follows [AKL13, p. 12, p. 76]:

Definition 4.9 (Delaunay triangulation)**.** Let $d \in \mathbb{N}_+$, and let $X \subseteq \mathbb{R}^d$ be locally finite and in general Delaunay position. The set

$$\mathcal{K}(X) := \left\{ T \subseteq X \;\middle|\; |T| = d+1,\ B(T) \cap X = \emptyset \right\}$$

is called *Delaunay triangulation (of X)*. ◀

Theorem 4.10. Let $d \in \mathbb{N}_+$, and let $X \subseteq \mathbb{R}^d$ be in general Delaunay position and locally finite. Then, the Delaunay triangulation $\mathcal{K}(X)$ is a triangulation of $\operatorname{conv}(X)$. ◀

The Delaunay triangulation is named after Boris Delaunay, who introduced it and proved fundamental results [Del34].

The term *triangulation* is also used for the case $d > 2$, although in this case, the partitions are higher-dimensional simplices instead of triangles. If $d = 3$, one can also use the term *tetrahedrization* [AKL13, p. 76]. Each element of $\mathcal{K}(X)$ is called *Delaunay triangle* or *Delaunay simplex*. By definition, the circumcircle generated by the vertices of a Delaunay triangle does not contain any knots in its interior.

Note that, if the knots are not in general Delaunay position, the triangulation could contain "holes", so that some of the resulting partitions would not be simplices. Hence, the result would be no triangulation but only a tessellation in this case. The definition of Delaunay triangulations can also be generalized to knot sets which contain more than $d + 1$ cospherical knots and, therefore, are not in general Delaunay position. However, the "holes" in the triangulation have to be triangulated appropriately.

The Delaunay triangulation has many appealing properties. For example, if $d = 2$, it is the triangulation that maximizes the minimal angle of its triangles [AKL13, p. 42f]. Since triangles with small angles are long, thin, and hence, less desirable [Nea01a], the Delaunay triangulation in some sense yields optimally shaped triangles.

Furthermore, the Delaunay triangulation of a given knot set in $\mathbb{R}^2$ can be computed efficiently in $\mathcal{O}(n \log n)$ time complexity, where n denotes the number of knots [LS80] [PS85, p. 221]. However, the complexity can grow rapidly when increasing d since the expected runtime complexity of the flipping algorithm is in $\mathcal{O}\left(n \log n + n^{\lceil d/2 \rceil}\right)$ [ES96]. For more information regarding Delaunay triangulations, we again refer to [AKL13].

4.3.3 Duality Relations

The interesting relation between Voronoi diagrams and Delaunay triangulations can be seen in the following observation for the case $d = 2$ (see also [AKL13, p. 12]):

Let $X \subseteq \mathbb{R}^2$ be locally finite and in general Delaunay position. We consider both Voronoi diagram and Delaunay triangulation as undirected graphs: The graph of the Voronoi diagram is given by $G := (V, E)$, where V denotes the Voronoi vertices and E the pairs of Voronoi vertices sharing a Voronoi edge of $\mathcal{V}(X)$. The graph of the Delaunay triangulation $\mathcal{K}(X)$ is given by $G' := (X, E')$, where the set of Delaunay

Delaunay triangulation	Voronoi diagram
Knot in X	Voronoi region
Delaunay edge	Voronoi edge
Delaunay triangle	Voronoi vertex

Tab. 4.1: The bijective duality relations between components of Delaunay triangulations and Voronoi diagrams for $d = 2$ [AKL13, p. 12]

edges E' contains all pairs of distinct knots of X which are vertices of the same Delaunay triangle, i.e.,

$$E' := \bigcup_{\{x,y,z\} \in \mathcal{K}(X)} \Big\{ \{x, y\}, \{y, z\}, \{z, x\} \Big\}.$$

Then, the graphs G and G' are dual. Therefore, two knots are connected by a Delaunay edge if and only if the corresponding Voronoi regions are adjacent, i.e.,

$$\mathcal{E}(X) = E'.$$

The bijective duality relations between the components of the Delaunay triangulation and the Voronoi diagram can be seen in Table 4.1, in accordance with [AKL13, p. 12]. Each Voronoi vertex is exactly the center of the circumcircle of the corresponding Delaunay triangle, which is not necessarily in the interior of the triangle. The stated duality also holds true for $d > 2$ [AKL13, p. 76].

As noted earlier, the number of Voronoi regions incident to a Voronoi vertex equals the number of knots with equal, minimal distance to the vertex. Consequently, if there are more than $d + 1$ incident Voronoi regions, more than $d + 1$ knots lie on a sphere around the vertex. Thus, the knot set is not in general Delaunay position as it does not satisfy Requirement (ii) in Definition 4.8. However, there are knot sets whose Voronoi vertices all have $d + 1$ incident Voronoi regions and which, therefore, yield a valid Delaunay triangulation but which are not in general Delaunay position. As a consequence, the requirement on the knot set to be in general Delaunay position is sufficient but not necessary for the definition of a valid Delaunay triangulation [AKL13, p. 12].

Figure 4.8 shows a two-dimensional knot set with its Delaunay triangulation and the duality to the Voronoi diagram.

Since, according to the duality, two knots are vertices of the same Delaunay triangle if and only if the corresponding Voronoi regions are adjacent, the vertices of a

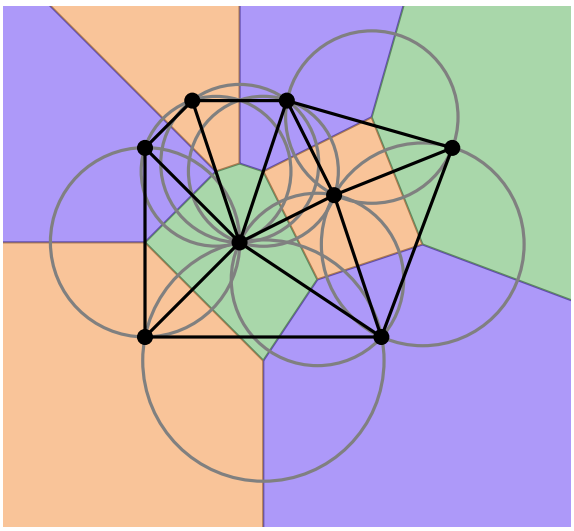

Fig. 4.8: Duality of Voronoi diagrams and Delaunay triangulations. The edges of Delaunay triangles *(black)* correspond to adjacent Voronoi regions. The circumcircles of Delaunay triangles *(gray)* do not contain any knot in its interior. Based on Figure 18 in [Nea01b].

Delaunay triangle are *neighbors* in some sense. Hence, the dual graph of the Voronoi diagram encodes proximity information of the knots. We will see that this notion of neighborhood can replace the concept of consecutivity in the construction of spline spaces. As encouragement, we consider the Delaunay triangulation for $d = 1$:

Remark 4.11. Let $n \in \mathbb{N}_+$, and let $x_0, \dots, x_n \in \mathbb{R}$ be an increasing sequence of knots. As a ball in $d = 1$ is just an interval, the circumcircle $B(x_i, x_j)$ of two knots x_i and x_j is the interval (x_i, x_j) for all $i, j \in \{0, \dots, n\}$ with $i < j$. That interval does not contain any of the knots $x_0, \dots, x_d$ if and only if $j = i + 1$. Hence, the Delaunay triangulation of $x_0, \dots, x_n$ is given by

$$\mathcal{K}(\{x_0, \dots, x_n\}) = \Big\{ \{x_{i-1}, x_i\} \;\Big|\; i \in \{1, \dots, n\} \Big\}.$$

Note that the intervals $[x_{i-1}, x_i]$, $i \in \{1, \dots, n\}$, of consecutive knots are exactly the supports of the B-splines of degree zero with respect to the knots $x_0, \dots, x_n$. ◀

This remark motivates the following consideration of a spline space of degree zero. A Delaunay triangle (or simplex) consists of $d + 1$ affinely independent knots, which can be used to generate a d-variate simplex spline of degree zero. We renormalize the simplex splines as follows: For any affinely independent knots $x_0, \dots, x_d \in \mathbb{R}^d$, let

$$\widetilde{M}(\cdot \mid x_0, \dots, x_d) := d! \operatorname{vol}_d(\operatorname{conv}(x_0, \dots, x_d))\, M(\cdot \mid x_0, \dots, x_d),$$

so that, for all $t \in \mathbb{R}^d$, one has

$$\widetilde{M}(t \mid x_0, \ldots, x_d) = \begin{cases} 1 & \text{if } t \in \operatorname{conv}(x_0, \ldots, x_d), \\ 0 & \text{otherwise.} \end{cases}$$

Let $X \subseteq \mathbb{R}^d$ be locally finite and in general Delaunay position, and let

$$A := \bigcup_{T \in \mathcal{K}(X)} \operatorname{conv}(T)^\circ.$$

Since the Delaunay triangulation is a tessellation, it follows that the renormalized simplex splines generated by the Delaunay simplices form a partition of unity on A, i.e.,

$$\sum_{T \in \mathcal{K}(X)} \widetilde{M}(t \mid T) = 1 \quad \text{for all } t \in A.$$

As $\operatorname{conv}(X) \backslash A$ contains only the faces of Delaunay simplices, which comprise the discontinuous regions of the corresponding simplex splines, and is a set of measure zero, the latter identity holds true almost everywhere [Nea01a]. Hence,

$$\operatorname{span}\Big\{ \widetilde{M}(\cdot \mid T) \;\Big|\; T \in \mathcal{K}(X) \Big\}$$

is almost everywhere in $\operatorname{conv}(X)$ a space of piecewise polynomials of degree zero which contains all polynomials of degree zero (i.e., constant functions) restricted to $\operatorname{conv}(X) \cap A$ and has a basis of compactly supported and linearly independent functions. Furthermore, it reduces to the common univariate splines for $d = 1$, according to Remark 4.11, and, therefore, is a promising starting point for a general solution of the Fundamental Problem. To extend these results to the whole set $\operatorname{conv}(X)$, a more sophisticated definition of simplex splines of degree zero would be necessary.

4.3.4 Higher-Order Voronoi Diagrams

In the previous subsection, we have seen means of defining a spline space of degree zero in arbitrary dimensions, which reduces to the univariate splines for $d = 1$. We are going to investigate now if this construction can be generalized to arbitrary degrees.

In [SH75], Shamos and Hoey introduced higher-order Voronoi diagrams as a generalization of the usual Voronoi diagrams. They are based on the fact that a Voronoi region corresponding to a given knot contains the points closest to that knot. A

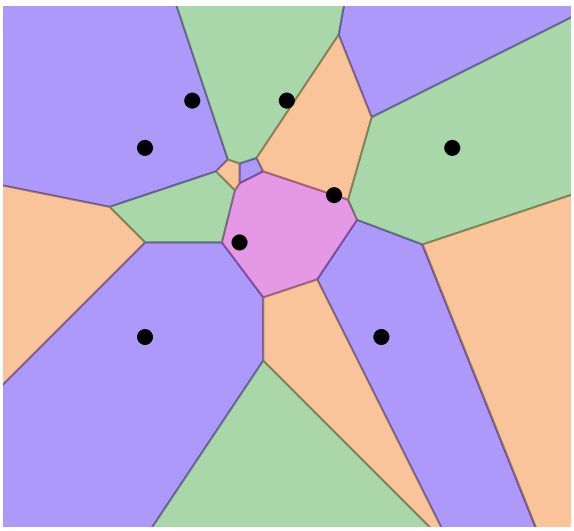

Fig. 4.9: Example of a Voronoi diagram of order two with respect to the given collection of knots. Based on Figure 14 in [Nea01b].

Voronoi region of a Voronoi diagram of order k, $k \in \mathbb{N}_+$, contains exactly the points which are closer to each knot of a given collection of k knots than to any other knot. This can be formalized as follows [Nea01b, p. 372]:

Definition 4.12 (Higher-order Voronoi diagram)**.** Let $d \in \mathbb{N}_+$, $k \in \mathbb{N}_+$, and choose a locally finite $X \subseteq \mathbb{R}^d$ with $|X| \geq k$. For all $Y \subseteq X$ with $|Y| = k$, the *Voronoi region of Y (with respect to X)* is the set of points

$$V_X(Y) := \left\{ t \in \mathbb{R}^d \;\middle|\; \max_{y \in Y} \|y - t\| = \inf_{\substack{Y' \subseteq X \\ |Y'| = k}} \max_{y' \in Y'} \|y' - t\| \right\},$$

which is closer to all knots in Y than to any other knot in X. The terms *adjacency* and *Voronoi diagram* are defined precisely as in Definition 4.6. ◀

Figure 4.9 depicts a Voronoi diagram of order two. Clearly, a Voronoi diagram of order one is the usual Voronoi diagram. It is easy to see that many Voronoi regions may be empty [Nea01b, p. 372]. However, knot sets corresponding to nonempty Voronoi regions are in some sense close to each other. This leads to the following consideration, which is due to Sabin [Sab89] (see also [Nea01b, p. 373f]):

Let $m \in \mathbb{N}_0$, and consider Voronoi diagrams of order $m+d+1$. Each set of $m+d+1$ knots gives rise to a d-variate simplex spline of degree m. When considering only simplex splines generated by knot sets corresponding to nonempty Voronoi

regions, all basis candidate functions are generated by knots close to each other and, therefore, have reasonably small support. However, it turns out that the resulting basis candidate functions are linearly dependent and, thus, do not yield a spline space solving the Fundamental Problem [Nea01b].

Therefore, we will consider another approach using higher-order analogues of Delaunay triangles, which are again closely related to higher-order Voronoi diagrams, in the next subsection.

4.3.5 Delaunay Configurations

When recalling the Delaunay triangulation, we defined it to be the unique triangulation with the property that the circumcircle of each triangle contains not a single knot of the given knot set in its interior. Similar to the higher-order analogue of Voronoi diagrams, this definition can be modified by requiring that each circumcircle has to contain exactly m knots, where $m \in \mathbb{N}_0$. This leads to the definition of *Delaunay configurations*, which is due to Neamtu [Nea01a; Nea01b] and is depicted in Figure 4.10.

Definition 4.13 (Delaunay configuration)**.** Let $d \in \mathbb{N}_+$, $m \in \mathbb{N}_0$, and let $X \subseteq \mathbb{R}^d$ be in general Delaunay position. An *(oriented Delaunay) configuration of degree* m is a tuple $K := (P, I)$ with

$$P, I \subseteq X, \quad |P| = d + 1, \quad |I| = m$$

and

$$\partial B(P) \cap X = P, \quad B(P) \cap X = I.$$

$\mathfrak{B}(K) := P$ is called the *boundary* of K, whereas $\mathfrak{I}(K) := I$ denotes the *interior* of K. The union $\mathfrak{U}(K) := P \cup I$ is the corresponding *unoriented Delaunay configuration*. The *circumcircle* of K is given as $B(P)$. $\mathcal{K}_m(X)$ denotes the set of all Delaunay configurations of degree m with respect to the knot set X. ◀

Examples of Delaunay configurations can be seen in Figure 4.11. If $m = 0$, a Delaunay configuration does not contain any interior knot and, thus, is just a Delaunay triangle. Note that the Delaunay configurations do not constitute a triangulation of the knots anymore if $m > 0$ [Nea01b, p. 378]. However, this does not pose a problem as we are only interested in finding suitable subsets of knots for the construction of a spline basis.

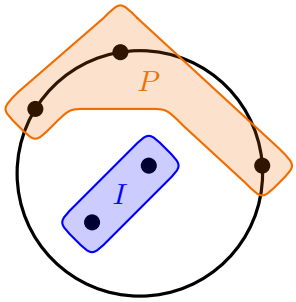

Fig. 4.10: Example of a Delaunay configuration of degree two. The ball generated by the $d+1$ boundary knots in P *(orange)* contains exactly the m knots of I in its interior *(blue)*. Based on Figure 21 in [Nea01b].

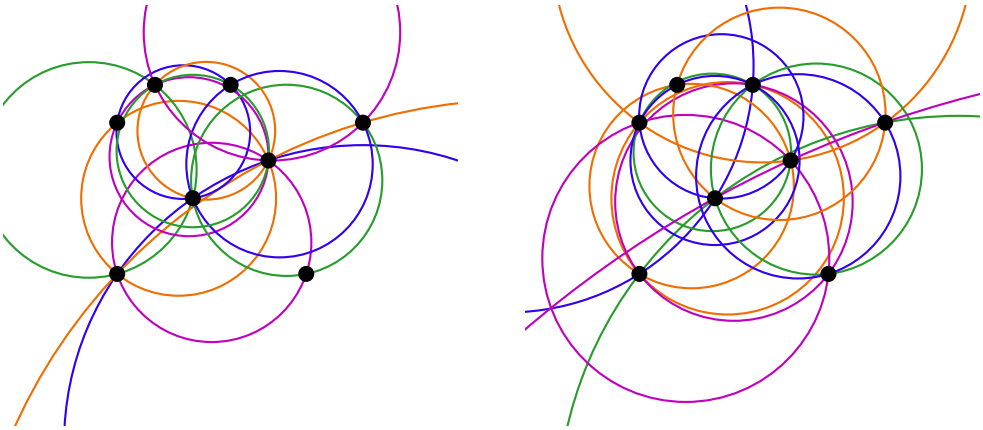

(a) Delaunay configurations of degree one

(b) Delaunay configurations of degree two

Fig. 4.11: All Delaunay configurations of degrees one and two with respect to the given knots

The relation between Delaunay configurations and higher-order Voronoi diagrams is pointed out in [Nea01b, p. 376f] for the case $d = 2$, $m = 1$ and Voronoi diagrams of order two: There are two types of Voronoi vertices, where the type depends on the knot sets assigned to the surrounding Voronoi regions. If each knot in one of these knot sets is also contained in another knot set associated to one of the Voronoi regions surrounding the Voronoi vertex, there are only three knots involved in total. On the contrary, if all three regions have the same knot in common, whereas the other knot of each region is not assigned to any of the other regions, the number of involved knots is four. The latter type of Voronoi vertex corresponds to a Delaunay configuration of degree one, where the interior knot is the one shared by all three Voronoi regions. For more details, we refer to [Nea01b, p. 376f]. A description of the relation for more general cases has not been given so far to the best of our knowledge.

By definition, a Delaunay configuration of degree m has $d+1$ knots on the boundary and exactly m knots in its interior. The union (i.e., the corresponding unoriented configuration) is a set of $d+m+1$ knots, which is exactly the number required for the construction of a d-variate simplex spline of degree m. Moreover, since Delaunay configurations of degree zero are just Delaunay triangles, one can use the reasoning in Subsection 4.3.3 to conclude that, in this special case, the Delaunay configurations give rise to a spline space containing constant functions supported on $\mathrm{conv}(X)$.

Neamtu proved in [Nea07] that this observation holds true for arbitrary degrees $m \in \mathbb{N}_0$ of Delaunay configurations and corresponding polynomial degrees. However, a renormalization of the simplex splines is necessary again, which motivates the following definition. It stems from [Nea01b] and has been adapted to our differently normalized original simplex splines:

Definition 4.14 (Normalized simplex spline)**.** Let $d \in \mathbb{N}_+$, $m \in \mathbb{N}_0$, and let $X \subseteq \mathbb{R}^d$ be in general Delaunay position. The *normalized simplex spline* with respect to a Delaunay configuration $K \in \mathcal{K}_m(X)$ is defined as

$$N(\cdot \mid K) := d!\, m!\, \mathrm{vol}_d(\mathrm{conv}(\mathfrak{B}(K)))\, M(\cdot \mid \mathfrak{U}(K)).$$

◀

Note that the normalization is chosen such that the normalized simplex splines of degree zero again form a partition of unity (everywhere on $\mathrm{conv}(X)$ except for the discontinuous boundaries), as it has been the case in Subsection 4.3.3.

Since a simplex spline M generated by a Delaunay configuration is defined with respect to the *unoriented* Delaunay configuration, the *role* of knots in the Delaunay configuration, i.e., whether it is an interior or a boundary knot, has no influence on the simplex spline. For normalized simplex splines, however, the normalization factor depends on the role of the knots.

To avoid boundary cases, Neamtu assumed X to cover the whole space, i.e., $\mathrm{conv}(X) = \mathbb{R}^d$, and to be locally finite, which are exactly the assumptions on the knot set in the Fundamental Problem (see Subsection 4.1.2). We summarize these assumptions in the following definition, as a reference for the remainder of the thesis.

Definition 4.15 (Strong conditions)**.** For $d \in \mathbb{N}_+$, a knot set $X \subseteq \mathbb{R}^d$ satisfies the *strong conditions* if

(i) X is locally finite, i.e., $|X \cap \Omega| < \infty$ for any compact $\Omega \subseteq \mathbb{R}^d$,

(ii) X is in general Delaunay position, as specified by Definition 4.8, and

(iii) X covers the whole $\mathbb{R}^d$, i.e., $\operatorname{conv}(X) = \mathbb{R}^d$. ◀

However, some of the results in this thesis are valid also for the following, more general class of knot sets:

Definition 4.16 (Weak conditions)**.** For $d \in \mathbb{N}_+$, a knot set $X \subseteq \mathbb{R}^d$ satisfies the *weak conditions* if

(i) X is nonempty and locally finite, i.e., $|X \cap \Omega| < \infty$ for any compact $\Omega \subseteq \mathbb{R}^d$, and

(ii) X is in general Delaunay position, as specified by Definition 4.8. ◀

For knot sets satisfying the strong conditions, we can now formulate Neamtu's theorem [Nea01b; Nea07]:

Theorem 4.17 (Neamtu)**.** Let $d \in \mathbb{N}_+$, $m \in \mathbb{N}_0$, and let $X \subseteq \mathbb{R}^d$ be a knot set satisfying the strong conditions. Let $p \in \Pi_m(\mathbb{R}^d)$ and P be its uniquely defined polar form. Then, the following identity holds true:

$$p(t) = \sum_{K \in \mathcal{K}_m(X)} P(\mathfrak{I}(K))\, N(t \mid K) \quad \text{for almost every } t \in \mathbb{R}^d. \tag{4.6}$$

In particular, if $m \geq 1$, one has

$$\Pi_m(\mathbb{R}^d) \subseteq \left\{ \sum_{K \in \mathcal{K}_m(X)} a_K\, N(\cdot \mid K) \;\middle|\; a_K \in \mathbb{R},\ K \in \mathcal{K}_m(X) \right\}.$$

◀

For $m = 0$, it would be necessary to exclude the edges of the Delaunay triangles (see Subsection 4.3.3) in order for the latter subset relation to hold true. For $m \geq 1$, Identity (4.6) holds pointwise [Nea07].

This result, which can be considered as an equivalent of Marsden's identity known from univariate splines (see Theorem 2.20), has been stated in [Nea01b] and proved

in [Nea07]. For $m = 0$, the result follows with the reasoning in Subsection 4.3.3. For $m \geq 1$, the proof is based on the recursive application of the identity

$$\sum_{K \in \mathcal{K}_m(X)} P(\mathfrak{I}(K))\, N(t \mid K) \quad = \sum_{K' \in \mathcal{K}_{m-1}(X)} P(\mathfrak{I}(K'), t)\, N(t \mid K'),$$

which in turn can be established for almost every $t \in \mathbb{R}^d$ using the following observation: When applying Micchelli's recursion formula (see Proposition 3.24) to the left-hand side and the multiaffinity of P to the right-hand side, some terms cancel out due to combinatorial properties of Delaunay configurations, and the remaining terms have a corresponding summand on the other side. We refer to [Nea07] for the complete proof.

Note that the polar form P is symmetric and, therefore, does not depend on the order of its arguments. Hence, using the *set* $\mathfrak{I}(K)$ as m-fold argument is a handy shorthand notation.

Corollary 4.18 (Partition of unity)**.** Let $d \in \mathbb{N}_+$, $m \in \mathbb{N}_0$, and let $X \subseteq \mathbb{R}^d$ satisfy the strong conditions. Then,

$$\sum_{K \in \mathcal{K}_m(X)} N(t \mid K) = 1 \quad \text{for almost every } t \in \mathbb{R}^d.$$

◀

The previous corollary follows directly from applying Identity (4.6) to the polynomial of degree zero that has value one. However, in the case $m = 0$, the identity again holds true only *almost everywhere*, as long as we have no consistent definition of simplex splines of degree zero on the (discontinuous) boundary.

Theorem 4.17 provides an *explicit* representation of polynomials of degree up to m by means of simplex splines associated with Delaunay configurations of degree m. Therefore, the generated spline space fulfills Requirement (C) of the Fundamental Problem.

When recalling univariate splines and DMS-splines, we encountered a more versatile variant of Marsden's identity in Theorem 2.22 and Theorem 4.5, which provides an explicit representation of all *piecewise* polynomials (with respect to the given knot sequence or the underlying triangulation) by means of B-splines and DMS-splines, respectively. Neamtu states in [Nea01b, p. 382] that a similar identity also holds true for the splines based on Delaunay configurations when reproducing piecewise polynomials with respect to the Delaunay triangulation:

Theorem 4.19. Let $d \in \mathbb{N}_+$, $m \in \mathbb{N}_0$, and let $X \subseteq \mathbb{R}^d$ satisfy the strong conditions. Let $f \in \mathcal{C}^{m-1}\left(\mathbb{R}^d\right)$ such that

$$f_T := f|_{\mathrm{conv}(T)} \in \Pi_m(\mathrm{conv}(T)) \quad \text{for all } T \in \mathcal{K}(X),$$

and let F_T be the polar form associated with f_T. Then,

$$f(\cdot) = \sum_{K \in \mathcal{K}_m(X)} F_{T(K)}(\mathfrak{I}(K))\, N(\cdot \mid K),$$

where $T(K)$ denotes *any* Delaunay triangle in the support of $N(\cdot \mid K)$. ◀

However, a proof of this theorem has not been given in [Nea01b]. Instead, there is a reference to a publication *"in preparation"*. A paper with the stated title was published some years later [Nea07], but it only deals with the proof of Theorem 4.17 and does not contain any information regardig this generalized formula. Despite the considerable time gone by since the original publication of [Nea01b], a proof of Theorem 4.19 has not been given so far in literature to the best of our knowledge.

4.3.6 Elimination of Duplicates

It would be a very appealing property of the Delaunay configuration construction if we could use the simplex splines generated by Delaunay configurations as a basis. However, this is not possible since there are linearly dependent functions, which result from Delaunay configurations that are the same when considered as unoriented Delaunay configurations but differ when taking the roles of the different knots into account, i.e., whether a knot is a boundary knot or an interior knot. Figure 4.12 displays the example presented in [Nea01b, p. 381] of two configurations of degree one, K and K', satisfying

$$\mathfrak{U}(K) = \mathfrak{U}(K'), \quad \mathfrak{B}(K) \neq \mathfrak{B}(K'), \quad \mathfrak{I}(K) \neq \mathfrak{I}(K').$$

Since unnormalized simplex splines do not respect the roles of the knots, normalized simplex splines associated with Delaunay configurations yielding the same *unoriented* configuration only differ by a constant factor and, hence, are clearly linearly dependent.

In [Nea01b, p. 381f], Neamtu proposes two different remedies to overcome this problem. The most straightforward way is to identify all configurations that are the same when considered as unoriented configurations using an equivalence relation $\sim$.

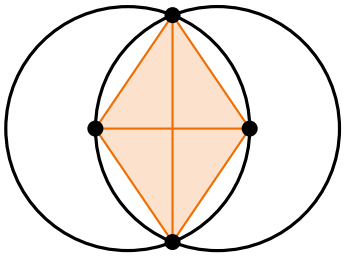

Fig. 4.12: Example of two different Delaunay configurations of degree one, which coincide when considered as unoriented configuration. Based on Figure 23 in [Nea01b].

The associated simplex splines only differ by a constant factor, which is why one representative of each equivalence class suffices. Hence, we define the corresponding splines space as follows:

Definition 4.20 (Nonpooled Delaunay configuration B-splines)**.** Let $d \in \mathbb{N}_+$, $m \in \mathbb{N}_0$, and let $X \subseteq \mathbb{R}^d$ satisfy the weak conditions. Define

$$\sim := \Big\{(K, K') \in \mathcal{K}_m(X) \times \mathcal{K}_m(X) \;\Big|\; \mathfrak{U}(K) = \mathfrak{U}(K')\Big\},$$

and let $\mathcal{R}$ be an arbitrary system of representatives of $\mathcal{K}_m(K)/\sim$. Define the space of *nonpooled Delaunay configuration B-splines (DCB-splines)* $\mathcal{S}_{m,X}$ as follows:

$$\mathcal{S}_{m,X} := \left\{ \sum_{R \in \mathcal{R}} a_R N(\cdot \mid R) \;\middle|\; a_R \in \mathbb{R},\ R \in \mathcal{R} \right\}.$$

The normalized basis candidate functions are given as

$$\mathcal{B}_{m,X} := \left\{ \left(d!\, m! \sum_{R' \in [R]_\sim} \mathrm{vol}_d(\mathrm{conv}(\mathfrak{B}(R'))) \right) M(\cdot \mid \mathfrak{U}(R)) \;\middle|\; R \in \mathcal{R} \right\}.$$

◀

As it is not yet clear if the functions in $\mathcal{B}_{m,X}$ are linearly independent, we will use the term *basis candidate function* instead of *basis function*. Note that, when using Theorem 4.17 on this spline space, the normalization factors from Definition 4.14 have to be summed up for identified simplex splines in order to maintain the validity. To that end, we formulated the normalized basis candidate functions explicitly in the previous definition.

The second possibility, which is also due to Neamtu [Nea01b], is motivated by a closer look on Theorem 4.17: Due to the arguments of the polar form in each summand, the coefficients only depend on the *interior* knots of the configurations. Therefore, configurations with the same collection of interior knots always have the same coefficient when representing a specific polynomial. This undesirable redundance can be avoided by identifying all configurations with the same set of interior knots via an equivalence relation

$$\simeq := \Big\{(K, K') \in \mathcal{K}_m(X) \times \mathcal{K}_m(X) \;\Big|\; \mathfrak{I}(K) = \mathfrak{I}(K')\Big\}.$$

In this case, however, the identified simplex splines are essentially different (i.e., not equal up to normalization). Hence, the corresponding simplex splines have to be summed up in order to maintain the validity of Theorem 4.17. Formally, we define the corresponding spline space as follows [Nea01b]:

Definition 4.21 (Pooled Delaunay configuration B-splines)**.** Let $d \in \mathbb{N}_+$, $m \in \mathbb{N}_0$, and let $X \subseteq \mathbb{R}^d$ satisfy the weak conditions. Let $\mathcal{I}_m(X) := \{\mathfrak{I}(K) \mid K \in \mathcal{K}_m(X)\}$ denote the set of all occurring collections of interior knots. Then, for each $I \in \mathcal{I}_m(X)$, one can define the set of Delaunay configurations identified with I as

$$\mathcal{K}_{I,m}(X) := \Big\{K \in \mathcal{K}_m(X) \;\Big|\; \mathfrak{I}(K) = I\Big\}.$$

The space of *pooled Delaunay configuration B-splines (pooled DCB-splines)* $\mathcal{S}'_{m,X}$ can be defined as follows:

$$\mathcal{S}'_{m,X} := \left\{ \sum_{I \in \mathcal{I}_m(X)} a_I \left(\sum_{K \in \mathcal{K}_{I,m}(X)} N(\cdot \mid K) \right) \;\middle|\; a_I \in \mathbb{R},\ I \in \mathcal{I}_m(X) \right\}.$$

In this case, the basis candidate functions are given as

$$\mathcal{B}'_{m,X} := \left\{ \sum_{K \in \mathcal{K}_{I,m}(X)} N(\cdot \mid K) \;\middle|\; I \in \mathcal{I}_m(X) \right\}.$$

◀

An example for the pooling of Delaunay configurations according to $\simeq$ and the resulting linear combination of simplex splines is presented in Figure 4.13. Note that the above definition is not reasonable in the case $m = 0$ as, in this case, the Delaunay configurations have no interior knots and, thus, have the same collection of interior knots. Hence, the spline space would only contain the constant one-function (when ignoring the inadequate definition of simplex splines at the discontinuities).

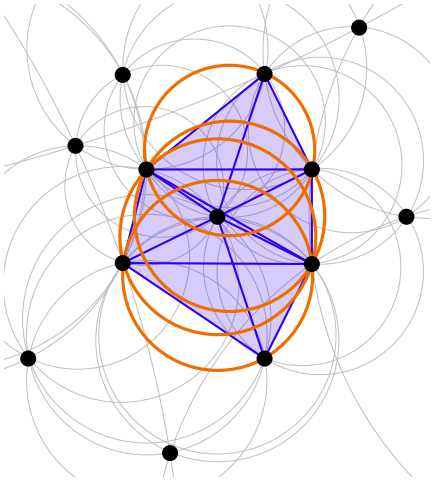

(a) Four configurations *(orange)* have the same interior knot and, thus, are identified. The shaded region *(blue)* refers to the support of the corresponding sum of normalized simplex splines.

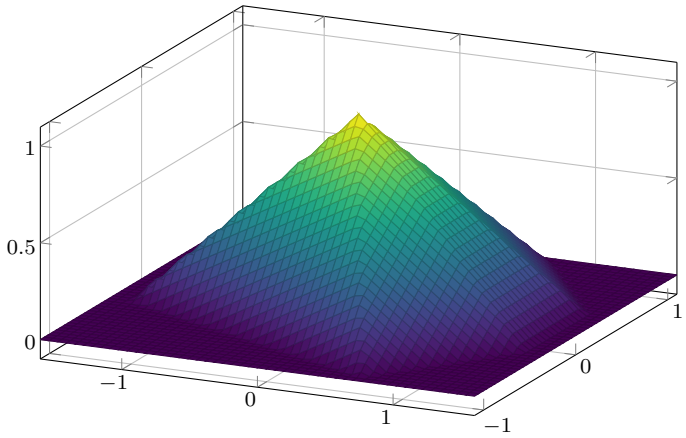

(b) The sum of the normalized simplex splines generated by the four pooled Delaunay configurations

Fig. 4.13: Example of the pooling of Delaunay configurations for $d = 2$, $m = 1$. The additional knots have been added in order to avoid that the pooling is incomplete due to an inadequate knot set.

Although this issue is not addressed in [Nea01b], a more reasonable convention would be to consider all Delaunay configurations as different with respect to $\simeq$ for $m = 0$. In particular, one has $\mathcal{S}_{0,X} = \mathcal{S}'_{0,X}$ with this interpretation.

The nonpooled DCB-splines are exactly as comprehensive as the span of all simplex splines associated with Delaunay configurations of the given degree since $\sim$ only identifies functions that are equal to each other up to a constant factor. On the contrary, the relation $\simeq$ pools different simplex splines, which is why the pooled

DCB-splines are more restrictive and, therefore, are less ample than nonpooled DCB-splines [Nea01b, p. 382].

The term *DCB-splines* has been introduced in [Cao+09] and, since then, has been used in a couple of publications [Cao+12; Zha+17; Cao+19], which is why we also use it here. However, no distinction has been made between the pooled and the nonpooled variant. For example, [Cao+09] and [Cao+12] use the nonpooled variant, whereas [Zha+17] employs pooled basis candidate functions. For the results in this thesis, we will state explicitly which spline space is considered.

For the linear combinations of simplex splines employed as basis candidate functions in the space of pooled DCB-splines, the term *multivariate B-spline* is established in [Nea01b]. However, we will refrain from using this term in the context of multivariate basis candidate functions since it is used frequently in literature whenever an approach seems to provide an appealing spline space similar to univariate B-splines and since little is known about the nature of the occurring linear combinations of simplex splines, although they reduce to the usual univariate B-splines when considered in one dimension as no pooling happens in that case. In order to avoid confusions, we will stick to the term *pooled simplex spline* or *pooled basis candidate function*.

4.3.7 DCB-Splines and the Fundamental Problem

The overall goal of this chapter is the definition of a multivariate spline space that is a solution to the Fundamental Problem (see Subsection 4.1.2). According to Neamtu [Nea01b, p 381ff], both nonpooled and pooled DCB-splines provide such a solution. We recall the specific requirements. To that end, let $d \in \mathbb{N}_+$, $m \in \mathbb{N}_0$, and let $X \subseteq \mathbb{R}^d$ be a knot set satisfying the strong conditions.

(A) Each simplex spline associated with a Delaunay configuration is a piecewise polynomial of degree m on each region bounded but not intersected by convex hulls of subsets of d different knots. Since each spline is a (possibly infinite) linear combination of such simplex splines, both nonpooled and pooled DCB-splines satisfy Requirement (A) of the Fundamental Problem. The set A in the formulation of this requirement can be specified as follows:

$$A = \bigcup_{K \in \mathcal{K}_m(X)} \bigcup_{\substack{L \subseteq \mathfrak{U}(K) \\ |L| = d}} \operatorname{conv}(L).$$

(B) We assume X to be in general Delaunay position and, therefore, also in general position, as specified by Definition 3.18. Hence, all simplex splines defined with respect to $m+d+1$ knots of X are $(m-1)$-times continuously differentiable. In particular, this holds true for simplex splines associated with Delaunay configurations and, thus, also for arbitrary linear combinations of such simplex splines. Hence, both spline spaces satisfy Requirement (B):

$$\mathcal{S}_{m,X} \subseteq \mathcal{C}^{m-1}(\mathbb{R}^d), \quad \mathcal{S}'_{m,X} \subseteq \mathcal{C}^{m-1}(\mathbb{R}^d).$$

(C) Theorem 4.19 ensures that the (possibly infinite) span of all simplex splines generated by Delaunay configurations of degree m contains all polynomials of degree up to m. By construction, this also holds true for both spline spaces, i.e.,

$$\Pi_m(\mathbb{R}^d) \subseteq \mathcal{S}_{m,X}, \quad \Pi_m(\mathbb{R}^d) \subseteq \mathcal{S}'_{m,X},$$

which ensures Requirement (C).

(D) It has been claimed that Requirement (D), which states that the spline space should be locally finite-dimensional, follows from *"the local nature of Delaunay configurations"* [Nea01b, p. 381]. The provided reference [Nea07] (*"in preparation"* at that time and published some years later), however, concentrates on the proof of Theorem 4.17 and contains no explicit results on this topic. Hence, a proof of that property has not been given so far to the best of our knowledge. We will deal with this issue in detail in Chapter 5.

(E) Requirement (E) states that, at each point, all but a finite set of basis candidate functions should vanish. This is closely related to the previous requirement and will also be dealt with in Chapter 5. Note that, for $m = 0$, this property directly follows from the fact that the Delaunay triangulation tessellates $\mathbb{R}^d$.

(F) Since each simplex spline is supported on the convex hull of its defining knots, each nonpooled basis candidate function has compact support. For pooled basis candidate functions, however, it could be possible that an infinite number of simplex splines is pooled, possibly yielding an unbounded support. For knot sets satisfying the strong conditions, we will see in Corollary 5.30 that the pooling involves only a finite number of simplex splines, though. Under this premise, also pooled basis candidate functions feature a compact support. Furthermore, it follows by construction of $\mathcal{S}_{m,X}$ and $\mathcal{S}'_{m,X}$, respectively, that each spline can be represented as (possibly infinite) linear combination of basis candidate simplex splines, which establishes Requirement (F).

(G) It has been stated in [Nea01b, p. 381ff] that the basis candidate functions spanning $\mathcal{S}_{m,X}$ and $\mathcal{S}'_{m,X}$ are linearly independent after identifying redundant configurations via $\sim$ and $\simeq$, respectively. However, also in this case, a proof has been provided neither in [Nea01b] nor in any other publication so far to the best of our knowledge. In Section 7.2, we will answer the question of linear independence negatively for the nonpooled spline space $\mathcal{S}_{m,X}$.

(H) Requirement (H) of the Fundamental Problem ensures that the construction yields the ordinary univariate spline space when considering the case $d = 1$. In Remark 4.11, we have noted that Delaunay triangles in one dimension are the pairs of consecutive knots. It is easy to see that Delaunay configurations of degree m reduce to sets of $m + 2$ consecutive knots for $d = 1$. Furthermore, univariate simplex splines are just (potentially renormalized) B-splines, which immediately yields that the space of simplex splines associated with Delaunay configurations of degree m equals the usual space of univariate splines in this case. As there are no redundancies in the set of Delaunay configurations for $d = 1$, i.e., each equivalence class of $\sim$ and $\simeq$ consists of exactly one element, the same holds true for both nonpooled and pooled DCB-splines. We refer to [Nea01b, p. 380] for more details on this topic.

We have defined two different spline spaces now, which both seem to provide a solution to the Fundamental Problem, according to [Nea01b]. But which one should be preferred?

The pooled approach avoids redundant summands in Identity 4.6 [Nea01b, p. 382]. Furthermore, it has been stated in [Nea01b, p. 383] that the spline space contains *exactly* the functions that are representable by means of Theorem 4.19, whereas the nonpooled version contains other functions, too. This is the reason why the pooled variant is favored in [Nea01b] and, therefore, is also more common in literature (see Subsection 4.3.8).

However, the pooled approach has the drawback that its basis candidate functions are no simplex splines but only (positive) linear combinations of simplex splines. Little is known about these linear combinations as, to the best of our knowledge, there is no publication so far explicitly dedicated to the investigation of their properties. Questions naturally arising are, for example, the following: Is there a lower or upper bound for the number of simplex splines pooled by such a linear combination? Could a linear combination yield a basis candidate function with a support whose interior is not connected? Is there always a unique maximum? Moreover, *"there is no associated recurrence relation relating these functions to basis [candidate] functions of lower degree"* [CLR13, p. 1669]. Such recurrence relations are very important

not only for theoretical but also for computational considerations. Neamtu defines the nonpooled DCB-splines only implicitly in [Nea01a] and the subsequent paper [Nea07], whereas he does not mention the pooled DCB-splines at all. However, at least for the latter publication, this could be due to the fact that he concentrates on the proof of Theorem 4.17.

Due to all these open questions involved when considering pooled DCB-splines, we think that the nonpooled variant, whose basis candidate functions are just the well-known simplex splines, is a better starting point for our considerations. However, our results partially also apply to the pooled spline space. We will leave a note hereof at the respective places and when summarizing our results in Section 8.1.

4.3.8 Related Work

So far, DCB-splines can rarely be found in practical applications. This may be mainly due to the fact that, on the one hand, there are both computational and numerical issues when computing simplex splines (see Section 8.2) and, on the other hand, the combinatorial nature of Delaunay configurations is very complex and not thoroughly understood. Nevertheless, pooled DCB-splines are used in [Han+08] to describe the deformation field in the process of parametric image registration. Nonpooled DCB-splines have been employed in [Cao+09] for the reconstruction of a smooth surface based on a closed triangulated surface of arbitrary topology. This approach requires to split the surface into several charts, which are topologically equivalent to a disk, and then to blend the pieces together. Later, [Cao+12] defined nonpooled DCB-splines directly on the sphere without the necessity of splitting and blending. Neamtu's approach and the idea of Delaunay configurations have been generalized by Liu and Snoeyink [LS07b; Liu08] by defining *generalized Delaunay configurations*. We will briefly introduce their approach in Section 4.4.3. In [DGN05], Dembart, Gonsor, and Neamtu deal with bivariate pooled DCB-splines of degree two in order to solve certain integral equations: They consider the approximation of a given function using pooled DCB-splines and sketch an algorithm for the efficient computation of Delaunay configurations in this special case. Furthermore, they investigate degenerate knot sets with a focus on repeated knots at the boundary of the convex hull of the knot set (see Subsection 8.2.2 for more details).

Although the concept of Delaunay configurations appeared implicitly in several publications dealing with higher-order Voronoi diagrams, its study as a separate entity by Neamtu seemed to be new [Nea01b, p. 377f]. Shortly after Neamtu's construction, [GHK02] introduced *Higher-order Delaunay triangulations* in order to

improve the quality of *Triangulated Irregular Networks* in *Geographic Information Systems*. These triangulations allow triangles with up to $k \in \mathbb{N}_0$ knots in the interior of their circumcircle and, therefore, provide more flexibility than the Delaunay triangulation. Hence, they consist of triangles associated with Delaunay configurations of degree up to k, which reveals a close relationship between both concepts. [SK09] and [Sil09] consider higher-order Delaunay triangulations of polygons and, as part of that, develop an algorithm for the computation of all Delaunay triangles up to the given order k, which, according to [Han+08], can also be employed for the efficient computation of Delaunay configurations.

4.4 Other Approaches

In the current chapter, we have given an overview of some important spline spaces using simplex splines so far. However, there are many other approaches, some of which we will name in this section.

4.4.1 Tensor Product Splines

One of the most popular approaches to multivariate splines are tensor product splines. For some $d \in \mathbb{N}_+$, assume that we have the information required for a univariate spline space for each dimension. Namely, this is the spline degree $m_i \in \mathbb{N}_0$ and the nondecreasing knot sequence $X_i = (x_{i,0}, \dots, x_{i,m_i+n_i}) \in \mathbb{R}^{m_i+n_i+1}$, $n_i \in \mathbb{N}_+$, for each $i \in \{1, \dots, d\}$.

The Cartesian product

$$X := \bigtimes_{i=1}^{d} X_i$$

of all knot sequences forms a d-dimensional grid of knots. Furthermore, using a tensor product construction, we can define higher dimensional analogues of B-splines as

$$\left(\bigotimes_{i=1}^{d} B_{j_i,m_i,X_i} \right) : \mathbb{R}^d \to \mathbb{R}, \quad (t_1, \dots, t_d) \mapsto \prod_{i=1}^{d} B_{j_i,m_i,X_i}(t_i),$$

where $j_i \in \{0, \dots, n_i - 1\}$ for each $i \in \{1, \dots, d\}$ [Sch07, p. 486]. These *tensor product B-splines* span a multivariate spline space on the grid X, which inherits many of the appealing properties known from univariate splines. For instance, the tensor product B-splines have compact support, which is a rectangle or cuboid now instead of a line segment, and form a partition of unity [Sch07, p. 487]. Additionally, they

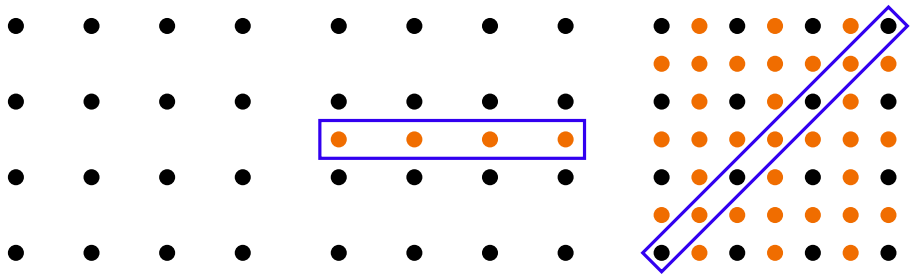

(a) Original knotset before refinement (b) Refinement along orthogonal direction (c) Refinement along diagonal direction

Fig. 4.14: Refining the knot set of tensor product splines. The original knots are depicted in *black*, whereas the inserted knots are displayed in *orange*. The *blue* area specifies the region in which a refinement is desired.

are polynomials of degree at most m_i, $i \in \{1, \ldots, d\}$, in the corresponding direction on each of the cuboids generated by neighboring knots [Sch07, p. 485].

However, tensor product splines have some drawbacks, which limit their suitability to certain applications. Two of the most severe problems are directly related to the simplicity of the tensor product structure:

1. The grid of knots X always has a rectangular structure. If one tries to approximate certain data using tensor product splines, the data also has to exhibit this special structure, i.e., the data points must form the mesh points of a rectangular grid. Otherwise, without further adaptions, no efficient approximation or interpolation is possible [Boo01, p. 310].

2. If the knot grid of a tensor product spline function shall be refined in a certain region in order to enhance the local approximation quality, it is not possible to add single knots. Instead, whole $(d-1)$-dimensional layers of knots have to be inserted. Whereas this may be feasible if the features necessitating the refinement are aligned with the directions of the tensor product grid, improving the approximation quality for diagonal features leads to a global refinement of the knot grid, as presented in Figure 4.14 [Boo01, p. 310].

Although these drawbacks limit the applicability of tensor product splines, their computational efficiency [Boo01, p. 291] causes an enormous popularity. An extension of tensor product splines are the *Non-Uniform Rational B-Splines (NURBS)*. They can be employed, for example, in *Isogeometric Analysis (IgA)*, which is an approach for integrating the solving of *Partial Differential Equations (PDEs)* into CAGD-tools [CHB09].

4.4.2 Polyhedral Splines and Box Splines

In [BH82b], de Boor and Höllig introduced a generalization of simplex splines, where the high-dimensional object that is projected on $\mathbb{R}^d$ is not restricted to simplices but can be an arbitrary bounded convex polytope instead, which is why these splines are called *polyhedral splines*. Further information on polyhedral splines can be found, for example, in [Boo93] and [Höl86].

One special type of polyhedral splines are the *box splines* introduced by [BD83], where the high-dimensional object is a parallelepiped. Properties as well as recurrence relations of box splines are given in [BH82a]. According to [Höl86], box splines can be viewed as generalization of univariate cardinal splines. For details on box splines, we refer to the book by de Boor, Höllig, and Riemenschneider [BHR93].

4.4.3 Generalized Delaunay Configurations

Liu and Snoeyink [LS07b; Liu08] distilled the two core ingredients in Neamtu's proof of Theorem 4.17, namely that it starts with a triangulation of a given set of knots for degree zero and that configuration sets of successive degrees exhibit a certain relation called *facet-matching property*. They provide the *link triangulation procedure* for the iterative construction of configurations of a certain degree. In each iteration, certain polygons have to be triangulated, and the specific choice of triangulation influences the resulting configurations. When starting with a Delaunay triangulation of the knots and performing a Delaunay triangulation of each polygon, one obtains Neamtu's Delaunay configurations. Otherwise, the resulting configurations are called *generalized Delaunay configurations*. As the link triangulation procedure ensures the facet-matching property, one can use a generalized version of Theorem 4.17 to obtain a Marsden identity for all spline spaces generated in this way. However, the link triangulation procedure can only be defined in two dimensions, and Liu and Snoeyink could prove the correctness only for a degree of at most three. Recently, Schmitt [Sch19] could show that the procedure works for arbitrary degrees.

Due to the freedom of choice with respect to the triangulations, one has certain control over the flexibility of the resulting spline space. According to [Liu08, p. 96] and [Zha+17], the result when approximating anisotropic functions or sharp features can be improved by using properly aligned generalized Delaunay configurations that are no ordinary Delaunay configurations.

Very recently, Barucq, Calandra, Diaz, and Frambati [Bar+22] used fine zonotopal tilings to generalize the link triangulation procedure to higher dimensions. Due to their combinatorial approach, they can also handle finite and degenerate knot sets. Furthermore, they provide algorithms for these (generalized) spline spaces, which can act as starting point for practical applications of these spaces.

4.4.4 Splines on Triangulations

In this chapter, we started with a certain kind of functions, namely simplex splines, and tried to choose an appropriate collection of basis candidate functions that spans a reasonable spline space with appealing properties. However, one can also proceed vice-versa and start with a certain space of piecewise polynomials. Afterwards, one can try to construct a compactly supported basis and derive properties [Nea01b, p. 358]. These spline spaces are frequently constructed on refinements (*"splits"*) of a certain triangulation, such as the Clough-Tocher split [CT66] and the Powell-Sabin split [PS77]. The corresponding Macro-element spaces, which emerge from Finite Element Methods, are presented for example in [LS07a]. For an application of Powell-Sabin splines to the Isogeometric Analysis of certain PDEs, we refer to [Spe+12]. Another approach based on simplex splines is given in [CLR13].

However, according to [Nea01b, p. 358], a partitioning of $\mathbb{R}^d$ ensuring the optimal smoothness of the splines (see Requirement (B) of the Fundamental Problem) may be very complicated. There are situations in which the ordinary space of piecewise polynomials on triangulations or other approaches yielding a simple partitioning do not contain any nontrivial spline that at the same time is optimally smooth and has compact support. Hence, these approaches in general do not satisfy both Requirements (B) and (F) at the same time and, therefore, are no solution to the Fundamental Problem [Nea01b, p. 358]. For an extensive study of this kind of piecewise polynomials on triangulations, we refer to the book on this subject by Lai and Schumaker [LS07a] and the references therein.

5 Local Finiteness

> *Der Worte sind genug gewechselt,*
> *Laßt mich auch endlich Taten sehn;*
>
> — **Johann Wolfgang von Goethe**
> Faust, Part One

In this chapter, we investigate the local finiteness property of DCB-splines, as introduced in our first research question. The essential consequence of this property is the fact that the splines spaces have a locally finite structure, even when considering infinite knot sets. This is also part of the requirements stated in the Fundamental Problem. Therefore, we start by recalling these requirements, formulating the local finiteness property, and settling reasonable assumptions on the knot set. Afterwards, we analyze the structure of appropriate knot sets and, finally, give a proof that the local finiteness property indeed holds true for both pooled and nonpooled DCB-splines under suitable conditions. Subsequently, we list several appealing consequences of this property, which in particular include the affected requirements of the Fundamental Problem, and close the chapter by formulating a practical criterion that can be used to check if the conditions on the knot set required for the local finiteness property to hold true on some compact region are satisfied.

5.1 Preliminaries

In the following subsection, we will formulate the local finiteness property. Subsequently, we will investigate which requirements on the knot set are necessary for the local finiteness property to hold true.

5.1.1 Problem Statement

DCB-splines have been constructed in order to provide a solution to the Fundamental Problem stated by Neamtu (see Subsection 4.1.2). Requirements (D) and (E) expect the spline space to exhibit a locally finite structure. More precisely, the following two

conditions are required to hold true for all spline degrees $m \in \mathbb{N}_0$ and appropriate knot sets $X \subseteq \mathbb{R}^d$, $d \in \mathbb{N}_+$:

(D) The spline spaces $\mathcal{S}_{m,X}$ and $\mathcal{S}'_{m,X}$ are locally finite-dimensional, i.e.,

$$\dim \mathcal{S}_{m,X}|_\Omega < \infty, \quad \dim \mathcal{S}'_{m,X}|_\Omega < \infty \quad \text{for all compact } \Omega \subseteq \mathbb{R}^d.$$

(E) At each point $t \in \mathbb{R}^d$, only a finite number of basis candidate functions in $\mathcal{B}_{m,X}$ and $\mathcal{B}'_{m,X}$, which are the basis candidates for the spline spaces $\mathcal{S}_{m,X}$ and $\mathcal{S}'_{m,X}$, respectively, are nonzero, i.e.,

$$\left|\left\{B \in \mathcal{B}_{m,X} \;\middle|\; t \in \operatorname{supp} B\right\}\right| < \infty, \quad \left|\left\{B' \in \mathcal{B}'_{m,X} \;\middle|\; t \in \operatorname{supp} B'\right\}\right| < \infty.$$

It was claimed that these properties follow from *"the local nature of Delaunay configurations"* [Nea01b, p. 381]. There was a reference to the publication [Nea07], which was *"in preparation"* at that time and was published some years later. However, to the best of our knowledge, neither [Nea07] nor any other publication contains any explicit results on the topic of local finiteness. Hence, we consider it worthwhile to spend the present chapter on these properties.

If X is finite, it is easy to see that both properties hold true as Delaunay configurations are specified uniquely by their boundary and interior knots and both collections are subsets of X.

Furthermore, in the case $m = 0$, the support of a basis candidate function is just the convex hull of its corresponding Delaunay triangle / simplex. Hence, Requirement (E) follows directly from the fact that Delaunay triangles tessellate $\operatorname{conv}(X)$. However, even if $m = 0$, it is not immediately clear that Requirement (D) holds true, as will be shown in Example 5.1.

The main result of this chapter is Theorem 5.29, which states that, for any compact $\Omega \subseteq \mathbb{R}^d$ and for any suitable knot set $X \subseteq \mathbb{R}^d$, whose properties will be settled in the following subsection, there is only a finite number of Delaunay configurations of some given degree $m \in \mathbb{N}_0$ whose circumcircles have a nonempty intersection with Ω, i.e.,

$$\left|\left\{K \in \mathcal{K}_m(X) \;\middle|\; B(\mathfrak{B}(K)) \cap \Omega \neq \emptyset\right\}\right| < \infty.$$

In the following, this will be referred to as the *local finiteness property*. Requirements (D) and (E) then follow as corollaries for both pooled and nonpooled DCB-splines.

The local finiteness property is utterly important not only for practical but also for theoretical considerations: In the definitions of both spline spaces, we allow an infinite number coefficients to be nonzero, whereas the *span* is usually restricted to *finite* linear combinations of basis candidate functions. Since every simplex spline has compact support, these infinite linear combinations are inevitable if one is interested in representing globally supported functions, such as polynomials. Immediately arising from the consideration of infinite sums is the question of convergence. Moreover, one is interested in the (possibly infinite) number of (nonnegative) basis candidate functions contributing to the function value at a certain position. Requirement (E) ensures that, for each point, only a finite set of functions is nonzero and, therefore, the number of nonzero summands is finite. Moreover, Requirement (D) suggests a certain *uniformity* of this property: For an arbitrary compact region Ω, no more than a finite number of basis candidate functions have to contribute to the value of a spline function *anywhere* inside of Ω.

The influence of the local finiteness property on practical aspects can be seen easily. Computers can only handle *finite* objects and, therefore, cannot evaluate infinite sums. Requirement (E) ensures that the evaluation of a spline function at a specific position $t \in \mathbb{R}^d$ involves only a finite number of functions. However, in order to decide *which* functions may contribute to the function value at t, it is necessary to compute all Delaunay configurations overlapping t, which, consequently, should be a finite set, too. This assumption is sharper than Requirement (E) since, for $d > 1$, the support of a basis candidate function is a proper subset of the circumcircle generated by the corresponding Delaunay configuration. The local finiteness property also comprises this sharper requirement, though. Furthermore, it follows from Requirement (D) that it is not necessary to handle infinite objects, even when considering infinite knot sets, as long as one restricts considerations on a compact and, thus, bounded region.

5.1.2 Prerequisites

The goal of this subsection is to determine suitable assumptions on the knot set $X \subseteq \mathbb{R}^d$, $d \in \mathbb{N}_+$. In Neamtu's Theorem 4.17 regarding DCB-splines, we assumed the knots to satisfy the strong conditions, as specified by Definition 4.15, i.e., to be in general Delaunay position, to be locally finite, and to cover the whole space $\mathbb{R}^d$. It would be desirable that these assumptions are sufficient to prove the local finiteness of DCB-splines. However, in order to keep the results as general as possible, we will check if one or several of these assumptions can be dropped without loosing the validity of the local finiteness property.

As we can define Delaunay configurations only with respect to knot sets in general Delaunay position, the corresponding assumption on X is inevitable. It is not very strong, however, since general Delaunay position can be enforced for any knot set by arbitrarily small perturbations of certain knots. In particular, it is not a contradiction to the Fundamental Problem as we expect Requirements (D) and (E) to hold true only for *almost every* knot set (see Subsection 4.1.2).

We defined Delaunay configurations as a generalization of Delaunay triangles, which, in some sense, encode neighborhood relations. Therefore, it seems reasonable to expect that, also in the case of Delaunay configurations, the structure of the corresponding spline space resembles the local neighborhood of knots within a certain region. Hence, if the knot set exhibits an accumulation point, also the set of Delaunay configurations can be expected to be infinitely dense in that region. On the contrary, a locally finite knot set can be expected to give rise to a locally finite set of Delaunay configurations. This justifies the assumption on X to be locally finite, i.e.,

$$|X \cap \Omega| < \infty \quad \text{for all compact } \Omega \subseteq \mathbb{R}^d.$$

The assumption $\operatorname{conv}(X) = \mathbb{R}^d$, however, does not seem to be necessary at first sight because there is no immediate reason for the local finiteness property to hold true only for knot sets without boundary. This consideration is disproved by the following example:

Example 5.1. Let $d = 2$, and consider the degrees zero and one. Define

$$X_0 := \{x_1, x_2, \dots\} \cup \{y_1, y_2, \dots\} \cup \{z_0\}, \quad X_1 := X_0 \cup \{z_1\},$$

where

$$x_i := \left(2^i - 1, \frac{1}{2^{i-1}}\right)^\intercal, \quad y_i := \left(2^i, \frac{1}{2^{i-1}}\right)^\intercal \quad \text{for all } i \in \mathbb{N}_+,$$
$$z_0 := (0,0)^\intercal, \quad z_1 := \left(0, -\frac{1}{2}\right)^\intercal.$$

The knots are depicted in Figure 5.1. We show in the upcoming Lemmas 5.2 and 5.3 that, for all $i, j \in \mathbb{N}_+$ with $i \neq j$, one has

$$x_j, y_j \notin \overline{B_i} := \overline{B(x_i, y_i, z_0)}. \tag{5.1}$$

Furthermore, Lemma 5.4 provides that

$$z_1 \in B_i \quad \text{for all } i \in \mathbb{N}_+. \tag{5.2}$$

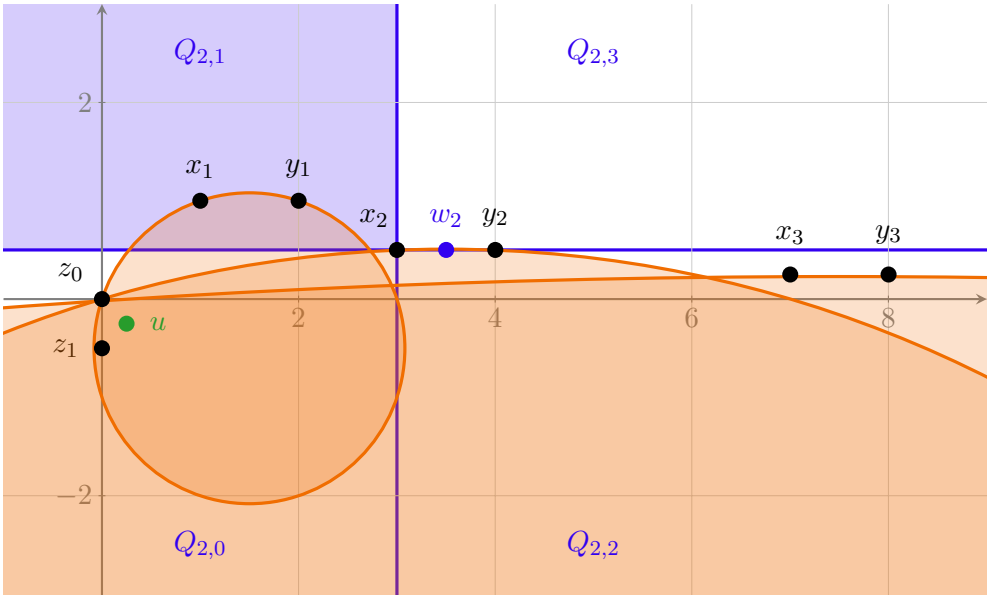

Fig. 5.1: Counterexample for the local finiteness property when dropping the assumption $\operatorname{conv}(X) = \mathbb{R}^d$. The tuples $(x_i, y_i, z_0), i \in \mathbb{N}_+$, give rise to an infinite set $\{B_i \mid i \in \mathbb{N}_+\}$ of overlapping circles corresponding to Delaunay configurations. Due to computational limitations, we only display a finite subset of these circles, namely those for $i \in \{1, \dots, 3\}$. The sets $Q_{2,1}, \dots, Q_{2,4}$ as well as the points u and w_2 are used in Example 5.1 and the proofs of Lemmas 5.2 and 5.5.

Consequently,

$$B(z_0, x_i, y_i) \cap X_0 = \emptyset \quad \text{and} \quad B(z_0, x_i, y_i) \cap X_1 = \{z_1\} \quad \text{for all } i \in \mathbb{N}_+.$$

To be able to compute Delaunay configurations for X_0 and X_1, respectively, we have to ensure that both sets are in general Delaunay position. As it is necessary to check every combination of three knots for collinearity and every combination of four knots for cocircularity, the proofs would be very tedious. Instead, we give evidence in Lemma 5.5 that, even if some combination of knots is collinear or cocircular, one of these knots can be relocated arbitrarily within some nonempty, open, bounded neighborhood U of the original position without violating any of the statements in (5.1) and (5.2). Considering a relocation of x_i or y_i for $i \in \mathbb{N}_+$ is sufficient since any combination of three or four knots contains at least one of these knots. The intersection of U with the union of all lines spanned by any two knots and of all circumcircles induced by any combination of three knots is a null set as it is a countable union of null sets and due to the σ-subadditivity of the Lebesgue measure. Since the Lebesgue measure of U as a nonempty, open set is positive, one can be sure to find a suitable relocation within any arbitrarily small neighborhood around the original position.

As a consequence, we can assume that

$$K_i := (\{z_0, x_i, y_i\}, \emptyset) \in \mathcal{K}_0(X_0) \quad \text{and} \quad K_i' := (\{z_0, x_i, y_i\}, \{z_1\}) \in \mathcal{K}_1(X_1)$$

for all $i \in \mathbb{N}_+$. These configurations are also displayed in Figure 5.1. Note that

$$K_i' \not\simeq K_j' \quad \text{but} \quad K_i' \simeq K_j' \quad \text{for all } i, j \in \mathbb{N}_+,\ i \neq j.$$

In particular, z_0 is a boundary knot of both an infinite set of configurations of degree zero and of an infinite set of configurations of degree one. Likewise, z_1 is an interior knot of an infinite number of Delaunay configurations of degree one.

Moreover, the point $u := (1/4, -1/4)^\intercal$ is in the support of each simplex spline generated by the Delaunay configurations K_i', $i \in \mathbb{N}_+$, of degree one, i.e.,

$$u \in \operatorname{supp} M(\cdot \mid z_0, z_1, x_i, y_i) \quad \text{for all } i \in \mathbb{N}_+,$$

which can be seen as follows: Let $i \in \mathbb{N}_+$, and consider the tuple $Y_i := (z_0, z_1, y_i)$ of knots in general position. The barycentric coordinates of u with respect to Y_i are positive since one can apply Cramer's rule, as shown in Remark 3.7, with the following determinants:

$$d(Y_i) = 2^{i-1} > 0, \qquad d_0(u \mid Y_i) = \frac{2^{i-1}(2^i - 1/2) - 1}{2^{i+1}} > 0,$$
$$d_1(u \mid Y_i) = \frac{2^{2i-1} + 1}{2^{i+1}} > 0, \qquad d_2(u \mid Y_i) = \frac{1}{8} > 0.$$

As a consequence,

$$u \in \operatorname{conv}(z_0, z_1, y_i) \subseteq \operatorname{conv}(z_0, z_1, x_i, y_i) = \operatorname{supp} M(\cdot \mid z_0, z_1, x_i, y_i)$$

for all $i \in \mathbb{N}_+$, according to Proposition 3.17.

This example can be generalized to arbitrary degrees by adding additional points like z_1 in the nonempty intersection of all circumcircles. Note that we have $\operatorname{conv}(X_0)$, $\operatorname{conv}(X_1) \subset \mathbb{R}^2$ as there is at most one knot in the lower half plane. On the contrary, if there would be more than $m \in \mathbb{N}_0$ knots in that half plane, each of these knots would be contained in the balls B_i for sufficiently large $i \in \mathbb{N}_+$. Hence, only a finite subset of the triples $\{(z_0, x_i, y_i) \mid i \in \mathbb{N}_+\}$ would give rise to circumcircles with m knots in their interior. Thus, we would not have an appropriate infinite collection of Delaunay configurations of degree m in that case, and therefore, the counterexample would not work any more. ◀

Example 5.1 leads to several interesting conclusions for DCB-splines with respect to knot sets satisfying the weak conditions, as specified in Definition 4.16:

1. For all $m \in \mathbb{N}_0$, there may be compact regions that have a nonempty intersection with the support of an infinite number of basis candidate functions. This can be seen, for instance, when considering $B_{1/4}(z_0)$ in the previous example. Since (at least for $m = 0$) the corresponding simplex splines are linearly independent, it follows that Requirement (D) does not hold true in general for pooled and nonpooled DCB-splines.

2. For all $m \in \mathbb{N}_+$, there may be points in the support of an infinite number of basis candidate functions, like u in the previous example, for instance. Therefore, Requirement (E) does not hold true in general for nonpooled DCB-splines and $m \geq 1$.

3. For all $m \in \mathbb{N}_0$, there may be points in the circumcircles of an infinite number of Delaunay configurations of degree m, like u in the previous example.

4. Since $K'_i \simeq K'_j$ for all $i, j \in \mathbb{N}_+$ in the previous example, i.e., all these configurations are in the same pool, it follows that, without further assumptions, the pooling of simplex splines for the construction of pooled basis candidate functions does not necessarily yield finite linear combinations. Therefore, a basis candidate function can be an infinite sum of simplex splines, which does not even have bounded support in this example.

As a consequence, all properties that we have hoped to gain from the local finiteness property do not hold true in general if we do not require the knot set to satisfy $\operatorname{conv}(X) = \mathbb{R}^d$. We will close the section with the pending Lemmas regarding the previous example.

Lemma 5.2. For all $i, j \in \mathbb{N}_+$ with $j < i$, one has $x_j, y_j \notin \overline{B_i}$.

Proof. Let $i, j \in \mathbb{N}_+$ with $j < i$. We define the sets

$$
\begin{aligned}
Q_{i,0} &:= \left\{ t \in \mathbb{R}^2 \;\middle|\; t_1 < 2^i - 1,\ t_2 < \frac{1}{2^{i-1}} \right\}, \\
Q_{i,1} &:= \left\{ t \in \mathbb{R}^2 \;\middle|\; t_1 < 2^i - 1,\ t_2 > \frac{1}{2^{i-1}} \right\}, \\
Q_{i,2} &:= \left\{ t \in \mathbb{R}^2 \;\middle|\; t_1 > 2^i - 1,\ t_2 < \frac{1}{2^{i-1}} \right\}, \\
Q_{i,3} &:= \left\{ t \in \mathbb{R}^2 \;\middle|\; t_1 > 2^i - 1,\ t_2 > \frac{1}{2^{i-1}} \right\}.
\end{aligned}
$$

One has $z_0 \in Q_{i,0} \cap \overline{B_i}$ by definition. Furthermore, we consider the point

$$w_i := \frac{1}{2}(x_i + y_i) = \left(2^i - \frac{1}{2}, \frac{1}{2^{i-1}}\right),$$

which lies on the line separating $Q_{i,2}$ and $Q_{i,3}$. Since $\overline{B_i}$ is strictly convex and $x_i, y_i \in \partial B_i$, it follows that w_i is an interior point of $\overline{B_i}$. Hence, one can find an $\epsilon > 0$ such that $B_\epsilon(w_i) \subseteq \overline{B_i}$. Let

$$w_i' := w_i - (0, \epsilon/2)^\intercal \in Q_{i,2} \cap \overline{B_i} \quad \text{and} \quad w_i'' := w_i + (0, \epsilon/2)^\intercal \in Q_{i,3} \cap \overline{B_i}.$$

We assume that $Q_{i,1} \cap \overline{B_i} \neq \emptyset$ and choose an arbitrary $v \in Q_{i,1} \cap \overline{B_i}$. Consequently, there is one of the points z_0, v, w_i', w_i'' in each of the sets $Q_{i,0}, \ldots, Q_{i,3}$. Therefore, we can express x_i, which is the point separating the four sets $Q_{i,0}, \ldots, Q_{i,3}$, as convex combination of z_0, v, w_i' and w_i''. As these points lie in $\overline{B_i}$, it follows from the strict convexity of $\overline{B_i}$ that x_i is an interior point of $\overline{B_i}$, which is a contradiction. As a consequence, one has

$$Q_{i,1} \cap \overline{B_i} = \emptyset \quad \text{for all } i \in \mathbb{N}_+. \tag{5.3}$$

In particular, due to the fact that $x_j, y_j \in Q_{i,1}$ for $j < i$, this implies that $x_j, y_j \notin \overline{B_i}$ for all $i, j \in \mathbb{N}_+$ with $j < i$. □

Lemma 5.3. For all $i, j \in \mathbb{N}_+$ with $j > i$, one has $x_j, y_j \notin \overline{B_i}$.

Proof. Let $i, j \in \mathbb{N}_+$ with $j > i$. The center of the circle B_i is given as

$$c_i := \left(2^i - \frac{1}{2},\ \frac{1}{2^i} + 2^{2i-2}(1 - 2^i)\right)^\intercal$$

since it can be verified easily that

$$r_i^2 := \|c_i\|^2 = \|c_i - z_0\|^2 = \|c_i - x_i\|^2 = \|c_i - y_i\|^2.$$

The claims $x_j, y_j \notin \overline{B_i}$ are equivalent to $\|x_j - c_i\|^2 - r_i^2 > 0$ and $\|y_j - c_i\|^2 - r_i^2 > 0$. Let $k := j - i \geq 1$. Straightforward calculation yields

$$\begin{aligned} \|x_j - c_i\|^2 - r_i^2 &= 2^{2j} - 2^{i+j+1} - 2^j + 2^{i+1} + \frac{1}{2^{2j-2}} - \frac{\frac{1}{2^i} + 2^{2i-2} - 2^{3i-2}}{2^{j-2}} \\ &\geq \frac{2^k - 1}{2^{2i+2k}}\left(2^{3i+k} - 4\right) > 0. \end{aligned} \tag{5.4}$$

Consequently, $x_j \notin \overline{B_i}$. The claim $y_j \notin \overline{B_i}$ is proved by similar calculations:

$$\|y_j - c_i\|^2 - r_i^2 = 2^{2j} - 2^{i+j+1} + 2^j + \frac{1}{2^{2j-2}} - \frac{\frac{1}{2^i} + 2^{2i-2} - 2^{3i-2}}{2^{j-2}} > 0. \tag{5.5}$$

□

Lemma 5.4. For all $i \in \mathbb{N}_+$, one has $z_1 \in B_i$.

Proof. Let $i \in \mathbb{N}_+$. Then,

$$r_i^2 - \|z_1 - c_i\|^2 = \frac{1}{2^{i+2}}\left(-4 - 2^{3i} + 2^{4i} - 2^i\right) \geq \frac{1}{4}\left(2^i - 1\right) \geq \frac{1}{4}, \tag{5.6}$$

which in particular yields the stated claim. □

Lemma 5.5. For each $i \in \mathbb{N}_+$, one can find open neighborhoods U_{x_i} and U_{y_i} around x_i and y_i, respectively, such that, for all $x_i' \in U_{x_i}$, $y_i' \in U_{y_i}$ and for any $j \in \mathbb{N}_+$, $i \neq j$, one has

$$x_j, y_j \notin \overline{B(x_i', y_i, z_0)}, \quad z_1 \in B(x_i', y_i, z_0), \tag{5.7}$$

$$x_j, y_j \notin \overline{B(x_i, y_i', z_0)}, \quad z_1 \in B(x_i, y_i', z_0), \tag{5.8}$$

$$x_i', y_i' \notin \overline{B(x_j, y_j, z_0)}. \tag{5.9}$$

Proof. Let $i \in \mathbb{N}_+$, and let r_i, c_i be defined as in Lemma 5.3. From (5.4) and (5.5), it follows that

$$\lim_{j\to\infty}\left(\|x_j - c_i\|^2 - r_i^2\right) = \infty \quad \text{and} \quad \lim_{j\to\infty}\left(\|y_j - c_i\|^2 - r_i^2\right) = \infty. \tag{5.10}$$

In combination with (5.1), i.e., $x_j, y_j \notin \overline{B}_i$ for all $j \in \mathbb{N}_+$ with $j \neq i$, this yields

$$\eta_1 := \inf_{\substack{j\in\mathbb{N}_+ \\ j\neq i}}\left\{\|x_j - c_i\|^2 - r_i^2\right\} > 0 \quad \text{and} \quad \eta_2 := \inf_{\substack{j\in\mathbb{N}_+ \\ j\neq i}}\left\{\|y_j - c_i\|^2 - r_i^2\right\} > 0$$

since, otherwise, the sequence of distances would contain a subsequence converging to zero, which would be a contradiction to (5.10). Furthermore, according to (5.6), one has

$$\begin{aligned}\eta_3 &:= \|c_i\| - \|z_1 - c_i\| = r_i - \|z_1 - c_i\| \geq \sqrt{\|z_1 - c_i\|^2 + 1/4} - \|z_1 - c_i\| \\ &> \sqrt{\|z_1 - c_i\|^2} - \|z_1 - c_i\| = 0.\end{aligned}$$

One can set

$$\epsilon := \frac{1}{2}\min\left\{\sqrt{\min\{\eta_1,\eta_2\}+\|c_i\|^2}-\|c_i\|,\ \eta_3\right\} > 0,$$

apply the triangle inequalities, and use the definitions of ϵ and η_1 to obtain for any $c_i' \in B_\epsilon(c_i)$ and for all $j \in \mathbb{N}_+$ with $j \neq i$ that

$$\begin{aligned}
\|x_j - c_i'\| - \|c_i'\| &\geq \big|\|x_j - c_i\| - \|c_i - c_i'\|\big| - (\|c_i' - c_i\| + \|c_i\|) \\
&> \|x_j - c_i\| - \|c_i\| - 2\epsilon \\
&\geq \|x_j - c_i\| - \|c_i\| - \left(\sqrt{\eta_1 + \|c_i\|^2} - \|c_i\|\right) \\
&\geq \|x_j - c_i\| - \sqrt{\|x_j - c_i\|^2} \\
&= 0.
\end{aligned}$$

Hence, one has $x_j \notin \overline{B_{\|c_i'\|}(c_i')}$. It follows analogously that $y_j \notin \overline{B_{\|c_i'\|}(c_i')}$. On the contrary, one has

$$\begin{aligned}
\|z_1 - c_i'\| - \|c_i'\| &\leq \|z_1 - c_i\| + \|c_i - c_i'\| - \Big|\|c_i' - c_i\| - \|c_i\|\Big| \\
&< \|z_1 - c_i\| - \|c_i\| + \eta_3 \\
&= 0,
\end{aligned}$$

and thus, $z_1 \in B_{\|c_i'\|}(c_i')$. Consequently, Relations (5.7) and (5.8) hold true if the relocation from x_i to x_i' or from y_i to y_i', respectively, causes a movement of the *center* of B_i from c_i to c_i' by a distance of less than ϵ.

To that end, let H_{x_i} be the open half plane generated by the hyperplane $\mathrm{aff}(z_0, y_i)$ such that $x_i \in H_{x_i}$, which is possible due to the affine independence of the knots z_0, x_i, y_i. Analogously, let H_{y_i} be the open half plane generated by $\mathrm{aff}(z_0, x_i)$ with $y_i \in H_{y_i}$. The maps

$$\begin{aligned}
&H_{x_i} \to \mathbb{R}^2, \quad x_i' \mapsto \mathrm{cen}(z_0, x_i', y_i) \quad \text{and} \\
&H_{y_i} \to \mathbb{R}^2, \quad y_i' \mapsto \mathrm{cen}(z_0, x_i, y_i')
\end{aligned}$$

are continuous on H_{x_i} and H_{y_i}, respectively, where cen denotes the center of the circumcircle generated by the given points. Hence, one can find $\delta_{x_i,1} > 0$ and $\delta_{y_i,1} > 0$ such that

$$\begin{aligned}
&\|c_i - \mathrm{cen}(z_0, x_i', y_i)\| < \epsilon \quad \text{for all } x_i' \in B_{\delta_{x_i,1}}(x_i), \\
&\|c_i - \mathrm{cen}(z_0, x_i, y_i')\| < \epsilon \quad \text{for all } y_i' \in B_{\delta_{y_i,1}}(y_i),
\end{aligned}$$

ensuring (5.7) for all $x_i' \in B_{\delta_{x_i,1}}(x_i)$ and (5.8) for all $y_i' \in B_{\delta_{y_i,1}}(y_i)$. In order to establish (5.9), we reutilize the sets $Q_{j,1}$ for $j \in \mathbb{N}_+$ from the proof of Lemma 5.2. From $x_i, y_i \in Q_{i+1,1}$, it follows that

$$\inf_{t \in Q_{i+1,1}^c} \|x_i - t\| = \min\left\{ \left| (2^{i+1} - 1) - (2^i - 1) \right|, \left| \frac{1}{2^{i-1}} - \frac{1}{2^i} \right| \right\} = \min\left\{ 2^i, \frac{1}{2^i} \right\} = \frac{1}{2^i}$$

and equivalently that

$$\inf_{t \in Q_{i+1,1}^c} \|y_i - t\| = \min\left\{ 2^i - 1, \ \frac{1}{2^i} \right\} = \frac{1}{2^i}.$$

By definition of $Q_{i+1,1}$, one has $Q_{i+1,1} \subseteq Q_{j,1}$ for all $j \in \mathbb{N}_+$ with $j \geq i+1$ and, therefore, also $Q_{j,1}^c \subseteq Q_{i+1,1}^c$. Consequently, one obtains together with (5.3) that

$$\inf_{t \in \overline{B_j}} \|x_i - t\| \geq \inf_{t \in Q_{j,1}^c} \|x_i - t\| \geq \inf_{t \in Q_{i+1,1}^c} \|x_i - t\| = \frac{1}{2^i}$$

and analogously that

$$\inf_{t \in \overline{B_j}} \|y_i - t\| \geq \frac{1}{2^i}$$

for all $j \in \mathbb{N}_+$ with $j \geq i+1$. Together with Lemma 5.3 and the fact that the set of remaining circles $\overline{B_1}, \dots \overline{B_{i-1}}$ clearly is finite, this yields that there are $\delta_{x_i,2}, \delta_{y_i,2} > 0$ such that, for each $j \in \mathbb{N}_+$ with $j \neq i$, one has

$$\begin{aligned} x_i' &\notin \overline{B_j} \quad \text{for all } x_i' \in B_{\delta_{x_i,2}}(x_i), \\ y_i' &\notin \overline{B_j} \quad \text{for all } y_i' \in B_{\delta_{y_i,2}}(y_i). \end{aligned}$$

Overall, we have shown that (5.7), (5.8), and (5.9) hold true for all $x_i' \in B_{\delta_{x_i}}(x_i)$ and $y_i' \in B_{\delta_{y_i}}(y_i)$, where $\delta_{x_i} := \min\{\delta_{x_i,1}, \delta_{x_i,2}\}$ and $\delta_{y_i} := \min\{\delta_{y_i,1}, \delta_{y_i,2}\}$, which finishes the proof. □

5.2 Density Cones

Unless stated otherwise, we will assume for the remainder of the current chapter that $d \in \mathbb{N}_+$, $m \in \mathbb{N}_0$, and that $X \subseteq \mathbb{R}^d$ is a knot set satisfying the strong conditions specified in Definition 4.15.

As starting point for a proof of the local finiteness property, we use the following observation: Delaunay configurations with a large circumcircle correspond to areas with only few knots. On the contrary, in areas with a high density of knots, the

circumcircles of Delaunay configurations are smaller. Therefore, we can hope to find a bound for the diameter of Delaunay configurations in some region, depending on the local density of knots.

At first, we consider an arbitrary point $t \in \mathbb{R}^d$. Without loss of generality, we can assume t to be the origin since we can translate all knots in X accordingly. In order to describe the density of knots *in a certain direction* around t, we consider *(infinite) cones* with apex in t. To that end, we give a definition of cones now, which is appropriate for our purposes, and show some basic properties. Afterwards, we use these cones to describe the density of knots in a certain direction and prove subsequently that one can find a bound *independently* of a specific direction.

5.2.1 Definition and Properties of Cones

Definition 5.6 (Cone)**.** Let $\theta \in \mathbb{R}^d$ with $\|\theta\| = 1$ and $a \in [0, 1]$. The *(infinite open) cone (with aperture a and direction / axis θ)* is defined as the set

$$C_a(\theta) := \left\{ w \in \mathbb{R}^d \backslash \{\mathbf{0}\} \;\middle|\; \frac{\langle \theta, w \rangle}{\|w\|} > 1 - 2a \right\}.$$

◀

Remark 5.7. We can identify all unit vectors in $\mathbb{R}^d$ with elements of the sphere $\mathbb{S}_{d-1}$. Therefore, we will henceforth write "$\theta \in \mathbb{S}_{d-1}$" instead of "$\theta \in \mathbb{R}^d$ with $\|\theta\| = 1$". ◀

Remark 5.8. Our definition of cones is consistent with the definition of cones in linear algebra in the sense that, for any cone C, one has

$$\lambda w \in C \quad \text{for all } w \in C,\ \lambda \in \mathbb{R}_+,$$

which follows directly from our definition. ◀

For a visualization of a cone, we refer to Figure 5.2. In all figures of this chapter, we parameterize the aperture of cones by an angle: For a cone with aperture a, this angle is given as $\alpha := 2 \arccos(1 - 2a)$.

Definition 5.9 (Convex cone)**.** Let C be a cone. C is a *convex cone* if, for arbitrary $v, w \in C$, one has $v + w \in C$. ◀

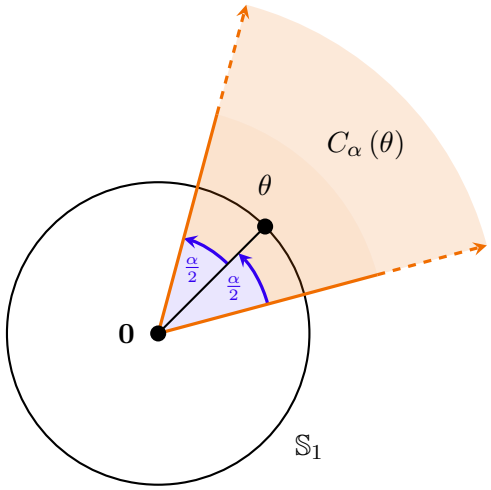

Fig. 5.2: Visualization of a cone in two dimensions ($d = 2$), parameterized by α and θ. The angle α corresponds to the aperture a, whereas θ denotes the direction / axis of the cone.

In particular, convex cones are convex [Itô93, p. 333]. Next, we formulate an easy criterion for cones in terms of our definition to be convex. Subsequently, we show that our definition of cones yields open sets.

Proposition 5.10. Let $\theta \in \mathbb{S}_{d-1}$ and $a \in [0, 1/2]$. Then, $C_a(\theta)$ is convex.

Proof. Let $v, w \in C_a(\theta)$. Then, $v \neq -w$ since, otherwise, one would have

$$1 - 2a < \frac{\langle \theta, v \rangle}{\|v\|} < -1 + 2a$$

and, thus, the contradiction $a > 1/2$. By using the linearity of $\langle \cdot, \theta \rangle$ and the triangle inequality, one can conclude that

$$\frac{\langle v + w, \theta \rangle}{\|v + w\|} > \frac{(1 - 2a)(\|v\| + \|w\|)}{\|v + w\|} \geq \frac{(1 - 2a)(\|v\| + \|w\|)}{\|v\| + \|w\|} = 1 - 2a,$$

and therefore, $v + w \in C_a(\theta)$. □

Proposition 5.11. Let $\theta \in \mathbb{S}_{d-1}$ and $a \in [0, 1]$. Then, $C_a(\theta)$ is open in $\mathbb{R}^d$.

Proof. The interval $(1 - 2a, 1]$ is open with respect to the topological space $[-1, 1]$ equipped with the topology inherited from $\mathbb{R}$. Furthermore, the map

$$h : \mathbb{R}^d \backslash \{\mathbf{0}\} \to [-1, 1], \quad w \mapsto \frac{\langle \theta, w \rangle}{\|w\|}$$

is continuous. Thus, the inverse image $C_a(\theta) = h^{-1}((1-2a,1])$ is open with respect to the topological space $\mathbb{R}^d\backslash\{\mathbf{0}\}$ equipped with the topology inherited from $\mathbb{R}^d$. Since $\mathbb{R}^d\backslash\{\mathbf{0}\}$ is open in $\mathbb{R}^d$, it follows with the properties of the induced topology that $C_a(\theta)$ is open in $\mathbb{R}^d$. □

In our last topological result regarding cones, we specify the boundary of a cone. We constrain the aperture to $a \in (0,1)$ and exclude the special cases $a \in \{0,1\}$. For $a = 0$, the cone is an empty set and, thus, has no boundary. The case $a = 1$ would require special treatment and will be omitted for the sake of simplicity since it will not be used throughout the thesis.

Proposition 5.12. Let $\theta \in \mathbb{S}_{d-1}$ and $a \in (0,1)$. Then,

$$\partial C_a(\theta) = \left\{ w \in \mathbb{R}^d\backslash\{\mathbf{0}\} \;\middle|\; \frac{\langle \theta, w\rangle}{\|w\|} = 1-2a \right\} \cup \{\mathbf{0}\} =: A.$$

Proof. "$\subseteq$" According to Proposition 5.11, $C_a(\theta)$ is open, i.e.,

$$\partial C_a(\theta) \subseteq C_a(\theta)^c = \left\{ w \in \mathbb{R}^d\backslash\{\mathbf{0}\} \;\middle|\; \frac{\langle \theta, w\rangle}{\|w\|} \leq 1-2a \right\} \cup \{\mathbf{0}\}. \tag{5.11}$$

Let

$$A' := \left\{ w \in \mathbb{R}^d\backslash\{\mathbf{0}\} \;\middle|\; \frac{\langle \theta, w\rangle}{\|w\|} < 1-2a \right\} \subseteq C_a(\theta)^c.$$

Since $A' = C_{1-a}(-\theta)$, one can apply Proposition 5.11 to obtain that A' is open. Consequently,

$$\partial C_a(\theta) \cap A' = \partial(C_a(\theta)^c) \cap A' = \emptyset,$$

yielding, together with (5.11), that $\partial C_a(\theta) \subseteq A$.

"$\supseteq$" Let $w \in A$. We show that $w \in \partial C_a(\theta)$ by constructing a sequence of points in $C_a(\theta)$ converging to w. Let

$$w_k := \left(1 - \frac{1}{k}\right) w + \frac{1}{k}\theta \quad \text{for all } k \in \mathbb{N}_+.$$

It follows from $a < 1$ that $w_k \neq \mathbf{0}$ for each $k \in \mathbb{N}_+$. Consequently, one obtains together with $\|\theta\| = 1$ and $\langle \theta, w\rangle = (1-2a)\|w\|$ as well as $1-2a < 1$ that

$$\frac{\langle \theta, w_k\rangle}{\|w_k\|} \geq \frac{\left(1-\frac{1}{k}\right)\langle \theta, w\rangle + \frac{1}{k}}{\left(1-\frac{1}{k}\right)\|w\| + \frac{1}{k}} > \frac{\left(1-\frac{1}{k}\right)(1-2a)\|w\| + \frac{1}{k}(1-2a)}{\left(1-\frac{1}{k}\right)\|w\| + \frac{1}{k}} = 1-2a.$$

Therefore, $w_k \in C_a(\theta)$ for all $k \in \mathbb{N}_+$. Since $(w_k)_{k\in\mathbb{N}_+}$ converges to w, this shows that $w \in \partial C_a(\theta)$. □

5.2.2 Density Description Using Cones

After these general preparations, we can now start to connect cones with the knot set X. To that end, we associate a cone with each direction around the point of consideration (which we assumed to be the origin). The aperture of the cone is chosen such that less than a given number $n \in \mathbb{N}_+$ of knots lie inside the cone but each cone with a larger aperture contains at least n knots. Hence, directions with a dense distribution of knots correspond to cones with a small aperture, whereas large apertures indicate sparse regions in the knot set.

Lemma 5.13. Let $\theta \in \mathbb{S}_{d-1}$ and $n \in \mathbb{N}_+$. The maximum

$$a_n(\theta) := \max A := \max\Big\{a \in [0,1] \;\Big|\; |C_a(\theta) \cap X| < n\Big\}$$

is well-defined.

Proof. As $C_0(\theta) = \emptyset$, one has $0 \in A$ and, in particular, $A \neq \emptyset$. Due to the fact that A is bounded and nonempty, it has a supremum $a := \sup A \in [0,1]$. We assume that $a \notin A$. Then, $|C_a(\theta) \cap X| \geq n$. Since

$$C_{a'}(\theta) \subseteq C_a(\theta) \quad \text{and} \quad |C_{a'}(\theta) \cap X| < n \quad \text{for all } 0 \leq a' < a,$$

there is an $x \in X$ satisfying

$$x \in C_a(\theta) \quad \text{and} \quad x \notin C_{a'}(\theta) \quad \text{for all } 0 \leq a' < a. \tag{5.12}$$

Consequently,

$$\widehat{a} := \frac{1}{2} - \frac{\langle \theta, x\rangle}{2\|x\|} < \frac{1}{2} - \frac{1}{2}(1-2a) = a.$$

Let $\epsilon := (a - \widehat{a})/2$. Then, $\epsilon > 0$ and $\widehat{a} + \epsilon < a$. Furthermore, $x \in C_{\widehat{a}+\epsilon}(\theta)$ since, by definition of $\widehat{a}$, one has

$$\frac{\langle \theta, x\rangle}{\|x\|} = 1 - 2\widehat{a} > 1 - 2(\widehat{a} + \epsilon),$$

which is a contradiction to (5.12). Hence, the assumption $a \notin A$ is false, and thus, the maximum is well-defined. □

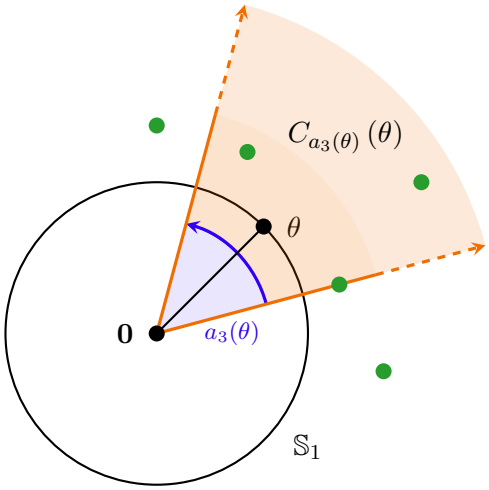

Fig. 5.3: Visualization of a cone ($d = 2$) in direction θ with aperture $a_n(\theta)$ for $n = 3$, as specified by Lemma 5.13. The knots in X are indicated by *green* dots. The aperture is chosen such that each cone with a larger aperture contains at least n knots.

Note that the consideration of *open* cones is essential for the preceding Lemma. The maximum does not exist in general when considering *closed* cones. A cone that is maximal in terms of Lemma 5.13 is depicted in Figure 5.3.

Corollary 5.14. For any $\theta \in \mathbb{S}_{d-1}$, $n \in \mathbb{N}_+$ and for all $\epsilon > 0$, one has

$$\left| C_{a_n(\theta)+\epsilon}(\theta) \cap X \right| \geq n.$$

Proof. Assume that $|C_{a_n(\theta)+\epsilon}(\theta) \cap X| < n$ for an $\epsilon > 0$, and define A as in Lemma 5.13. Then, $a_n(\theta) + \epsilon \in A$. Due to $a_n(\theta) + \epsilon > a_n(\theta)$, this is a contradiction to the definition of $a_n(\theta)$. □

Corollary 5.15. Let $\theta \in \mathbb{S}_{d-1}$, $n \in \mathbb{N}_+$, and $a \in [0, 1]$. If $|C_a(\theta) \cap X| \geq n$, there is an $\epsilon > 0$ such that $|C_{a-\epsilon}(\theta) \cap X| \geq n$.

Proof. Assume that the claim does not hold true. Then, for all $\epsilon > 0$, one has $|C_{a-\epsilon}(\theta) \cap X| < n$. Hence, $a \leq \sup A$, where A is again defined as in Lemma 5.13. The latter provides $a \leq \max A$, and therefore, $a \in A$, which yields the contradiction $|C_a(\theta) \cap X| < n$. Consequently, the assumption is incorrect, and one can find a suitable $\epsilon > 0$. □

We can use the assumption $\operatorname{conv}(X) = \mathbb{R}^d$ now to ensure that $a_n(\theta)$ is strictly smaller than $1/2$ for every direction $\theta \in \mathbb{S}_{d-1}$ and for all $n \in \mathbb{N}_+$.

Proposition 5.16. If X satisfies the strong conditions, then, for all $\theta \in \mathbb{S}_{d-1}$ and for any $n \in \mathbb{N}_+$, one has $a_n(\theta) < 1/2$.

Proof. Let $n \in \mathbb{N}_+$, and assume that there is a $\theta \in \mathbb{S}_{d-1}$ with $a_n(\theta) \geq 1/2$. The cone $C_{1/2}(\theta)$ is an open half space, which will be called H. Consequently,

$$n > \left|C_{a_n(\theta)}(\theta) \cap X\right| \geq \left|C_{1/2}(\theta) \cap X\right| = |H \cap X|. \tag{5.13}$$

Without loss of generality, assume that $H = \{u \in \mathbb{R}^d \mid u_1 > 0\}$. Choose

$$x_1^* := \begin{cases} 0 & \text{if } H \cap X = \emptyset, \\ \max\{x_1 \mid x \in H \cap X\} & \text{otherwise,} \end{cases}$$

which is well-defined due to the finiteness of $H \cap X$, according to (5.13). Hence, for all $x \in X$, one has $x_1 \leq x_1^*$ by definition of x_1^* and H, respectively. Let $t \in \operatorname{conv}(X)$. Then, there is a family $(\mu_x)_{x \in X}$ in $\mathbb{R}$ satisfying

$$t = \sum_{x \in X} \mu_x x, \quad \sum_{x \in X} \mu_x = 1, \quad \text{and} \quad \mu_x \geq 0 \text{ for all } x \in X.$$

Consequently,

$$t_1 = \sum_{x \in X} \mu_x x_1 \leq \sum_{x \in X} \mu_x x_1^* = x_1^* \sum_{x \in X} \mu_x = x_1^*,$$

and hence,

$$\operatorname{conv}(X) \subseteq \{u \in \mathbb{R}^d \mid u_1 \leq x_1^*\} \subset \mathbb{R}^d,$$

which is a contradiction to $\operatorname{conv}(X) = \mathbb{R}^d$. Therefore, the assumption is incorrect, yielding that one has $a_n(\theta) < 1/2$ for all $\theta \in \mathbb{S}_{d-1}$. □

5.2.3 Uniformity of Density Cones

The next goal is to find a global upper bound for $a_n(\cdot)$ that is independent of the direction on the one hand and smaller than $1/2$ on the other hand. Proposition 5.16 ensures that we can find an appropriate bound for any direction. As there is an infinite number of directions, we cannot just take the maximum, though. It is clear that $1/2$ is an upper bound, but the following proposition ensures that we can do better and find an upper bound which is strictly smaller than $1/2$.

Proposition 5.17. Let $n \in \mathbb{N}_+$, and let $X \subseteq \mathbb{R}^d$ satisfy the strong conditions. There is an $a \in (0, 1/2)$ such that, for all $\theta \in \mathbb{S}_{d-1}$, one has $|C_a(\theta) \cap X| \geq n$.

Proof. Assume that the claim does not hold true. Then, for all $a \in (0, 1/2)$, one can find a $\theta \in \mathbb{S}_{d-1}$ such that $|C_a(\theta) \cap X| < n$. Since

$$\frac{1}{2} - \frac{1}{4k} \in \left(0, \frac{1}{2}\right) \quad \text{for all } k \in \mathbb{N}_+,$$

there is a sequence $(\theta_k)_{k\in\mathbb{N}_+}$ in $\mathbb{S}_{d-1}$ such that

$$\left|C_{\left(\frac{1}{2}-\frac{1}{4k}\right)}(\theta_k) \cap X\right| < n \quad \text{for all } k \in \mathbb{N}_+. \tag{5.14}$$

As $\mathbb{S}_{d-1}$ is compact, this sequence has a convergent subsequence $(\theta_{k_\ell})_{\ell\in\mathbb{N}_+}$ with limit $\theta^* \in \mathbb{S}_{d-1}$. Proposition 5.16 provides that

$$a' := \max\Big\{a \in [0,1] \;\Big|\; |C_a(\theta^*) \cap X| < n\Big\} < \frac{1}{2}.$$

Let $a^* := a'/2 + 1/4$. Then, one has $a' < a^* < 1/2$. Thus, Corollary 5.14 yields

$$|C_{a^*}(\theta^*) \cap X| \geq n. \tag{5.15}$$

Let $\epsilon := 1/2 - a^* > 0$. Since $(\theta_{k_\ell})_{\ell\in\mathbb{N}_+}$ converges to θ^*, it follows from the continuity of $\langle \cdot, \theta^* \rangle$ that

$$\lim_{\ell\to\infty} \langle \theta_{k_\ell}, \theta^* \rangle = \left\langle \lim_{\ell\to\infty} \theta_{k_\ell}, \theta^* \right\rangle = \|\theta^*\|^2 = 1.$$

Hence, there is an $\widetilde{\ell} \in \mathbb{N}_+$ such that $\langle \theta^*, \theta_{k_\ell} \rangle > 1 - \epsilon^2/2$ for all $\ell \geq \widetilde{\ell}$. Choose $\ell^* \in \mathbb{N}_+$ such that

$$k_{\ell^*} \geq \max\left\{\frac{1}{2\epsilon}, k_{\widetilde{\ell}}\right\}.$$

Then, $1/k_{\ell^*} \leq 2\epsilon$. We claim now that

$$C_{a^*}(\theta^*) \subseteq C_{\frac{1}{2}-\frac{1}{4k_{\ell^*}}}(\theta_{k_{\ell^*}}). \tag{5.16}$$

To that end, let $t \in C_{a^*}(\theta^*)$. As a consequence of

$$\|\theta^* - \theta_{k_{\ell^*}}\|^2 = 2 - 2\langle \theta^*, \theta_{k_{\ell^*}} \rangle < \epsilon^2$$

and the Cauchy-Schwarz inequality, one obtains

$$\begin{aligned}\frac{\langle t, \theta_{k_{\ell^*}} \rangle}{\|t\|} = \frac{\langle t, \theta^* \rangle - \langle t, \theta^* - \theta_{k_{\ell^*}} \rangle}{\|t\|} &\geq 1 - 2a^* - \|\theta^* - \theta_{k_{\ell^*}}\| \\ &> 1 - 2a^* - \epsilon = \epsilon \geq \frac{1}{2k_{\ell^*}} = 1 - 2\left(\frac{1}{2} - \frac{1}{4k_{\ell^*}}\right),\end{aligned}$$

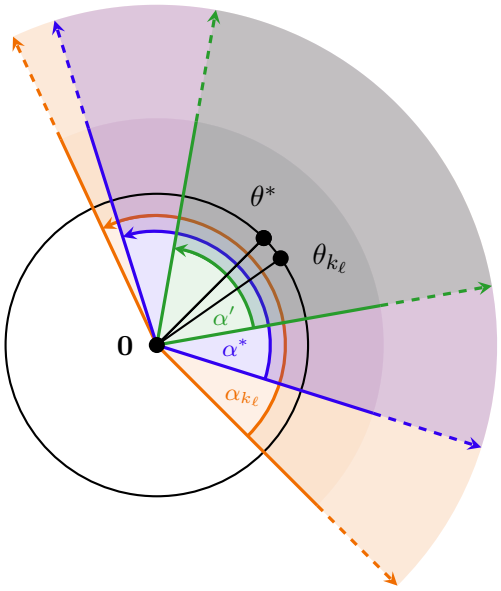

Fig. 5.4: The key idea in the proof of Proposition 5.17. At some point of the convergent subsequence of "counterexamples", the corresponding cone *(orange)*, which contains less than n knots, encloses the cone $C_{a^*}(\theta^*)$ *(blue)*, which is by definition a proper superset of the limit cone $C_{a'}(\theta^*)$ *(green)* and, therefore, contains at least n knots, yielding a contradiction.

and thus, (5.16) holds true. Together with (5.15) and (5.14), this yields the contradiction

$$n \leq |C_{a^*}(\theta^*) \cap X| \leq \left| C_{\frac{1}{2} - \frac{1}{4k_{\ell^*}}}(\theta_{k_{\ell^*}}) \cap X \right| < n.$$

Hence, the assumption is false, and one can find a suitable $a \in (0, 1/2)$. □

The key idea of the previous proof is the construction of a sequence of cones whose apertures grow towards $1/2$ and whose directions converge to the axis of some limit cone. The contradiction then follows from the fact that, for a sufficiently large index, the cones of the sequence enclose the limit cone, as depicted in Figure 5.4.

The same strategy can be used to show that we can also find an $R \in \mathbb{R}_+$ such that each cone with an aperture as specified by the previous proposition contains at least $n \in \mathbb{N}_+$ knots within a distance to the apex / origin of at most R:

Proposition 5.18. Let $n \in \mathbb{N}_+$, and let $X \subseteq \mathbb{R}^d$ satisfy the strong conditions. There is an $a \in (0, 1/2)$ and an $R \in \mathbb{R}_+$ such that

$$|C_a(\theta) \cap B_R(\mathbf{0}) \cap X| \geq n \quad \text{for all } \theta \in \mathbb{S}_{d-1}.$$

Proof. Proposition 5.17 ensures the existence of an $a \in (0, 1/2)$ such that

$$|C_a(\theta) \cap X| \geq n \quad \text{for all } \theta \in \mathbb{S}_{d-1}.$$

Assume that we cannot find an appropriate $R \in \mathbb{R}_+$. Then, for all $R \in \mathbb{R}_+$, we can find a $\theta_R \in \mathbb{S}_{d-1}$ such that $|C_a(\theta_R) \cap B_R(\mathbf{0}) \cap X| < n$. By picking any of these directions for a given radius, one can construct a sequence $(\theta_k)_{k\in\mathbb{N}_+}$ in $\mathbb{S}_{d-1}$ satisfying

$$|C_a(\theta_k) \cap B_k(\mathbf{0}) \cap X| < n \quad \text{for all } k \in \mathbb{N}_+. \tag{5.17}$$

As $\mathbb{S}_{d-1}$ is compact, this sequence has a convergent subsequence $(\theta_{k_\ell})_{\ell\in\mathbb{N}_+}$ with limit $\theta^* \in \mathbb{S}_{d-1}$. Since $|C_a(\theta^*) \cap X| \geq n$, Corollary 5.15 yields the existence of an $\epsilon > 0$ such that $|C_{a-\epsilon}(\theta^*) \cap X| \geq n$. Thus, one can find an $R^* \in \mathbb{R}_+$ such that

$$|C_{a-\epsilon}(\theta^*) \cap B_{R^*}(\mathbf{0}) \cap X| \geq n. \tag{5.18}$$

The sequence $(\theta_{k_\ell})_{\ell\in\mathbb{N}_+}$ converges to θ^*, and therefore, it follows in the same way as in the proof of Proposition 5.17 that one can find an $\widetilde{\ell} \in \mathbb{N}_+$ such that

$$\langle \theta_{k_\ell}, \theta^* \rangle > 1 - 2\epsilon^2 \quad \text{for all } \ell \geq \widetilde{\ell}. \tag{5.19}$$

Choose $\ell^* \in \mathbb{N}_+$ such that $k_{\ell^*} \geq \max\{k_{\widetilde{\ell}}, R^*\}$. We claim now that

$$C_{a-\epsilon}(\theta^*) \subseteq C_a(\theta_{k_{l^*}}). \tag{5.20}$$

To that end, let $t \in C_{a-\epsilon}(\theta^*)$. Together with

$$\|\theta^* - \theta_{k_{\ell^*}}\|^2 = 2 - 2\langle \theta^*, \theta_{k_{\ell^*}} \rangle < 4\epsilon^2$$

and the Cauchy-Schwarz inequality, one obtains

$$\frac{\langle t, \theta_{k_{\ell^*}} \rangle}{\|t\|} = \frac{\langle t, \theta^* \rangle - \langle t, \theta^* - \theta_{k_{\ell^*}} \rangle}{\|t\|} > 1 - 2(a - \epsilon) - \|\theta^* - \theta_{k_{\ell^*}}\| > 1 - 2a.$$

Consequently, $t \in C_a(\theta_{k_{\ell^*}})$, and therefore, (5.20) holds true, which, together with (5.18), the definition of k_{ℓ^*}, and (5.17), yields the contradiction

$$\begin{aligned} n &\leq |C_{a-\epsilon}(\theta^*) \cap B_{R^*}(\mathbf{0}) \cap X| \leq \left|C_{a-\epsilon}(\theta^*) \cap B_{k_{\ell^*}}(\mathbf{0}) \cap X\right| \\ &\leq \left|C_a(\theta_{k_{\ell^*}}) \cap B_{k_{\ell^*}}(\mathbf{0}) \cap X\right| < n. \end{aligned}$$

As a consequence, the assumption is incorrect, yielding the existence of an appropriate $R \in \mathbb{R}_+$. □

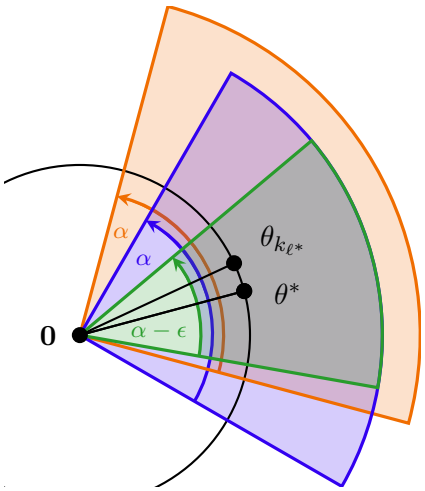

Fig. 5.5: The key idea in the proof of Proposition 5.18. Despite being a proper subset of the cone $C_a(\theta^*)$ *(blue)*, the cone $C_{a-\epsilon}(\theta^*)$ *(green)* still contains at least n knots within a certain radius. However, for a sufficiently large index l^* in the convergent subsequence of "counterexamples", the corresponding cone *(orange)* encloses the cone $C_{a-\epsilon}(\theta^*)$, which is a contradiction to the assumption that every counterexample contains less than n knots within an even larger radius.

The situation in the preceding proposition is presented in Figure 5.5.

5.3 Geometry of Cones and Balls

In the previous section, we ensured that, for all $n \in \mathbb{N}_+$, we can find a distance and an aperture such that each cone with this aperture contains at least n knots within that distance from the apex, independently of the direction of the cone.

Delaunay configurations are based on balls instead of cones, though. Hence, we show several geometric results in this section regarding cones, balls, and the interactions between them. Many of the results appear obvious for $d \in \{2, 3\}$. However, proofs are still necessary since we consider an arbitrary number of dimensions and geometric intuition is very limited for $d > 3$. Many of the proofs can be simplified considerably by specific assumptions that do not limit the overall generality.

5.3.1 Geometry of Balls

We start with a formula for the center of a circumcircle through $d + 1$ points in the case that all but one point take certain positions:

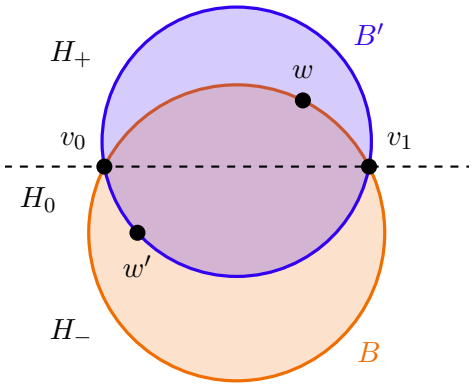

Fig. 5.6: Points, circles, and half spaces as introduced by Lemma 5.20, which examines the subset relations between the balls B and B' in the half spaces H_+ and H_-

Lemma 5.19. Consider $v_0, \dots, v_d \in \mathbb{R}^d$ such that

$$v_0 = -\mathbf{e}_1, \quad v_1 = \mathbf{e}_1, \quad v_2 = \mathbf{e}_2, \quad \dots, \quad v_{d-1} = \mathbf{e}_{d-1} \quad \in \mathbb{R}^d.$$

If $v_0, \dots, v_d$ are affinely independent, the center of the circumcircle $B(v_0, \dots, v_d)$ is given as

$$c := (0, \dots, 0, \widehat{c})^\intercal \in \mathbb{R}^d, \quad \text{where } \widehat{c} := \frac{\|v_d\|^2 - 1}{2v_{d,d}},$$

and its radius is $\sqrt{\widehat{c}^2 + 1}$.

Proof. We can assume that $v_{d,d} \neq 0$ since, otherwise, the $d+1$ points would lie in a $(d-1)$-dimensional hyperplane and, thus, would not be affinely independent. Hence, the denominator in the expression for $\widehat{c}$ is nonzero.

It is clear that $\|v_i - c\|^2 = \widehat{c}^2 + 1$ for all $i \in \{0, \dots, d-1\}$. But also for v_d, one has

$$\|v_d - c\|^2 = \sum_{i=1}^{d-1} v_{d,i}^2 + (v_{d,d} - \widehat{c})^2 = \sum_{i=1}^{d-1} v_{d,i}^2 + v_{d,d}^2 - \frac{2v_{d,d}(\|v_d\|^2 - 1)}{2v_{d,d}} + \widehat{c}^2 = \widehat{c}^2 + 1,$$

which yields the stated claim. □

Next, we use the formula shown in the previous Lemma to derive certain subset relationships between two circumcircles generated by sets that only differ by one point, as visualized in Figure 5.6.

Lemma 5.20. Let $v'_0, \dots, v'_{d-1} \in \mathbb{R}^d$ be affinely independent and $w, w' \in \mathbb{R}^d \backslash H_0$, where $H_0 := \operatorname{aff}(v'_0, \dots, v'_{d-1})$. The hyperplane H_0 divides $\mathbb{R}^d$ into two open half

spaces H_+, H_-, indexed such that $w' \in H_-$. The following statements are equivalent:

(i) $w' \in B\Big(w, v'_0, \ldots, v'_{d-1}\Big)$,

(ii) $\overline{B\Big(w', v'_0, \ldots, v'_{d-1}\Big)} \cap H_- \subseteq B\Big(w, v'_0, \ldots, v'_{d-1}\Big) \cap H_-$,

(iii) $\overline{B\Big(w, v'_0, \ldots, v'_{d-1}\Big)} \cap H_+ \subseteq B\Big(w', v'_0, \ldots, v'_{d-1}\Big) \cap H_+$.

Proof. Since $w, w' \notin \operatorname{aff}(v'_0, \ldots, v'_{d-1})$, it is clear that the two sets $\{w, v'_0, \ldots, v'_{d-1}\}$ and $\{w', v'_0, \ldots, v'_{d-1}\}$ are affinely independent and, therefore, give rise to circumcircles. Without loss of generality, assume that

$$H_0 = \{t \in \mathbb{R}^d \mid t_d = 0\} \quad \text{and} \quad H_+ = \{t \in \mathbb{R}^d \mid t_d > 0\}.$$

The points $v'_0, \ldots, v'_{d-1}$ give rise to a hypersphere which is contained in H_0. Further, we can assume without loss of generality that, for this hypersphere, one has

$$\operatorname{rad}(v'_0, \ldots, v'_{d-1}) = 1 \quad \text{and} \quad \operatorname{cen}(v'_0, \ldots, v'_{d-1}) = \mathbf{0},$$

where rad and cen denote radius and center, respectively, of the circumcircle generated by the given points. We consider the points

$$v_0 := -\mathbf{e}_1, \quad v_1 := \mathbf{e}_1, \quad v_2 := \mathbf{e}_2, \quad \ldots, \quad v_{d-1} := \mathbf{e}_{d-1} \quad \in \mathbb{R}^d.$$

It is easy to see that $v_0, \ldots, v_{d-1} \in \partial B(v'_0, \ldots, v'_{d-1})$ and that these points are affinely independent. Consequently, $B(v_0, \ldots, v_{d-1}) = B(v'_0, \ldots, v'_{d-1})$, and also

$$\begin{aligned} B &:= B(w, v_0, \ldots, v_{d-1}) = B(w, v'_0, \ldots, v'_{d-1}), \\ B' &:= B(w', v_0, \ldots, v_{d-1}) = B(w', v'_0, \ldots, v'_{d-1}). \end{aligned}$$

Hence, we can work with $v_0, \ldots, v_{d-1}$ instead of $v'_0, \ldots, v'_{d-1}$ from now on and, thus, can apply Lemma 5.19 to obtain that

$$\begin{aligned} b &:= \operatorname{cen}(w, v_0, \ldots, v_{d-1}) = (0, \ldots, 0, \widehat{b})^\intercal, \\ c &:= \operatorname{cen}(w', v_0, \ldots, v_{d-1}) = (0, \ldots, 0, \widehat{c})^\intercal, \\ r &:= \operatorname{rad}(w, v_0, \ldots, v_{d-1}) = \sqrt{\widehat{b}^2 + 1}, \\ s &:= \operatorname{rad}(w', v_0, \ldots, v_{d-1}) = \sqrt{\widehat{c}^2 + 1}, \end{aligned}$$

where

$$\widehat{b} = \frac{\|w\|^2 - 1}{2w_d} \quad \text{and} \quad \widehat{c} = \frac{\|w'\|^2 - 1}{2w'_d}.$$

"(i) $\Rightarrow$ (iii)" Let $u \in \overline{B} \cap H_+$. Then, $u_d > 0$ and $\|u - b\|^2 \leq r^2$. Consequently,

$$\|u\|^2 - 1 = \|u - b\|^2 + 2\widehat{b}u_d - \widehat{b}^2 - 1 = \|u - b\|^2 - r^2 + 2\widehat{b}u_d \leq 2\widehat{b}u_d. \tag{5.21}$$

Since $w' \in B$, it follows as in (5.21) that $\|w'\|^2 - 1 < 2\widehat{b}w'_d$. Furthermore, we have chosen H_- such that $w' \in H_-$, yielding $w'_d < 0$. As a consequence,

$$\begin{aligned}
\|u - c\|^2 &= \|u\|^2 + \widehat{c}^2 - \frac{u_d}{w'_d}(\|w'\|^2 - 1) \\
&< \|u\|^2 + \widehat{c}^2 - 2\widehat{b}u_d \\
&\leq \|u\|^2 + \widehat{c}^2 - (\|u\|^2 - 1) \\
&= s^2,
\end{aligned}$$

and thus, $\overline{B} \cap H_+ \subseteq B'$.

"(iii) $\Rightarrow$ (ii)" We set $z := (0, \ldots, 0, \widehat{b} + r) \in \mathbb{R}^d$. Then,

$$\|z - b\|^2 = r^2 \quad \text{and} \quad z_d = \widehat{b} + \sqrt{\widehat{b}^2 + 1} > \widehat{b} + |\widehat{b}| \geq 0.$$

Therefore, $z \in \partial B \cap H_+$ and, in particular, $z \notin H_0$. Hence, the points $v_0, \ldots, v_{d-1}, z$ are affinely independent, and their circumcircle is given as $B(v_0, \ldots, v_{d-1}, z) = B$. Thus, also the centers of both spheres coincide, yielding with Lemma 5.19 that

$$\widehat{b} = \frac{\|z\|^2 - 1}{2z_d}.$$

From the assumption that (iii) holds true, one obtains $z \in \overline{B} \cap H_+ \subseteq B' \cap H_+$. Similar to (5.21), this can be expressed by the inequality $\|z\|^2 - 1 < 2\widehat{c}z_d$. Now, let $u \in \overline{B'} \cap H_-$, i.e., $\|u\|^2 - 1 \leq 2\widehat{c}u_d$ and $u_d < 0$. Then,

$$\begin{aligned}
\|u - b\|^2 &= \|u\|^2 - \frac{u_d}{z_d}(\|z\|^2 - 1) + \widehat{b}^2 \\
&< \|u\|^2 - 2\widehat{c}u_d + \widehat{b}^2 \\
&\leq \|u\|^2 - (\|u\|^2 - 1) + \widehat{b}^2 \\
&= r^2,
\end{aligned}$$

and therefore, $u \in B$, which yields the stated claim.

"(ii) $\Rightarrow$ (i)" It directly follows from (ii) that $w' \in B$, which finishes the proof. $\square$

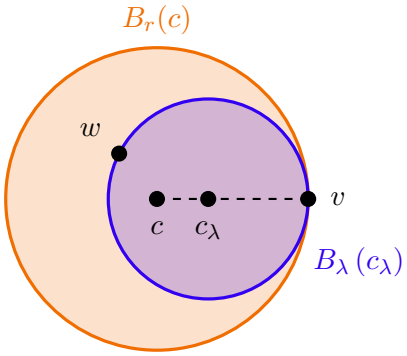

Fig. 5.7: The situation in the proof of Lemma 5.22. All circles $B_\lambda(c_\lambda)$ *(blue)* passing through v are contained in the circle $B_r(c)$ *(orange)* if $c_\lambda \in \operatorname{conv}(c, v)$. For a particular choice of λ, one can ensure additionally that $B_\lambda(c_\lambda)$ passes through w.

In the previous proof, we made assumptions and claimed that they do not reduce its generality. The assumption on position and orientation of the hyperplane H_0 takes several rotational degrees of freedom and one translational degree of freedom, whereas the assumption on H_+ determines the flip along H_0. The assumption on the radius can be fulfilled by appropriate scaling, and positioning the center in the origin within the hyperplane H_0 consumes the remaining $d-1$ translational degrees of freedom. Hence, each set of points can be forced to fulfill all assumptions by a transformation containing a rotation, a translation, scaling, and in some circumstances a reflection. As subset relations are invariant under such transformations, the assumptions do not diminish the generality of the proof.

We add another two results regarding the subset relationship between certain balls, which will only be used in the next section but fit into the current context.

Lemma 5.21. Let $c, c' \in \mathbb{R}^d$, $r, r' \in \mathbb{R}_+$ such that there exists a $v \in \partial B_r(c) \cap \partial B_{r'}(c')$. If there is a $\lambda \in \mathbb{R}$ with $\lambda \geq 1$ and $(c' - v) = \lambda(c - v)$, it follows that $B_r(c) \subseteq B_{r'}(c')$.

Proof. Without loss of generality, assume that $c = (0, \ldots, 0)^\intercal$ and $v = (1, 0, \ldots, 0)^\intercal$. It follows that

$$c' = (1 - \lambda, 0, \ldots, 0)^\intercal, \quad r = 1, \quad r' = \lambda.$$

Let $w \in B_r(c)$. Then, $\|w\| < 1$ and, in particular, $w_1 < 1$. With $\lambda \geq 1$, it follows that

$$\|w - c'\|^2 = \|w\|^2 - 2(1-\lambda)w_1 + (1-\lambda)^2 < 1 - 2(1-\lambda) + (1-\lambda)^2 = r'^2,$$

and therefore, $w \in B_{r'}(c')$, yielding the stated claim. □

Lemma 5.22. Let $c \in \mathbb{R}^d$, $r \in \mathbb{R}_+$, $v \in \partial B_r(c)$, and $w \in \overline{B_r(c)}$. Then, there are $c' \in \operatorname{conv}(c, v)$ and $r' \in \mathbb{R}_+$ such that

$$v, w \in \partial B_{r'}(c') \quad \text{and} \quad B_{r'}(c') \subseteq B_r(c).$$

Proof. If $w \in \partial B_r(c)$, the claim follows directly by choosing $c' = c$ and $r' = r$. Hence, it is sufficient to consider the case $w \in B_r(c)$.

Without loss of generality, assume that $c = (0, \dots, 0)^\intercal$ and $v = (1, 0, \dots, 0)^\intercal$, so that $r = 1$. For all $\lambda \in (0, 1)$, define $c_\lambda := (1 - \lambda, 0, \dots, 0)^\intercal$, so that $v \in \partial B_\lambda(c_\lambda)$. Let $\lambda \in (0, 1)$ and $u \in B_\lambda(c_\lambda)$. One has $1 - u_1 > 0$ since, otherwise, the inequality

$$\|u - c_\lambda\|^2 - \lambda^2 \geq (u_1 - 1 + \lambda)^2 - \lambda^2 = u_1^2 - 2u_1 + 1 - 2\lambda(1 - u_1) \geq (u_1 - 1)^2 \geq 0$$

would yield the contradiction $u \notin B_\lambda(c_\lambda)$. Consequently,

$$\begin{aligned} \|u\|^2 &= \|u - c_\lambda\|^2 - (1 - \lambda)^2 + 2u_1(1 - \lambda) < \lambda^2 - (1 - \lambda)^2 + 2u_1(1 - \lambda) \\ &= 1 - 2(1 - \lambda)(1 - u_1) < 1, \end{aligned}$$

which provides $B_\lambda(c_\lambda) \subseteq B_r(c)$ for all $\lambda \in (0, 1)$. The claim is proved if we can find a specific $\lambda \in (0, 1)$ with $w \in \partial B_\lambda(c_\lambda)$. We make the particular choice

$$\lambda := 1 - \frac{1 - \|w\|^2}{2(1 - w_1)}.$$

As we assumed that $w \in B_r(c)$, we have $\|w\| < 1$ and, in particular, $w_1 < 1$. Then, $\lambda \in (0, 1)$ since, on the one hand, both nominator and denominator are positive and, on the other hand,

$$\lambda \geq 1 - \frac{1 - w_1^2}{2(1 - w_1)} = 1 - \frac{1 + w_1}{2} > 0.$$

Furthermore, we have

$$\begin{aligned} \|w - c_\lambda\|^2 &= \|w\|^2 + \frac{w_1(\|w\|^2 - 1)}{1 - w_1} + (1 - \lambda)^2 \\ &= 1 + \frac{(1 - w_1)(\|w\|^2 - 1) + w_1(\|w\|^2 - 1)}{1 - w_1} + (1 - \lambda)^2 \\ &= 1 + \frac{\|w\|^2 - 1}{1 - w_1} + (1 - \lambda)^2 \\ &= 1 - 2(1 - \lambda) + (1 - \lambda)^2 \\ &= \lambda^2, \end{aligned}$$

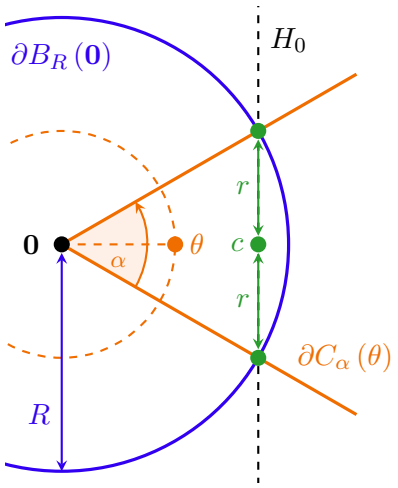

Fig. 5.8: The intersection of the boundary of a cone *(orange)* with apex in the origin and a sphere *(blue)* with center in the origin is a sphere *(green)* in the $(d-1)$-dimensional affine subspace H_0. Note that a sphere in one dimension, like $\partial B_r^{H_0}(c)$ in this example, just consists of two points.

and therefore, $w \in \partial B_\lambda(c_\lambda)$, which shows that $B_\lambda(c_\lambda)$ satisfies all conditions stated in the claim. □

A visualization of the preceding Lemma is presented in Figure 5.7.

5.3.2 Interactions of Cones and Balls

After showing several properties of balls, we now aim at a formulation of the main result of the previous section, Proposition 5.18, in terms of balls instead of cones. To that end, several geometric preparations are necessary. The following result is a direct consequence of the Minkowski theorem (see [Brø83, p. 35f] or [Roc70, p. 167], for example).

Lemma 5.23. Let $A \subseteq \mathbb{R}^d$ be compact and convex. Then, $\operatorname{conv}(\partial A) = A$. ◀

For $c \in H_0$, $r \in \mathbb{R}_+$, and some hyperplane $H_0 \subseteq \mathbb{R}^d$, let $B_r^{H_0}(c) := B_r(c) \cap H_0$ denote the restriction of the ball $B_r(c)$ to H_0. In the expression $\partial B_r^{H_0}(c)$, we consider the relative boundary with respect to H_0 instead of the boundary with respect to the topological space $\mathbb{R}^d$.

In the next Lemma, which is visualized in Figure 5.8, we examine the intersection of a sphere and the boundary of a cone.

Lemma 5.24. Let $\theta \in \mathbb{S}_{d-1}$, $a \in (0,1)$, and $R \in \mathbb{R}_+$. Define

$$c := R(1-2a)\theta, \quad r := R\sqrt{1-(1-2a)^2}, \quad H_0 := \{w \in \mathbb{R}^d \mid \langle w-c, \theta\rangle = 0\}.$$

Then, one has

$$A := \partial C_a(\theta) \cap \partial B_R(\mathbf{0}) = \partial B_r^{H_0}(c).$$

Proof. "$\subseteq$" Let $v \in A$. Then, $\|v\| = R$ and $\langle v, \theta\rangle/\|v\| = 1-2a$, according to Proposition 5.12. Consequently,

$$\begin{aligned}\|v-c\|^2 &= \|v\|^2 - 2\langle v, c\rangle + \|c\|^2 \\ &= R^2 - 2R(1-2a)\langle v, \theta\rangle + R^2(1-2a)^2 \\ &= r^2,\end{aligned}$$

which shows that, in fact, A is a sphere of radius r around c. This sphere is restricted to the lower-dimensional affine subspace H_0 since

$$\langle v-c, \theta\rangle = (1-2a)\|v\| - R(1-2a)\langle \theta, \theta\rangle = 0.$$

"$\supseteq$" Conversely, every point $w \in \mathbb{R}^d$ satisfying $\langle w-c, \theta\rangle = 0$ and $\|w-c\| = r$ is an element of A, which can be seen by

$$\begin{aligned}\|w\|^2 &= \|w-c\|^2 + \|c\|^2 + 2\langle w-c, c\rangle \\ &= R^2\Big(1-(1-2a)^2\Big) + R^2(1-2a)^2 + 2R(1-2a)\langle w-c, \theta\rangle = R^2\end{aligned}$$

and

$$\frac{\langle w, \theta\rangle}{\|w\|} = \frac{\langle w-c, \theta\rangle + \langle c, \theta\rangle}{R} = \frac{R(1-2a)}{R}\langle \theta, \theta\rangle = (1-2a).$$

□

As shown in the previous Lemma, the intersection of a sphere with the boundary of a cone yields a lower-dimensional sphere whose affine hull is a hyperplane. We state now that the intersection of the cone with one of the closed half spaces generated by this hyperplane can be expressed as convex hull of certain points if $a < 1/2$:

Lemma 5.25. Let $\theta \in \mathbb{S}_{d-1}$, $a \in (0, 1/2)$, $R \in \mathbb{R}_+$, and $A := \partial C_a(\theta) \cap \partial B_R(\mathbf{0})$. The hyperplane $H_0 := \mathrm{aff}(A)$ generates two open half spaces H_+, H_-, numbered such that $\mathbf{0} \in H_+$. Let $H := H_0 \cup H_+$. Then,

$$\overline{C_a(\theta)} \cap H = \mathrm{conv}(A \cup \{\mathbf{0}\}).$$

Proof. Lemma 5.24 ensures that $\dim \operatorname{aff}(A) = d-1$, and therefore, the half spaces are well-defined. Additionally, it confirms that A is a $(d-1)$-dimensional sphere in H_0, i.e., $A = \partial B_r^{H_0}(c)$, where H_0, the center $c \in H_0$, and the radius $r \in \mathbb{R}_+$ are specified by Lemma 5.24.

"$\supseteq$": Due to $a < 1/2$, it follows with Proposition 5.10 that $\overline{C_a(\theta)}$ is convex. Together with the convexity of H, it follows that $\overline{C_a(\theta)} \cap H$ as intersection of convex sets is also convex. From $A \cup \{\mathbf{0}\} \subseteq \overline{C_a(\theta)} \cap H$ and the fact that $\operatorname{conv}(A \cup \{\mathbf{0}\})$ is the smallest convex set containing A and $\mathbf{0}$, one obtains that $\operatorname{conv}(A \cup \{\mathbf{0}\}) \subseteq \overline{C_a(\theta)} \cap H$.

"$\subseteq$": Assume without loss of generality that $\theta = (0, \dots, 0, 1) \in \mathbb{S}_{d-1}$, and choose an arbitrary $v \in \overline{C_a(\theta)} \cap H$. If $v = \mathbf{0}$, the claim follows immediately. Hence, we consider the case $v \neq \mathbf{0}$ now. Definition 5.6 yields

$$v_d = \langle \theta, v \rangle \geq (1-2a)\|v\| > 0.$$

From $\langle w - c, \theta \rangle = w_d - R(1-2a)$ for all $w \in \mathbb{R}^d$, it follows that

$$H_0 = \Big\{ w \in \mathbb{R}^d \;\Big|\; w_d = R(1-2a) \Big\}.$$

Hence, $v_d = R(1-2a)$ if $v \in H_0$. In the case $v \in H_+$, one obtains

$$\operatorname{sgn}(v_d - R(1-2a)) = \operatorname{sgn}\langle v - c, \theta \rangle = \operatorname{sgn}\langle \mathbf{0} - c, \theta \rangle = \operatorname{sgn}(-R(1-2a)) = -1$$

due to $\mathbf{0} \in H_+$ and $R(1-2a) > 0$. As a consequence, one has $v_d \leq R(1-2a)$ in both cases. Let

$$\lambda := \frac{v_d}{R(1-2a)} \in (0,1] \quad \text{and} \quad v' := \frac{1}{\lambda} v,$$

so that $v'_d = R(1-2a)$ and, therefore, $v' \in H_0$. Together with $1/\lambda > 0$ and Remark 5.8, one obtains that $v' \in \overline{C_a(\theta)} \cap H_0$. Next, we claim that $v' \in \overline{B_r^{H_0}(c)}$. Since $v' \in \overline{C_a(\theta)} \backslash \{\mathbf{0}\}$, it follows that

$$\|v'\| \leq \frac{\langle \theta, v' \rangle}{1-2a} = \frac{v'_d}{1-2a} = R,$$

and thus,

$$\|v' - c\|^2 = \big\|v' - R(1-2a)\theta\big\|^2 = \|v'\|^2 - v'^2_d \leq R^2 - R^2(1-2a)^2 = r^2.$$

Consequently, one has $v' \in \overline{B_r^{H_0}(c)}$, which yields together with Lemma 5.23 that $v' \in \overline{B_r^{H_0}(c)} = \operatorname{conv}\Big(\partial B_r^{H_0}(c)\Big) = \operatorname{conv}(A)$. Since $v = \lambda v' + (1-\lambda)\mathbf{0}$ and $\lambda \in (0,1]$, it follows that $v \in \operatorname{conv}(A \cup \{\mathbf{0}\})$, which finishes the proof. □

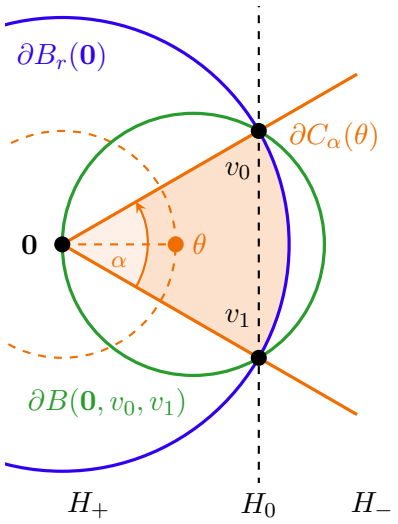

Fig. 5.9: The situation in Proposition 5.26. All knots in the cone $C_a(\theta)$ *(orange)* within a certain radius r *(blue)* of the origin are contained in the ball $\overline{B(\mathbf{0}, v_0, v_1)}$ *(green)*.

Many of the results presented in this section are used in the following proposition, which reveals an important geometric relationship between balls and cones, as pictured in Figure 5.9.

Proposition 5.26. Let $\theta \in \mathbb{S}_{d-1}$, $a \in (0, 1/2)$, and $r \in \mathbb{R}_+$. For each collection of affinely independent points $v_0, \ldots, v_{d-1} \in A := \partial C_a(\theta) \cap \partial B_r(\mathbf{0})$, one has

$$C_a(\theta) \cap \overline{B_r(\mathbf{0})} \subseteq \overline{B(\mathbf{0}, v_0, \ldots, v_{d-1})}.$$

Proof. According to Lemma 5.24, the set A is a sphere in a $(d-1)$-dimensional affine subspace H_0. In particular, this ensures the existence of affinely independent points $v_0, \ldots, v_{d-1} \in A$. From $a < 1/2$, it follows that $\mathbf{0} \notin H_0$. The hyperplane H_0 generates two open half spaces H_+ and H_-, where we choose H_+ such that $\mathbf{0} \in H_+$.

Now, let $u \in C_a(\theta) \cap \overline{B_r(\mathbf{0})}$. We have to distinguish two different cases: First, we assume that $u \in H := H_0 \cup H_+$. Applying Lemma 5.25 yields

$$\overline{C_a(\theta)} \cap H = \operatorname{conv}(A \cup \{\mathbf{0}\}).$$

Since A is a sphere in $d-1$ dimensions, the boundary (relative with respect to H_0) of the circumcircle determined by the affinely independent points $v_0, \ldots, v_{d-1} \in A$

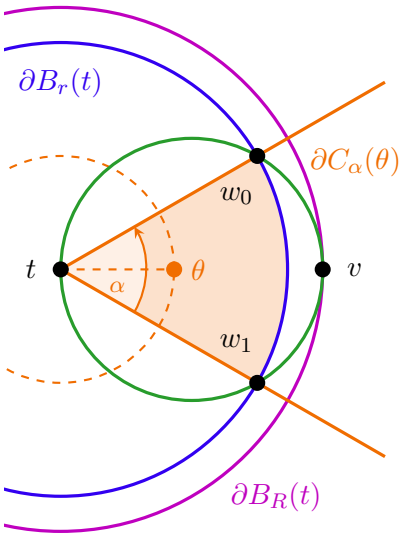

Fig. 5.10: This slightly adapted version of Figure 5.9 visualizes the situation in Proposition 5.27. For any point t, one can find a distance R *(purple)* such that each point v with that distance to t gives rise to a ball *(green)* through t and v with center $(t+v)/2$ containing at least n knots. This is due to the fact that R is chosen such that this ball *(green)* encloses all points in the cone $C_a(\theta)$ *(orange)* within distance r *(blue)* of t. This set contains at least n knots if a and r are chosen appropriately, as ensured by Proposition 5.18.

is exactly the sphere A. Therefore, $A \cup \{\mathbf{0}\} \subseteq \overline{B(\mathbf{0}, v_0, \dots, v_{d-1})}$. The convexity of $\overline{B(\mathbf{0}, v_0, \dots, v_{d-1})}$ yields the stated claim as follows:

$$u \in C_a(\theta) \cap \overline{B_r(\mathbf{0})} \cap H \subseteq \overline{C_a(\theta)} \cap H = \operatorname{conv}(A \cup \{\mathbf{0}\}) \subseteq \overline{B(\mathbf{0}, v_0, \dots, v_{d-1})}.$$

The case $u \in H_-$ remains to be considered. From $\mathbf{0} \in B_r(\mathbf{0}) \cap H_+$, it follows that there is a $w \in \partial B_r(\mathbf{0}) \cap H_+$. In particular, $w \notin H_0$, and thus, the points $v_0, \dots, v_{d-1}, w$ are affinely independent and give rise to a circumcircle. Due to the fact that $v_0, \dots, v_{d-1}, w \in \partial B_r(\mathbf{0})$, the two balls coincide, i.e., $B(v_0, \dots, v_{d-1}, w) = B_r(\mathbf{0})$. In particular, $\mathbf{0} \in B(w, v_0, \dots, v_{d-1}) \cap H_+$. Hence, one can apply Lemma 5.20 to obtain

$$u \in C_a(\theta) \cap \overline{B_r(\mathbf{0})} \cap H_- \subseteq \overline{B(w, v_0, \dots, v_{d-1})} \cap H_- \subseteq \overline{B(\mathbf{0}, v_0, \dots, v_{d-1})},$$

which finishes the proof. □

The previous proposition is the core ingredient in the proof of the following result, which can be considered as an equivalent of Proposition 5.18 using balls instead of cones. After all, this was the goal of the current subsection. We refer to Figure 5.10 for a visualization.

Proposition 5.27. Let $X \subseteq \mathbb{R}^d$ satisfy the strong conditions. Let $t \in \mathbb{R}^d$ and $n \in \mathbb{N}_+$. There is an $R \in \mathbb{R}_+$ such that, for all $v \in \partial B_R(t)$, one has

$$\left|\overline{B_{\frac{R}{2}}\left(\frac{t+v}{2}\right)} \cap X\right| \geq n.$$

Proof. Without loss of generality, assume that $t = \mathbf{0}$. Proposition 5.18 ensures the existence of $r \in \mathbb{R}_+$ and $a \in (0, 1/2)$ such that one has

$$|C_a(\theta) \cap B_r(\mathbf{0}) \cap X| \geq n \quad \text{for all } \theta \in \mathbb{S}_{d-1}. \tag{5.22}$$

Let $R := r/(1-2a)$ and $v \in \partial B_R(\mathbf{0})$. Without loss of generality, assume that $v = (\widehat{v}, 0, \ldots, 0)^\intercal$ with $\widehat{v} > 0$. Let

$$\theta := v/\|v\| = (1, 0, \ldots, 0) \in \mathbb{S}_{d-1}, \quad s := \sqrt{1-(1-2a)^2},$$

and define $w_0, \ldots, w_{d-1} \in \mathbb{R}^d$ as follows:

$$w_0 := \begin{pmatrix} r(1-2a) \\ -rs \\ 0 \\ \vdots \\ 0 \end{pmatrix}, \quad w_1 := \begin{pmatrix} r(1-2a) \\ rs \\ 0 \\ \vdots \\ 0 \end{pmatrix},$$

$$w_2 := \begin{pmatrix} r(1-2a) \\ 0 \\ rs \\ 0 \\ \vdots \\ 0 \end{pmatrix}, \quad \ldots, \quad w_{d-1} := \begin{pmatrix} r(1-2a) \\ 0 \\ \vdots \\ 0 \\ rs \end{pmatrix}.$$

It follows from $1-2a \in (0,1)$ and $r > 0$ that $w_0, \ldots, w_{d-1}$ are linearly independent and, therefore, also that $\mathbf{0}, w_0, \ldots, w_{d-1}$ are *affinely* independent. Consequently, these points give rise to a circumcircle $B(\mathbf{0}, w_0, \ldots, w_{d-1})$. For all $i \in \{0, \ldots, d-1\}$, one has $\|w_i\| = r$ and, consequently,

$$\frac{\langle w_i, \theta \rangle}{\|w_i\|} = 1 - 2a,$$

yielding

$$w_0, \ldots, w_{d-1} \in \partial C_a(\theta) \cap \partial B_r(\mathbf{0}).$$

Thus, one can apply Proposition 5.26 to obtain

$$C_a(\theta) \cap B_r(\mathbf{0}) \subseteq \overline{B(\mathbf{0}, w_0, \dots, w_{d-1})}. \tag{5.23}$$

Since $v \in \partial B_R(\mathbf{0})$ and $\widehat{v} > 0$, one has $\widehat{v} = R$. As a consequence, one obtains for all $i \in \{0, \dots, d-1\}$ that

$$\left\| w_i - \frac{v}{2} \right\|^2 = \left(r(1-2a) - \frac{R}{2} \right)^2 + r^2 \left(1 - (1-2a)^2 \right) = \left(\frac{R}{2} \right)^2.$$

Together with $\|v/2\| = R/2$, this yields

$$\mathbf{0}, w_0, \dots, w_{d-1} \in \partial B_{\frac{R}{2}} \left(\frac{v}{2} \right),$$

and therefore,

$$B(\mathbf{0}, w_0, \dots, w_{d-1}) = B_{\frac{R}{2}} \left(\frac{v}{2} \right),$$

which can be utilized together with (5.23) and (5.22) to obtain

$$\left| \overline{B_{\frac{R}{2}} \left(\frac{t+v}{2} \right)} \cap X \right| = \left| \overline{B(\mathbf{0}, w_0, \dots, w_{d-1})} \cap X \right| \geq |C_a(\theta) \cap B_r(\mathbf{0}) \cap X| \geq n.$$

□

5.4 Local Finiteness Theorem

After the preparations in the previous sections, the goal of the current section is to prove that the local finiteness property holds true if the knot set satisfies the strong conditions specified in Definition 4.15.

5.4.1 Generalization to Compact Sets

So far, we considered cones and circles only to describe the neighborhood of one specific point. However, as stated in the introductory part of this chapter, we aim at a proof of the local finiteness property that holds true for arbitrary compact sets instead of single points.

Most of the work necessary for this generalization is done by the following Lemma, which is again based on the idea of building a sequence of counterexamples and obtaining a contradiction using the limit of a convergent subsequence. To keep track

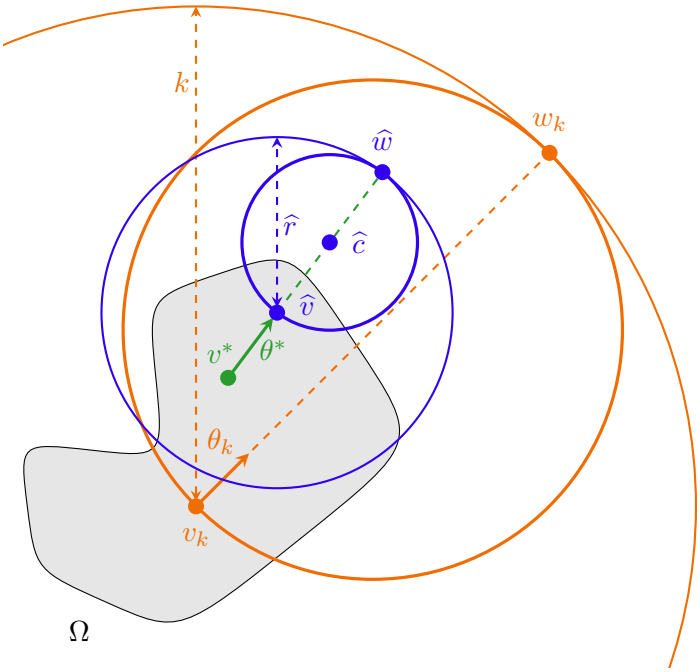

Fig. 5.11: The situation in Lemma 5.28 with compact Ω. The circle with center v_k through w_k with radius k *(orange)* corresponds to an element of the sequence of counterexamples. The limit (v^*, θ^*) *(green)* of a convergent subsequence is used to construct a ball with center $\widehat{c}$ and radius $\widehat{r}/2$ *(blue)* containing at least n knots. If the index k is chosen large enough, this ball is contained in the ball corresponding to the k-th counterexample *(orange)*, which is a contradiction.

of the different quantities used during the course of the proof, we display most of the points and vectors in Figure 5.11.

Lemma 5.28. Let $X \subseteq \mathbb{R}^d$ satisfy the strong conditions. Let $\Omega \subseteq \mathbb{R}^d$ be compact and $n \in \mathbb{N}_+$. There is an $R \in \mathbb{R}_+$ such that, for all $v \in \Omega$ and for all $w \in \partial B_R(v)$, one has

$$\left| B_{\frac{R}{2}}\left(\frac{v+w}{2}\right) \cap X \right| \geq n.$$

Proof. According to Proposition 5.27, one can find an $r(v) \in \mathbb{R}_+$ for each $v \in \Omega$ such that one has

$$\left| \overline{B_{\frac{r(v)}{2}}\left(\frac{v+w}{2}\right)} \cap X \right| \geq n \quad \text{for all } w \in \partial B_{r(v)}(v).$$

Assume that there is no $R \in \mathbb{R}_+$ satisfying

$$\left| B_{\frac{R}{2}}\left(\frac{v+w}{2}\right) \cap X \right| \geq n \quad \text{for all } v \in \Omega,\ w \in \partial B_R(v).$$

Then, for all $R \in \mathbb{R}_+$, one can find $v \in \Omega$ and $w \in \partial B_R(v)$ such that

$$\left| B_{\frac{R}{2}}\left(\frac{v+w}{2}\right) \cap X \right| < n.$$

Hence, we can construct a sequence $(v_k, w_k)_{k\in\mathbb{N}_+}$ of counterexamples in $\Omega \times \mathbb{R}^d$ such that, for each $k \in \mathbb{N}_+$, one has

$$w_k \in \partial B_k(v_k) \quad \text{and} \quad \left| B_{\frac{k}{2}}\left(\frac{v_k+w_k}{2}\right) \cap X \right| < n.$$

For $k \in \mathbb{N}_+$, let

$$\theta_k := (w_k - v_k)/\|w_k - v_k\| \in \mathbb{S}_{d-1}.$$

From now on, we consider the sequence $(v_k, \theta_k)_{k\in\mathbb{N}_+}$ in $\Omega \times \mathbb{S}_{d-1}$, which has a convergent subsequence $(v_{k_\ell}, \theta_{k_\ell})_{\ell\in\mathbb{N}_+}$ with limit (v^*, θ^*) since both Ω and $\mathbb{S}_{d-1}$ are compact and, therefore, $\Omega \times \mathbb{S}_{d-1}$ is compact, too. We choose an arbitrary $\epsilon > 0$ now, consider θ^* as unit vector in $\mathbb{R}^d$, and set $\widehat{v} := v^* + \epsilon\theta^*$. Then, $\widehat{v}$ is not necessarily in Ω, but one can apply Proposition 5.27 nevertheless, yielding the existence of an $\widehat{r} \in \mathbb{R}_+$ such that

$$\left| \overline{B_{\widehat{r}/2}\left(\frac{\widehat{v}+w}{2}\right)} \cap X \right| \geq n \quad \text{for all } w \in \partial B_{\widehat{r}}(\widehat{v}).$$

In particular, this holds true for $\widehat{w} := \widehat{v} + \widehat{r}\theta^*$. As $(\theta_{k_\ell})_{\ell\in\mathbb{N}_+}$ converges to θ^*, one can find an $\ell_1 \in \mathbb{N}_+$ such that

$$\|\theta_{k_\ell} - \theta^*\| < \frac{\epsilon}{2\epsilon + \widehat{r}} \quad \text{for all } \ell \geq \ell_1.$$

Due to the fact that $(v_{k_\ell})_{\ell\in\mathbb{N}_+}$ converges to v^*, one can find an $\ell_2 \in \mathbb{N}_+$ satisfying

$$\|v_{k_\ell} - v^*\| < \frac{\epsilon}{2} \quad \text{for all } \ell \geq \ell_2.$$

Furthermore, there is an $\ell_3 \in \mathbb{N}_+$ such that $k_\ell \geq \widehat{r} + 2\epsilon$ for all $\ell \geq \ell_3$. Define $\ell := \max\{\ell_1, \ell_2, \ell_3\}$ and $k := k_\ell$. Let $\widehat{c} := (\widehat{v} + \widehat{w})/2$ and $u \in \overline{B_{\widehat{r}/2}(\widehat{c})}$. Then,

$$\begin{aligned}
&\left\| u - \frac{v_k + w_k}{2} \right\| \\
&= \left\| u - \left(v_k + \frac{\theta_k \|w_k - v_k\|}{2} \right) \right\| \\
&\leq \|u - \widehat{c}\| + \left\| \widehat{c} - \left(v_k + \frac{k}{2}\theta_k \right) \right\| \\
&\leq \frac{\widehat{r}}{2} + \left\| \widehat{v} + \frac{\widehat{r}}{2}\theta^* - \left(v_k + \frac{k}{2}\theta_k \right) \right\|
\end{aligned}$$

$$
\begin{aligned}
&= \frac{\widehat{r}}{2} + \left\| v^* - v_k + \left(\epsilon + \frac{\widehat{r}}{2}\right)\theta^* - \frac{k}{2}\theta_k \right\| \\
&\leq \frac{\widehat{r}}{2} + \|v^* - v_k\| + \left\| \left(\epsilon + \frac{\widehat{r}}{2}\right)(\theta^* - \theta_k) + \left(\frac{\widehat{r} - k}{2} + \epsilon\right)\theta_k \right\| \\
&\leq \frac{\widehat{r}}{2} + \|v^* - v_k\| + \left|\epsilon + \frac{\widehat{r}}{2}\right| \|\theta^* - \theta_k\| + \left|\frac{\widehat{r} - k}{2} + \epsilon\right| \\
&= \frac{\widehat{r}}{2} + \|v^* - v_k\| + \left(\epsilon + \frac{\widehat{r}}{2}\right) \|\theta^* - \theta_k\| + \frac{k - \widehat{r}}{2} - \epsilon \\
&< \frac{\epsilon}{2} + \left(\frac{2\epsilon + \widehat{r}}{2}\right) \frac{\epsilon}{2\epsilon + \widehat{r}} - \epsilon + \frac{k}{2} \\
&= \frac{k}{2}.
\end{aligned}
$$

Thus, due to the arbitrary choice of u, one obtains

$$
\overline{B_{\hat{r}/2}(\widehat{c})} \subseteq B_{k/2}\left(\frac{v_k + w_k}{2}\right)
$$

and, therefore, the contradiction

$$
n \leq \left| \overline{B_{\hat{r}/2}\left(\frac{\widehat{v} + \widehat{w}}{2}\right)} \cap X \right| \leq \left| B_{k/2}\left(\frac{v_k + w_k}{2}\right) \cap X \right| < n.
$$

As a consequence, the assumption is incorrect, and the existence of an appropriate $R \in \mathbb{R}_+$ is guaranteed. □

5.4.2 Main Result

Finally, we can merge the previous results into the following theorem proving the local finiteness property for both pooled and nonpooled DCB-splines.

Theorem 5.29 (Local Finiteness)**.** Let $d \in \mathbb{N}_+$, $m \in \mathbb{N}_0$, and let $\Omega \subseteq \mathbb{R}^d$ be compact. Choose a knot set $X \subseteq \mathbb{R}^d$ satisfying the strong conditions. The set

$$
\left\{ K \in \mathcal{K}_m(X) \;\middle|\; \overline{B(\mathfrak{B}(K))} \cap \Omega \neq \emptyset \right\}
$$

is finite.

Proof. As Ω is bounded, one can find a closed ball $\overline{B}$ containing Ω. Without loss of generality, assume that $\Omega \subseteq \overline{B} = \overline{B_1(\mathbf{0})}$. Then, for all $v \in \Omega$, one has $\|v\| \leq 1$. Let $n := m + 1$. According to Lemma 5.28, there is an $R \in \mathbb{R}_+$ such that one has

$$
\left| B_{\frac{R}{2}}\left(\frac{v + w}{2}\right) \cap X \right| \geq n > m \quad \text{for all } v \in \Omega,\ w \in \partial B_R(v). \tag{5.24}
$$

Assume now that there is a $K^* \in \mathcal{K}_m(X)$ satisfying

$$\overline{B(\mathfrak{B}(K^*))} \cap \Omega \neq \emptyset \quad \text{and} \quad \overline{B(\mathfrak{B}(K^*))} \not\subseteq \overline{B_{R+1}(\mathbf{0})}.$$

Then, there is a $w \in \partial B(\mathfrak{B}(K^*))$ with $w \notin \overline{B_{R+1}(\mathbf{0})}$ since, otherwise, Lemma 5.23, which can be applied due to the convexity and compactness of $\overline{B(\mathfrak{B}(K^*))}$, would yield the contradiction

$$\overline{B(\mathfrak{B}(K^*))} = \operatorname{conv}(\partial B(\mathfrak{B}(K^*))) \subseteq \operatorname{conv}\Big(\overline{B_{R+1}(\mathbf{0})}\Big) = \overline{B_{R+1}(\mathbf{0})}.$$

Furthermore, we can choose any $v \in \overline{B(\mathfrak{B}(K^*))} \cap \Omega$. Lemma 5.22 provides the existence of a $\widetilde{c} \in \mathbb{R}^d$ and an $\widetilde{r} \in \mathbb{R}_+$ such that

$$v, w \in \partial B_{\widetilde{r}}(\widetilde{c}) \quad \text{and} \quad B_{\widetilde{r}}(\widetilde{c}) \subseteq B(\mathfrak{B}(K^*)). \tag{5.25}$$

Moreover, let

$$c' := v + \frac{R}{2\|\widetilde{c} - v\|}(\widetilde{c} - v), \quad w' := 2c' - v, \quad \lambda := \frac{2\|\widetilde{c} - v\|}{R}.$$

Then, with

$$\begin{aligned}\|\widetilde{c} - v\| &= \frac{\|\widetilde{c} - v\| + \|\widetilde{c} - w\|}{2} \geq \frac{\|\widetilde{c} - v\| + \|\widetilde{c} - w\| + \|v\| - 1}{2} \\ &\geq \frac{\|\widetilde{c}\| - \|v\| + \|w - \widetilde{c}\| + \|v\| - 1}{2} \geq \frac{\|\widetilde{c} + w - \widetilde{c}\| - 1}{2} > \frac{R}{2},\end{aligned}$$

it follows that $\lambda > 1$. Furthermore, $\lambda(c' - v) = \widetilde{c} - v$ and $v \in \partial B_{R/2}(c')$. Consequently, one can apply Lemma 5.21, yielding

$$B_{\frac{R}{2}}(c') \subseteq B_{\widetilde{r}}(\widetilde{c}). \tag{5.26}$$

Additionally, $\|w' - v\| = 2\|c' - v\| = R$, and therefore, $w' \in \partial B_R(v)$. Hence, (5.24) is applicable to w', which, together with (5.26) and (5.25), yields the contradiction

$$\begin{aligned}m &< \left|B_{\frac{R}{2}}\left(\frac{v + w'}{2}\right) \cap X\right| = \left|B_{\frac{R}{2}}(c') \cap X\right| \\ &\leq |B_{\widetilde{r}}(\widetilde{c}) \cap X| \leq |B(\mathfrak{B}(K^*)) \cap X| = m.\end{aligned}$$

Consequently, there is no Delaunay configuration K^* such that

$$\overline{B(\mathfrak{B}(K^*))} \cap \Omega \neq \emptyset \quad \text{and} \quad \overline{B(\mathfrak{B}(K^*))} \not\subseteq \overline{B_{R+1}(\mathbf{0})},$$

and thus, for all $K \in \mathcal{K}_m(X)$ with $\overline{B(\mathfrak{B}(K))} \cap \Omega \neq \emptyset$, one has $\overline{B(\mathfrak{B}(K))} \subseteq \overline{B_{R+1}(\mathbf{0})}$.

As X is locally finite, the set $\overline{B_{R+1}(\mathbf{0})} \cap X$ is finite. Since a Delaunay configuration is uniquely identified by its $d+1$ boundary knots and since there is only a finite number of different choices of boundary knots in $\overline{B_{R+1}(\mathbf{0})} \cap X$, the set

$$\left\{ K \in \mathcal{K}_m(X) \;\middle|\; \mathfrak{B}(K) \subseteq \overline{B_{R+1}(\mathbf{0})} \cap X \right\}$$

is also finite. From $\mathfrak{B}(K) \subseteq \overline{B(\mathfrak{B}(K))} \cap X$, it follows that

$$\begin{aligned}
&\left| \left\{ K \in \mathcal{K}_m(X) \;\middle|\; \overline{B(\mathfrak{B}(K))} \cap \Omega \neq \emptyset \right\} \right| \\
&= \left| \left\{ K \in \mathcal{K}_m(X) \;\middle|\; \overline{B(\mathfrak{B}(K))} \cap \Omega \neq \emptyset,\ \overline{B(\mathfrak{B}(K))} \subseteq \overline{B_{R+1}(\mathbf{0})} \right\} \right| \\
&\leq \left| \left\{ K \in \mathcal{K}_m(X) \;\middle|\; \overline{B(\mathfrak{B}(K))} \subseteq \overline{B_{R+1}(\mathbf{0})} \right\} \right| \\
&\leq \left| \left\{ K \in \mathcal{K}_m(X) \;\middle|\; \overline{B(\mathfrak{B}(K))} \cap X \subseteq \overline{B_{R+1}(\mathbf{0})} \right\} \right| \\
&\leq \left| \left\{ K \in \mathcal{K}_m(X) \;\middle|\; \mathfrak{B}(K) \subseteq \overline{B_{R+1}(\mathbf{0})} \cap X \right\} \right| \\
&< \infty,
\end{aligned}$$

which finishes the proof of the theorem. □

5.5 Consequences

In this final section of the current chapter, we will first list results following from the local finiteness theorem and, then, try to mitigate the conditions on the knot set X.

5.5.1 Corollaries

In Section 5.1.2, we presented an example to show that, without the assumption $\operatorname{conv}(X) = \mathbb{R}^d$, several undesirable situations may happen. We show now that these situations can be excluded if the local finiteness property holds true, which is in particular the case if $\operatorname{conv}(X) = \mathbb{R}^d$, as shown by Theorem 5.29. Hence, let $d \in \mathbb{N}_+$, $m \in \mathbb{N}_0$, and assume again that $X \subseteq \mathbb{R}^d$ satisfies the strong conditions specified by Definition 4.15.

Corollary 5.30. If $X \subseteq \mathbb{R}^d$ satisfies the strong conditions and if $m \geq 1$, every pooled basis candidate function is a linear combination of a finite number of simplex splines.

Proof. Let $B \in \mathcal{B}'_{m,X}$. There is an $I \in \mathcal{I}_m(X)$ such that

$$B = \sum_{K \in \mathcal{K}_{I,m}(X)} N(\cdot \mid K).$$

Therefore, it remains to be shown that $\mathcal{K}_{I,m}(X)$ is finite. As $\mathfrak{I}(K) \subseteq \overline{B(\mathfrak{B}(K))}$ for all $K \in \mathcal{K}_{I,m}(X)$, it follows from $I \neq \emptyset$ and the fact that one can apply Theorem 5.29 to I, which is a finite set and, thus, compact, that

$$\begin{aligned}
|\mathcal{K}_{I,m}(X)| &= \left|\left\{K \in \mathcal{K}_m(X) \;\middle|\; \mathfrak{I}(K) = I\right\}\right| \\
&= \left|\left\{K \in \mathcal{K}_m(X) \;\middle|\; \mathfrak{I}(K) = I,\ I \subseteq \overline{B(\mathfrak{B}(K))}\right\}\right| \\
&\leq \left|\left\{K \in \mathcal{K}_m(X) \;\middle|\; I \subseteq \overline{B(\mathfrak{B}(K))}\right\}\right| \\
&\leq \left|\left\{K \in \mathcal{K}_m(X) \;\middle|\; I \cap \overline{B(\mathfrak{B}(K))} \neq \emptyset\right\}\right| \\
&< \infty.
\end{aligned}$$

□

Since sets containing only one element are trivially compact, the following two corollaries in particular yield pointwise results. Therefore, they ensure that Requirement (E) of the Fundamental Problem holds true for both $\mathcal{S}_{m,X}$ and $\mathcal{S}'_{m,X}$.

Corollary 5.31. If $X \subseteq \mathbb{R}^d$ satisfies the strong conditions, the set

$$\left\{B \in \mathcal{B}_{m,X} \;\middle|\; \text{supp } B \cap \Omega \neq \emptyset\right\}$$

is finite for all compact $\Omega \subseteq \mathbb{R}^d$.

Proof. As the basis candidate functions are simplex splines, their support is the convex hull of their knots. Each basis candidate function is generated by one or several Delaunay configurations corresponding to the same unoriented Delaunay configuration (see Definition 4.20). Both boundary and interior knots lie in the closed circumcircle of the Delaunay configuration. Hence, it follows with Theorem 5.29 that

$$\begin{aligned}
\left|\left\{B \in \mathcal{B}_{m,X} \;\middle|\; \text{supp } B \cap \Omega \neq \emptyset\right\}\right| &\leq \left|\left\{K \in \mathcal{K}_m(X) \;\middle|\; \text{supp } N(\cdot \mid K) \cap \Omega \neq \emptyset\right\}\right| \\
&\leq |\{K \in \mathcal{K}_m(X) \;\big|\; \overline{B(\mathfrak{B}(K))} \cap \Omega \neq \emptyset\}| < \infty.
\end{aligned}$$

□

Corollary 5.32. If $X \subseteq \mathbb{R}^d$ satisfies the strong conditions, the set

$$\left\{ B \in \mathcal{B}'_{m,X} \;\middle|\; \text{supp } B \cap \Omega \neq \emptyset \right\}$$

is finite for all compact $\Omega \subseteq \mathbb{R}^d$.

Proof. The basis candidate functions are finite linear combinations of simplex splines. Hence, all basis candidate functions that have a nonempty intersection with Ω involve at least one simplex spline whose support has a nonempty intersection with Ω. Every such simplex spline is generated by a Delaunay configuration, and its support is a subset of the circumcircle of the Delaunay configuration. Consequently, Theorem 5.29 yields

$$\begin{aligned}
&\left| \left\{ B \in \mathcal{B}'_{m,X} \;\middle|\; \text{supp } B \cap \Omega \neq \emptyset \right\} \right| \\
&\leq \left| \left\{ I \in \mathcal{I}_m(X) \;\middle|\; \text{there exists a } K \in \mathcal{K}_{I,m}(X) \text{ with supp } N(\cdot \mid K) \cap \Omega \neq \emptyset \right\} \right| \\
&\leq \left| \left\{ K \in \mathcal{K}_m(X) \;\middle|\; \text{supp } N(\cdot \mid K) \cap \Omega \neq \emptyset \right\} \right| \\
&\leq \left| \left\{ K \in \mathcal{K}_m(X) \;\middle|\; \overline{B(\mathfrak{B}(K))} \cap \Omega \neq \emptyset \right\} \right| < \infty.
\end{aligned}$$

□

Corollary 5.33. If $X \subseteq \mathbb{R}^d$ satisfies the strong conditions, the spaces of pooled and nonpooled DCB-splines are locally finite-dimensional, i.e.,

$$\dim \mathcal{S}_{m,X}|_\Omega < \infty, \quad \dim \mathcal{S}'_{m,X}|_\Omega < \infty \quad \text{for all compact } \Omega \subseteq \mathbb{R}^d.$$

Proof. The claim follows directly from Corollaries 5.31 and 5.32, respectively, and the fact that zero-functions are trivially linearly dependent. □

In particular, the previous corollary ensures that Requirement (D) of the Fundamental Problem holds true for both pooled and nonpooled DCB-splines. Consequently, all desired properties related to local finiteness hold true if we assume that $\operatorname{conv}(X) = \mathbb{R}^d$ or, trivially, if X is finite.

5.5.2 Local Finiteness Condition

In the introductory section of the current chapter, we have seen that, without the condition $\operatorname{conv}(X) = \mathbb{R}^d$, we cannot expect the local finiteness property to hold

true for infinite knot sets. This assumption is very strong, though. When recalling the proof of the local finiteness property, it turns out that the only point at which we used this condition was in the proof of Proposition 5.16. Therefore, the local finiteness property and, in turn, the corollaries of the previous subsection hold true even for knot sets with $\mathrm{conv}(X) \subset \mathbb{R}^d$ if one can guarantee that Proposition 5.16 holds true.

When we analyze the proof of that particular proposition, it follows readily that it also holds true if we assume that each open half space generated by any hyperplane contains at least a given number $n := m+1$ of knots, where $m \in \mathbb{N}_0$ again denotes the spline degree. Since these hyperplanes can be placed arbitrarily, it is easy to see that this assumption is equivalent to the initial assumption $\mathrm{conv}(X) = \mathbb{R}^d$. However, we can utilize this observation to obtain a *local* variant of the local finiteness property. To that end, we consider a compact region $\Omega \subseteq \mathbb{R}^d$ now and assume that X satisfies the following *local finiteness condition*, which in particular implies the weak conditions specified in Definition 4.16.

Definition 5.34 (Local finiteness condition)**.** Let $d \in \mathbb{N}_+$, $n \in \mathbb{N}_+$, and let $\Omega \subseteq \mathbb{R}^d$ be compact. $X \subseteq \mathbb{R}^d$ satisfies the *local finiteness condition (with respect to Ω and n)* if X fulfills the weak conditions and if there is an $\widehat{\Omega} \subseteq \mathbb{R}^d$ with $\Omega \subseteq \widehat{\Omega}^\circ$ and

$$|H(t,\theta) \cap X| \geq n \quad \text{for all } t \in \widehat{\Omega},\ \theta \in \mathbb{S}_{d-1}, \tag{5.27}$$

where $H(t,\theta)$ denotes

$$H(t,\theta) := \{u \in \mathbb{R}^d \mid \langle u - t, \theta \rangle > 0\},$$

which is one of the half spaces generated by the hyperplane passing through t with normal vector θ. ◀

Note that, for the local finiteness condition, we require (5.27) to hold true on a set $\widehat{\Omega}$ which is *larger* than the original domain Ω. This is due to the fact that, in the proof of Lemma 5.28, we invoke Proposition 5.27 on a point $\widehat{v} := v^* + \epsilon\theta^*$ which is possibly outside of Ω. This procedure is uncritical when considering the local finiteness property *globally*, as we did in Lemma 5.28. In a *local* version, however, it is crucial to keep $\widehat{v}$ inside the controlled region. Since we do not have any control over the values of $v^* \in \Omega$ and $\theta^* \in \mathbb{S}_{d-1}$, it is not possible to enforce that $\widehat{v} \in \Omega$. As $\epsilon > 0$ can be chosen arbitrarily, the distance of $\widehat{v}$ to Ω can be made arbitrarily small, though. Hence, it is sufficient to choose any region $\widehat{\Omega}$ with $\Omega \subseteq \widehat{\Omega}^\circ$, as can be seen

easily: Any point $v^* \in \Omega$ is an interior point of $\widehat{\Omega}$, and therefore, one can find an $\epsilon > 0$ such that

$$\widehat{v} = v^* + \epsilon\theta^* \in B_{2\epsilon}(v^*) \subseteq \widehat{\Omega}.$$

Let $C_a(t,\theta)$ denote the open cone with aperture $a \in [0,1]$, direction $\theta \in \mathbb{S}_{d-1}$, and apex in $t \in \mathbb{R}^d$. This is consistent with Definition 5.6 in the sense that $C_a(\mathbf{0},\theta) = C_a(\theta)$ for all $a \in [0,1]$ and $\theta \in \mathbb{S}_{d-1}$. The following proposition provides the conclusion that Proposition 5.16 holds true on a suitable $\widehat{\Omega} \supset \Omega$ for knot sets satisfying the local finiteness condition with respect to Ω.

Proposition 5.35. Let $n \in \mathbb{N}_+$, and choose a compact $\Omega \subseteq \mathbb{R}^d$. Let $X \subseteq \mathbb{R}^d$ be a knot set satisfying the local finiteness condition with respect to Ω and n. There is an $\widehat{\Omega} \subseteq \mathbb{R}^d$ with $\Omega \subseteq \widehat{\Omega}^\circ$ and

$$a_n(t,\theta) := \max\Big\{a \in [0,1] \;\Big|\; |C_a(t,\theta) \cap X| < n\Big\} < \frac{1}{2} \quad \text{for all } t \in \widehat{\Omega},\ \theta \in \mathbb{S}_{d-1},$$

where $C_a(t,\theta)$ denotes the open cone in direction $\theta \in \mathbb{S}_{d-1}$ with aperture $a \in [0,1]$ and apex in $t \in \mathbb{R}^d$, i.e.,

$$C_a(t,\theta) := \Big\{w \in \mathbb{R}^d \backslash \{t\} \;\Big|\; \langle \theta, w-t\rangle / \|w-t\| > 1 - 2a\Big\}.$$

Proof. The definition of the local finiteness condition yields the existence of a suitable $\widehat{\Omega}$ such that (5.27) holds true on $\widehat{\Omega}$. The assumption that there is a $t \in \widehat{\Omega}$ and a $\theta \in \mathbb{S}_{d-1}$ with $a_n(t,\theta) \geq 1/2$ directly yields the contradiction

$$n > |C_{a_n(t,\theta)}(t,\theta) \cap X| \geq |H(t,\theta) \cap X| \geq n.$$

□

The choice $n := m+1$ in the preceding proposition, where $m \in \mathbb{N}_0$ again denotes the spline degree, readily yields the following corollary:

Corollary 5.36. Let $d \in \mathbb{N}_+$, $m \in \mathbb{N}_0$, and let $\Omega \subseteq \mathbb{R}^d$ be compact. If $X \subseteq \mathbb{R}^d$ satisfies the local finiteness condition with respect to Ω and $m+1$, the local finiteness property, i.e.,

$$\Big|\Big\{K \in \mathcal{K}_m(X) \;\Big|\; \overline{B(\mathfrak{B}(K))} \cap \Omega \neq \emptyset\Big\}\Big| < \infty,$$

holds true for both spline spaces $\mathcal{S}_{m',X}|_\Omega$ and $\mathcal{S}'_{m',X}|_\Omega$ restricted to Ω. ◀

For a given region $\Omega \subseteq \mathbb{R}^d$ and a given knot set $X \subseteq \mathbb{R}^d$, the following question directly arises from this result: Can we show *practically* whether X satisfies the local

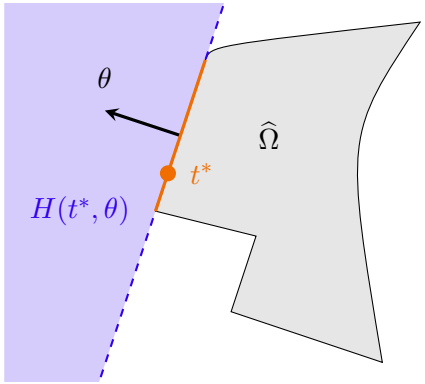

Fig. 5.12: Example of extremal points. The marked line *(orange)* represents all extremal points in direction θ with respect to $\widehat{\Omega}$. One exemplary extremal point and its associated half space $H(t^*, \theta)$ *(blue)* is given by t^* *(orange)*.

finiteness condition with respect to Ω? As a first step, we show that the consideration of certain boundary points of a suitable $\widehat{\Omega}$, which we will call *extremal points*, is sufficient.

Definition 5.37 (Extremal point)**.** Let $\theta \in \mathbb{S}_{d-1}$, and let $\widehat{\Omega} \subseteq \mathbb{R}^d$ be nonempty and compact. An *extremal point in direction θ (with respect to $\widehat{\Omega}$)* is a point $t \in \widehat{\Omega}$ satisfying

$$\langle t, \theta \rangle = \max_{t' \in \widehat{\Omega}} \langle t', \theta \rangle.$$

◀

The maximum is well-defined since one can apply the extreme value theorem due to the compactness of $\widehat{\Omega}$ and the continuity of $\langle \cdot, \theta \rangle$. We refer to Figure 5.12 for an exemplary visualization of extremal points. Note that all extremal points are necessarily boundary points since the maximum cannot be assumed on interior points due to the linearity of $\langle \cdot, \theta \rangle$. Conversely, if $\widehat{\Omega}$ is chosen to be convex, each boundary point is an extremal point in at least one direction.

The significance of extremal points for the local finiteness condition can be seen as follows. Let $\widehat{\Omega} \subseteq \mathbb{R}^d$ be nonempty and compact, and choose $\theta \in \mathbb{S}_{d-1}$. Let $t^* \in \widehat{\Omega}$ be an extremal point in direction θ. Then, $H(t^*, \theta) \subseteq H(t, \theta)$ for all $t \in \widehat{\Omega}$ since for any $u \in H(t^*, \theta)$ one has

$$\langle u - t, \theta \rangle = \langle u, \theta \rangle - \langle t, \theta \rangle \geq \langle u, \theta \rangle - \langle t^*, \theta \rangle = \langle u - t^*, \theta \rangle > 0$$

and, therefore, also $u \in H(t, \theta)$. In particular, this subset relation ensures that the half spaces $H(t_1, \theta)$, $H(t_2, \theta)$ associated to *different* extremal points t_1, t_2 with

respect to the *same* direction θ coincide, as can be seen easily when looking at Figure 5.12. As a consequence, it is sufficient to consider extremal points when checking a given knot set X for the local finiteness condition in a region $\widehat{\Omega}$:

Proposition 5.38. Let $n \in \mathbb{N}_+$, and let $\widehat{\Omega} \subseteq \mathbb{R}^d$ be nonempty and compact. For all $\theta \in \mathbb{S}_{d-1}$, let $t_\theta \in \mathbb{R}^d$ denote an arbitrary extremal point in direction θ with respect to $\widehat{\Omega}$. If $X \subseteq \mathbb{R}^d$ satisfies the weak conditions and if

$$|H(t_\theta, \theta) \cap X| \geq n \quad \text{for all } \theta \in \mathbb{S}_{d-1}, \tag{5.28}$$

then X fulfills the local finiteness condition with respect to n and any compact Ω with $\Omega \subseteq \widehat{\Omega}^\circ$.

Proof. The proof follows immediately from the previous observation since, for all $t \in \widehat{\Omega}$ and for any $\theta \in \mathbb{S}_{d-1}$, one has $|H(t, \theta) \cap X| \geq |H(t_\theta, \theta) \cap X| \geq n$. □

Without further assumptions on $\widehat{\Omega}$, we still have to consider a possibly infinite set of extremal points. For example, if we choose $\widehat{\Omega}$ to be a closed ball, $\widehat{\Omega}$ is convex and, therefore, each point on the boundary of $\widehat{\Omega}$ is an extremal point. Moreover, it is the *unique* extremal point in a specific direction. Hence, we will assume now that $\widehat{\Omega}$ has a considerably simpler structure:

Remark 5.39. Let $X \subseteq \mathbb{R}^d$ satisfy the weak conditions, and let $\widehat{\Omega} \subseteq \mathbb{R}^d$ be a nonempty, closed polytope, as displayed exemplarily in Figure 5.13. In particular, $\widehat{\Omega}$ is convex, bounded, and also compact. Hence, the prerequisites of Proposition 5.38 are fulfilled if one can show that (5.28) holds true.

However, due to the fact that $\widehat{\Omega}$ is an intersection of a finite number of half-spaces and due to the linearity of $\langle \cdot, \theta \rangle$ for all $\theta \in \mathbb{S}_{d-1}$, it follows that each extremal point is a solution of a linear optimization problem with linear side conditions. It is known from linear optimization theory (see [BT97, p. 65], for example) that, for such optimization problems, one can always find a vertex (i.e., a corner) of the feasible region (in this case $\widehat{\Omega}$) solving the problem. Thus, for each $\theta \in \mathbb{S}_{d-1}$, one can find a vertex of $\widehat{\Omega}$ that is an extremal point in direction θ.

Therefore, according to Proposition 5.38, if $\widehat{\Omega}$ is a nonempty, closed polytope, it is sufficient to check that (5.28) holds true at the vertices of $\widehat{\Omega}$ in the corresponding directions (for which the vertex is an extremal point) in order to ensure that the local finiteness condition and, thus, also the local finiteness property hold true on any compact Ω with $\Omega \subseteq \widehat{\Omega}^\circ$. In practice, this is a much more feasible endeavor than the initial local finiteness condition. ◀

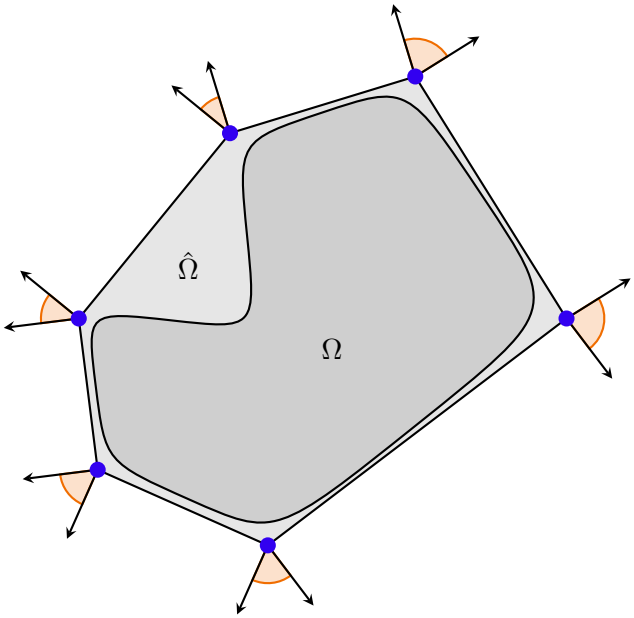

Fig. 5.13: Local finiteness condition for polytopes. If $\widehat{\Omega}$ is chosen to be a polytope that contains Ω in its interior, it is sufficient to consider half spaces only at the vertices *(blue)* of that polytope (which are in particular extremal points) in order to ensure that the local finiteness property holds true on Ω. We also display the range of half space normals *(orange)* that has to be checked at each vertex.

6 Knot Insertion

> *We seem to be made to suffer. It's our lot in life.*
>
> **— Star Wars: Episode IV – A New Hope**

When introducing univariate splines, we also recalled knot insertion in Subsection 2.3.5, which ensures that each spline with respect to some knot sequence can also be expressed in terms of any refined knot sequence. We will refer to this as *knot insertion property* and investigate if it also holds true for nonpooled DCB-splines. We explicitly focus on nonpooled DCB-splines, although some results may also be applied to pooled DCB-splines. Moreover, we prefer to consider the unnormalized simplex splines M instead of the normalized version N in order to avoid notational overhead. For the question *if* the knot insertion property holds true, the normalization of basis candidate functions clearly does not matter.

Throughout the chapter, we once again assume that $d \in \mathbb{N}_+$, $m \in \mathbb{N}_0$, and that $X \subseteq \mathbb{R}^d$ satisfies the weak conditions specified in Definition 4.16.

6.1 Preliminaries

The fundamental question we are going to answer in this chapter is the following: For two knot sets X, X' with the specified properties and $X \subseteq X'$, does the subset relation $\mathcal{S}_{m,X} \subseteq \mathcal{S}_{m,X'}$ hold true, like it does for univariate splines?

Due to the same argument as in the univariate case, one can restrict considerations on the insertion of a single knot since the general case follows by repeated application (at least for a finite number of new knots). Hence, we assume that $x^* \in \mathbb{R}^d$ and add x^* to the existing knot set X to obtain the refined knot set $X^* := X \cup \{x^*\}$. Furthermore, we require X^* to be in general Delaunay position, which in particular implies that $x^* \notin X$. We have to check now if the relation $\mathcal{S}_{m,X} \subseteq \mathcal{S}_{m,X^*}$ holds true. The question is answered by the following example:

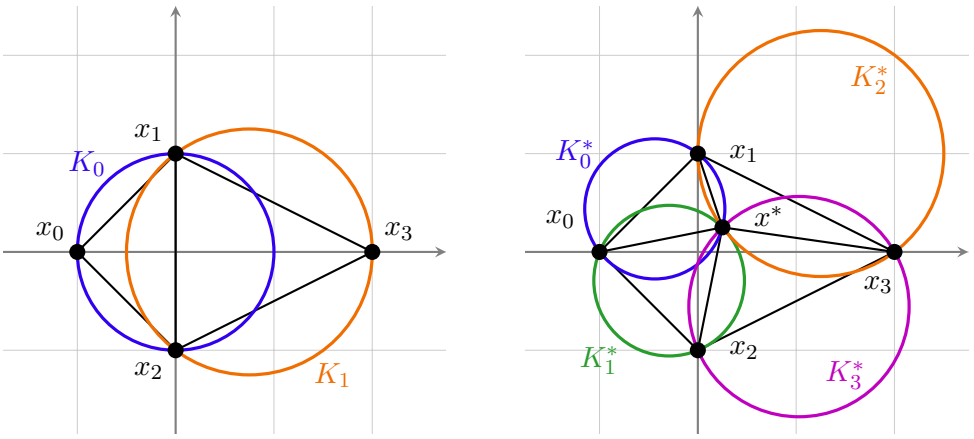

(a) Situation for original knot set X (b) Situation for refined knot set X^*

Fig. 6.1: Counterexample for the knot insertion property. There are splines in the spline space $\mathcal{S}_{0,X}$ *(left)* which cannot be represented with respect to the refined spline space $\mathcal{S}_{0,X^*}$ *(right)*. The circles represent the circumcircles of Delaunay configurations, whereas the black lines indicate the boundary of the support of the corresponding simplex splines.

Example 6.1. Choose $d := 2$, $m := 0$, and the knots

$$x_0 := \begin{pmatrix} -1 \\ 0 \end{pmatrix}, \quad x_1 := \begin{pmatrix} 0 \\ 1 \end{pmatrix}, \quad x_2 := \begin{pmatrix} 0 \\ -1 \end{pmatrix}, \quad x_3 := \begin{pmatrix} 2 \\ 0 \end{pmatrix}, \quad x^* := \begin{pmatrix} 1/4 \\ 1/4 \end{pmatrix}.$$

When looking at Figure 6.1, it can be seen that these knots are in general Delaunay position. We choose an arbitrary locally finite knot set X^* in general Delaunay position with $\operatorname{conv}(X^*) = \mathbb{R}^d$ such that $x_0, \dots, x_3, x^* \in X^*$ and

$$X^* \backslash \{x_0, \dots, x_3, x^*\} \cap \bigcup_{i=0}^{1} \overline{B(\mathfrak{B}(K_i))} \cap \bigcup_{i=0}^{3} \overline{B(\mathfrak{B}(K_i^*))} = \emptyset, \tag{6.1}$$

where the Delaunay configurations $K_0, K_1, K_0^*, \dots, K_3^*$ are defined with respect to the finite knot sets $\{x_0, \dots, x_3\}$ and $\{x_0, \dots, x_3, x^*\}$, respectively, and will be defined below. Due to (6.1), these configurations are not influenced by the remaining knots in X^*. Hence, the additional knots do not require further consideration. We extend X^* in this way to show that the counterexample also works for knot sets satisfying $\operatorname{conv}(X^*) = \mathbb{R}^d$. Moreover, define $X := X^* \backslash \{x^*\}$, which is also a locally finite knot set in general Delaunay position. It generates the Delaunay configurations

$$K_0 := (\{x_0, x_1, x_2\}, \emptyset), \quad K_1 := (\{x_1, x_2, x_3\}, \emptyset)$$

of degree zero, i.e., without interior knots (see Definition 4.13), as can be verified easily when looking at Figure 6.1. On the contrary, Delaunay configurations of the refined knot set X^* are

$$K_0^* := (\{x_0, x_1, x^*\}, \emptyset), \qquad K_1^* := (\{x_0, x_2, x^*\}, \emptyset),$$
$$K_2^* := (\{x_1, x_3, x^*\}, \emptyset), \qquad K_3^* := (\{x_2, x_3, x^*\}, \emptyset).$$

It can be seen in Figure 6.1 that $K_0^*, \ldots, K_3^* \in \mathcal{K}_0(X^*)$ but $K_0, K_1 \notin \mathcal{K}_0(X^*)$. Furthermore, since Delaunay triangulations tessellate $\mathbb{R}^2$, there is no other configuration in $\mathcal{K}_0(X^*)$ that gives rise to a simplex spline whose support has a nonempty intersection with $\operatorname{conv}(x_0, \ldots, x_3)^\circ$. We consider the spline function

$$g := \sum_{K \in \mathcal{K}_0(X)} a_K M(\cdot \mid \mathfrak{U}(K)) \quad \in \mathcal{S}_{0,X}$$

with coefficients

$$a_K := \begin{cases} 2 \operatorname{vol}_d(\operatorname{conv}(x_0, x_1, x_2)) & \text{if } K = K_0, \\ 0 & \text{otherwise,} \end{cases} \quad \text{for all } K \in \mathcal{K}_0(X).$$

According to Definition 3.15, g can be represented for all $t \in \mathbb{R}^2$ as

$$g(t) = 2 \operatorname{vol}_d(\operatorname{conv}(x_0, x_1, x_2))\, M(t \mid \mathfrak{U}(K_0)) = \begin{cases} 1 & \text{if } t \in \operatorname{conv}(x_0, x_1, x_2), \\ 0 & \text{otherwise.} \end{cases}$$

We assume now that it is possible to express g in terms of the refined spline space $\mathcal{S}_{0,X^*}$. Due to the fact that there are no further basis candidate functions with support in $\operatorname{conv}(x_0, \ldots, x_3)^\circ$, there are coefficients $a_{K_0^*}, a_{K_1^*}, a_{K_2^*}, a_{K_3^*} \in \mathbb{R}$ such that

$$g^*(t) := \sum_{i=0}^{3} a_{K_i^*} M(t \mid \mathfrak{U}(K_i^*)) = g(t) \quad \text{for all } t \in \mathbb{R}^2 \backslash A^*.$$

Here, A^* contains the boundaries of the supports of the simplex splines, i.e.,

$$A^* := \bigcup_{i=0}^{4} \bigcup_{j=i+1}^{4} \operatorname{conv}(x_i, x_j),$$

where $x_4 := x^*$. Let us consider the point $t = (-1/2, 1/4)^\intercal \in \mathbb{R}^2 \backslash A^*$, for which $g(t) = 1$ holds. Due to $t \in \operatorname{conv}(x_0, x_1, x^*)^\circ$ and the pairwise disjointness of

$$\operatorname{conv}(x_0, x_1, x^*)^\circ,\ \operatorname{conv}(x_0, x_2, x^*)^\circ,\ \operatorname{conv}(x_1, x_3, x^*)^\circ,\ \operatorname{conv}(x_2, x_3, x^*)^\circ,$$

it follows that $a_{K_0^*} = 1$. Equivalently, one can conclude for the point $(-1/2, -1/4)^\intercal$ that $a_{K_1^*} = 1$. On the contrary, the points $(1/2, 1/4)^\intercal$ and $(1/2, -1/4)^\intercal$ yield that $a_{K_2^*} = a_{K_3^*} = 0$. If we finally consider the point $t' = (1/8, 1/8)^\intercal$, it follows with

$$t' \in \operatorname{conv}(x_0, x_2, x^*)^\circ \quad \text{and} \quad t' \notin \operatorname{conv}(x_0, x_1, x_2)$$

that $g(t') = 0 \neq 1 = g^*(t')$, which is a contradiction to the assumption that $g(t) = g^*(t)$ for all $t \in \mathbb{R}^2 \backslash A^*$. Hence, g cannot be expressed in terms of the refined spline space $\mathcal{S}_{0,X^*}$, which shows that the knot insertion property does not hold true in general for nonpooled DCB-splines. Note that this example also works for pooled DCB-splines of degree zero (according to our definition). As a consequence, the knot insertion property does not hold true in general for pooled DCB-splines either. ◀

As the knot insertion property does not hold true in general, we spend the remainder of the current chapter on the characterization of situations where the insertion of an additional knot yields a spline space that contains all functions of the coarser space. In the following section, we will formulate a necessary criterion which has to be fulfilled if the relation $\mathcal{S}_{m,X} \subseteq \mathcal{S}_{m,X^*}$ holds true. Afterwards, we will try to show that this criterion is also sufficient.

6.2 Necessary Criterion

When recalling Example 6.1, it can be seen that the key problem is the disappearance of the edge between x_1 and x_2 after inserting the additional knot x^*. All splines that can be expressed with respect to the refined knot set are continuous across that edge. Hence, not all splines of the coarse spline space can be represented in that way since it contains functions with discontinuities across this edge, even when considering only the interior of the supports and ignoring the improperly defined boundary.

As it turns out, this is the key idea towards a general necessary criterion for the knot insertion property. Without this criterion being satisfied, the refined spline space does not contain all functions of the coarser one.

6.2.1 Limits of Differentiability

We have recalled in Theorem 3.20 that a simplex spline of degree m has $m - 1$ continuous derivatives if the corresponding knots are in general position. In the

following two lemmas, we will show that this differentiability is optimal in the following sense: In each convex hull of a subset of d knots, there are points at which the $(m-1)$-th derivative is not continuously differentiable. The following results are sufficient for our subsequent considerations. A more detailed treatment of the exact differentiability of simplex splines and more general results on this topic are presented in [Hak82].

Lemma 6.2. Let $X \subseteq \mathbb{R}^d$ satisfy the weak conditions, and choose a $Z \subseteq X$ with $|Z| = d$. Let $\mathcal{A}$ be a system of subsets of knots such that $\mathcal{A} \subseteq \{A \subseteq X \mid |A| = d\}$ and $Z \notin \mathcal{A}$. Then,

$$\mathrm{vol}_{d-1}\left(\mathrm{conv}(Z) \cap \bigcup_{A \in \mathcal{A}} \mathrm{conv}(A)\right) = 0.$$

Proof. The claim is clear if $\mathcal{A} = \emptyset$. Otherwise, we can choose an $A \in \mathcal{A}$. Since $A \neq Z$, one has $|Z \cap A| \leq d-1$. We assume now that

$$\mathrm{vol}_{d-1}(\mathrm{conv}(Z) \cap \mathrm{conv}(A)) \neq 0. \tag{6.2}$$

Both convex hulls are subsets of hyperplanes in $\mathbb{R}^d$, and the intersection of two *distinct* hyperplanes is empty or a lower-dimensional affine subspace of dimension $d-2$. As this would yield $\mathrm{vol}_{d-1}(\mathrm{conv}(Z) \cap \mathrm{conv}(A)) = 0$, which would be a contradiction to Assumption (6.2), it follows that both hyperplanes coincide. Hence, all knots in $Z \cup A$ lie in the same hyperplane. However, due to

$$|Z \cup A| = |Z| + |A| - |Z \cap A| \geq 2d - (d-1) = d+1,$$

these (at least) $d+1$ knots in a common hyperplane constitute a contradiction to the requirement on X that no $d+2$ knots are affinely dependent. Consequently, Assumption (6.2) is incorrect, and one has

$$\mathrm{vol}_{d-1}(\mathrm{conv}(Z) \cap \mathrm{conv}(A)) = 0 \quad \text{for all } A \in \mathcal{A}. \tag{6.3}$$

$\mathcal{A}$ is countable since it consists of subsets containing exactly d elements of the countable set X. Hence, the claim follows due to (6.3) and the σ-subadditivity of the Lebesgue measure:

$$0 \leq \mathrm{vol}_{d-1}\left(\mathrm{conv}(Z) \cap \bigcup_{A \in \mathcal{A}} \mathrm{conv}(A)\right) \leq \sum_{A \in \mathcal{A}} \mathrm{vol}_{d-1}(\mathrm{conv}(Z) \cap \mathrm{conv}(A)) = 0.$$

□

Lemma 6.3. Let $X \subseteq \mathbb{R}^d$ satisfy the weak conditions. Choose $Y \subseteq X$ such that $|Y| = d + m + 1$, and let $Z \subseteq Y$ with $|Z| = d$. Moreover, choose $\mathcal{A}$ such that

$$\mathcal{A} \subseteq \Big\{ A \subseteq X \;\Big|\; |A| = d,\ A \neq Z \Big\} \quad \text{and} \quad \Big\{ A \subseteq Y \;\Big|\; |A| = d,\ A \neq Z \Big\} \subseteq \mathcal{A}.$$

We set

$$W := \operatorname{conv}(Z) \Big\backslash \bigcup_{A \in \mathcal{A}} \operatorname{conv}(A).$$

Then, $\operatorname{vol}_{d-1}(W) > 0$, and $M(\cdot \mid Y)$ is at all points in W *not* m-times continuously differentiable.

Proof. Since $\mathcal{A}$ satisfies the conditions in Lemma 6.2, one can apply this lemma to obtain that

$$\operatorname{vol}_{d-1}\left(\operatorname{conv}(Z) \cap \bigcup_{A \in \mathcal{A}} \operatorname{conv}(A) \right) = 0.$$

Furthermore, one has $\operatorname{vol}_{d-1}(\operatorname{conv}(Z)) > 0$ as X is in general Delaunay position. Hence, one can conclude that

$$\begin{aligned} \operatorname{vol}_{d-1}(W) &= \operatorname{vol}_{d-1}(\operatorname{conv}(Z)) - \operatorname{vol}_{d-1}\left(\operatorname{conv}(Z) \cap \bigcup_{A \in \mathcal{A}} \operatorname{conv}(A) \right) \\ &= \operatorname{vol}_{d-1}(\operatorname{conv}(Z)) > 0. \end{aligned}$$

We prove the remainder of the claim via induction on m.

Simplex splines of degree zero are just scaled characteristic functions of the convex hull of Y. As the scaling factor is nonzero, the claim follows for $m = 0$ directly from the fact that $\mathbb{1}_{\operatorname{conv}(Y)}$ is discontinuous at the boundary of $\operatorname{conv}(Y)$.

Consider $m \to m + 1$ now. Since $\operatorname{vol}_{d-1}(W) > 0$, it follows that $W \neq \emptyset$, so that we can choose a $t \in W$. Moreover, we number $x_0, \ldots, x_{d+m+1} \in Y$ such that

$$Z = \{x_0, \ldots, x_{d-1}\} \quad \text{and} \quad Y = Z \cup \{x_d, \ldots, x_{d+m+1}\}.$$

Consider the barycentric direction

$$\mu := (-1, \underbrace{0, \ldots, 0}_{(d-1)\text{-times}}, 1, \underbrace{0, \ldots, 0}_{(m+1)\text{-times}}) \in \mathbb{R}^{d+m+2}.$$

According to Theorem 3.19, one can represent the directional derivative of $M(\cdot \mid Y)$ in direction

$$y := \sum_{k=0}^{d+m+1} \mu_k x_k = x_d - x_0$$

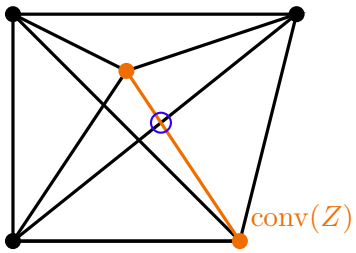

Fig. 6.2: The situation in Lemma 6.3. The quadratic simplex spline with respect to the given knots is *not* twice differentiable at almost every point of $\operatorname{conv}(Z)$ *(orange)*. The endpoints of $\operatorname{conv}(Z)$ *(orange)* as well as the intersection point *(blue)* are excluded from the set W.

in terms of two simplex splines of degree m:

$$D_y M(\cdot \mid Y) = M(\cdot \mid x_0, \dots, x_{d-1}, x_{d+1}, \dots, x_{d+m+1}) - M(\cdot \mid x_1, \dots, x_{d+m+1}). \quad (6.4)$$

Since $t \in W$ and $\mathcal{A}$ satisfies the corresponding conditions, we can apply the induction hypothesis to the first simplex spline $M(\cdot \mid x_0, \dots, x_{d-1}, x_{d+1}, \dots, x_{d+m+1})$ to obtain that it is *not* m-times continuously differentiable at t.

We show now that the second simplex spline is m-times continuously differentiable at t. To that end, we note that, for all $A \subseteq \{x_1, \dots, x_{d+m+1}\}$ with $|A| = d$, one has $x_0 \notin A$ and, therefore, $A \neq Z$. Consequently, $A \in \mathcal{A}$, and thus, $t \notin \operatorname{conv}(A)$. Hence, Theorem 3.20 yields that $M(\cdot \mid x_1, \dots, x_{d+m+1})$ is a polynomial locally around t and, in particular, m-times continuously differentiable at t. According to (6.4), this yields that $D_y M(\cdot \mid Y)$ is *not* m-times continuously differentiable at t since, otherwise, one would obtain the contradiction that

$$M(\cdot \mid x_0, \dots, x_{d-1}, x_{d+1}, \dots, x_{d+m+1}) = M(\cdot \mid x_1, \dots, x_{d+m+1}) + D_y M(\cdot \mid Y)$$

as a sum of functions which are m-times continuously differentiable at t would also be m-times continuously differentiable at t. Consequently, $M(\cdot \mid Y)$ is *not* $(m+1)$-times continuously differentiable at all points in W. □

The nondifferentiable points covered by the previous lemma are presented in Figure 6.2. Note that, in most cases, $M(\cdot \mid Y)$ is not m-times continuously differentiable at *all* points in $\operatorname{conv}(Z)$. However, for some choices of $A \in \mathcal{A}$, it can happen that *both* simplex splines in (6.4) are not m-times continuously differentiable at $t \in \operatorname{conv}(Z) \cap \operatorname{conv}(A)$. Since it could happen theoretically that these nondifferentiabilities cancel out, one cannot conclude in general that also $D_y M(\cdot \mid Y)$ is not

m-times continuously differentiable at t. As the scope of the previous lemma is sufficient for our purposes, we will not consider these special situations in more detail and instead refer to [Hak82].

6.2.2 Definition of the Criterion

We can use the nonexistence of m-th derivatives now to formulate the following criterion, which is a necessary condition for the knot insertion property.

Theorem 6.4. Let $d \in \mathbb{N}_+$, $m \in \mathbb{N}_0$, and let $X \subseteq \mathbb{R}^d$ satisfy the weak conditions. Furthermore, choose

$$\begin{aligned} Y \subseteq X, &\quad |Y| = d + m + 1, \\ Z \subseteq Y, &\quad |Z| = d, \end{aligned}$$

and let

$$\mathcal{A} \subseteq \left\{ A \subseteq X \;\middle|\; |A| = m + d + 1 \right\}$$

such that

$$\left| \left\{ A \in \mathcal{A} \;\middle|\; \text{supp } M(\cdot \mid A) \cap \Omega \neq \emptyset \right\} \right| < \infty \tag{6.5}$$

for all compact $\Omega \subseteq \mathbb{R}^d$. If $Z \not\subseteq A$ for all $A \in \mathcal{A}$, then there is *no* family of real-valued coefficients $(c_A)_{A \in \mathcal{A}}$ such that

$$M(\cdot \mid Y) = \sum_{A \in \mathcal{A}} c_A M(\cdot \mid A).$$

Proof. Assume that one has $Z \not\subseteq A$ for all $A \in \mathcal{A}$, and define

$$W := \left(\bigcup_{\substack{Z' \subseteq Y \\ |Z'| = d \\ Z' \neq Z}} \operatorname{conv}(Z') \right) \cup \bigcup_{A \in \mathcal{A}} \underbrace{\bigcup_{\substack{A' \subseteq A \\ |A'| = d}} \operatorname{conv}(A')}_{=: W_A}.$$

Then, one can apply Lemma 6.3 to obtain that $\operatorname{vol}_{d-1}(\operatorname{conv}(Z) \backslash W) > 0$. In particular, there is a $t \in \operatorname{conv}(Z) \backslash W$. Lemma 6.3 additionally provides that, for all open neighborhoods $U \subseteq \mathbb{R}^d$ of t, one has

$$M(\cdot \mid Y)\big|_U \notin \mathcal{C}^m(U). \tag{6.6}$$

Let $A \in \mathcal{A}$. Then, $W_A \subseteq W$ and $t \notin W$ imply $t \notin W_A$. Moreover, W_A is closed as finite union of closed sets, and therefore, W_A^c is open. Hence, there is an $\epsilon_A > 0$ such that $B_{\epsilon_A}(t) \cap W_A = \emptyset$. Thus, Theorem 3.20 provides that

$$M(\cdot \mid A)\Big|_{B_{\epsilon_A}(t)} \in \Pi_m(B_{\epsilon_A}(t)). \tag{6.7}$$

Assume now that there is a family of real-valued coefficients $(c_A)_{A\in\mathcal{A}}$ such that

$$M(\cdot \mid Y) = \sum_{A\in\mathcal{A}} c_A M(\cdot \mid A). \tag{6.8}$$

Choose an arbitrary $\epsilon' > 0$, and consider

$$\mathcal{A}' := \left\{ A \in \mathcal{A} \;\middle|\; \overline{B_{\epsilon'}(t)} \cap \operatorname{supp} M(\cdot \mid A) \neq \emptyset \right\} \quad \text{and} \quad \epsilon := \min\left\{ \epsilon', \min_{A\in\mathcal{A}'} \epsilon_A \right\} > 0,$$

so that

$$M(\cdot \mid A)\Big|_{B_\epsilon(t)} \equiv 0 \quad \text{for all } A \in \mathcal{A}\backslash\mathcal{A}'.$$

With Assumption (6.5), it follows that $\mathcal{A}'$ is finite and, therefore, that ϵ is well-defined. Consequently, $M(\cdot \mid Y)$ can locally be represented as

$$M(\cdot \mid Y)\Big|_{B_\epsilon(t)} = \sum_{A\in\mathcal{A}} c_A M(\cdot \mid A)\Big|_{B_\epsilon(t)} = \sum_{A\in\mathcal{A}'} c_A M(\cdot \mid A)\Big|_{B_\epsilon(t)}, \tag{6.9}$$

which is a finite linear combination of polynomials, according to (6.7). Hence,

$$M(\cdot \mid Y)\Big|_{B_\epsilon(t)} \in \Pi_m(B_\epsilon(t)) \subseteq \mathcal{C}^m(B_\epsilon(t)),$$

i.e., $M(\cdot \mid Y)$ is locally a polynomial and, in particular, has m continuous derivatives at t, which is a contradiction to (6.6). Thus, a family of coefficients satisfying (6.8) does not exist with the stated premises. □

When setting $\mathcal{A}$ to the set of unoriented Delaunay configurations of degree m with respect to the knot set X, Condition 6.5 follows directly from the local finiteness property (see Theorem 5.29 and Corollary 5.31). Although the previous theorem looks fairly abstract at first sight, its application to DCB-splines is straightforward:

Corollary 6.5. Let $d \in \mathbb{N}_+$, $m \in \mathbb{N}_0$, and let $X^* \subseteq \mathbb{R}^d$ be a knot set satisfying the strong conditions. Choose $x^* \in X^*$. Define the coarser knot set as $X := X^*\backslash\{x^*\}$. If there exists a $K \in \mathcal{K}_m(X)$ and a $Z \subseteq \mathfrak{U}(K)$ with $|Z| = d$ such that $Z \not\subseteq \mathfrak{U}(K^*)$ for all $K^* \in \mathcal{K}_m(X^*)$, then $\mathcal{S}_{m,X} \not\subseteq \mathcal{S}_{m,X^*}$.

Proof. Let

$$\mathcal{A} := \Big\{ \mathfrak{U}(K^*) \;\Big|\; K^* \in \mathcal{K}_m(X^*) \Big\}.$$

Since X^* satisfies the strong conditions, Corollary 5.31 yields that

$$\Big| \Big\{ A \in \mathcal{A} \;\Big|\; \text{supp } M(\cdot \mid A) \cap \Omega \neq \emptyset \Big\} \Big| < \infty \quad \text{for all compact } \Omega \subseteq \mathbb{R}^d.$$

Thus, one can apply Theorem 6.4 to obtain that $M(\cdot \mid \mathfrak{U}(K)) \in \mathcal{S}_{m,X} \setminus \mathcal{S}_{m,X^*}$. □

Definition 6.6 (Necessary criterion for knot insertion)**.** Let $d \in \mathbb{N}_+$, $m \in \mathbb{N}_0$, and let $X^* \subseteq \mathbb{R}^d$ be a knot set satisfying the weak conditions. Choose $x^* \in X^*$, and define the coarser knot set as $X := X^* \backslash \{x^*\}$. Then, X^* satisfies the *necessary criterion for knot insertion (with respect to x^*)* if, for all $K \in \mathcal{K}_m(X)$ and for any $Z \subseteq \mathfrak{U}(K)$ with $|Z| = d$, one can find a $K^* \in \mathcal{K}_m(X^*)$ such that $Z \subseteq \mathfrak{U}(K^*)$. ◀

In the previous definition, we required X^* to satisfy only the weak conditions, in order to keep the results in the next section as general as possible. However, only for knot sets satisfying the strong conditions, we have shown that the criterion is really necessary. The following result is just the contraposition of Corollary 6.5.

Corollary 6.7. Let $d \in \mathbb{N}_+$, $m \in \mathbb{N}_0$, and let $X^* \subseteq \mathbb{R}^d$ be a knot set satisfying the strong conditions. Choose $x^* \in X^*$, and define $X := X^* \backslash \{x^*\}$. If one has $\mathcal{S}_{m,X} \subseteq \mathcal{S}_{m,X^*}$, then X^* satisfies the necessary criterion for knot insertion. ◀

Remark 6.8. The usual univariate splines exhibit the knot insertion property, as stated in Subsection 2.3.5. Since DCB-splines reduce to these univariate splines when considered in one dimension, the necessary criterion is required to hold true for $d = 1$ *in any case*. This is indeed true as Z is then just a single knot, which is contained in each collection of knots corresponding to the $m + 2$ overlapping or adjacent B-splines. ◀

Remark 6.9. The necessary criterion requires that every set of d knots appearing as subset of any unoriented Delaunay configuration in the coarse knot set also appears in at least one of the configurations of the refined knot set. One possibility to enforce that the necessary criterion holds true, of course, would be to modify the definition of the spline space as to incorporate these subsets by adding further basis candidate functions that are *not* generated by Delaunay configurations. Such a modification is clearly a severe intervention, which is incompatible with the whole approach based on Delaunay configurations. Another issue with enforcing the necessary criterion is the following: In Figure 6.3a, there are only few knots and it is reasonable to

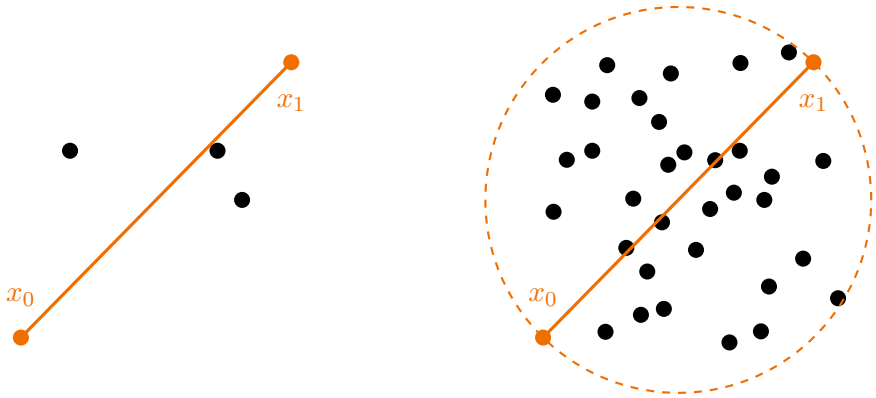

(a) Sparse knot set (b) Knot set after repeated refinement

Fig. 6.3: Enforcing the necessary criterion. In a sparse knot set *(left)*, it may be reasonable to consider two knots as neighbors even though they are fairly far apart *(orange)*. After repeated insertion of knots *(right)*, however, it may be not reasonable any more to consider these knots as neighbors.

consider the knots x_0 and x_1 as neighbors, i.e., there is a Delaunay configuration incorporating both knots. When enforcing the necessary criterion and inserting knots iteratively, this neighborhood relation has to be retained. This contrasts the desired locality of spline basis candidate functions, as presented in Figure 6.3b. ◀

6.3 Sufficiency of the Criterion

The definition of a sufficient criterion ensuring that the knot insertion property holds true for a specific knot set would be at least as interesting as a necessary criterion, like the one formulated in the previous section. Ideally, this necessary criterion is already sufficient, which would show the equivalence of the criterion and the knot insertion property. In this section, we try to give a proof for this circumstance.

In the following subsection, we will recall a knot insertion formula for simplex splines. Subsequently, we will show step-by-step that the necessary criterion implies the existence of specific Delaunay configurations, which, under certain circumstances, can be combined using the knot insertion formula. We try to use these combinations to prove the sufficiency of the criterion. To show the relationship $\mathcal{S}_{m,X} \subseteq \mathcal{S}_{m,X^*}$ for a knot set X and a refined knot set X^*, it is clearly sufficient to show that $\mathcal{B}_{m,X} \subseteq \mathcal{S}_{m,X^*}$ since $\mathcal{B}_{m,X}$ is a generating system for $\mathcal{S}_{m,X}$. Therefore, we will pick an arbitrary basis candidate function in $\mathcal{B}_{m,X}$ and try to prove that it is also contained in the refined spline space $\mathcal{S}_{m,X^*}$.

6.3.1 Knot Insertion Formula

The first ingredient needed to show the sufficiency of the necessary criterion is a knot insertion formula which enables the expression of a simplex spline of a certain degree by means of several other simplex splines of the same degree. Note that Micchelli's recursion formula (see Proposition 3.24) uses simplex splines of a lower degree for that purpose. We will see, however, that the recursion formula is closely related to the knot insertion formula presented in this subsection.

The knot insertion formula is also due to Micchelli since, in fact, it has been used in [Mic80] to prove the recursion formula. Therefore, it is called *Micchelli's knot insertion formula* in [PBP02, p. 264]. In literature, different proofs of this formula have been presented: The proofs in [Mic80] and [Mic95, p. 165f] are based on divided differences, whereas [Mic95, p. 164f] and [PBP02, p. 263f] employ different, geometric approaches. In the following, we present another, novel proof for the knot insertion formula for the case $m \geq 2$, which utilizes Micchelli's recursion formula and, to the best of our knowledge, has not been given in literature so far.

To keep things clear, we use the following shorthand notation, which has been employed, for example, in [Nea07], [PBP02], and [Mic95] in a similar way: For any $x_0, \ldots, x_d, t \in \mathbb{R}^d$, $Z := (x_0, \ldots, x_d)$, and $i, j \in \{0, \ldots, d\}$, we define

$$Z_i^\dagger := (x_0, \ldots, x_{i-1}, t, x_{i+1}, \ldots, x_d), \qquad Z_i^* := (x_0, \ldots, x_{i-1}, x^*, x_{i+1}, \ldots, x_d),$$
$$Z_i := (x_0, \ldots, x_{i-1}, x_{i+1}, \ldots, x_d).$$

We can now give the following proof for Micchelli's knot insertion formula for $m \geq 2$:

Theorem 6.10 (Micchelli's knot insertion formula)**.** Let $d, m \in \mathbb{N}_+$, $m \geq 2$, and choose $x_0, \ldots, x_{m+d}, x^* \in \mathbb{R}^d$ in general position. Set $Z := (x_0, \ldots, x_d)$. Then,

$$M(t \mid x_0, \ldots, x_{m+d}) = \sum_{i=0}^{d} u_i(x^* \mid Z) M(t \mid x_0, \ldots, x_{i-1}, x_{i+1}, \ldots, x_{m+d}, x^*)$$

for every $t \in \mathbb{R}^d$.

Proof. Let $Y := (x_{d+1}, \ldots, x_{m+d})$ and $t \in \mathbb{R}$. Since the definition of simplex splines is independent of the order of knots, one has

$$M(\cdot \mid (Z_j^*)_i, Y) = M(\cdot \mid (Z_i^*)_j, Y) \quad \text{for all } i, j \in \{0, \ldots, d\},\ i \neq j.$$

Together with Micchelli's recursion formula (see Proposition 3.24), Identity (3.3) regarding barycentric coordinates, and the manipulation of sums

$$\sum_{i=0}^{d}\sum_{j=i+1}^{d} a_{i,j} = \sum_{j=0}^{d}\sum_{i=0}^{j-1} a_{i,j} = \sum_{i=0}^{d}\sum_{j=0}^{i-1} a_{j,i}$$

shown in [GKP89, p. 36], one obtains

$$\begin{aligned}
&\sum_{i=0}^{d} u_i(x^* \mid Z) M\Big(t \;\Big|\; x_0,\dots,x_{i-1},x_{i+1},\dots,x_{m+d},x^*\Big)\\
&= \frac{1}{d(Z)}\sum_{i=0}^{d} d(Z_i^*) M\Big(t \;\Big|\; Z_i^*, Y\Big)\\
&= \frac{1}{md(Z)}\sum_{i=0}^{d} d(Z_i^*)\left(u_i(t \mid Z_i^*) M\Big(t \;\Big|\; Z_i, Y\Big) + \sum_{j=0, j\neq i}^{d} u_j(t \mid Z_i^*) M\Big(t \;\Big|\; (Z_i^*)_j, Y\Big)\right)\\
&= \frac{1}{md(Z)}\sum_{i=0}^{d}\left(d\Big(Z_i^\dagger\Big) M\Big(t \;\Big|\; Z_i, Y\Big) + \sum_{j=0, j\neq i}^{d} d\Big((Z_i^*)_j^\dagger\Big) M\Big(t \;\Big|\; (Z_i^*)_j, Y\Big)\right)\\
&= \frac{1}{md(Z)}\left(\sum_{i=0}^{d} d\Big(Z_i^\dagger\Big) M\Big(t \;\Big|\; Z_i, Y\Big) + \sum_{i=0}^{d}\sum_{j=0}^{i-1} d\Big((Z_i^*)_j^\dagger\Big) M\Big(t \;\Big|\; (Z_i^*)_j, Y\Big)\right.\\
&\qquad \left. + \sum_{i=0}^{d}\sum_{j=0}^{i-1} d\Big((Z_j^*)_i^\dagger\Big) M\Big(t \;\Big|\; (Z_j^*)_i, Y\Big)\right)\\
&= \frac{1}{md(Z)}\left(\sum_{i=0}^{d} d\Big(Z_i^\dagger\Big) M\Big(t \;\Big|\; Z_i, Y\Big)\right.\\
&\qquad \left. + \sum_{i=0}^{d}\sum_{j=0}^{i-1} \underbrace{\Big(d\Big((Z_i^*)_j^\dagger\Big) + d\Big((Z_j^*)_i^\dagger\Big)\Big)}_{=0} M\Big(t \;\Big|\; (Z_i^*)_j, Y\Big)\right)\\
&= M\Big(t \;\Big|\; x_0,\dots,x_{m+d}\Big).
\end{aligned}$$

□

As we have to apply the recursion formula, the proof does not cover the case $m \in \{0, 1\}$. For $m = 0$, the occurring functions are piecewise constant, and the stated identity reduces to a combinatorial relationship between the support of these functions. This relationship is basically the core of the geometric proof of the knot insertion formula in [PBP02, p. 263f]. In the case $m = 1$, the above result still does not hold pointwise as we cannot apply the recursion formula due to the discontinuities in the occurring simplex splines of degree zero. This could be remedied by a consistent definition of degree zero simplex splines on the boundary of their support (see Subsection 8.2.1).

The original formulation of Theorem 6.10 is more general in two ways: Firstly, it also allows for the case $m \in \{0, 1\}$ and more general collections of knots. Secondly, it facilitates the use of an arbitrary number of nonzero coefficients in the affine combination of x^*, whereas we assumed that at most $d + 1$ coefficients are different from zero. Nevertheless, due to Carathéodory's theorem, every choice of x^* can be represented in this way.

Despite these limitations, our proof reveals the interesting insight that the intimate relationship between Micchelli's recursion formula and the knot insertion formula is in some sense *bidirectional* since, in [Mic80], Micchelli used the knot insertion formula to prove the recursion formula and we proceeded vice versa.

Remark 6.11. The knot insertion formula provides rich possibilities for the combination of simplex splines of the same degree. In particular, if one has $d + 1$ simplex splines such that each pair is defined with respect to collections of knots that differ by exactly one knot, the total number of involved knots is $m + d + 2$. In this case, the knot insertion formula enables the combination of any simplex spline that is defined with respect to a subset of $m + d + 1$ knots. Hence, there are exactly $m + d + 2$ possible choices. Clearly, $d + 1$ of these choices yield the original simplex splines, whereas the remaining $m + 1$ possibilities generate functions which are not part of the initial set of simplex splines. ◀

Remark 6.12. In the univariate case, the coefficients in the knot insertion formula (see Theorem 2.26) are always nonnegative when combining a specific B-spline. However, this is not necessarily the case in the multivariate analogue. The coefficients are nonnegative if and only if the barycentric coordinates $u_i(x^* \mid Z)$ are nonnegative for all $i \in \{0, \dots, d\}$. This is clearly the case if and only if $x^* \in \operatorname{conv}(x_0, \dots, x_d)$. We display this behavior in Figure 6.4. ◀

6.3.2 Critical Configurations

We aim at a proof of the existence of certain Delaunay configurations now, which we will call *critical configurations* and which, under certain circumstances, enable us to apply Micchelli's knot insertion formula to obtain a linear combination of a given basis candidate function in $\mathcal{B}_{m,X}$ in terms of basis candidate functions generated by the refined knot set X^*. As mentioned earlier, it is sufficient to show that $\mathcal{B}_{m,X} \subseteq \mathcal{S}_{m,X^*}$ in order to prove that $\mathcal{S}_{m,X} \subseteq \mathcal{S}_{m,X^*}$.

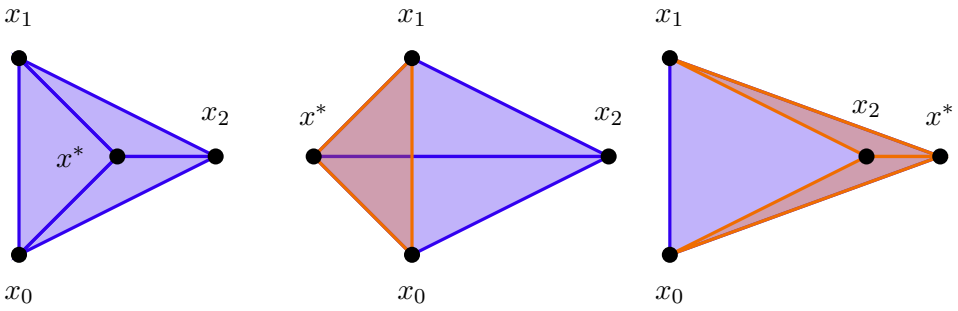

(a) All coefficients are positive **(b)** One coefficient is negative **(c)** Two coefficients are negative

Fig. 6.4: Different signs of coefficients when applying the knot insertion formula in order to represent the simplex spline $M(\cdot \mid x_0, x_1, x_2)$ by means of other simplex splines of degree zero with respect to three knots of the set $\{x_0, x_1, x_2, x^*\}$. Regions shaded in *blue* refer to the support of simplex splines with a positive coefficient, whereas *orange* regions indicate a negative coefficient.

To that end, several geometric preliminaries are necessary again. One of these results cannot be generalized for $d > 2$, though (see the remarks following Lemma 6.16). Since the case $d = 1$ is clear as the knot insertion property holds true for univariate splines in any case, we will formulate the final result of this subsection only for $d = 2$. Nevertheless, we provide generic proofs that work for arbitrary $d \in \mathbb{N}_+$ for the following auxiliary results.

One of the most important results for the following considerations is Lemma 5.20. We will extend its statement now by the following two results:

Lemma 6.13. Let $d \in \mathbb{N}_+$, and choose affinely independent $v_0, \ldots, v_{d-1} \in \mathbb{R}^d$. Let H_+ and H_- denote the two open half spaces generated by the hyperplane $\mathrm{aff}(v_0, \ldots, v_{d-1})$. Choose $w, w' \in H_+ \cup H_-$ such that $\{v_0, \ldots, v_{d-1}, w, w'\}$ is in general Delaunay position. Then, *exactly one* of the following properties holds true:

(i) $\overline{B(v_0, \ldots, v_{d-1}, w)} \cap H_+ \subseteq B(v_0, \ldots, v_{d-1}, w')$,

(ii) $\overline{B(v_0, \ldots, v_{d-1}, w')} \cap H_+ \subseteq B(v_0, \ldots, v_{d-1}, w)$.

Proof. Due to the affine independence of the points, both balls are well-defined. We make the same transformations as in Lemma 5.20 to simplify the proof, so that one has $H_+ = \{t \in \mathbb{R}^d \mid t_d > 0\}$ and

$$b := \mathrm{cen}(v_0, \ldots, v_{d-1}, w) = (0, \ldots, 0, \widehat{b})^\intercal,$$
$$c := \mathrm{cen}(v_0, \ldots, v_{d-1}, w') = (0, \ldots, 0, \widehat{c})^\intercal,$$

$$r := \operatorname{rad}(v_0, \dots, v_{d-1}, w) = \sqrt{\widehat{b}^2 + 1},$$
$$s := \operatorname{rad}(v_0, \dots, v_{d-1}, w') = \sqrt{\widehat{c}^2 + 1},$$

where

$$\widehat{b} = \frac{\|w\|^2 - 1}{2w_d} \quad \text{and} \quad \widehat{c} = \frac{\|w'\|^2 - 1}{2w'_d}.$$

As the points are in general Delaunay position, it follows that $\widehat{b} \neq \widehat{c}$. Assume that $\widehat{c} < \widehat{b}$, and choose $u \in \overline{B_s(c)} \cap H_+$. Then, it follows as in (5.21) that

$$\|u\|^2 - 1 \leq 2u_d\widehat{c} < 2u_d\widehat{b},$$

and therefore, $u \in B_r(b)$. Consequently, (ii) holds true. Otherwise, one has $\widehat{b} < \widehat{c}$, and it follows analogously that (i) holds true.

The assumption that both (i) and (ii) hold true yields the contradiction

$$\overline{B_r(b)} \cap H_+ \subseteq B_s(c) \cap H_+ \subset \overline{B_s(c)} \cap H_+ \subseteq B_r(b) \cap H_+ \subset \overline{B_r(b)} \cap H_+,$$

which finishes the proof. □

Corollary 6.14. Let $d \in \mathbb{N}_+$, and choose affinely independent $v_0, \dots, v_{d-1} \in \mathbb{R}^d$. Let H_+ and H_- denote the two open half spaces generated by the hyperplane $H_0 := \operatorname{aff}(v_0, \dots, v_{d-1})$. Choose $w \in H_+ \cup H_-$ and $u \in H_+ \backslash B(v_0, \dots, v_{d-1}, w)$ such that $\{v_0, \dots, v_{d-1}, w, u\}$ is in general Delaunay position. Then,

$$\overline{B(v_0, \dots, v_{d-1}, w)} \cap H_+ \subseteq B(v_0, \dots, v_{d-1}, u) \cap H_+ \quad \text{and}$$
$$\overline{B(v_0, \dots, v_{d-1}, u)} \cap H_- \subseteq B(v_0, \dots, v_{d-1}, w) \cap H_-.$$

Proof. Since $u \in H_+ \cap \overline{B(v_0, \dots, v_{d-1}, u)}$, one has

$$\overline{B(v_0, \dots, v_{d-1}, u)} \cap H_+ \not\subseteq B(v_0, \dots, v_{d-1}, w),$$

and consequently, Lemma 6.13 yields

$$\overline{B(v_0, \dots, v_{d-1}, w)} \cap H_+ \subseteq B(v_0, \dots, v_{d-1}, u).$$

The second formula then follows by applying Lemma 5.20. □

We can use previous results to show that points in a half space can be ordered strictly in the following way:

Lemma 6.15. Let $d \in \mathbb{N}_+$, and choose affinely independent $v_0, \dots, v_{d-1} \in \mathbb{R}^d$. Let H_+ be one of the open half spaces generated by the hyperplane $\operatorname{aff}(v_0, \dots, v_{d-1})$. Choose $W := \{w_i \in H_+ \mid i \in I\}$ such that $W \cup \{v_0, \dots, v_{d-1}\}$ is in general Delaunay position, where I is a nonempty index set. Then, the relation

$$\prec := \left\{(w, w') \in W \times W \;\middle|\; w \in B(v_0, \dots, v_{d-1}, w')\right\}$$

is a strict total order on W.

Proof. a) *Irreflexivity:* It follows from the definition that $w \not\prec w$ for all $w \in W$.

b) *Connectedness:* Let $w, w' \in W$ with $w \neq w'$. Lemma 6.13 provides that either

$$\overline{B(v_0, \dots, v_{d-1}, w)} \cap H_+ \subseteq B(v_0, \dots, v_{d-1}, w'),$$

yielding $w \prec w'$, or

$$\overline{B(v_0, \dots, v_{d-1}, w')} \cap H_+ \subseteq B(v_0, \dots, v_{d-1}, w),$$

which in turn implies that $w' \prec w$.

c) *Transitivity:* Let $w_1, w_2, w_3 \in W$ such that $w_1 \prec w_2$ and $w_2 \prec w_3$. Then, $w_2 \in B(v_0, \dots, v_{d-1}, w_3) \cap H_+$, and thus,

$$w_1 \in B(v_0, \dots, v_{d-1}, w_2) \cap H_+ \subseteq B(v_0, \dots, v_{d-1}, w_3)$$

due to Lemma 5.20. Therefore, it follows that $w_1 \prec w_3$, which finishes the proof. □

Whereas the formal definition of this order seems to be new in the context of Delaunay configurations, it already appeared implicitly in literature, for example in [SK09]. For a visualization of the previous result, we refer to Figure 6.5. In the following lemma, we again extend the statement of a geometric result that has been presented earlier, namely Lemma 5.22:

Lemma 6.16. Let $d \in \mathbb{N}_+$, $c \in \mathbb{R}^d$, $r \in \mathbb{R}_+$, and $v, v' \in \overline{B_r(c)}$. There are $c' \in \mathbb{R}^d$, $r' \in \mathbb{R}_+$ such that $v, v' \in \partial B_{r'}(c')$ and $B_{r'}(c') \subseteq B_r(c)$.

Proof. If $v, v' \in \partial B_r(c)$, the claim follows immediately. If only one of the points v, v' is on the boundary $\partial B_r(c)$, applying Lemma 5.22 yields the stated claim. Otherwise,

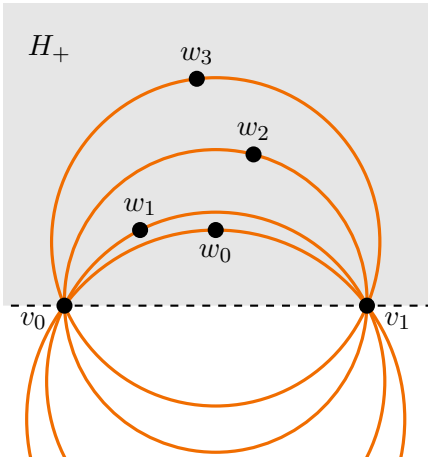

Fig. 6.5: Strict total order of points in a half space. The points $w_0, \dots, w_3$ in the half space H_+ can be ordered according to the nesting of the circles $B(v_0, v_1, w_i)$, $i \in \{0, \dots, 3\}$, in H_+. In this example, one has $w_0 \prec w_1 \prec w_2 \prec w_3$.

$v, v' \in B_r(c)$. We choose an arbitrary $w \in \partial B_r(c)$ and apply Lemma 5.22 both to v, w and to v', w, yielding $b, b' \in \operatorname{conv}(c, w)$ and $s, s' \in \mathbb{R}_+$ such that

$$\begin{aligned} v, w &\in \partial B_s(b), & B_s(b) &\subseteq B_r(c), \\ v', w &\in \partial B_{s'}(b'), & B_{s'}(b') &\subseteq B_r(c). \end{aligned}$$

Since $b, b' \in \operatorname{conv}(c, w)$, there are $\lambda, \lambda' \in [0, 1]$ such that

$$b = \lambda c + (1 - \lambda) w \quad \text{and} \quad b' = \lambda' c + (1 - \lambda') w.$$

Consequently,

$$\|b - b'\| = |\lambda - \lambda'| \|c - w\| = \Big| |\lambda| - |\lambda'| \Big| \|c - w\| = \Big| \|b - w\| - \|b' - w\| \Big| = |s - s'|.$$

If $s \geq s'$, one obtains

$$\|v' - b\| \leq \|v' - b'\| + \|b' - b\| = s' + |s - s'| = s$$

and, therefore, $v' \in \overline{B_s(b)}$. Applying Lemma 5.22 once again to v and v' results in $c' \in \operatorname{conv}(b, v)$ and $r' \in \mathbb{R}_+$ satisfying

$$v, v' \in \partial B_{r'}(c') \quad \text{and} \quad B_{r'}(c') \subseteq B_s(b) \subseteq B_r(c),$$

which yields the stated claim. If $s < s'$, the claim follows analogously. □

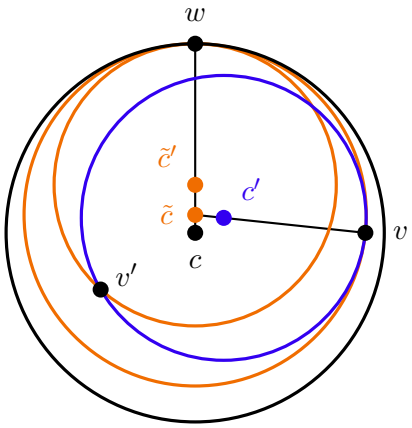

Fig. 6.6: The situation in Lemma 6.16. Lemma 5.22 ensures the existence of circles *(orange)* through w and v or v', respectively, where w can be chosen arbitrarily on the boundary of the initial circle *(black)*. Applying the same result once again to the larger of the two *orange* circles yields the existence of another circle *(blue)* through v and v', which is contained in the initial circle *(black)*.

The situation in the previous lemma is illustrated in Figure 6.6. Note that it *cannot* be generalized to d points in a d-dimensional ball for $d \geq 3$. As an example, consider the case $d = 3$, and assume that we have three distinct points $v, v', v'' \in \overline{B}$, where B is an arbitrary open ball. If $v, v' \in \partial B$ and $v'' \in B$, there is no ball B' satisfying both $v, v', v'' \in \partial B'$ and $\overline{B}' \subseteq \overline{B}$ since every $\overline{B}' \subset \overline{B}$ touches ∂B at no more than one point and, therefore, it is impossible that both $v \in \partial B'$ and $v' \in \partial B'$. On the contrary, if $v, v' \in \partial B \cap \partial B'$ and $\overline{B}' \subseteq \overline{B}$, it follows that $B = B'$ and, hence, $v'' \notin \partial B'$.

In the last preparation for the main result of this subsection, we show a very simple property of certain maps. Despite its simplicity, it is a core ingredient in the proofs of the following propositions.

Lemma 6.17. Let $m \in \mathbb{N}_0$ and $n \in \mathbb{N}_+$. Let $\varphi : \{1, \dots, n\} \to \mathbb{N}_0$ be a map satisfying

$$\varphi(k) \geq \varphi(k+1) - 1 \quad \text{for all } k \in \{1, \dots, n-1\}.$$

as well as $\varphi(1) \leq m$ and $\varphi(n) \geq m$. Then, there is a $k^* \in \{1, \dots n\}$ with $\varphi(k^*) = m$.

Proof. The claim trivially holds true for $n = 1$ since $m \leq \varphi(1) \leq m$. Consider $n \to n+1$ now. If $\varphi(2) \geq m+1$, one has $m \geq \varphi(1) \geq \varphi(2) - 1 \geq m$ and, thus, can choose $k^* = 1$. If $\varphi(2) \leq m$, apply the induction hypothesis to the function $\widetilde{\varphi} : \{1, \dots, n\} \to \mathbb{N}_0,\ k \to \varphi(k+1)$, yielding the existence of a $\widetilde{k} \in \{1, \dots, n\}$ such that $\widetilde{\varphi}(\widetilde{k}) = m$. Consequently, setting $k^* := \widetilde{k} + 1 \in \{2, \dots, n+1\}$ yields $\varphi(k^*) = \widetilde{\varphi}(\widetilde{k}) = m$ and, therefore, finishes the proof. □

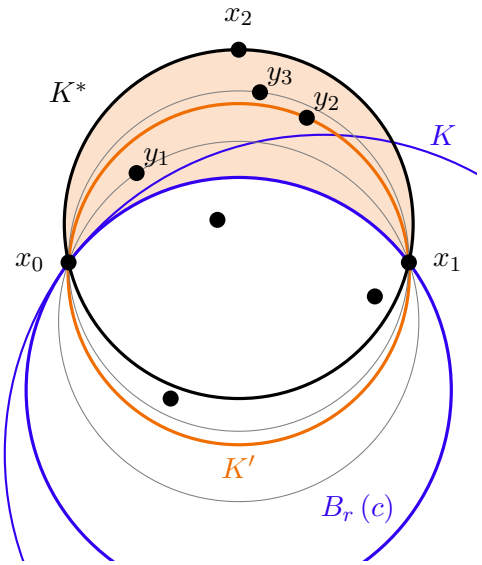

Fig. 6.7: The situation in Proposition 6.18 for $m = 4$. We require the existence of the Delaunay configuration K *(blue)* and define I as the set of knots in the shaded region *(orange)*. Together with x_0 and x_1, at least one of these knots (namely $\widehat{x} = y_2$ in this example) is a boundary knot of a Delaunay configuration K' *(orange)*, which we will call critical configuration.

We are able to prove the existence of specific Delaunay configurations now, which we will subsequently define as *critical configurations*. As elucidated in the introduction of this subsection and the remarks following Lemma 6.16, we have to restrict ourselves to $d = 2$ for that purpose.

The requirements of the following proposition are in particular fulfilled when one considers X as a *refined* knot set satisfying the necessary criterion for knot insertion (see Definition 6.6). K^* can be considered as Delaunay configuration (formerly of degree m) which is not an element of $\mathcal{K}_m(X)$ any more due to the insertion of the new knot. Therefore, it is a Delaunay configuration of degree $m+1$ now. The necessary criterion implies the existence of a suitable configuration K. The proof is illustrated in Figure 6.7.

Proposition 6.18 (Critical configurations)**.** Let $X \subseteq \mathbb{R}^2$ be a knot set satisfying the weak conditions. Let $m \in \mathbb{N}_0$ and $x_0, x_1 \in X$ such that there are

$$\begin{aligned} K^* \in \mathcal{K}_{m+1}(X) \quad &\text{with } x_0, x_1 \in \mathfrak{B}(K^*), \\ K \in \mathcal{K}_m(X) \quad &\text{with } x_0, x_1 \in \mathfrak{U}(K). \end{aligned}$$

Then, there is an $\widehat{x} \in \mathfrak{I}(K^*)$ and a $K' \in \mathcal{K}_m(X)$ with $\{x_0, x_1, \widehat{x}\} = \mathfrak{B}(K')$.

Proof. Let $B := B(\mathfrak{B}(K^*))$. According to Lemma 6.16, there is a $c \in \mathbb{R}^2$ and an $r \in \mathbb{R}_+$ such that $x_0, x_1 \in \partial B_r(c)$ and $B_r(c) \subseteq B(\mathfrak{B}(K))$. Hence, one has

$$|B_r(c) \cap X| \leq |B(\mathfrak{B}(K)) \cap X| = m \tag{6.10}$$

and, in particular, $B_r(c) \neq B$ since $|B \cap X| = m + 1$. Let H_+, H_- denote the two open half planes generated by the hyperplane $\operatorname{aff}(x_0, x_1)$. Since $x_0, x_1 \in \partial B \cap \partial B_r(c)$, one can apply Lemma 6.13, yielding that

$$\text{either} \quad \overline{B} \cap H_+ \subseteq B_r(c) \quad \text{or} \quad \overline{B_r(c)} \cap H_+ \subseteq B.$$

According to Lemma 5.20, the latter would imply $\overline{B} \cap H_- \subseteq B_r(c)$. As we have not imposed any restrictions on the roles of H_+ and H_- yet, we can number them such that

$$\overline{B_r(c)} \cap H_+ \subseteq B \quad \text{and} \quad \overline{B} \cap H_- \subseteq B_r(c). \tag{6.11}$$

Define $I := (B \backslash B_r(c)) \cap X$. Due to (6.11), one has

$$I \subseteq H_+. \tag{6.12}$$

Moreover, as X is in general Delaunay position, (6.11), (6.12), and (6.10) yield

$$\begin{aligned} m + 1 &= |B \cap H_+ \cap X| + |B \cap H_- \cap X| \\ &= |B_r(c) \cap H_+ \cap X| + |(B \backslash B_r(c)) \cap H_+ \cap X| + |B \cap H_- \cap X| \\ &\leq |B_r(c) \cap H_+ \cap X| + |I| + |B_r(c) \cap H_- \cap X| \leq m + |I|, \end{aligned}$$

and hence, $I \neq \emptyset$. According to Lemma 6.15 and (6.12), we can define a strict total ordering $\prec$ on I such that, for any $y, y' \in I$ with $y \prec y'$, one has $y \in B(x_0, x_1, y')$, which in turn implies $B(x_0, x_1, y) \cap H_+ \subseteq B(x_0, x_1, y')$, according to Lemma 5.20. Moreover, we label the elements in I as $\{y_1, \ldots, y_n\} := I$ with $n := |I|$ such that, for all $i, j \in \{1, \ldots, n\}$ with $i < j$, one has $y_i \prec y_j$. Then,

$$B(x_0, x_1, y_i) \cap I = \{y_1, \ldots, y_{i-1}\} \quad \text{for all } i \in \{1, \ldots, n\}, \tag{6.13}$$

and, due to Lemma 5.20, also

$$B(x_0, x_1, y_j) \cap H_- \subseteq B(x_0, x_1, y_i) \quad \text{for all } i, j \in \{1, \ldots, n\},\ i < j. \tag{6.14}$$

For all $i \in \{1, \ldots, n\}$, it follows from $y_i \in H_+ \backslash B_r(c)$ and Corollary 6.14 that

$$B_r(c) \cap H_+ \subseteq B(x_0, x_1, y_i) \quad \text{and} \quad B(x_0, x_1, y_i) \cap H_- \subseteq B_r(c). \tag{6.15}$$

Moreover, $y_i \in B \cap H_+$ together with Lemma 5.20 yields

$$B(x_0, x_1, y_i) \cap H_+ \subseteq B \quad \text{and} \quad B \cap H_- \subseteq B(x_0, x_1, y_i) \tag{6.16}$$

for all $i \in \{1, \ldots, n\}$. As a consequence of (6.15), (6.16), (6.12), and (6.13), one has

$$\begin{aligned} &|B(x_0, x_1, y_i) \cap H_+ \cap X| \\ &= |B_r(c) \cap H_+ \cap X| + |(B(x_0, x_1, y_i) \backslash B_r(c)) \cap H_+ \cap X| \\ &= |B_r(c) \cap H_+ \cap X| + |B(x_0, x_1, y_i) \cap H_+ \cap (B \backslash B_r(c)) \cap X| \\ &= |B_r(c) \cap H_+ \cap X| + i - 1 \end{aligned} \tag{6.17}$$

for all $i \in \{1, \ldots, n\}$. Our goal is to apply Lemma 6.17 to the map

$$\varphi : \{1, \ldots, n\} \to \mathbb{N}_0, \quad i \mapsto |B(x_0, x_1, y_i) \cap X|.$$

The remainder of the proof shows that the prerequisites of that lemma hold true. From (6.17) and (6.15), it follows that

$$\begin{aligned} \varphi(1) &= |B(x_0, x_1, y_1) \cap H_- \cap X| + |B_r(c) \cap H_+ \cap X| \\ &\leq |B_r(c) \cap H_- \cap X| + |B_r(c) \cap H_+ \cap X| \leq m, \end{aligned}$$

whereas (6.14) and (6.17) yield

$$\begin{aligned} \varphi(i) &\geq |B(x_0, x_1, y_{i+1}) \cap H_- \cap X| + |B(x_0, x_1, y_i) \cap H_+ \cap X| \\ &= |B(x_0, x_1, y_{i+1}) \cap H_- \cap X| + |B(x_0, x_1, y_{i+1}) \cap H_+ \cap X| - 1 \\ &= \varphi(i+1) - 1. \end{aligned}$$

for all $i \in \{1, \ldots, n-1\}$. It remains to be shown that $\varphi(n) \geq m$. One has

$$y_n \in A := (B \backslash B(x_0, x_1, y_n)) \cap H_+ \cap X.$$

Assume that there is another $y \in A$ with $y \neq y_n$. Then, from (6.15) and applying Corollary 6.14 to $y \in H_+ \backslash B(x_0, x_1, y_n)$, one obtains

$$y \notin B(x_0, x_1, y) \cap H_+ \supseteq B(x_0, x_1, y_n) \cap H_+ \supseteq B_r(c) \cap H_+.$$

As a consequence, $y \notin B_r(c)$, and therefore, $y \in I$. Due to the maximality of y_n in I with respect to $\prec$, one has $y \in B(x_0, x_1, y_n)$, which is a contradiction to $y \in A$. Thus, there is no such y, and it follows that $|(B \backslash B(x_0, x_1, y_n)) \cap H_+ \cap X| = 1$.

Consequently, one obtains together with (6.16) that

$$\begin{aligned}\varphi(n) &= |B \cap H_+ \cap X| - |(B \backslash B(x_0, x_1, y_n)) \cap H_+ \cap X| + |B(x_0, x_1, y_n) \cap H_- \cap X| \\ &\geq |B \cap H_+ \cap X| - 1 + |B \cap H_- \cap X| = m.\end{aligned}$$

Finally, one can apply Lemma 6.17, yielding the existence of an $i^* \in \{1, \ldots, n\}$ such that $|B(x_0, x_1, y_{i^*}) \cap X| = \varphi(i^*) = m$. Hence, by choosing $\widehat{x} := y_{i^*} \in \mathfrak{I}(K^*)$, one obtains the stated claim. □

In the proof of Proposition 6.18, we ensured the existence of an $\widehat{x} \in I$ such that

$$|B(x_0, x_1, \widehat{x}) \cap X| = m. \tag{6.18}$$

However, this knot is in general not uniquely defined. In this case, we choose of all knots in I satisfying (6.18) the one which is maximal with respect to $\prec$.

Definition 6.19 (Critical configuration, Rank)**.** Let $X \subseteq \mathbb{R}^2$ satisfy the weak conditions, and let $x_0, x_1, x' \in X$ such that there are

$$\begin{aligned} K^* \in \mathcal{K}_{m+1}(X) \quad &\text{with } x_0, x_1 \in \mathfrak{B}(K^*) \text{ and } x' \in \mathfrak{I}(K^*), \\ K' \in \mathcal{K}_m(X) \quad &\text{with } \{x_0, x_1, x'\} = \mathfrak{B}(K'). \end{aligned}$$

Let H_+, H_- be the open half planes generated by the hyperplane $\mathrm{aff}(x_0, x_1)$, indexed such that $x' \in H_+$. Let $I := \mathfrak{I}(K^*) \cap H_+$. Since $x' \in I$, one has $I \neq \emptyset$. Define a strict ordering $\prec$ on I such that, for any $y, y' \in I$ with $y \prec y'$, one has $y \in B(x_0, x_1, y')$, and whose existence is guaranteed by Lemma 6.15. Let

$$\widehat{x} := \max_{\prec} \Big\{ y \in I \;\Big|\; |B(x_0, x_1, y) \cap X| = m \Big\}.$$

Then, the Delaunay configuration $K \in \mathcal{K}_m(X)$ with $\mathfrak{B}(K) = \{x_0, x_1, \widehat{x}\}$ is a *critical configuration of K^* (with respect to x_0 and x_1)*. The number

$$\Big| \mathfrak{I}(K^*) \Big\backslash \mathfrak{U}(K) \Big| \in \mathbb{N}_0$$

denotes the *rank* of the critical configuration. ◀

Note that the set I has been defined differently in Proposition 6.18 and Definition 6.19 in order to avoid the dependence of the ball $B_r(c)$ in the latter. Since

$$(B \backslash B_r(c)) \cap X = (B \backslash B_r(c)) \cap H_+ \cap X = (\mathfrak{I}(K^*) \cap H_+) \backslash B_r(c) \subseteq \mathfrak{I}(K^*) \cap H_+,$$

the set I in Proposition 6.18 is a subset of the one in Definition 6.19. According to (6.15), no knot in $B_r(c)$ can be maximal with respect to $\prec$, though. Moreover, Proposition 6.18 ensures that there is always an $\widehat{x} \in (\mathfrak{I}(K^*) \cap H_+) \backslash B_r(c)$ under the stated assumptions. Hence, the resulting critical configuration would be the same for both definitions of I.

The critical configuration has been chosen as the Delaunay configuration generated by x_0, x_1, and some point in I which has the largest overlap with $\mathfrak{I}(K^*)$ in terms of common knots, as displayed in Figure 6.8a. However, despite the unambiguous choice of $\widehat{x}$ in I, a critical configuration with respect to x_0, x_1 is not necessarily unique since it also depends on the roles of the half planes H_- and H_+, which in turn depend on the choice of K'. This ambiguity is presented in Figure 6.9.

Since $\widehat{x} \in \mathfrak{U}(K) \cap \mathfrak{I}(K^*)$ and $|\mathfrak{I}(K^*)| = m + 1$, it is clear that the rank of a critical configuration can be at most m.

Remark 6.20. Consider a knot set $X^* \subseteq \mathbb{R}^2$ satisfying the weak conditions, and let $X := X^* \backslash \{x^*\}$ denote the coarser knot set for an arbitrary inserted knot $x^* \in X^*$. Then, X also satisfies the weak conditions. We choose any $K \in \mathcal{K}_m(X)$ with $x^* \in B(\mathfrak{B}(K))$ and set $K^* := (\mathfrak{B}(K), \mathfrak{I}(K) \cup \{x^*\}) \in \mathcal{K}_{m+1}(X^*)$. Moreover, let $x_0, x_1, x_2 \in X$ such that $\mathfrak{B}(K) = \{x_0, x_1, x_2\}$. If we assume now that the necessary criterion for knot insertion (Definition 6.6) holds true, we can find configurations $K_0', K_1', K_2' \in \mathcal{K}_m(X^*)$ such that

$$x_1, x_2 \in \mathfrak{U}(K_0'), \quad x_2, x_0 \in \mathfrak{U}(K_1'), \quad x_0, x_1 \in \mathfrak{U}(K_2').$$

Invoking Proposition 6.18 on each of these configurations yields the existence of critical configurations $K_0, K_1, K_2 \in \mathcal{K}_m(X^*)$ and not necessarily distinct interior knots $\widehat{x}_0, \widehat{x}_1, \widehat{x}_2 \in \mathfrak{I}(K^*)$ such that

$$\{\widehat{x}_0, x_1, x_2\} = \mathfrak{B}(K_0), \quad \{x_0, \widehat{x}_1, x_2\} = \mathfrak{B}(K_1), \quad \{x_0, x_1, \widehat{x}_2\} = \mathfrak{B}(K_2).$$

We assume now that all three critical configurations have rank zero, which is equivalent to $|\mathfrak{I}(K^*) \backslash \mathfrak{U}(K_i)| = 0$ and, in turn, $\mathfrak{I}(K^*) \subseteq \mathfrak{U}(K_i)$ for all $i \in \{0, 1, 2\}$. As $|\mathfrak{I}(K^*)| = m + 1$ and $|\mathfrak{U}(K_0)| = m + 3$, it follows from $x_1, x_2 \in \mathfrak{U}(K_0) \backslash \mathfrak{I}(K^*)$ that

$$\mathfrak{U}(K_0) = \mathfrak{I}(K^*) \cup \{x_1, x_2\}.$$

Since it follows analogously that

$$\mathfrak{U}(K_1) = \mathfrak{I}(K^*) \cup \{x_2, x_0\} \quad \text{and} \quad \mathfrak{U}(K_2) = \mathfrak{I}(K^*) \cup \{x_0, x_1\},$$

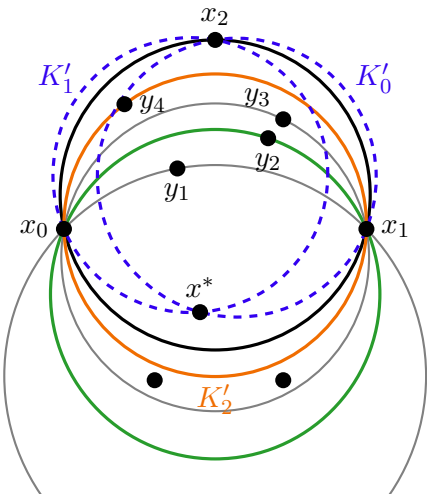

(a) The Delaunay configuration through y_2 *(green)* is no critical configuration as y_2 is not maximal with respect to $\prec$ in the set $\{y \in \{y_1, \dots, y_4\} \mid |B(x_0, x_1, y) \cap X| = m\}$.

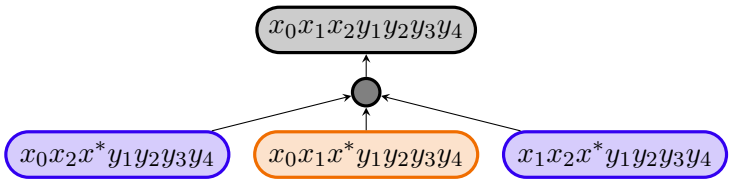

(b) Scheme of the combination of simplex splines above

Fig. 6.8: Using critical configurations to combine a simplex spline for $m = 4$. The critical configuration K_2' through x_0, x_1 and y_4 *(orange)* has rank zero. Together with the critical configurations K_0' and K_1' with respect to x_0, x_2 and x_1, x_2, respectively, of rank zero *(blue, dashed)*, one can use the knot insertion formula to combine the simplex spline $M(\cdot \mid x_0, x_1, x_2, y_1, \dots, y_4)$, which has been generated by the configuration of degree m with the boundary knots x_0, x_1, x_2 *(black)* before inserting the knot x^*.

the Delaunay configurations K_0, K_1, and K_2 differ pairwise by exactly one knot. Therefore, according to Remark 6.11, we can apply the knot insertion formula, yielding coefficients $a_0, a_1, a_2 \in \mathbb{R}$ such that

$$M(\cdot \mid K) = \sum_{i=0}^{2} a_i M(\cdot \mid K_i)$$

is a linear combination of the simplex spline corresponding to the original configuration $K \in \mathcal{K}_m(X)$ with respect to the coarser knot set, which uses the simplex splines generated by the configurations $K_0, K_1, K_2 \in \mathcal{K}_m(X^*)$ with respect to the refined knot set. After all, this has been our goal, as presented in Figure 6.8. Since the rank of any critical configuration is at most m, we have proved the following corollary. ◀

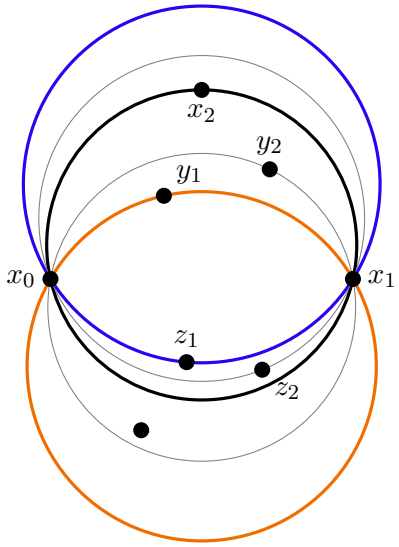

Fig. 6.9: We consider the Delaunay configuration of degree $m+1$ *(black)* with the boundary knots x_0, x_1, and x_2. There exist two different critical configurations *(orange / blue)* of that configuration with respect to the same knots x_0 and x_1.

Corollary 6.21. Let $m = 0$, and choose a knot set $X^* \subseteq \mathbb{R}^2$ satisfying the weak conditions. Let $X := X^* \backslash \{x^*\}$ for an arbitrary $x^* \in X^*$. If the necessary criterion for knot insertion (Definition 6.6) holds true with respect to x^*, one has $\mathcal{S}_{0,X} \subseteq \mathcal{S}_{0,X^*}$, i.e., the necessary criterion is also sufficient. ◀

If $m > 0$, however, the critical configurations do not have rank zero in general. In that case, their corresponding simplex splines cannot be combined directly using Micchelli's knot insertion formula, and we have to find another strategy:

We will see in the following subsection that the existence of a critical configuration of nonzero rank also implies the existence of specific configurations, which will be called *companion configurations* and, under certain circumstances, can be used to combine the original simplex spline by *repeated* application of the knot insertion formula.

The fact that these companion configurations automatically come with a critical configuration also justifies the term *critical configuration* that we have introduced in this subsection.

Remark 6.22. Critical configurations of rank zero reveal an interesting connection to Neamtu's proof of Theorem 4.17 in [Nea07]. For a knot set X satisfying the strong conditions, he defined a *face of degree* m as a tuple (P, I), where $P, I \subseteq X$, $|P| = d$, and $|I| = m$ such that there is an open ball $\widetilde{B}$ with $P \subseteq \partial\widetilde{B}$ and $I = \widetilde{B} \cap X$.

He proved that, for each face (P, I), there are exactly two distinct knots $x, x' \in X \backslash P$ such that there are open balls B, B' with

$$\begin{aligned} P \cup \{x\} &\subseteq \partial B, & P \cup I \cup \{x\} &= \overline{B} \cap X, \\ P \cup \{x'\} &\subseteq \partial B', & P \cup I \cup \{x'\} &= \overline{B'} \cap X. \end{aligned}$$

Clearly, either zero, one, or two of the points x, x' are contained in I. Depending on this number, Neamtu classified the face as *nonessential face*, *essential face*, or *phantom face*, respectively.

Let $K^* \in \mathcal{K}_{m+1}(X)$, and choose two distinct $x_0, x_1 \in \mathfrak{B}(K^*)$. As it turns out, there exists a critical configuration K' of K^* with respect to x_0, x_1 and of rank zero if and only if $(\{x_0, x_1\}, \mathfrak{I}(K^*))$ is an essential face of degree $m+1$. In this case, the sets $\{x_0, x_1, x\}$ and $\{x_0, x_1, x'\}$ are the boundary knots of the original configuration K^* and the critical configuration K', respectively, where x and x' denote the two distinct knots from Neamtu's proof. However, it does not seem possible to take immediate advantage from this connection, in particular as it seems to exist only for critical configurations of rank zero. ◀

6.3.3 Companion Configurations

Throughout the whole subsection, we again have to restrict ourselves to $d = 2$. We begin with further geometrical preparations, which give information on the subset relationships of circles for *two different* divisions of $\mathbb{R}^2$ into half planes. So far, all results only considered *one* separating hyperplane, which is not sufficient for the subsequent proof regarding companion configurations.

Lemma 6.23. Let $u, v, w \in \mathbb{R}^2$ be affinely independent, and define G_+, G_- as the two open half planes generated by $\operatorname{aff}(u, v)$ with $w \in G_+$. Furthermore, define H_+, H_- as the two open half planes generated by $\operatorname{aff}(u, w)$ with $v \in H_-$. Then, one has $B(u, v, w) \cap G_- \subseteq H_-$.

Proof. In a similar way as in the proof of Lemma 5.20, assume without loss of generality that

$$u = (1, 0)^\intercal, \quad v = (-1, 0)^\intercal, \quad G_+ = \{(z_1, z_2)^\intercal \in \mathbb{R}^2 \mid z_2 > 0\}. \tag{6.19}$$

Hence, $w_2 > 0$, and one can apply Lemma 5.19 to obtain that

$$c := \operatorname{cen}(u, v, w) = (0,\ \widehat{c})^\intercal, \quad r := \operatorname{rad}(u, v, w) = \sqrt{\widehat{c}^2 + 1},$$

where

$$\widehat{c} := \frac{w_1^2 + w_2^2 - 1}{2w_2}.$$

Let $n := u - c$, and define the tangent on $B(u, v, w)$ at u as

$$F_0 := \{z \in \mathbb{R}^2 \mid \langle z - u, n\rangle = 0\}.$$

This tangent generates the open half plane $F_- := \{z \in \mathbb{R}^2 \mid \langle z - u, n\rangle < 0\}$. Let $z \in B(u, v, w)$. Then, it follows in the same way as in (5.21) that $\|z\|^2 - 1 < 2\widehat{c}z_2$, and, due to the choices in (6.19), one has

$$\langle z - u, n\rangle = z_1 - 1 - z_2\widehat{c} < \frac{-z_1^2 + 2z_1 - 1 - z_2^2}{2} = \frac{-(z_1 - 1)^2 - z_2^2}{2} \leq 0,$$

which shows that

$$B(u, v, w) \subseteq F_-. \tag{6.20}$$

Let $n' := (w_2, 1 - w_1)^\intercal$. Due to

$$\langle n', w - u\rangle = w_2(w_1 - 1) + (1 - w_1)w_2 = 0,$$

one has $n' \perp \operatorname{aff}(u, w)$. Therefore, it follows together with $\langle v - u, n'\rangle = -2w_2 < 0$ that $H_+^0 := H_+ \cup H_0$ can be expressed as $H_+^0 = \{y \in \mathbb{R}^2 \mid \langle y - u, n'\rangle \geq 0\}$. Assume that there is a $y \in F_- \cap G_- \cap H_+^0$. Then, $y_2 < 0$ due to the definition of G_-. Moreover, $y \in H_+^0$ yields

$$0 \leq \langle y - u, n'\rangle = (y_1 - 1)w_2 + y_2(1 - w_1),$$

which is equivalent to

$$y_1 - 1 \geq -\frac{y_2}{w_2}(1 - w_1)$$

since $w_2 > 0$. Then, $y \in F_-$ yields the contradiction

$$\begin{aligned}
0 &> \langle y - u, n\rangle \\
&= (y_1 - 1) - \frac{y_2}{w_2}\frac{w_1^2 + w_2^2 - 1}{2} \\
&\geq -\frac{y_2}{w_2}\left(1 - w_1 + \frac{w_1^2}{2} + \frac{w_2^2}{2} - \frac{1}{2}\right) \\
&= \underbrace{-\frac{y_2}{w_2}}_{>0}\left(\underbrace{\left(\frac{w_1}{\sqrt{2}} - \frac{1}{\sqrt{2}}\right)^2}_{\geq 0} + \underbrace{\left(\frac{w_2}{\sqrt{2}}\right)^2}_{\geq 0}\right) \\
&\geq 0.
\end{aligned}$$

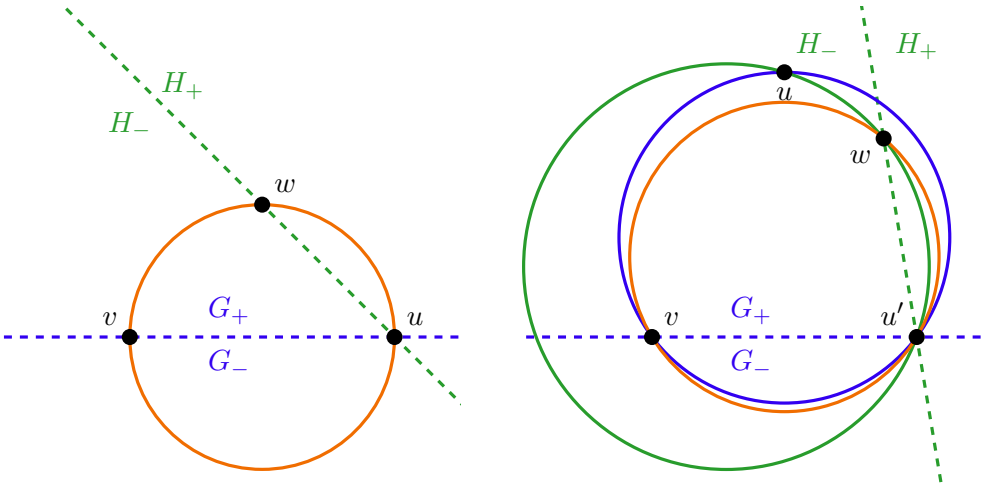

(a) The situation in Lemma 6.23 (b) The situation in Lemma 6.24

Fig. 6.10: Points, circles, and half planes as specified in Lemmas 6.23 and 6.24

Therefore, $F_- \cap G_- \cap H_+^0 = \emptyset$, and thus, it follows with (6.20) that

$$B(u,v,w) \cap G_- \subseteq F_- \cap G_- \subseteq H_-,$$

which finishes the proof. □

The points, circles, and half planes used in the previous and the following lemma are presented in Figure 6.10.

Lemma 6.24. Let $u, u', v, w \in \mathbb{R}^2$ be in general Delaunay position. Let G_+, G_- denote the two open half planes generated by $\mathrm{aff}(u', v)$, and suppose that $u, w \in G_+$. Furthermore, assume that $w \in B(u,u',v)$ and $v \in B(u,u',w)$. Then,

$$B(u',v,w) \cap G_- \subseteq B(u,u',w).$$

Proof. Assume that $u \in B(u',v,w)$. Then, from $w \in B(u,u',v) \cap G_+$, the fact that $u \in G_+$, and applying Lemma 5.20 twice, one obtains the contradiction

$$\overline{B(u,u',v)} \cap G_+ \subseteq B(u',v,w) \cap G_+ \subset \overline{B(u',v,w)} \cap G_+ \subset \overline{B(u,u',v)} \cap G_+.$$

Hence, one has

$$u \notin B(u',v,w). \tag{6.21}$$

Define H_+, H_- as the two open half planes generated by $\mathrm{aff}(u', w)$, indexed such that $v \in H_-$. Since $w \in G_+$, one can apply Lemma 6.23 to obtain

$$B(u', v, w) \cap G_- \subseteq H_-. \tag{6.22}$$

Assume that $u \in H_+$. Together with (6.21), Corollary 6.14 yields $\overline{B(u, u', w)} \cap H_- \subseteq B(u', v, w)$. However, together with $v \in B(u, u', w) \cap H_-$ and Lemma 5.20, one again obtains the contradiction

$$\overline{B(u, u', w)} \cap H_- \subseteq B(u', v, w) \cap H_- \subset \overline{B(u', v, w)} \cap H_- \subset \overline{B(u, u', w)} \cap H_-.$$

Hence, one can deduce that $u \in H_-$. Consequently, due to (6.21), one can apply Corollary 6.14 to obtain together with (6.22) that

$$B(u', v, w) \cap G_- \subseteq B(u', v, w) \cap H_- \subseteq B(u, u', w),$$

which finishes the proof. □

Corollary 6.25. Let $u, u', v, w, w' \in \mathbb{R}^2$ be in general Delaunay position. Let G_+, G_- denote the open half planes generated by $\mathrm{aff}(u', v)$, and assume that $u, w, w' \in G_+$. Furthermore, suppose that

$$w \in B(u', v, w'), \quad w \in B(u, u', v), \quad v \in B(u, u', w).$$

Then, $B(u', v, w') \cap G_- \subseteq B(u, u', w)$.

Proof. Since $w \in B(u', v, w') \cap G_+$, Lemmas 5.20 and 6.24 yield

$$B(u', v, w') \cap G_- \subseteq B(u', v, w) \cap G_- \subseteq B(u, u', w).$$

□

Lemma 6.26. Let $u, v, w \in \mathbb{R}^2$ be in general position. Then,

(i) $\overline{B(u, v, w)} \cap \mathrm{aff}(u, v) = \mathrm{conv}(u, v)$,

(ii) $B(u, v, w) \cap \mathrm{aff}(u, v) = \mathrm{conv}(u, v) \backslash \{u, v\}$.

Proof. We only give a proof for (i) as (ii) follows similarly.

"$\supseteq$" This direction directly follows from $u, v \in \overline{B(u, v, w)} \cap \mathrm{aff}(u, v)$ and the fact that $\overline{B(u, v, w)} \cap \mathrm{aff}(u, v)$ is convex as intersection of convex sets.

"$\subseteq$" Let $t \in \overline{B(u,v,w)} \cap \operatorname{aff}(u,v)$. Then, there is a $\lambda \in \mathbb{R}$ satisfying

$$t = \lambda u + (1-\lambda)v.$$

Choose $c \in \mathbb{R}^2$ and $r \in \mathbb{R}_+$ such that $B(u,v,w) = B_r(c)$. Assume that $t \notin \operatorname{conv}(u,v)$, which is equivalent to $\lambda \notin [0,1]$ and, in turn, yields $\lambda(1-\lambda) < 0$. From the law of cosines and $u \neq v$, it follows that

$$\begin{aligned}
\|t-c\|^2 &= \lambda^2\|u-c\|^2 + (1-\lambda)^2\|v-c\|^2 + 2\lambda(1-\lambda)\langle u-c, v-c\rangle \\
&= \Big(\lambda^2 + (1-\lambda)^2\Big)r^2 + \lambda(1-\lambda)\Big(\|u-c\|^2 + \|v-c\|^2 - \|u-v\|^2\Big) \\
&= \Big(2\lambda^2 - 2\lambda + 1\Big)r^2 + 2\lambda(1-\lambda)r^2 - \lambda(1-\lambda)\|u-v\|^2 \\
&> r^2,
\end{aligned}$$

which is a contradiction to $t \in \overline{B(u,v,w)}$. Consequently, the assumption is false, and one has $t \in \operatorname{conv}(u,v)$. □

We can now introduce companion configurations. We will start by a formal definition and prove afterwards that, for $d = 2$, the existence of companion configurations is *guaranteed* by the existence of a critical configuration of nonzero rank. The term *companion configuration* is also motivated by the fact that these configurations automatically come with a critical configuration.

Definition 6.27. Let $m \in \mathbb{N}_+$, and let $X \subseteq \mathbb{R}^2$ be a knot set satisfying the weak conditions. Suppose that there are $x_0, x_1, x_2, \widehat{x} \in X$ and

$$\begin{array}{lll}
K^* \in \mathcal{K}_{m+1}(X) & \text{with} & \{x_0,x_1,x_2\} = \mathfrak{B}(K^*), \qquad \widehat{x} \in \mathfrak{I}(K^*), \\
K \in \mathcal{K}_m(X) & \text{with} & \{x_0,x_1,\widehat{x}\} = \mathfrak{B}(K)
\end{array}$$

such that K is a critical configuration of K^* with respect to x_0, x_1. Then, for all $x' \in \mathfrak{I}(K)\backslash\mathfrak{I}(K^*)$, a configuration $K' \in \mathcal{K}_m(X)$ is called *companion configuration for x' (with respect to K and K^*)* if

$$B(\mathfrak{B}(K')) \;\subseteq\; B(\mathfrak{B}(K)) \cup B(\mathfrak{B}(K^*))$$

and if either $x_0, x' \in \mathfrak{B}(K')$ or $x_1, x' \in \mathfrak{B}(K')$. ◀

As the set $\mathfrak{I}(K)\backslash\mathfrak{I}(K^*)$ is empty if the critical configuration K has rank zero, companion configurations can only exist if the corresponding critical configuration has a nonzero rank. For this case, we can now prove the existence of at least two

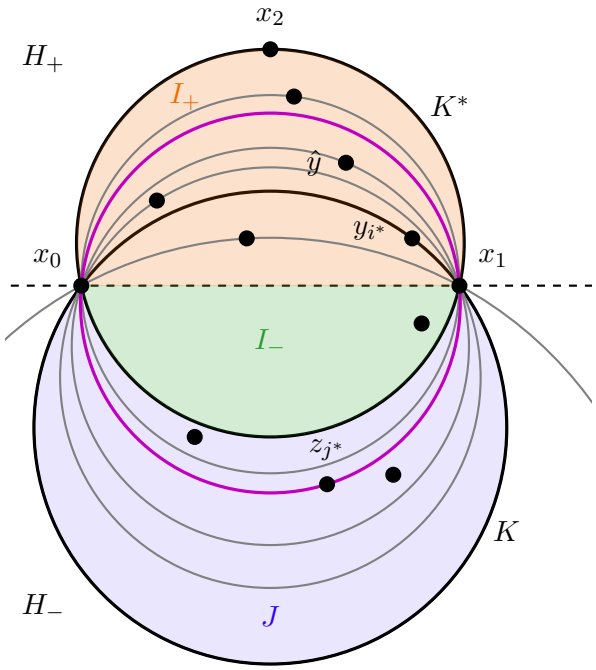

Fig. 6.11: Important quantities in the first half of the proof of Proposition 6.28. We display the half planes H_+, H_- and the regions for the knot sets I_+ *(orange)*, I_- *(green)*, and J *(blue)*. We also show the important knots z_{j^*}, y_{i^*}, and $\widehat{y} := y_{i^*-j^*+|J|+1}$, as well as the circle $B(x_0, x_1, z_{j^*})$ *(purple)*.

companion configurations for any knot in $\mathfrak{I}(K)\backslash\mathfrak{I}(K^*)$. The proof is rather long and technical since the consideration of many different circles is necessary.

Proposition 6.28 (Companion configurations)**.** Let $m \in \mathbb{N}_+$, and let $X \subseteq \mathbb{R}^2$ be a knot set satisfying the weak conditions. Suppose that we can choose $x_0, x_1, x_2, \widehat{x} \in X$ and

$$\begin{aligned} K^* \in \mathcal{K}_{m+1}(X) \qquad &\text{with} \qquad \{x_0, x_1, x_2\} = \mathfrak{B}(K^*), \qquad \widehat{x} \in \mathfrak{I}(K^*), \\ K \in \mathcal{K}_m(X) \qquad &\text{with} \qquad \{x_0, x_1, \widehat{x}\} = \mathfrak{B}(K) \end{aligned}$$

such that K is a critical configuration of K^* with respect to x_0, x_1 of nonzero rank. Then, for all $x' \in \mathfrak{I}(K)\backslash\mathfrak{I}(K^*)$, there are configurations $K_{0,x'}, K_{1,x'} \in \mathcal{K}_m(X)$ with

$$\begin{aligned} x_0, x' \in \mathfrak{B}(K_{0,x'}), \quad x_1 \notin \mathfrak{B}(K_{0,x'}), \quad B(\mathfrak{B}(K_{0,x'})) \subseteq B(\mathfrak{B}(K)) \cup B(\mathfrak{B}(K^*)), \\ x_1, x' \in \mathfrak{B}(K_{1,x'}), \quad x_0 \notin \mathfrak{B}(K_{1,x'}), \quad B(\mathfrak{B}(K_{1,x'})) \subseteq B(\mathfrak{B}(K)) \cup B(\mathfrak{B}(K^*)). \end{aligned}$$

In particular, there are at least two companion configurations for x' with respect to K and K^*.

Proof. We only prove the existence of a suitable $K_{1,x'}$ since the existence of $K_{0,x'}$ follows analogously due to symmetry. We divide the proof into several parts and refer to Figure 6.11 for an overview.

Part 1: In the first part of the proof, we define several quantities.

Let H_+, H_- denote the two open half planes generated by $H_0 := \operatorname{aff}(x_0, x_1)$, indexed such that $\widehat{x} \in H_+$. Due to the assumption that X is in general Delaunay position, it follows that $H_0 \cap X \backslash \{x_0, x_1\} = \emptyset$. Furthermore, define

$$I := \mathfrak{I}(K^*) = B(x_0, x_1, x_2) \cap X, \quad I_+ := I \cap H_+, \quad I_- := I \cap H_-.$$

Clearly, $|I| = m + 1$. According to Lemma 6.15, there is a strict total order $\prec$ on I_+ such that, for any $y, y' \in I_+$ with $y \prec y'$, one has $y \in B(x_0, x_1, y')$. We label the elements as $\{y_1, \ldots, y_{|I_+|}\} := I_+$ such that, for all $i, i' \in \{1, \ldots, |I_+|\}$ with $i < i'$, one has $y_i \prec y_{i'}$. Since $\widehat{x} \in I_+$, there is an $i^* \in \{1, \ldots, |I_+|\}$ such that $\widehat{x} = y_{i^*}$. In particular, I_+ is nonempty. From $K \in \mathcal{K}_m(X)$, it follows that

$$|B(x_0, x_1, y_{i^*}) \cap X| = m. \tag{6.23}$$

Part 2: The goal of this part is to show that $|B(x_0, x_1, y_i) \cap X| \geq m + 1$ for all $i \in \{i^* + 1, \ldots, |I_+|\}$.

With $y_i \in B(x_0, x_1, x_2) \cap H_+$ and Lemma 5.20, it follows that

$$\overline{B(x_0, x_1, x_2)} \cap H_- \subseteq B(x_0, x_1, y_i), \tag{6.24}$$

$$\overline{B(x_0, x_1, y_i)} \cap H_+ \subseteq B(x_0, x_1, x_2) \tag{6.25}$$

for all $i \in \{1, \ldots, |I_+|\}$. Furthermore, from the maximality of $y_{|I_+|}$ with respect to $\prec$, one obtains that

$$\left| I_+ \setminus B\left(x_0, x_1, y_{|I_+|}\right) \right| = \left| \left\{ y_{|I_+|} \right\} \right| = 1. \tag{6.26}$$

Consequently, using (6.25), (6.24), and (6.26) yields

$$\begin{aligned}
&\left| B\left(x_0, x_1, y_{|I_+|}\right) \cap X \right| \\
&= \left| B\left(x_0, x_1, y_{|I_+|}\right) \cap B(x_0, x_1, x_2) \cap H_+ \cap X \right| + \left| B\left(x_0, x_1, y_{|I_+|}\right) \cap H_- \cap X \right| \\
&\geq \left| I_+ \right| - \left| I_+ \setminus B\left(x_0, x_1, y_{|I_+|}\right) \right| + \left| I_- \right| \\
&= m.
\end{aligned} \tag{6.27}$$

By definition of $\prec$ on I_+, one has

$$B(x_0, x_1, y_i) \cap I_+ \;=\; \{y_1, \ldots, y_{i-1}\} \quad \text{for all } i \in \{1, \ldots, |I_+|\} \tag{6.28}$$

and $y_i \in B(x_0, x_1, y_{i+1})$ for all $i \in \{1, \ldots, |I_+| - 1\}$. Hence, Lemma 5.20 provides

$$B(x_0, x_1, y_{i+1}) \cap H_- \;\subseteq\; B(x_0, x_1, y_i) \tag{6.29}$$

for $i \in \{1, \ldots, |I_+| - 1\}$. According to (6.25), (6.29), and (6.28), one can deduce that

$$\begin{aligned}
&|B(x_0, x_1, y_i) \cap X| \\
&\geq |B(x_0, x_1, y_i) \cap B(x_0, x_1, x_2) \cap H_+ \cap X| + |B(x_0, x_1, y_{i+1}) \cap H_- \cap X| \\
&= |B(x_0, x_1, y_{i+1}) \cap B(x_0, x_1, x_2) \cap H_+ \cap X| - 1 + |B(x_0, x_1, y_{i+1}) \cap H_- \cap X| \\
&= |B(x_0, x_1, y_{i+1}) \cap X| - 1.
\end{aligned} \tag{6.30}$$

Assume now that there is an $i \in \{i^* + 1, \ldots, |I_+|\}$ such that $|B(x_0, x_1, y_i) \cap X| \leq m$. Then, together with (6.27) and (6.30), it follows that we can apply Lemma 6.17 to the map

$$\varphi : \{i, \ldots, |I_+|\}, \quad k \mapsto |B(x_0, x_1, y_k) \cap X|,$$

yielding the existence of an $i' \in \{i, \ldots, |I_+|\}$ with $|B(x_0, x_1, y_{i'}) \cap X| = \varphi(i') = m$. Since $i' \geq i \geq i^* + 1$ and, hence, $y_{i'} \succ y_{i^*}$, this is a contradiction to the fact that K is a critical configuration due to the maximality of y_{i^*} in Definition 6.19. As a consequence, there is no such i, and one can conclude that

$$|B(x_0, x_1, y_i) \cap X| \geq m + 1 \quad \text{for all } i \in \{i^* + 1, \ldots, |I_+|\}. \tag{6.31}$$

Part 3: In this part, we consider the knots in $\mathfrak{I}(K) \backslash \mathfrak{I}(K^*)$.

Let $J := \mathfrak{I}(K) \backslash \mathfrak{I}(K^*) = (B(x_0, x_1, y_{i^*}) \cap X) \backslash I$. Then, (6.25) provides

$$J \subseteq H_-. \tag{6.32}$$

As the critical configuration K has nonzero rank, it follows that $\mathfrak{I}(K^*) \backslash \mathfrak{U}(K) \neq \emptyset$, and thus, $\mathfrak{I}(K^*) \not\subseteq \mathfrak{U}(K)$. Therefore, one obtains together with $|\mathfrak{I}(K^*)| = m + 1$ that $|\mathfrak{I}(K^*) \cap \mathfrak{U}(K)| \leq m$. In combination with $y_{i^*} \in \mathfrak{I}(K^*) \cap \mathfrak{B}(K)$, this yields $|\mathfrak{I}(K^*) \cap \mathfrak{I}(K)| \leq m - 1$. Consequently, by using $|\mathfrak{I}(K)| = m$, one obtains that

$$J = \mathfrak{I}(K) \backslash \mathfrak{I}(K^*) \neq \emptyset.$$

According to (6.32), Lemma 6.15 guarantees the existence of a strict total ordering $\prec$ on J such that one has $z \in B(x_0, x_1, z')$ for all $z, z' \in J$ with $z \prec z'$. We label the elements in J as $\{z_1, \ldots, z_{|J|}\} := J$ such that $z_j \prec z_{j'}$ for any $j, j' \in \{1, \ldots, |J|\}$ with $j < j'$.

We have to prove the existence of companion configurations for all $x' \in J$. To that end, let $x' \in J$ and choose $j^* \in \{1, \ldots, |J|\}$ such that $x' = z_{j^*}$. Set

$$I'_{+,j^*} := \Big\{ y \in I_+ \;\Big|\; z_{j^*} \in B(x_0, x_1, y) \Big\} \subseteq I_+.$$

Part 4: We consider the particular knot $y_{i^*-j^*+|J|+1}$ and show $y_{i^*-j^*+|J|+1} \in I'_{+,j^*}$.

The knot $y_{i^*-j^*+|J|+1}$ is well-defined since, on the one hand,

$$i^* - j^* + |J| + 1 \geq i^* + 1 \tag{6.33}$$

and, on the other hand, (6.23), (6.25), (6.28), (6.24), and (6.32) yield

$$\begin{aligned} m = |B(x_0, x_1, y_{i^*}) \cap X| \; &= \; i^* - 1 + |B(x_0, x_1, y_{i^*}) \cap H_- \cap X| \\ &= i^* - 1 + |I_-| + |(B(x_0, x_1, y_{i^*}) \cap H_- \cap X) \backslash I_-| \; = \; i^* - 1 + |I_-| + |J|, \end{aligned} \tag{6.34}$$

which in turn provides that

$$i^* - j^* + |J| + 1 \; = \; m - |I_-| - j^* + 2 \; \leq \; m - |I_-| + 1 \; = \; |I_+|.$$

By definition of $\prec$ on I_+ and (6.33), one has $y_{i^*} \in B\Big(x_0, x_1, y_{i^*-j^*+|J|+1}\Big) \cap H_+$, and hence, due to Lemma 5.20,

$$B\Big(x_0, x_1, y_{i^*-j^*+|J|+1}\Big) \cap H_- \; \subseteq \; B(x_0, x_1, y_{i^*}). \tag{6.35}$$

Applying Lemma 5.20 once more to $y_{i^*-j^*+|J|+1} \in B(x_0, x_1, x_2) \cap H_+$ yields

$$I_- \; = \; B(x_0, x_1, x_2) \cap H_- \cap X \; \subseteq \; B\Big(x_0, x_1, y_{i^*-j^*+|J|+1}\Big). \tag{6.36}$$

Consequently, one obtains with (6.36), (6.35), and (6.32) that

$$\begin{aligned} &B\Big(x_0, x_1, y_{i^*-j^*+|J|+1}\Big) \cap H_- \cap X \\ &= I_- \cup \Big(\Big(B\Big(x_0, x_1, y_{i^*-j^*+|J|+1}\Big) \cap H_- \cap X\Big) \Big\backslash I\Big) \\ &\subseteq I_- \cup \Big(\Big(B(x_0, x_1, y_{i^*}) \cap X\Big) \Big\backslash I\Big) \cap H_- \\ &= I_- \cup J. \end{aligned} \tag{6.37}$$

Assume now that

$$y_{i^*-j^*+|J|+1} \notin I'_{+,j^*}, \tag{6.38}$$

which is equivalent to

$$z_{j^*} \notin B\Big(x_0, x_1, y_{i^*-j^*+|J|+1}\Big). \tag{6.39}$$

We are going to show now that, under this assumption,

$$z_{j^*+1}, \ldots, z_{|J|} \notin B\Big(x_0, x_1, y_{i^*-j^*+|J|+1}\Big). \tag{6.40}$$

Indeed, if we assume that $z_j \in B\Big(x_0, x_1, y_{i^*-j^*+|J|+1}\Big)$ for a $j \in \{j^*+1, \ldots, |J|\}$, applying Lemma 5.20 twice yields

$$\overline{B(x_0, x_1, z_{j^*})} \cap H_- \subseteq B(x_0, x_1, z_j) \cap H_- \subseteq B\Big(x_0, x_1, y_{i^*-j^*+|J|+1}\Big),$$

which is a contradiction to (6.39). As a consequence, by using (6.34), (6.28), (6.25), and $J \cap I_- = \emptyset$, one obtains

$$\begin{aligned}
m &= i^* - 1 + |I_-| + |J| + |\{z_1, \ldots, z_{j^*-1}\}| - (j^* - 1) \\
&= (i^* - j^* + |J|) + |I_-| + |J \backslash \{z_{j^*}, \ldots, z_{|J|}\}| \\
&= \Big|B\Big(x_0, x_1, y_{i^*-j^*+|J|+1}\Big) \cap I_+\Big| + \Big|I_-\Big| + \Big|J \Big\backslash \{z_{j^*}, \ldots, z_{|J|}\}\Big| \\
&= \Big|B\Big(x_0, x_1, y_{i^*-j^*+|J|+1}\Big) \cap H_+ \cap X\Big| + \Big|\Big(I_- \cup J\Big) \Big\backslash \{z_{j^*}, \ldots, z_{|J|}\}\Big|
\end{aligned}$$

and, by further applying (6.37), (6.39), (6.40), (6.33), and (6.31), the contradiction

$$\begin{aligned}
m &\geq \Big|B\Big(x_0, x_1, y_{i^*-j^*+|J|+1}\Big) \cap H_+ \cap X\Big| + \\
&\qquad \Big|\Big(B\Big(x_0, x_1, y_{i^*-j^*+|J|+1}\Big) \cap H_- \cap X\Big) \Big\backslash \{z_{j^*}, \ldots, z_{|J|}\}\Big| \\
&= \Big|B\Big(x_0, x_1, y_{i^*-j^*+|J|+1}\Big) \cap H_+ \cap X\Big| + \Big|B\Big(x_0, x_1, y_{i^*-j^*+|J|+1}\Big) \cap H_- \cap X\Big| \\
&\geq m + 1.
\end{aligned}$$

Hence, Assumption (6.38) is false and one has

$$y_{i^*-j^*+|J|+1} \in I'_{+,j^*}. \tag{6.41}$$

Part 5: The aim of the following part is to show that $|B(x_0, x_1, z_{j^*}) \cap X| \geq m + 1$.

To that end, let $\widetilde{y}_{j^*} := \max_{\prec} I'_{+,j^*}$, which is well-defined since I'_{+,j^*} is nonempty due to (6.41). According to (6.41) and the fact that $I'_{+,j^*} \subseteq I_+$, one can find an

$$\ell \in \{i^* - j^* + |J| + 1, \ \ldots, \ |I_+|\}$$

such that $\widetilde{y}_{j^*} = y_\ell$. From $y_1, \dots, y_{\ell-1} \in B(x_0, x_1, y_\ell) \cap H_+$, the definition of I'_{+,j^*}, and (6.32), it follows with Lemma 5.20 that

$$\overline{B(x_0, x_1, y_i)} \cap H_+ \subseteq \overline{B(x_0, x_1, y_\ell)} \cap H_+ \subseteq B(x_0, x_1, z_{j^*})$$

for all $i \in \{1, \dots, \ell\}$. In particular,

$$y_1, \dots, y_\ell \in B(x_0, x_1, z_{j^*}) \cap H_+ \cap X. \tag{6.42}$$

Due to (6.32), one has $z_{j^*} \in B(x_0, x_1, y_{i^*}) \cap H_-$. Thus, Lemma 5.20 yields

$$\overline{B(x_0, x_1, z_{j^*})} \cap H_- \subseteq B(x_0, x_1, y_{i^*}), \tag{6.43}$$
$$\overline{B(x_0, x_1, y_{i^*})} \cap H_+ \subseteq B(x_0, x_1, z_{j^*}). \tag{6.44}$$

From the strict total order on J and (6.32) as well as (6.43), one obtains

$$\{z_1, \dots, z_{j^*-1}\} = B(x_0, x_1, z_{j^*}) \cap H_- \cap J = \big(B(x_0, x_1, z_{j^*}) \cap H_- \cap X\big) \backslash I_-. \tag{6.45}$$

By definition of J, one has $z_{j^*} \notin I = B(x_0, x_1, x_2) \cap X$, and therefore, (6.32) and Corollary 6.14 yield

$$I_- = B(x_0, x_1, x_2) \cap H_- \cap X \subseteq B(x_0, x_1, z_{j^*}), \tag{6.46}$$
$$B(x_0, x_1, z_{j^*}) \cap H_+ \subseteq B(x_0, x_1, x_2). \tag{6.47}$$

Hence, due to (6.46), (6.42), (6.45), and (6.34), one can conclude that

$$\begin{aligned}
&|B(x_0, x_1, z_{j^*}) \cap X| \\
&= |B(x_0, x_1, z_{j^*}) \cap H_+ \cap X| + |(B(x_0, x_1, z_{j^*}) \cap H_- \cap X) \backslash I_-| + |I_-| \\
&\geq |\{y_1, \dots, y_\ell\}| + |\{z_1, \dots, z_{j^*-1}\}| + |I_-| \\
&\geq i^* + |J| + |I_-| \\
&= m + 1.
\end{aligned} \tag{6.48}$$

Part 6: We introduce a second hyperplane G_0 and consider the corresponding half planes. Throughout the remainder of the proof, we refer to Figure 6.12 for an overview.

The hyperplane $G_0 := \operatorname{aff}(x_1, z_{j^*})$ divides $\mathbb{R}^2$ into two open half planes G_+, G_-, indexed such that $x_0 \in G_+$. Since $z_{j^*} \in H_-$, Lemma 6.23 yields

$$B(x_0, x_1, z_{j^*}) \cap G_- \subseteq H_-. \tag{6.49}$$

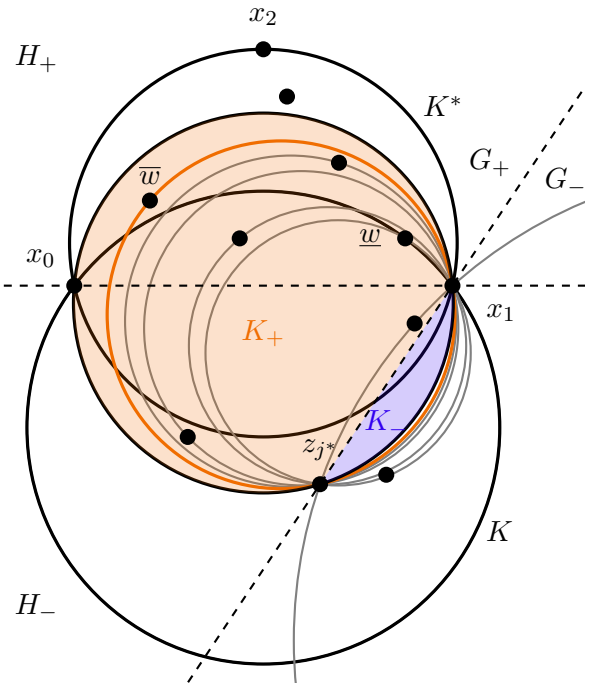

Fig. 6.12: Important quantities in the second half of the proof of Proposition 6.28. We display the regions for the knots sets K_+ *(orange)* and K_- *(blue)*, the important knots $\underline{w}$ and $\overline{w}$, as well as the resulting companion configuration *(orange)*.

Define

$$K_- := B(x_0, x_1, z_{j^*}) \cap G_- \cap X, \quad K_+ := B(x_0, x_1, z_{j^*}) \cap G_+ \cap X.$$

Then, according to (6.49), (6.46), (6.45), and (6.34),

$$\begin{aligned} |K_-| \leq |B(x_0, x_1, z_{j^*}) \cap H_- \cap X| &= |(B(x_0, x_1, z_{j^*}) \cap H_- \cap X) \backslash I_-| + |I_-| \\ &= |\{z_1, \dots, z_{j^*-1}\}| + |I_-| \leq |J| - 1 + |I_-| = m - i^* \leq m - 1. \end{aligned} \tag{6.50}$$

Since, according to (6.48),

$$|K_-| + |K_+| = |B(x_0, x_1, z_{j^*}) \cap X| \geq m + 1, \tag{6.51}$$

one can conclude with (6.50) that

$$|K_+| \geq m + 1 - |K_-| \geq 2. \tag{6.52}$$

Part 7: Our next goal is to define two specific knots $\underline{w}, \overline{w} \in K_+$ which will be the extremes of our subsequent considerations.

According to Lemma 6.15, there is a strict total ordering $\triangleleft$ on K_+ with respect to the half plane G_+ such that, for any $w, w' \in K_+$ with $w \triangleleft w'$, one has

$$w \in B(x_1, z_{j^*}, w'). \tag{6.53}$$

The different symbol $\triangleleft$ is used to distinguish between the different orderings with respect to H_+, H_- and G_+, G_-, respectively. Moreover, label the elements in K_+ as $\{w_1, \ldots, w_{|K_+|}\} := K_+$ such that $w_1 \triangleleft \ldots \triangleleft w_{|K_+|}$. For $w, w' \in K_+$, let $w \trianglelefteq w'$ denote that $w = w'$ or $w \triangleleft w'$. Let $s := m - |K_-| + 1$. Due to (6.50) and (6.51), one has

$$2 \leq s \leq |K_+|, \tag{6.54}$$

and therefore, the element $\overline{w} := w_s$ is well-defined. Next, consider the set

$$L := \Big(H_+ \Big\backslash B(x_0, x_1, y_{i^*})\Big) \cap K_+.$$

The assumption $y_{i^*} \in G_-$ yields together with $y_{i^*} \in H_+$, (6.44), and (6.49) the contradiction $y_{i^*} \in H_-$. Hence, $y_{i^*} \in G_+$, and also $y_{i^*} \in K_+$, according to (6.44). Moreover, one has $y_{i^*} \in L$ since $y_{i^*} \notin B(x_0, x_1, y_{i^*})$. In particular, $L \neq \emptyset$, and thus, the element $\underline{w} := \min_{\triangleleft} L$ is well-defined.

Part 8: We prove now that $\underline{w} \triangleleft \overline{w}$.

Assume that $\overline{w} \trianglelefteq \underline{w}$, which is equivalent to $\overline{w} \in \overline{B(x_1, z_{j^*}, \underline{w})}$. Due to (6.54), the set $L' := \{w_1, \ldots, w_{s-1}\}$ is nonempty. Let $w' \in L'$. Then, $w' \in K_+$ as well as

$$w' \triangleleft \overline{w} \trianglelefteq \underline{w}. \tag{6.55}$$

Assuming $w' \in H_+ \backslash B(x_0, x_1, y_{i^*})$ yields $w' \in K_+ \cap H_+ \backslash B(x_0, x_1, y_{i^*}) = L$, which, together with (6.55), is a contradiction to the minimality of $\underline{w}$ in L. Hence, it follows that $w' \notin H_+ \backslash B(x_0, x_1, y_{i^*})$, and as a consequence,

$$L' \subseteq H_- \cup B(x_0, x_1, y_{i^*}) = H_- \cup \Big(B(x_0, x_1, y_{i^*}) \cap H_+\Big). \tag{6.56}$$

Therefore, one can conclude using (6.23), (6.43), and (6.49) that

$$\begin{aligned}
m &= |B(x_0, x_1, y_{i^*}) \cap H_+ \cap X| + |B(x_0, x_1, y_{i^*}) \cap H_- \cap X| \\
&\geq |B(x_0, x_1, y_{i^*}) \cap H_+ \cap X| + |B(x_0, x_1, z_{j^*}) \cap H_- \cap X| + |\{z_{j^*}\}| \\
&= |B(x_0, x_1, y_{i^*}) \cap H_+ \cap X| + |B(x_0, x_1, z_{j^*}) \cap H_- \cap G_+ \cap X| \\
&\qquad + |B(x_0, x_1, z_{j^*}) \cap G_- \cap X| + 1
\end{aligned}$$

and further, due to (6.56), that

$$\begin{aligned} m &\geq |B(x_0, x_1, y_{i^*}) \cap H_+ \cap K_+| + |H_- \cap K_+| + |K_-| + 1 \\ &\geq |K_+ \cap L'| + |K_-| + 1 \\ &= |\{w_1, \ldots, w_{s-1}\}| + |K_-| + 1 \\ &= m + 1, \end{aligned}$$

which is clearly a contradiction. Thus, our initial assumption is incorrect and one has

$$\underline{w} \triangleleft \overline{w}. \tag{6.57}$$

Part 9: Next, we show the first of three important subset relations that hold for all elements of K_+ between $\underline{w}$ and $\overline{w}$.

Let $w \in K_+$ such that $\underline{w} \trianglelefteq w \trianglelefteq \overline{w}$ and whose existence is guaranteed by (6.57). Since $w \in B(x_0, x_1, z_{j^*}) \cap G_+$, Lemma 5.20 yields

$$\overline{B(x_1, w, z_{j^*})} \cap G_+ \subseteq B(x_0, x_1, z_{j^*}), \tag{6.58}$$

and, together with (6.43), one obtains

$$B(x_1, w, z_{j^*}) \cap G_+ \cap H_- \subseteq B(x_0, x_1, z_{j^*}) \cap H_- \subseteq B(x_0, x_1, y_{i^*}). \tag{6.59}$$

Since $\underline{w} \in L \subseteq B(x_0, x_1, z_{j^*}) \cap H_+$, one can apply Lemma 5.20 to obtain

$$z_{j^*} \in \overline{B(x_0, x_1, z_{j^*})} \cap H_- \subseteq B(x_0, x_1, \underline{w}). \tag{6.60}$$

Furthermore, one has $x_0, w, \underline{w} \in G_+$ and $\underline{w} \in B(x_0, x_1, z_{j^*})$ by definition of K_+. If $\underline{w} = w$, Lemma 6.24 can be applied due to (6.60), and consequently,

$$B(x_1, w, z_{j^*}) \cap G_- = B(x_1, \underline{w}, z_{j^*}) \cap G_- \subseteq B(x_0, x_1, \underline{w}). \tag{6.61}$$

Otherwise, one has $\underline{w} \triangleleft w$ and, thus, $\underline{w} \in B(x_1, w, z_{j^*})$. Together with (6.60), one can apply Corollary 6.25 to obtain also in this case that

$$B(x_1, w, z_{j^*}) \cap G_- \subseteq B(x_0, x_1, \underline{w}). \tag{6.62}$$

As $\underline{w} \in L \subseteq H_+ \backslash B(x_0, x_1, y_{i^*})$, Corollary 6.14 yields

$$\overline{B(x_0, x_1, \underline{w})} \cap H_- \subseteq B(x_0, x_1, y_{i^*}). \tag{6.63}$$

By using Lemma 6.26, the convexity of $B(x_0, x_1, y_{i^*})$, and $z_{j^*} \in B(x_0, x_1, y_{i^*})$, one obtains

$$B(x_1, w, z_{j^*}) \cap G_0 \cap H_- \subseteq \operatorname{conv}(x_1, z_{j^*}) \backslash \{x_1, z_{j^*}\} \subseteq B(x_0, x_1, y_{i^*}). \tag{6.64}$$

Hence, (6.59), (6.64), (6.61), (6.62), and (6.63) can be used to establish

$$\begin{aligned} B(x_1, w, z_{j^*}) \cap H_- &\subseteq B(x_0, x_1, y_{i^*}) \cup (B(x_1, w, z_{j^*}) \cap G_- \cap H_-) \\ &\subseteq B(x_0, x_1, y_{i^*}) \cup (B(x_0, x_1, \underline{w}) \cap H_-) \\ &= B(x_0, x_1, y_{i^*}). \end{aligned} \tag{6.65}$$

Part 10: In the following, we show a second subset relation, which again holds true for all elements of K_+ between $\underline{w}$ and $\overline{w}$.

To that end, we again choose a $w \in K_+$ with $\underline{w} \trianglelefteq w \trianglelefteq \overline{w}$, whose existence is guaranteed by (6.57). Let $P := \overline{B(x_1, w, z_{j^*})}$, and assume that

$$\partial P \cap H_+ = \emptyset. \tag{6.66}$$

Then, one has $\partial P \subseteq H_0 \cup H_-$. Since $H_0 \cup H_-$ is convex and P is convex and compact, one obtains $P = \operatorname{conv}(\partial P) \subseteq H_0 \cup H_-$, according to Lemma 5.23. Hence, $\underline{w} \trianglelefteq w$ yields $\underline{w} \in P \subseteq H_0 \cup H_-$, which is a contradiction to $\underline{w} \in L \subseteq H_+$. Thus, Assumption (6.66) is false, and therefore, we can choose an arbitrary $\widetilde{x} \in \partial P \cap H_+$, which, independently of the specific choice, satisfies

$$\overline{B(x_1, \widetilde{x}, z_{j^*})} = P = \overline{B(x_1, w, z_{j^*})}.$$

From $x_1, \widetilde{x}, z_{j^*} \in \partial P$, $\widetilde{x} \in H_+$, $z_{j^*} \in H_-$, and $x_1 \in H_0$, it follows that H_0, considered as a line, is a secant of the circle ∂P. Therefore, one can find an $\widetilde{x}_0 \in \partial P \cap H_0 \backslash \{x_1\}$, and one has

$$\overline{B(x_1, \widetilde{x}_0, z_{j^*})} = P. \tag{6.67}$$

We claim now that $\widetilde{x}_0 \in G_+$, which is clear by definition of G_+ if $\widetilde{x}_0 = x_0$. Hence, we consider $\widetilde{x}_0 \neq x_0$ and show that the assumption

$$\widetilde{x}_0 \notin G_+ \tag{6.68}$$

yields a contradiction.

First, we first consider the case $\widetilde{x}_0 \in G_0$. Then, it follows with $\widetilde{x}_0 \neq x_1$ and $x_1, \widetilde{x}_0 \in H_0$ that $z_{j^*} \in G_0 = \operatorname{aff}(x_1, \widetilde{x}_0) = H_0$, which is a contradiction to $z_{j^*} \in H_-$.

Secondly, we consider the case $\widetilde{x}_0 \in G_-$. As $x_0 \in G_+$ and $x_1 \in G_0$, it follows with the convexity of $G_0 \cup G_+$ that $\operatorname{conv}(x_0, x_1) \subseteq G_0 \cup G_+$. Together with Lemma 6.26, this yields

$$\widetilde{x}_0 \notin \operatorname{conv}(x_0, x_1) \;=\; \overline{B(x_0, x_1, y_{i^*})} \cap H_0. \tag{6.69}$$

Since $\widetilde{x}_0 \in H_0$ by definition, one obtains from (6.69) that $\widetilde{x}_0 \notin \overline{B(x_0, x_1, y_{i^*})}$. As $\overline{B(x_0, x_1, y_{i^*})}$ is closed, its complement is open, and one can find an open neighborhood U around $\widetilde{x}_0$ such that

$$\overline{B(x_0, x_1, y_{i^*})} \cap U \;=\; \emptyset. \tag{6.70}$$

Next, we define the sequence $(q_k)_{k \in \mathbb{N}_+}$, where

$$q_k := \frac{1}{k+1} z_{j^*} + \left(1 - \frac{1}{k+1}\right) \widetilde{x}_0 \quad \text{for all } k \in \mathbb{N}_+.$$

Due to the definition of q_k and Lemma 6.26, one obtains for all $k \in \mathbb{N}_+$ that

$$q_k \in \operatorname{conv}(\widetilde{x}_0, z_{j^*}) \backslash \{\widetilde{x}_0, z_{j^*}\} \;=\; B(x_1, \widetilde{x}_0, z_{j^*}) \cap \operatorname{aff}(\widetilde{x}_0, z_{j^*}) \;\subseteq\; B(x_1, \widetilde{x}_0, z_{j^*}).$$

Moreover, from $\widetilde{x}_0 \in H_0$, $z_{j^*} \in H_-$, and the convexity of $H_- \cup H_0$, it follows that $q_k \in \operatorname{conv}(\widetilde{x}_0, z_{j^*}) \subseteq H_- \cup H_0$ for all $k \in \mathbb{N}_+$. Assume now that there is a $k \in \mathbb{N}_+$ such that $q_k \in H_0$. Then,

$$z_{j^*} = (k+1)\left(q_k - \left(1 - \frac{1}{k+1}\right)\widetilde{x}_0\right) = (k+1)q_k - k\widetilde{x}_0 \in \operatorname{aff}(q_k, \widetilde{x}_0) = H_0,$$

which is a contradiction to $z_{j^*} \in H_-$. Hence, one has

$$q_k \in B(x_1, \widetilde{x}_0, z_{j^*}) \cap H_- \;=\; B(x_1, w, z_{j^*}) \cap H_- \quad \text{for all } k \in \mathbb{N}_+.$$

Since $(q_k)_{k \in \mathbb{N}_+}$ converges to $\widetilde{x}_0$, it follows that $B(x_1, w, z_{j^*}) \cap H_- \cap U \neq \emptyset$. This, however, is a contradiction to

$$B(x_1, w, z_{j^*}) \cap H_- \cap U \;\subseteq\; B(x_0, x_1, y_{i^*}) \cap U \;=\; \emptyset,$$

which follows from (6.65) and (6.70). Hence, we obtained a contradiction for both $\widetilde{x}_0 \in G_0$ and $\widetilde{x}_0 \in G_-$. Thus, Assumption (6.68) is false, yielding $\widetilde{x}_0 \in G_+$.

As $H_0 = \operatorname{aff}(x_0, x_1) = \operatorname{aff}(\widetilde{x}_0, x_1)$ and since $\widetilde{x}_0 \in G_+$ and $z_{j^*} \in H_-$, one can apply Lemma 6.23 with interchanged names of the half planes, yielding together with (6.67) and the definition of P that

$$B(x_1, w, z_{j^*}) \cap H_+ \;=\; B(x_1, \widetilde{x}_0, z_{j^*}) \cap H_+ \;\subseteq\; G_+.$$

Hence, one can conclude together with (6.58) and (6.47) that

$$\begin{aligned} B(x_1, w, z_{j^*}) \cap H_+ &= B(x_1, w, z_{j^*}) \cap H_+ \cap G_+ \\ &\subseteq B(x_0, x_1, z_{j^*}) \cap H_+ \cap G_+ \qquad (6.71) \\ &\subseteq B(x_0, x_1, x_2). \qquad (6.72) \end{aligned}$$

Part 11: We show the third and last subset relation now.

Let $w \in K_+$ with $\underline{w} \trianglelefteq w \trianglelefteq \overline{w}$, and assume that there is a

$$t \in \left(B(x_1, w, z_{j^*}) \Big\backslash \overline{B(x_0, x_1, x_2)} \right) \cap H_0. \qquad (6.73)$$

Since

$$B(x_1, w, z_{j^*}) \backslash \overline{B(x_0, x_1, x_2)} \;=\; B(x_1, w, z_{j^*}) \cap \overline{B(x_0, x_1, x_2)}^{\,c}$$

is open as intersection of open sets, one can find an open neighborhood U' around t with $U' \subseteq B(x_1, w, z_{j^*}) \backslash \overline{B(x_0, x_1, x_2)}$. As $\partial H_+ = H_0$, it follows that $U' \cap H_+ \neq \emptyset$. This is a contradiction to (6.72), though. Hence, Assumption (6.73) is false, and one has

$$B(x_1, w, z_{j^*}) \cap H_0 \;\subseteq\; \overline{B(x_0, x_1, x_2)} \cap H_0 \;=\; \operatorname{conv}(x_0, x_1),$$

where the latter equality is established by Lemma 6.26. However, $x_1 \notin B(x_1, w, z_{j^*})$, and, according to (6.58) and $x_0 \in G_+ \backslash B(x_0, x_1, z_{j^*})$, also

$$x_0 \notin \overline{B(x_1, w, z_{j^*})}. \qquad (6.74)$$

Consequently, applying Lemma 6.26 once again yields

$$B(x_1, w, z_{j^*}) \cap H_0 \;\subseteq\; \operatorname{conv}(x_0, x_1) \backslash \{x_0, x_1\} \;=\; B(x_0, x_1, x_2) \cap H_0. \qquad (6.75)$$

Part 12: In the following, we consider the number of knots in the extremal circumcircles defined by x_1, z_{j^*}, and $\underline{w}$ or $\overline{w}$, respectively.

One has $\overline{w} \in K_+ \subseteq B(x_0, x_1, z_{j^*}) \cap G_+$, and hence, Lemma 5.20 yields

$$B(x_0, x_1, z_{j^*}) \cap G_- \;\subseteq\; B(x_1, \overline{w}, z_{j^*}).$$

Therefore, by recalling the definitions of $\triangleleft$ and $\overline{w} = w_{m-|K_-|+1}$, it follows that

$$\begin{aligned} |B(x_1, \overline{w}, z_{j^*}) \cap X| &\geq |B(x_1, \overline{w}, z_{j^*}) \cap G_+ \cap X| + |B(x_0, x_1, z_{j^*}) \cap G_- \cap X| \\ &= \left| \{w_1, \ldots, w_{m-|K_-|}\} \right| + |K_-| \;=\; m. \qquad (6.76) \end{aligned}$$

Next, we consider $\underline{w}$. One has

$$B(x_1, \underline{w}, z_{j^*}) \cap H_+ \cap K_+ \subseteq B(x_0, x_1, y_{i^*}) \tag{6.77}$$

as any $x \in B(x_1, \underline{w}, z_{j^*}) \cap L$ would satisfy $x \lhd \underline{w}$, which would be a contradiction to the minimality of $\underline{w}$ in L. As a consequence, due to (6.71), the definition of K_+, and (6.77), one has

$$\begin{aligned} B(x_1, \underline{w}, z_{j^*}) \cap H_+ \cap X &\subseteq B(x_1, \underline{w}, z_{j^*}) \cap H_+ \cap B(x_0, x_1, z_{j^*}) \cap G_+ \cap X \\ &\subseteq B(x_0, x_1, y_{i^*}). \end{aligned} \tag{6.78}$$

Finally, one obtains in combination with $H_0 \cap X = \{x_0, x_1\}$, (6.74), (6.65), (6.78), and (6.23) that

$$\begin{aligned} &|B(x_1, \underline{w}, z_{j^*}) \cap X| \\ &= |B(x_1, \underline{w}, z_{j^*}) \cap H_+ \cap X| + |B(x_1, \underline{w}, z_{j^*}) \cap H_- \cap X| \\ &\le |B(x_0, x_1, y_{i^*}) \cap H_+ \cap X| + |B(x_0, x_1, y_{i^*}) \cap H_- \cap X| \\ &= m. \end{aligned} \tag{6.79}$$

Part 13: The last missing requirement for an application of Lemma 6.17 to the knots $\underline{w} \trianglelefteq w \trianglelefteq \overline{w}$ is the relationship of the number of knots in successive circumcircles, which will be shown now.

Let $s' \in \{1, \dots, |K_+| - 1\}$, which is well-defined since $|K_+| \ge 2$, according to (6.52). Then, due to the definition of the ordering $\lhd$ in (6.53), one has

$$|B(x_1, w_{s'}, z_{j^*}) \cap K_+| = s' - 1, \qquad |B(x_1, w_{s'+1}, z_{j^*}) \cap K_+| = s'. \tag{6.80}$$

Since $w_{s'}, w_{s'+1} \in K_+ \subseteq B(x_0, x_1, z_{j^*}) \cap G_+$, Lemma 5.20 yields

$$\overline{B(x_1, w, z_{j^*})} \cap G_+ \subseteq B(x_0, x_1, z_{j^*}) \quad \text{for both } w \in \{w_{s'}, w_{s'+1}\}. \tag{6.81}$$

Therefore, by recalling that $K_+ = B(x_0, x_1, z_{j^*}) \cap G_+ \cap X$ and applying (6.81) as well as (6.80), one obtains

$$\begin{aligned} &|B(x_1, w_{s'+1}, z_{j^*}) \cap G_+ \cap X| \\ &= |B(x_1, w_{s'+1}, z_{j^*}) \cap B(x_0, x_1, z_{j^*}) \cap G_+ \cap X| \\ &= |B(x_1, w_{s'}, z_{j^*}) \cap B(x_0, x_1, z_{j^*}) \cap G_+ \cap X| + 1 \\ &= |B(x_1, w_{s'}, z_{j^*}) \cap G_+ \cap X| + 1. \end{aligned} \tag{6.82}$$

Furthermore, one has $w_{s'} \in B(x_1, w_{s'+1}, z_{j^*}) \cap G_+$, and consequently, it follows with Lemma 5.20 that

$$B(x_1, w_{s'+1}, z_{j^*}) \cap G_- \subseteq B(x_1, w_{s'}, z_{j^*}). \tag{6.83}$$

By combining (6.82) and (6.83), one obtains

$$\begin{aligned} &|B(x_1, w_{s'+1}, z_{j^*}) \cap X| \\ &\leq |B(x_1, w_{s'}, z_{j^*}) \cap X \cap G_-| + |B(x_1, w_{s'}, z_{j^*}) \cap X \cap G_+| + 1 \\ &= |B(x_1, w_{s'}, z_{j^*}) \cap X| + 1. \end{aligned} \tag{6.84}$$

Conclusion: We can finally combine our results to prove the stated claim. In particular, we apply Lemma 6.17, which guarantees the existence of an appropriate Delaunay configuration.

Let $\overline{s} := m - |K_-| + 1 \leq |K_+|$, so that $w_{\overline{s}} = \overline{w}$. Due to $\underline{w} \in K_+$ and (6.57), there is an $\underline{s} \in \{1, \ldots, \overline{s} - 1\}$ such that $w_{\underline{s}} = \underline{w}$. Then, according to (6.84), one obtains

$$|B(x_1, w_{s'}, z_{j^*}) \cap X| \geq |B(x_1, w_{s'+1}, z_{j^*}) \cap X| - 1 \tag{6.85}$$

for all $s' \in \{\underline{s}, \ldots, \overline{s} - 1\}$. From (6.76), (6.79), and (6.85), it follows that we can now apply Lemma 6.17 to the map

$$\varphi : \{\underline{s}, \ldots, \overline{s}\} \to \mathbb{N}_0, \quad s' \mapsto |B(x_1, w_{s'}, z_{j^*}) \cap X|,$$

yielding the existence of an $s^* \in \{\underline{s}, \ldots, \overline{s}\}$ such that

$$|B(x_1, w_{s^*}, z_{j^*}) \cap X| = \varphi(s^*) = m.$$

Therefore, we found an appropriate Delaunay configuration of degree m. It remains to be shown that the stated subset relation holds true and the configuration, thus, is a companion configuration. We have made preparations in (6.65), (6.72), and (6.75), so that

$$\begin{aligned} &B(x_1, w_{s^*}, z_{j^*}) \\ &= (B(x_1, w_{s^*}, z_{j^*}) \cap H_+) \cup (B(x_1, w_{s^*}, z_{j^*}) \cap H_-) \cup (B(x_1, w_{s^*}, z_{j^*}) \cap H_0) \\ &\subseteq B(x_0, x_1, x_2) \cup B(x_0, x_1, y_{i^*}) \\ &= B(\mathfrak{B}(K^*)) \cup B(\mathfrak{B}(K)) \end{aligned}$$

finally yields the stated claim. □

Let us recall the steps in the proof briefly: In the first part, we introduce the sets I_+ and I_-, which contain the interior knots of the configuration K^* in the half planes H_+ and H_-, respectively. The half planes H_+ and H_- are generated by the hyperplane $H_0 = \mathrm{aff}(x_0, x_1)$. In the second part, we show that, for all knots $y \in \mathfrak{I}(K^*)\backslash\mathfrak{U}(K)$, where K is the critical configuration of K^* with respect to x_0 and x_1, the ball $B(x_0, x_1, y)$ contains at least $m+1$ knots. On the contrary, the third part considers the knots in $\mathfrak{I}(K)\backslash\mathfrak{I}(K^*)$, which are the possible choices for x'. Parts 4 and 5 show that, for each choice of x', also the ball $B(x_0, x_1, x')$ contains at least $m+1$ knots. Afterwards, we introduce the alternative division of $\mathbb{R}^2$ by the hyperplane $G_0 = \mathrm{aff}(x_1, x')$, which is necessary for the consideration of circles that contain x' instead of x_0 on their boundary. Part 7 introduces two specific knots $\underline{w}, \overline{w} \in K_+$, where K_+ contains the knots in $B(x_0, x_1, x') \cap G_+$ and G_+ is one of the two half planes generated by G_0. The knots $\underline{w}$ and $\overline{w}$ are in some sense extremal for the following considerations. After showing that $\underline{w} \triangleleft \overline{w}$ in Part 8, where $\triangleleft$ is a specific order on the knots in K_+, we prove fragments of the subset relation stated in the claim during the course of Parts 9 to 11 for all knots in K_+ that are between $\underline{w}$ and $\overline{w}$ with respect to $\triangleleft$. Here, Parts 9, 10, and 11 consider the subset relation on H_-, H_+, and H_0, respectively. Subsequently, Parts 12 and 13 ensure that the requirements of Lemma 6.17 hold true for the knots between $\underline{w}$ and $\overline{w}$, so that we can apply this lemma in the Conclusion.

Remark 6.29. Define X, m, K^*, K, x_0, x_1, x_2, and $\widehat{x}$ as in Definition 6.27, and consider the case where the critical configuration K has rank one. Since the rank is bounded by the degree, this trivially holds true for critical configurations of nonzero rank if $m = 1$. In Figure 6.13, the situation is depicted for $m = 1$, where the knot labeled y is the unique knot in $\mathfrak{I}(K^*)\backslash\mathfrak{U}(K)$ and z denotes the interior knot in the critical configuration K. For $m > 1$, the additional knots would be interior knots of both K^* and K. Since these knots are of minor interest in the subsequent considerations, we assume that $m = 1$. However, the reasoning remains valid for arbitrary degrees as long as the critical configuration has rank one.

We can use the facts that $\widehat{x} \in \mathfrak{I}(K^*) \cap \mathfrak{B}(K)$, that $|\mathfrak{I}(K^*)| = 2$, and that K has rank one to obtain that $z \notin \mathfrak{I}(K^*)$. Hence, the unoriented companion configurations for z with respect to K and K^* are given by

$$\mathfrak{U}(K_{0,z}) = \{x_0, z, y, \widehat{x}\} \quad \text{and} \quad \mathfrak{U}(K_{1,z}) = \{x_1, z, y, \widehat{x}\}.$$

As the unoriented critical configuration is given by $\mathfrak{U}(K) = \{x_0, x_1, \widehat{x}, z\}$, the three configurations $K_{0,z}$, $K_{1,z}$, and K differ from each other by exactly one knot. According to Remark 6.11, one can use the knot insertion formula to obtain the simplex

spline $M(\cdot \mid x_0, x_1, \widehat{x}, y)$. This function, however, would be the simplex spline corresponding to the (nonexistent) critical configuration of rank zero. Therefore, we can apply the strategy in Remark 6.20 (including another application of the knot insertion formula) to obtain a linear combination of the original basis candidate function using simplex splines generated by Delaunay configurations of the refined knot set also in this case. This procedure is illustrated in Example 6.31. Thus, we have shown the following corollary, where the case $m = 0$ has already been proved in Corollary 6.21. ◀

Corollary 6.30. Let $m \in \{0, 1\}$, and let $X^* \subseteq \mathbb{R}^2$ be a knot set satisfying the weak conditions. Define $X := X^* \backslash \{x^*\}$ for an arbitrary $x^* \in X^*$. If the necessary criterion for knot insertion, as introduced in Definition 6.6, holds true with respect to x^*, one has

$$\mathcal{S}_{m,X} \subseteq \mathcal{S}_{m,X^*},$$

i.e., the necessary criterion is also sufficient. ◀

Example 6.31. Let us again consider the situation depicted in Figure 6.13. Namely, one has $m = 1$ and a knot set $X \subseteq \mathbb{R}^2$ satisfying the weak conditions. Choose $K^* \in \mathcal{K}_2(X)$, and let $x_0, x_1, x_2, \widehat{x}, y \in X$ such that one has $\mathfrak{B}(K^*) = \{x_0, x_1, x_2\}$ and $\mathfrak{I}(K^*) = \{\widehat{x}, y\}$. Suppose that $\widehat{x}$ is a newly inserted knot and that we are interested in representing the simplex spline $M(\cdot \mid x_0, x_1, x_2, y)$, which is *not* generated by a Delaunay configuration of degree one anymore due to the inserted knot $\widehat{x}$. Further, suppose that the necessary criterion for knot insertion (Definition 6.6) with respect to the new knot $\widehat{x}$ holds true. In this case, Proposition 6.18 ensures the existence of critical configurations $K_0, K_1, K_2 \in \mathcal{K}_1(X)$ of K^* with respect to x_1, x_2 and x_0, x_2 as well as x_0, x_1, respectively. Moreover, assume that K_0 and K_1 have rank zero, whereas K_2 has rank one. As in the previous remark, suppose that y is the unique knot in $\mathfrak{I}(K^*) \backslash \mathfrak{U}(K_2)$, which implies that $\widehat{x} \in \mathfrak{B}(K_2)$. Furthermore, let z denote the interior knot of the critical configuration K_2. Invoking Proposition 6.28 on K_2 yields the existence of two companion configurations $K_2', K_2'' \in \mathcal{K}_1(X)$ for z with respect to K_2 and K^*, indexed such that $x_0 \in \mathfrak{B}(K_2')$. In total, we have the following five unoriented Delaunay configurations of degree one:

$$\begin{aligned} \mathfrak{U}(K_0) &= \{x_1, x_2, \widehat{x}, y\}, & \mathfrak{U}(K_1) &= \{x_0, x_2, \widehat{x}, y\}, \\ \mathfrak{U}(K_2) &= \{x_0, x_1, \widehat{x}, z\}, & \mathfrak{U}(K_2') &= \{x_0, \widehat{x}, y, z\}, \\ \mathfrak{U}(K_2'') &= \{x_1, \widehat{x}, y, z\}. \end{aligned}$$

Set $Y := (x_0, x_1, x_2)$ and $Z := (x_0, x_1, y)$. By applying Micchelli's knot insertion formula (Theorem 6.10) twice, one can represent the desired simplex spline

$M(\cdot \mid x_0, x_1, x_2, y)$ in terms of simplex splines generated by Delaunay configurations in $\mathcal{K}_1(X)$ as follows:

$$\begin{aligned} M(\cdot \mid x_0, x_1, x_2, y) &= u_0(\widehat{x} \mid Y) M(\cdot \mid x_1, x_2, \widehat{x}, y) + u_1(\widehat{x} \mid Y) M(\cdot \mid x_0, x_2, \widehat{x}, y) \\ &\quad + u_2(\widehat{x} \mid Y) M(\cdot \mid x_0, x_1, \widehat{x}, y) \\ &= u_0(\widehat{x} \mid Y) M(\cdot \mid x_1, x_2, \widehat{x}, y) + u_1(\widehat{x} \mid Y) M(\cdot \mid x_0, x_2, \widehat{x}, y) \\ &\quad + u_2(\widehat{x} \mid Y) u_2(z \mid Z) M(\cdot \mid x_0, x_1, \widehat{x}, z) \\ &\quad + u_2(\widehat{x} \mid Y) u_1(z \mid Z) M(\cdot \mid x_0, \widehat{x}, y, z) \\ &\quad + u_2(\widehat{x} \mid Y) u_0(z \mid Z) M(\cdot \mid x_1, \widehat{x}, y, z). \end{aligned}$$

This formula is schematically also reflected in Figure 6.13b. ◀

Corollary 6.30 is restricted to $m \in \{0, 1\}$. However, both Propositions 6.18 and 6.28, apply to arbitrary degrees $m \in \mathbb{N}_0$. Does the strategy of Remark 6.29 and Example 6.31 also work in the general case? This is indeed true for some cases, as depicted in Figure 6.14 exemplarily: The critical configuration can be combined with two companion configurations, yielding a simplex spline that can be combined with another two companion configurations to obtain the simplex spline that would have been generated by the (nonexistent) critical configuration of rank zero.

On the contrary, the strategy does not work for the example presented in Figure 6.15: No pair of companion configurations can be combined with the critical configuration. The core of the problem is the fact that the orderings with respect to the half planes generated by $\mathrm{aff}(x_0, x')$ and $\mathrm{aff}(x_1, x')$, respectively, are not necessarily equivalent. Nevertheless, it is possible to combine the desired simplex spline also in this example. Further auxiliary configurations, whose circumcircles are contained in the union of the circumcircles of original and critical configuration (like it is the case for companion configurations), are necessary, though.

Despite numerous experiments regarding these combinations, no general strategy for the construction of the simplex spline that would have been generated by the critical configuration of rank zero could be found. In numerical experiments checking for combinability in more than 12,000 cases, this simplex spline could always be reconstructed using critical, companion, and auxiliary configurations, though. The results of the simulation are presented in Table 6.1. This leads to the conjecture that, for all $m \in \mathbb{N}_0$ and at least for $d = 2$, the necessary criterion formulated in Definition 6.6 is sufficient for the knot insertion property to hold true.

	Rank					
Degree	2	3	4	5	6	7
2	1744					
3	1461	1207				
4	972	814	622			
5	809	687	331	154		
6	798	658	186	139	144	
7	546	527	180	144	58	60

Tab. 6.1: Numerical experiments for the combination of simplex splines: We tried to construct the simplex spline corresponding to the (nonexistent) critical configuration of rank zero using the (existent) critical configuration, its companion configurations, and auxiliary configurations for randomly chosen knot sets. In this table, the number of simulated cases is displayed for different degrees m and for different ranks of the critical configuration.

Conjecture 6.32. Let $m \in \mathbb{N}_0$, and let $X^* \subseteq \mathbb{R}^2$ be a knot set satisfying the weak conditions. Define $X := X^* \backslash \{x^*\}$ for an arbitrary $x^* \in X^*$. If the necessary criterion for knot insertion introduced in Definition 6.6 holds true with respect to x^*, one has

$$\mathcal{S}_{m,X} \subseteq \mathcal{S}_{m,X^*},$$

i.e., the necessary criterion is also sufficient. ◀

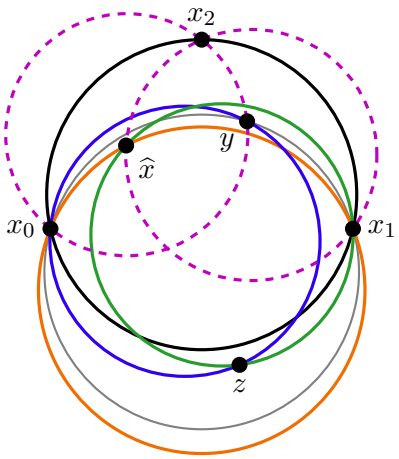

(a) Delaunay configurations used for the combination of simplex splines

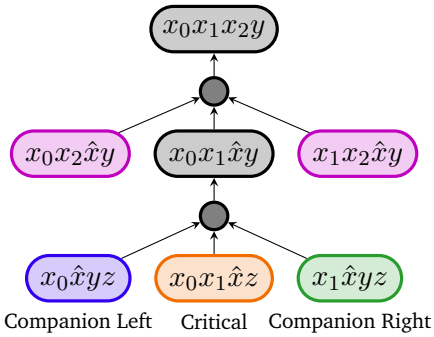

(b) Scheme of the combination of simplex splines

Fig. 6.13: Combination of critical and companion configurations for $m = 1$. The critical configuration *(orange)* of the original configuration *(black)* with respect to x_0, x_1 has rank one. The simplex splines corresponding to the critical configuration and its two companion configurations *(blue, green)* can be combined using the knot insertion formula to obtain a simplex spline with respect to the knots x_0, x_1, $\widehat{x}$, and y. Together with the critical configurations with respect to x_0, x_2 and x_0, x_1 *(purple, dashed)*, which have rank zero in this example, this yields the original simplex spline by another application of the knot insertion formula.

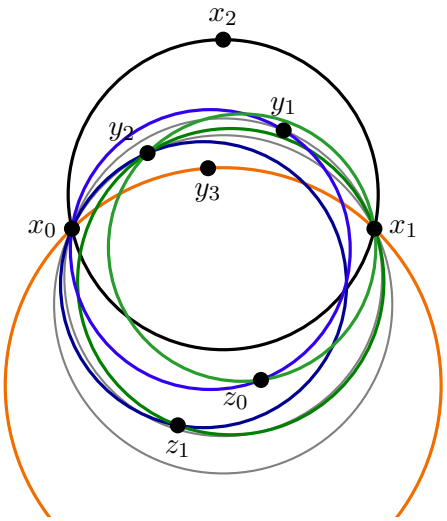

(a) Delaunay configurations used for the combination of simplex splines

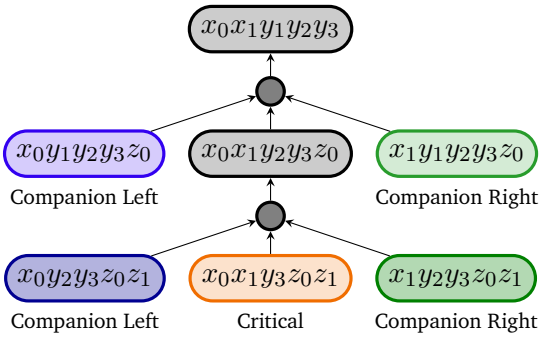

(b) Scheme of the combination of simplex splines

Fig. 6.14: Example of a critical configuration of rank two where the strategy of Remark 6.29 can be applied. The critical configuration *(orange)* can be combined with two companion configurations *(dark blue, dark green)* to obtain a simplex spline that would have been generated by the critical configuration of rank one. This simplex spline can in turn be combined with another two companion configurations *(blue, green)* to the simplex spline corresponding to the (nonexistent) critical configuration of rank zero. The critical configurations with respect to x_1, x_2 and x_0, x_2 are not displayed in this figure.

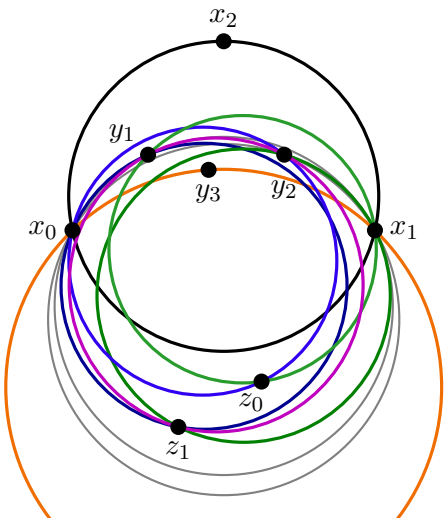

(a) Delaunay configurations used for the combination of simplex splines

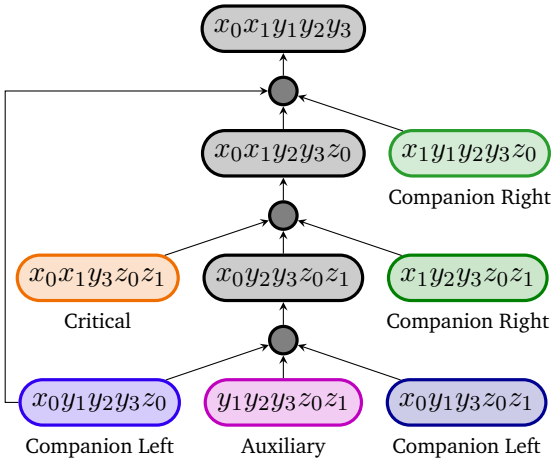

(b) Scheme of the combination of simplex splines

Fig. 6.15: Example of a critical configuration of rank two where the strategy of Remark 6.29 *cannot* be applied since no pair of companion configurations *(blue, green, dark blue, dark green)* can be combined with the critical configuration *(orange)*. Nevertheless, the simplex spline corresponding to the (nonexistent) critical configuration of rank zero can be combined using an auxiliary configuration *(purple)*, as presented in the displayed scheme.

7 Approximation and Condition

> *True learning must not be content with ideas, which are, in fact, signs, but must discover things in their individual truth.*
>
> **— Umberto Eco**
> The Name of the Rose

After the theoretical results in the previous chapters, we investigate two aspects of splines now which are particularly important for practical considerations, namely the approximation quality of the spline spaces and the condition of the spline space basis candidates.

7.1 Approximation

In the introductory chapter of this thesis, we motivated the definition of splines with their suitability for approximation problems. Regarding multivariate DCB-splines, however, we have little information about their approximation quality so far. The goal of the current section is the definition of a multivariate generalization of the Schoenberg operator, which we have introduced in Subsection 2.3.4 for univariate splines, and the determination of an upper bound for the error that can occur when we use this operator to approximate a given, sufficiently smooth function.

We will see that all definitions and proofs in this section are straightforward generalizations of the univariate analogues, which is possible due to the fact that both univariate and DCB-splines provide a Marsden-like identity, which is the core ingredient in the determination of an error bound. To be able to apply the corresponding Theorem 4.17, we assume throughout the section that $m \in \mathbb{N}_+$ denotes the spline degree and that $X \subseteq \mathbb{R}^d$ for $d \in \mathbb{N}_+$ is a knot set satisfying the strong conditions specified in Definition 4.15.

Note that a generalization of Greville sites and the Schoenberg operator to DCB-splines has already been given in [DGN05] for the special case of bivariate quadratic DCB-splines, i.e., $d = m = 2$. Our results can be applied to arbitrary dimensions and

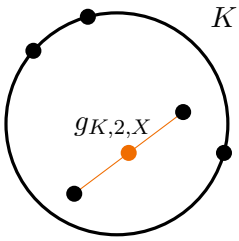

Fig. 7.1: Generalized Greville site $g_{K,2,X}$ *(orange dot)* with respect to the configuration K *(black circle)* and the given knot set X *(black dots)*

degrees but are equivalent to the results in [DGN05] when considered in this special case.

7.1.1 Multivariate Schoenberg Operator

The definition of the univariate Schoenberg operator is based on Greville sites. When recalling Definition 2.23, it can be seen that each Greville site is associated with one particular B-spline and that the site is the mean of m knots in the support of this B-spline. Each B-spline is defined with respect to $m+2$ knots, but only the m *interior* knots contribute to the Greville site, whereas the two *boundary* knots are ignored. This motivates the following straightforward generalization to DCB-splines:

Definition 7.1 (Greville site)**.** Let $d, m \in \mathbb{N}_+$, and let $X \subseteq \mathbb{R}^d$ satisfy the strong conditions. For all $K \in \mathcal{K}_m(X)$, the point

$$g_{K,m,X} := \frac{1}{m} \sum_{x \in \mathfrak{I}(K)} x$$

denotes the *(generalized) Greville site with respect to* K*.* ◀

For an example of the Greville site with respect to a given configuration, we refer to Figure 7.1. Using generalized Greville sites, the Schoenberg operator can be defined equivalently to the univariate case:

Definition 7.2 (Schoenberg operator)**.** Let $d, m \in \mathbb{N}_+$. Choose $X \subseteq \mathbb{R}^d$ satisfying the strong conditions, and let $f : \mathbb{R}^d \to \mathbb{R}$. Then,

$$S_{m,X} f := \sum_{K \in \mathcal{K}_m(X)} f(g_{K,m,X}) N(\cdot \mid K) \quad \in \mathcal{S}_{m,X} \cap \mathcal{S}'_{m,X}.$$

defines the *Schoenberg operator (of degree* m *with respect to* X*).* ◀

It is easy to see that the Schoenberg operator is linear. The fact that the approximant resulting from an application of the Schoenberg operator is a spline both in $\mathcal{S}_{m,X}$ and $\mathcal{S}'_{m,X}$ can be seen as follows: The nonpooled DCB-splines identify only simplex splines that are identical up to normalization. Hence, the coefficient in the Schoenberg operator corresponding to a basis candidate function in $\mathcal{B}_{m,X}$ is just the sum of properly weighted function evaluations at the corresponding Greville sites. Formally,

$$\sum_{K\in\mathcal{K}} f(g_{K,m,X})N(\cdot \mid K) = \left(d!m! \sum_{K\in\mathcal{K}} f(g_{K,m,X})\mathrm{vol}_d(\mathrm{conv}(\mathfrak{B}(K)))\right) M(\cdot \mid \mathfrak{U}(K^*)),$$

where $\mathcal{K} \subseteq \mathcal{K}_m(X)$ is a set of configurations such that $K_1 \sim K_2$ for all $K_1, K_2 \in \mathcal{K}$, and $K^* \in \mathcal{K}$ can be chosen arbitrarily. Here, $\sim$ denotes the equivalence relation introduced in Definition 4.20.

When considering pooled DCB-splines instead, also simplex splines that are essentially different (i.e., not equal up to normalization) are identified. However, the pooling according to $\simeq$ only involves Delaunay configurations with the same collection of interior knots. Hence, the corresponding Greville sites and, in turn, the coefficients in the Schoenberg operator coincide.

Similar generalizations of the Schoenberg operator have already been presented earlier for other spline spaces employing simplex splines, for example in [GL81] for the geometric approach in the case $d = 2$ and in [DMS92, p. 111] for DMS-splines. It is not surprising that they are very similar both to the original univariate Schoenberg operator and to our definition in terms of DCB-splines.

7.1.2 Approximation Quality

As the Schoenberg operator evaluates a given function only at the discrete Greville sites, the approximation quality, like in the univariate case, heavily depends on the behavior of the function *between* the Greville sites. For univariate B-splines, we recalled the linear exactness property in Subsection 2.3.4, which ensures that, for $m \geq 1$, affine functions (i.e., polynomials of degree at most one) are reproduced by the Schoenberg operator and, thus, the error is zero. As it turns out, it follows from Neamtu's generalization of Marsden's identity that this also holds true for pooled and nonpooled DCB-splines. This fact has already been claimed in [DGN05] for the special case $d = m = 2$. For a proof, we first have to compute the polar form of a multivariate polynomial of degree at most one. Our result agrees with the one given in [DMS92, p. 111].

Lemma 7.3. Choose $p \in \Pi_1(\mathbb{R}^d)$. Let $a \in \mathbb{R}^d$ and $b \in \mathbb{R}$ be the uniquely defined coefficients such that $p(t) = a^\intercal t + b$ for all $t \in \mathbb{R}^d$. The polar form P of p is given by

$$P(t_1, \ldots, t_m) = b + \frac{1}{m} a^\intercal \left(\sum_{i=1}^{m} t_i \right) \quad \text{for all } t_1, \ldots, t_m \in \mathbb{R}^d.$$

Proof. According to Theorem 2.18, we have to show that P is symmetric, multiaffine, and that it has the diagonal property.

(i) *Symmetry:* The symmetry follows directly from the commutativity of vector addition in $\mathbb{R}^d$.

(ii) *Multiaffinity:* Choose affinely independent $z_0, \ldots, z_d \in \mathbb{R}^d$. Moreover, let $Z := (z_0, \ldots, z_d)$ and $k \in \{1, \ldots, m\}$. Then, for all $t_1, \ldots, t_m \in \mathbb{R}^d$, one has

$$\begin{aligned}
&\sum_{\ell=0}^{d} u_\ell(t_k \mid Z) P(t_1, \ldots, t_{k-1}, z_\ell, t_{k+1}, \ldots, t_m) \\
&= \frac{1}{m} a^\intercal \underbrace{\left(\sum_{\ell=0}^{d} u_\ell(t_k \mid Z) z_l \right)}_{=t_k} + \left(b + \sum_{\substack{i=1 \\ i \neq k}}^{m} \frac{a^\intercal t_i}{m} \right) \underbrace{\left(\sum_{\ell=0}^{d} u_\ell(t_k \mid Z) \right)}_{=1} \\
&= P(t_1, \ldots, t_m).
\end{aligned}$$

(iii) *Diagonal property:* For all $t \in \mathbb{R}^d$, one has

$$P(t, \ldots, t) = b + \sum_{i=1}^{m} \frac{a^\intercal t}{m} = b + a^\intercal t = p(t).$$

□

Using the previous Lemma, the linear exactness property follows directly from the equivalent of Marsden's identity for DCB-splines formulated in Theorem 4.17.

Proposition 7.4 (Linear exactness)**.** Let $d, m \in \mathbb{N}_+$, and choose a knot set $X \subseteq \mathbb{R}^d$ satisfying the strong conditions. For all $p \in \Pi_1(\mathbb{R}^d)$, one has $S_{m,X} p = p$.

Proof. Let $a \in \mathbb{R}^d$ and $b \in \mathbb{R}$ be the uniquely defined coefficients such that, for all $t \in \mathbb{R}^d$, one has $p(t) = a^\intercal t + b$. It follows with Lemma 7.3 and Theorem 4.17 that

$$S_{m,X} p(t) = \sum_{K \in \mathcal{K}_m(X)} p\left(\frac{1}{m} \sum_{x \in \mathfrak{I}(K)} x \right) N(t \mid K)$$

$$
\begin{aligned}
&= \sum_{K \in \mathcal{K}_m(X)} \left(b + \sum_{x \in \mathfrak{I}(K)} \frac{a^\intercal x}{m} \right) N(t \mid K) \\
&= \sum_{K \in \mathcal{K}_m(X)} P(\mathfrak{I}(K)) N(t \mid K) \\
&= p(t)
\end{aligned}
$$

for all $t \in \mathbb{R}^d$. □

Of course, one is interested in a result regarding the approximation quality of a much broader class of functions, and indeed, if we assume a given function to be at least two times continuously differentiable, we can use the linear exactness property to obtain an upper bound for the approximation error. It has been stated in several publications, like in [Boo82, p. 68f] or in [DMS92, p. 111] for example, that, for suitable operators which reproduce polynomials of degree up to m', the error decreases as $h^{m'+1}$, where h denotes the maximum (local) distance between neighboring knots. Nevertheless, we give an explicit upper bound for the approximation error in order to confirm the approximation order, derive also the constant factor, and enable a comparison to the univariate equivalent provided in Theorem 2.25. The proof follows the sketch for general approximation operators in [Boo82, p. 68f].

Theorem 7.5 (Approximation order)**.** Let $m, d \in \mathbb{N}_+$, and choose a knot set $X \subseteq \mathbb{R}^d$ satisfying the strong conditions. Moreover, let $f \in \mathcal{C}^2(\mathbb{R}^d)$, and let $H_f(z')$ denote the Hessian of f at z'. Then, under the condition that both supremums exist, one has

$$
\|f - S_{m,X} f\|_\infty \leq 2r^2 \sup_{z' \in \mathbb{R}^d} \|H_f(z')\|_{\mathrm{F}},
$$

where

$$
r := \sup_{K \in \mathcal{K}_m(X)} \operatorname{rad}(\mathfrak{B}(K)).
$$

Proof. For $v \in \mathbb{R}^d$, let

$$
\mathcal{K}^*_{m,v}(X) := \left\{ K \in \mathcal{K}_m(X) \;\middle|\; v \in \operatorname{supp} N(\cdot \mid K) \right\} \subseteq \mathcal{K}_m(X)
$$

denote the set of all Delaunay configurations whose corresponding simplex splines contain v in their support. Then, in particular, $v \in \overline{B(\mathfrak{B}(K))}$ for all $K \in \mathcal{K}^*_{m,v}(X)$, and thus, one has

$$
\|v - w\| \leq \|v - \operatorname{cen}(\mathfrak{B}(K))\| + \|\operatorname{cen}(\mathfrak{B}(K)) - w\| < 2 \operatorname{rad}(\mathfrak{B}(K))
$$

for all $w \in B(\mathfrak{B}(K))$. Since the Greville site with respect to a configuration K is a convex combination of interior knots of K, which are clearly in $B(\mathfrak{B}(K))$, it follows from the convexity of $B(\mathfrak{B}(K))$ that $g_{K,m,X} \in B(\mathfrak{B}(K))$, and hence,

$$\|v - g_{K,m,X}\| < 2\operatorname{rad}(\mathfrak{B}(K)) \quad \text{for all } v \in \mathbb{R}^d,\ K \in \mathcal{K}^*_{m,v}(X). \tag{7.1}$$

Furthermore, for all $v, w \in \mathbb{R}^d$, the multivariate Taylor expansion of f at v yields the existence of a $z \in \operatorname{conv}(v, w)$ such that

$$f(w) = \underbrace{f(v) + \langle \nabla f(v), w - v\rangle}_{=:T_{1,v}f(w)} + \underbrace{\frac{1}{2}(w-v)^\intercal H_f(z)(w-v)}_{=:T_{\mathrm{r},v}f(w)}.$$

For all $v, w \in \mathbb{R}^d$ and a suitable choice of $z \in \operatorname{conv}(v, w)$, one can use the Cauchy-Schwarz inequality and the compatibility of the Frobenius and the Euclidean norm, i.e.,

$$\|Au\|_2 \le \|A\|_{\mathrm{F}}\|u\|_2 \quad \text{for all } u \in \mathbb{R}^d,\ A \in \mathbb{R}^{d\times d},$$

to bound the absolute value of the remainder term $T_{\mathrm{r},v}f(w)$ of the Taylor expansion:

$$\begin{aligned}|T_{\mathrm{r},v}f(w)| &= \frac{1}{2}|(w-v)^\intercal H_f(z)(w-v)| \le \frac{1}{2}\|w-v\|\|H_f(z)(w-v)\| \\ &\le \frac{1}{2}\|H_f(z)\|_{\mathrm{F}}\|w-v\|^2 \le \frac{1}{2}\|w-v\|^2 \sup_{z'\in\mathbb{R}^d}\|H_f(z')\|_{\mathrm{F}}.\end{aligned}$$

In combination with (7.1), this yields that, for all $K \in \mathcal{K}^*_{m,v}(X)$, one has

$$|T_{\mathrm{r},v}f(g_{K,m,X})| \le \frac{(2\operatorname{rad}(\mathfrak{B}(K)))^2}{2}\sup_{z'\in\mathbb{R}^d}\|H_f(z')\|_{\mathrm{F}} \le 2r^2 \sup_{z'\in\mathbb{R}^d}\|H_f(z')\|_{\mathrm{F}}.$$

Together with the identity $T_{1,v}f(v) = f(v)$ for all $v \in \mathbb{R}^d$, the linear exactness and linearity of the Schoenberg operator, the nonnegativity of simplex splines, and the partition of unity (Corollary 4.18), we obtain the final estimate

$$\begin{aligned}\|f - S_{m,X}f\|_\infty &= \sup_{v\in\mathbb{R}^d}|T_{1,v}f(v) - S_{m,X}f(v)| = \sup_{v\in\mathbb{R}^d}|S_{m,X}(T_{1,v}f)(v) - S_{m,X}f(v)| \\ &= \sup_{v\in\mathbb{R}^d}|S_{m,X}(T_{\mathrm{r},v}f)(v)| \le \sup_{v\in\mathbb{R}^d}\sum_{K\in\mathcal{K}^*_{m,v}(X)}|T_{\mathrm{r},v}f(g_{K,m,X})||N(v \mid K)| \\ &\le 2r^2\left(\sup_{z'\in\mathbb{R}^d}\|H_f(z')\|_{\mathrm{F}}\right)\left(\sup_{v\in\mathbb{R}^d}\sum_{K\in\mathcal{K}^*_{m,v}(X)}|N(v \mid K)|\right) \\ &= 2r^2\sup_{z'\in\mathbb{R}^d}\|H_f(z')\|_{\mathrm{F}}.\end{aligned}$$

□

Equivalently to this global result, one can also derive a *local* error bound. To that end, we consider a convex, open $\Omega \subseteq \mathbb{R}^d$ and $f \in \mathcal{C}^2(\Omega)$. However, the supremum of the Frobenius norm of the Hessian of f has to be taken on a convex region $\widehat{\Omega} \supseteq \Omega$ which contains all Greville sites corresponding to Delaunay configurations in $\{\mathcal{K}^*_{m,v}(X) \mid v \in \Omega\}$. The set $\widehat{\Omega}$ is in general larger than Ω, but if Ω is bounded, the local finiteness theorem (Theorem 5.29) ensures that $\widehat{\Omega}$ is bounded, too.

When comparing this bound to the univariate equivalent in Theorem 2.25, we miss the dependency on the spline degree m at first sight. However, as the circumcircle of Delaunay configurations becomes larger when the spline degree increases, the value of m is already encoded in the factor r^2. In fact, our multivariate bound employing $2r^2$ is even slightly better than the univariate bound in Theorem 2.25 since it can be expressed as $1/2\,(\sup_{i\in\mathbb{Z}} |x_{i+m+1} - x_i|)^2 \|f''\|_\infty$ in the univariate case.

Theorem 7.5 ensures that the maximum approximation error decreases quadratically as the maximum configuration size decreases. Since Neamtu's Theorem 4.17, as foundation for the results in this section, applies to both pooled and nonpooled DCB-splines, the same holds true for Theorem 7.5. Hence, both pooled and nonpooled DCB-splines can be utilized for the efficient approximation of $\mathcal{C}^2(\mathbb{R}^d)$-functions.

If one is able to construct an operator ensuring an exactness of a higher degree, it can be expected that also the approximation order would increase accordingly, as has been suggested by several publications, such as [Boo82, p. 68f]. Most parts of our proof could be reused by employing a higher-order Taylor expansion.

7.2 Condition

It is the goal of this section to provide bounds that relate the maximum absolute value of some set of coefficients with the maximum absolute value of the spline function generated by these coefficients. If the bounds are relatively close to one, the basis candidates for DCB-splines are well-conditioned and, in particular, really a basis. An equivalent result for univariate splines has been presented in Subsection 2.3.6.

7.2.1 Bounding the Spline Value

The supremum norm of a spline function can be bounded easily by employing the partition of unity for DCB-splines, as presented in Corollary 4.18. The result follows analogously for both nonpooled and pooled DCB-splines.

Proposition 7.6. Let $d \in \mathbb{N}_+$, $m \in \mathbb{N}_0$, and choose a knot set $X \subseteq \mathbb{R}^d$ satisfying the weak conditions. Let $g \in \mathcal{S}_{m,X}$ be a nonpooled DCB-spline and $a := (a_B)_{B \in \mathcal{B}_{m,X}}$ be its bounded, real-valued family of coefficients. Then, one has $\|g\|_\infty \leq \|a\|_\infty$.

Proof. Let $t \in \mathbb{R}^d$. Due to the definition of $\mathcal{B}_{m,X}$, the nonnegativity of simplex splines, and the partition of unity (Corollary 4.18), it follows that

$$|g(t)| \leq \|a\|_\infty \sum_{B \in \mathcal{B}_{m,X}} |B(t)| = \|a\|_\infty \sum_{K \in \mathcal{K}_m(X)} N(t \mid K) \leq \|a\|_\infty.$$

□

Proposition 7.7. Let $d \in \mathbb{N}_+$, $m \in \mathbb{N}_0$, and choose a knot set $X \subseteq \mathbb{R}^d$ satisfying the weak conditions. Let $g \in \mathcal{S}'_{m,X}$ be a pooled DCB-spline and $a := (a_B)_{B \in \mathcal{B}_{m,X}}$ be its bounded, real-valued family of coefficients. Then, one has $\|g\|_\infty \leq \|a\|_\infty$. ◀

7.2.2 Bounding the Coefficients

For an estimate in the other direction, we only consider nonpooled DCB-splines. Stability can be considered as "quantized version of linear independence". In particular, a linear dependent basis candidate cannot be stable. During our experiments, we encountered the following example, which shows that the basis candidate functions for nonpooled DCB-splines are not necessarily linear independent and, thus, renders the existence of a constant $C_m > 0$ such that $\|a\|_\infty \leq C_m \|g\|_\infty$ for all spline functions $g \in \mathcal{S}_{m,X}$ with a bounded, real-valued family of coefficients $a := (a_B)_{B \in \mathcal{B}_{m,X}}$ impossible.

Example 7.8. Let $d = 2$, $m = 2$, and

$$x_0 := (-1, 0)^\intercal, \qquad x_1 := (1, 0)^\intercal, \qquad x_2 := \left(\frac{1}{4}, -\frac{1}{2}\right)^\intercal,$$
$$x_3 := \left(-\frac{1}{4}, -1\right)^\intercal, \qquad x_4 := \left(-\frac{1}{4}, \frac{1}{2}\right)^\intercal, \qquad x_5 := \left(\frac{1}{4}, 1\right)^\intercal.$$

When looking at Figure 7.2, it is easy to see that $x_0, \ldots, x_5$ are in general Delaunay position and give rise to the following Delaunay configurations:

$$\widetilde{K}_0 := (\{x_0, x_1, x_2\}, \{x_4, x_5\}), \qquad \widetilde{K}_1 := (\{x_0, x_1, x_3\}, \{x_2, x_4\}),$$
$$\widetilde{K}_2 := (\{x_0, x_1, x_4\}, \{x_2, x_3\}), \qquad \widetilde{K}_3 := (\{x_0, x_1, x_5\}, \{x_2, x_4\}),$$
$$\widetilde{K}_4 := (\{x_2, x_3, x_5\}, \{x_0, x_4\}), \qquad \widetilde{K}_5 := (\{x_3, x_4, x_5\}, \{x_1, x_2\}).$$

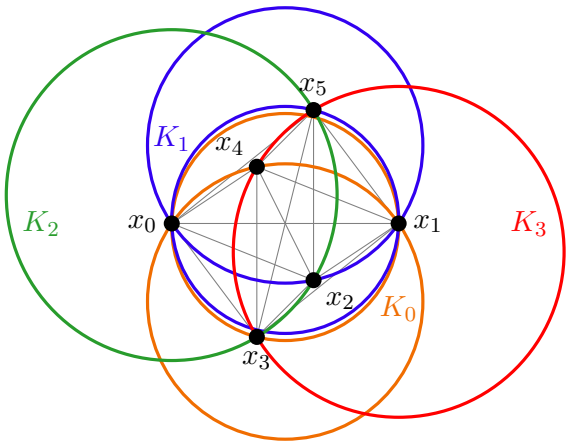

Fig. 7.2: Knots and configurations as introduced in Example 7.8. Delaunay configurations of the same color are equivalent with respect to $\sim$.

When we consider unoriented Delaunay configurations and eliminate duplicates according to $\sim$, the following four configurations remain:

$$\begin{aligned}
K_0 &:= \{x_0, x_1, x_2, x_3, x_4\} = \mathfrak{U}\big(\widetilde{K_1}\big) = \mathfrak{U}\big(\widetilde{K_2}\big),\\
K_1 &:= \{x_0, x_1, x_2, x_4, x_5\} = \mathfrak{U}\big(\widetilde{K_0}\big) = \mathfrak{U}\big(\widetilde{K_3}\big),\\
K_2 &:= \{x_0, x_2, x_3, x_4, x_5\} = \mathfrak{U}\big(\widetilde{K_4}\big),\\
K_3 &:= \{x_1, x_2, x_3, x_4, x_5\} = \mathfrak{U}\big(\widetilde{K_5}\big).
\end{aligned}$$

We extend the knot set $\{x_0, \dots, x_5\}$ to a knot set $X \subseteq \mathbb{R}^2$ satisfying the strong conditions such that $x_0, \dots, x_5 \in X$ and

$$\big(X \backslash \{x_0, \dots, x_5\}\big) \cap \bigcup_{i=0}^{5} \overline{B\Big(\mathfrak{B}\big(\widetilde{K_i}\big)\Big)} = \emptyset.$$

Then, $\widetilde{K_0}, \dots, \widetilde{K_5} \in \mathcal{K}_2(X)$, and therefore, $c_0 M(\cdot \mid K_0), \dots, c_3 M(\cdot \mid K_3) \in \mathcal{B}_{2,X}$ for appropriately chosen normalization factors $c_0, \dots, c_3 \in \mathbb{R}_+$. This expansion of the simple knot set $\{x_0, \dots, x_5\}$ is necessary in order to ensure $\operatorname{conv}(X) = \mathbb{R}^d$. Define

$$b := \frac{1}{d(x_0, x_1, x_5)} = \frac{1}{2}, \quad b' := \frac{1}{d(x_0, x_1, x_3)} = -\frac{1}{2},$$

and the nonzero coefficients

$$\begin{aligned}
a_0 &:= bd(x_0, x_1, x_2) = -1/2, && a_1 := -b'd(x_0, x_1, x_2) = -1/2,\\
a_2 &:= bd(x_0, x_2, x_5) - b'd(x_0, x_2, x_3) = 15/16 - 7/16 = 1/2,\\
a_3 &:= bd(x_2, x_1, x_5) - b'd(x_2, x_1, x_3) = 9/16 - 1/16 = 1/2.
\end{aligned}$$

It follows from Micchelli's knot insertion formula (see Theorem 6.10) that, for all $t \in \mathbb{R}^d$, one has

$$\begin{aligned}
&\sum_{i=0}^{3} a_i M(t \mid K_i) \\
&= b\Big(d(x_0, x_1, x_2)M(t \mid K_0) + d(x_0, x_2, x_5)M(t \mid K_2) \\
&\qquad + d(x_2, x_1, x_5)M(t \mid K_3)\Big) \\
&\quad - b'\Big(d(x_0, x_1, x_2)M(t \mid K_1) + d(x_0, x_2, x_3)M(t \mid K_2) \\
&\qquad + d(x_2, x_1, x_3)M(t \mid K_3)\Big) \\
&= M(t \mid x_0, x_1, x_3, x_4, x_5) - M(t \mid x_0, x_1, x_3, x_4, x_5) = 0.
\end{aligned}$$

As all coefficients $a_0, \ldots, a_3$ are nonzero, we have found a nontrivial linear combination of the zero-function, which shows in particular that the basis candidate functions in $\mathcal{B}_{m,X}$ are linearly dependent.

This has also been confirmed by the numerical evaluation presented in Figure 7.3: The maximum absolute deviation from the zero-function is $5.7745 \cdot 10^{-16}$, which is small enough to be caused by numerical inaccuracies. ◀

The previous example is a contradiction to the claim in [Nea01b, p. 381] that the basis candidate functions in $\mathcal{B}_{m,X}$ are linearly independent. In particular, this shows that $\mathcal{B}_{m,X}$ is in general *not* a basis for the space of nonpooled DCB-splines $\mathcal{S}_{m,X}$. Furthermore, the knots in the example can be varied slightly without changing the validity of the example, as follows from the fact that the set of Delaunay configurations does not change as long as none of the knots crosses the circumcircle of any Delaunay configuration and the knot set remains in general Delaunay position. Within that range, the circumcircles of Delaunay configurations follow the knot positions "continuously". This insight ensures that the set of knot configurations leading to dependent basis candidate functions is not a set of measure zero. In particular, this counterexample is not some kind of degenerate case which could have been excluded by additional constraints on the knot set.

Remark 7.9. When we consider pooled DCB-splines and look at the Delaunay configurations $\widetilde{K}_0, \ldots \widetilde{K}_5$ in the previous counterexample, it turns out that there are five different collections of interior knots and, thus, also five different pooled basis candidate functions. In particular, this collection of functions comprises all the basis candidate functions generated by the nonpooled approach, $c_0 M(\cdot \mid K_0), \ldots, c_3 M(\cdot \mid K_3)$,

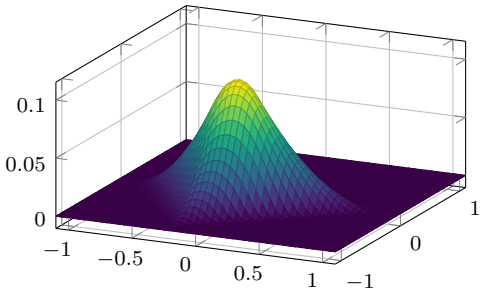

(a) The simplex spline $M(\cdot \mid K_0)$

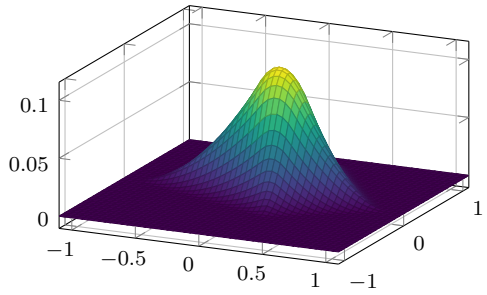

(b) The simplex spline $M(\cdot \mid K_1)$

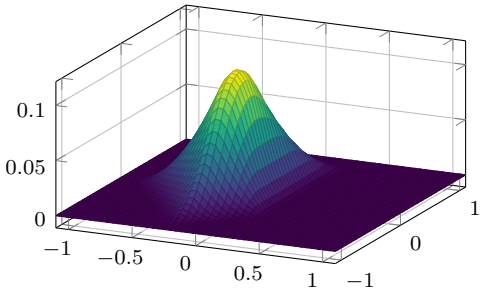

(c) The simplex spline $M(\cdot \mid K_2)$

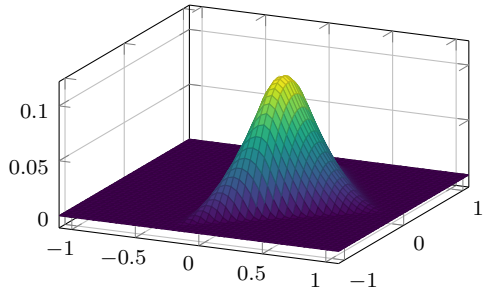

(d) The simplex spline $M(\cdot \mid K_3)$

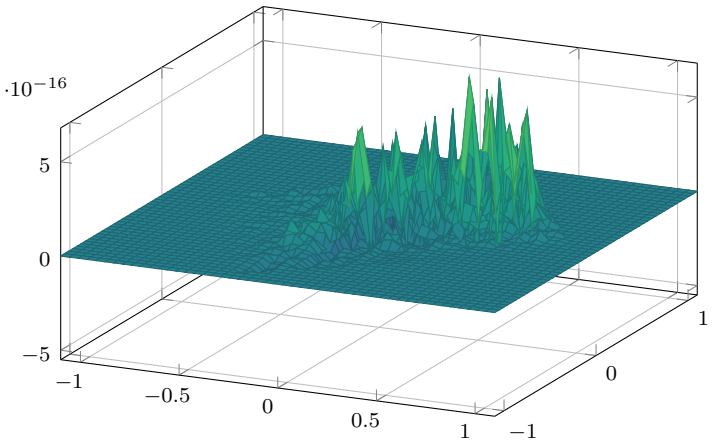

(e) A linear combination of the simplex splines displayed above

Fig. 7.3: Plots of the functions in Example 7.8. A linear combination of the four displayed simplex splines with appropriate nonzero coefficients yields the zero-function. It is presented in Figure 7.3e, where the small deviations from zero are caused by numerical inaccuracies.

up to normalization. Therefore, the counterexample also works for the pooled approach at first sight. However, when expanding the set of knots $\{x_0, \dots, x_5\}$ to the knot set X with $\operatorname{conv}(X) = \mathbb{R}^2$, new Delaunay configurations arise, and each of the configurations $\widetilde{K_0}$, $\widetilde{K_2}$, $\widetilde{K_4}$, and $\widetilde{K_5}$ will be pooled with at least one of these new Delaunay configurations. This also influences the generated basis candidate functions, of course, and thus, the counterexample does not apply to pooled DCB-splines with respect to knot sets satisfying the strong conditions. As the pooling also influences the value of the pooled basis candidate functions inside the convex hull $\operatorname{conv}(x_0, \dots, x_5)$, it is even unclear if there is a linear combination of pooled basis candidate functions yielding the zero function when restricting them to the region $\operatorname{conv}(x_0, \dots, x_5)$. Hence, the counterexample does not contain any statement about the *local linear independence* (see [DM85], for example) of pooled basis candidate functions either. ◀

The supremum norm of the constant zero-function is clearly zero. Due to linear dependence, it is possible to combine the zero-function with nonzero coefficient sets. This immediately shows that a constant $C_m > 0$ satisfying

$$\|a\|_\infty \leq C_m \|g\|_\infty$$

for all spline functions $g \in \mathcal{S}_{m,X}$ with a bounded, real-valued family of coefficients $a := (a_B)_{B \in \mathcal{B}_{m,X}}$ does not exist in general. After all, $\mathcal{B}_{m,X}$ is not necessarily a basis.

8 Conclusion

> *Of course it is happening inside your head, Harry, but why on earth should that mean that it is not real?*
>
> **— J. K. Rowling**
> Harry Potter and the Deathly Hallows

This final chapter starts with a summary of the results gained in the previous chapters, followed by some issues that arise when employing DCB-splines for practical applications. Afterwards, we will close the chapter with open questions and ideas for future research.

8.1 Summary

In the introduction of the thesis, we formulated four research questions regarding DCB-splines, which have been answered in the previous chapters. When recalling the properties of univariate splines presented in Section 2.3, it turns out that, for each property, we have investigated to what extent it applies to DCB-splines, with a focus on the nonpooled approach. We will summarize our insights now.

In Chapter 5, we investigated the local finiteness property. For knot sets X satisfying the strong conditions specified in Definition 4.15, in particular $\operatorname{conv}(X) = \mathbb{R}^d$, we proved for both pooled and nonpooled DCB-splines that each point is in the support of only a finite number of basis candidate functions and that the restriction of the spline space to a compact region has finite dimensions. This is an affirmative answer to our first research question. However, we could also provide an example showing that the local finiteness property does not hold true in general if $\operatorname{conv}(X) \subset \mathbb{R}^d$. We also formulated the local finiteness condition, which is a sufficient criterion for the local finiteness property in a compact domain even if $\operatorname{conv}(X) \subset \mathbb{R}^d$. For appropriately chosen domains, the local finiteness condition can be checked practically.

For nonpooled DCB-splines, we found a counterexample in Section 7.2 showing that the basis candidate functions are not necessarily linearly independent, which

answers our second research question. Consequently, nonpooled DCB-splines are not a solution to the Fundamental Problem formulated in Section 4.1.2. Note that the counterexample does not apply to the pooled approach to DCB-splines favored by Neamtu.

The third research question, which is answered in Section 7.1, concerns approximation by DCB-splines. A Schoenberg operator can be defined equivalently to the univariate case. We verified that it features linear exactness and used this result to provide an upper bound for the approximation error. Like in the univariate case, this error decreases quadratically as the maximum radius of the circumcircles of Delaunay configurations is reduced. These circumcircles seem to be a "natural" measure.

The knot insertion property is an important feature of univariate splines. However, both pooled and nonpooled DCB-splines do *not* exhibit this property, as shown by a counterexample in Chapter 6. Inspired by this example, we provide a necessary criterion for the knot insertion property to hold true for a given inserted knot. We also succeeded in proving that this criterion is sufficient for bivariate, nonpooled DCB-splines of degrees zero and one. Numerical experiments suggest that the sufficiency even holds true for arbitrary degrees. All these results are contributions to our fourth research question.

8.2 Practical Considerations

While the focus of this work lies in theoretical properties of DCB-splines, splines have primarily been designed to be used in practical applications. In this section, we consider three different issues that arise when implementing DCB-splines, namely the efficient evaluation of simplex splines, the handling of degenerate and finite knot sets, and the efficient computation of Delaunay configurations.

8.2.1 Efficient Evaluation of Simplex Splines

Let $d \in \mathbb{N}_+$ and $m \in \mathbb{N}_0$. Clearly, one of the most important tasks in practical applications using simplex splines is their evaluation. The key ingredient for an efficient evaluation procedure is Micchelli's recursion formula (see Proposition 3.24). For $m \geq 2$, it can be employed to express the value of a simplex spline of degree m at $t \in \mathbb{R}^d$ as weighted sum of several simplex splines of degree $m-1$ evaluated at t. If the recursion formula would also be valid for $m = 1$, one could apply it recursively

to express every simplex spline in terms of simplex splines of degree zero, i.e., scaled characteristic functions of simplices.

However, a more sophisticated definition of the value of simplex splines of degree zero on the discontinuous boundary of their support would be necessary to be able to apply the recursion formula for $m = 1$. There *"does not seem to exist a simple convention which is compatible with the recurrence relations"* [Höl86, p. 104], though. [Mic79] assigns specific values to that boundary in order to obtain a valid formula for $m = 1$. Unfortunately, it turns out that it is impossible to choose these values appropriately in a way that the recursion identity holds pointwise independently of the specific relative position of the knots. For univariate splines, the problem is solved by simply choosing to make the B-splines continuous from either the left or from the right [Gra88]; note that we have chosen the latter in Definition 2.11. An equivalent approach for the multivariate case is proposed in [Sei92a, p. 263] by introducing *half-open convex hulls*, and similarly in [Gra88]. Although being theoretically correct, this approach does not allow a numerically stable implementation, which renders it infeasible for practical applications [Gra88]. Instead, Grandine shows in [Gra88] how to evaluate continuous simplex splines of degree one directly. By applying the recursion formula for the case $m \geq 2$, this enables an efficient evaluation of all simplex splines of degree at least one with respect to knots in general position. For other knot sets, the issue remains for evaluations on the $(d-1)$-simplices spanned by subsets of d knots, though.

Assume that $m \geq 2$. When using Micchelli's recursion formula to evaluate a d-variate simplex spline of degree m at some site $t \in \mathbb{R}^d$, it is necessary to express t as affine combination of the $d+m+1$ knots. The weights associated to the knots are then used as coefficients in the linear combination of the simplex splines of degree $m-1$. Due to Carathéodory's theorem, at most $d+1$ nonzero coefficients are sufficient to represent t in this way (see Remark 3.25). According to [Gra88], one should choose the $d+1$ nonzero coefficients such that all coefficients are nonnegative in order to increase numerical accuracy: As simplex splines are nonnegative, this strategy avoids inaccuracies due to cancellation. [Gra88] formulates these requirements on the coefficients and uses a Tucker tableau to derive a suitable solution.

Another question regarding the efficiency of function evaluation in a specific spline space is the following: Can simplex splines of degree $m-1$ be reused for the computation of *several* basis candidate functions of degree m? If this would be possible, branches of the recursive evaluation tree could be memoized. For the combinatorial approach presented in Subsection 4.2.2, [Gra87] provides the negative result that a simplex spline of degree $m-1$ contributes to at most two simplex

splines of degree m. To the best of our knowledge, a similar result regarding DCB-splines has not been published so far. Thus, it may still be possible that an efficient evaluation procedure is available for these spline spaces.

8.2.2 Degenerate and Finite Knot Sets

Throughout the thesis, we had different requirements on the knot set $X \subseteq \mathbb{R}^d$, $d \in \mathbb{N}_+$. For many theorems, we assumed that X satisfies the *strong conditions* specified in Definition 4.15, i.e., that X is locally finite, in general Delaunay position, and that $\operatorname{conv}(X) = \mathbb{R}^d$. Whereas most knot sets in practical applications are certainly locally finite, the restriction to knot sets satisfying $\operatorname{conv}(X) = \mathbb{R}^d$ is more severe since this implies in particular that X contains an infinite number of knots. Moreover, it would also be desirable to be able to cope with knot sets that are not in general Delaunay position, such as knots on a grid. Relaxations of the requirements on the knot sets are investigated in [DGN05] for bivariate, quadratic, pooled DCB-splines.

The problem with degenerate knot sets, i.e., knot sets that are not in general Delaunay position, is twofold: Firstly, if we construct a simplex spline with respect to a collection of knots which contains a subset $A \subseteq X$ of $d+1$ knots such that $\dim \operatorname{aff}(A) < d$, this simplex spline is not $(m-1)$-times continuously differentiable, i.e., does not have maximum smoothness [Hak82]. This is not necessarily a problem, but one should be aware of this fact, for example when constructing DCB-splines with respect to a grid-like knot set. Secondly, the construction of basis candidate functions for DCB-splines is based on Delaunay configurations, which can only be defined for knot sets in general Delaunay position. Namely, if more than $d+1$ knots lie on a sphere, it is unclear if the additional knot(s) should be treated as interior knot(s) of the configuration. This circumstance corresponds to the situation where the Delaunay triangulation contains untriangulated holes (see Subsection 4.3.2). If these holes are triangulated arbitrarily, for example via symbolic perturbation, however, one obtains a suitable space of DCB-splines of degree zero [DGN05]. This approach can be employed for arbitrary spline degrees. The resulting spline spaces depend on the specific perturbation, though [DGN05].

Whereas knot sets with an infinite number of knots may be of theoretical interest, almost every practical application is restricted to finite knot sets, which in particular do *not* satisfy $\operatorname{conv}(X) = \mathbb{R}^d$. We demanded the knot set X to satisfy this requirement in order to ensure the local finiteness property (see Theorem 5.29) and the validity of Neamtu's equivalent of Marsden's identity for DCB-splines (see Theorem 4.17). We

only have to consider the latter since the local finiteness property is trivially satisfied for finite knot sets. Marsden's identity can be used to obtain the spline representation of polynomials, which, except for the zero-function, do not have a bounded support and, thus, cannot be expressed using a finite knot set and compactly supported basis candidate functions. The following insights regarding this topic can be found in [DGN05]. Let $m \in \mathbb{N}_+$, and choose a finite knot set $X \subseteq \mathbb{R}^d$ in general Delaunay position. Then, $\Omega := \operatorname{conv}(X)$ is our convex and compact domain of interest. As all basis candidate functions in $\mathcal{B}_{m,X}$ and $\mathcal{B}'_{m,X}$, respectively, are continuous and supported on Ω, they vanish on $\partial\Omega$, which is in particular a contradiction to the partition of unity (see Corollary 4.18). Thus, Theorem 4.17 can only hold true on a subset of Ω. One possible approach to handle this issue would be to add knots outside of Ω to the knot set X. However, since there is no canonical choice for these knots and as this method involves further drawbacks, [DGN05] propose to allow knots with multiplicity at the boundary of Ω and apply symbolic perturbation to obtain a space of DCB-splines. Although the resulting spline space depends on the specific perturbation, Theorem 4.17 holds true on Ω if each knot on the boundary has multiplicity $m + 1$, which is also the usual choice in the univariate case. As [DGN05] point out, the discontinuities of the basis candidate functions at the boundary of Ω can propagate to the interior of Ω, though. In their specific case ($d = 2$, $m = 2$), the continuity of the resulting spline functions can be ensured by choosing the same coefficient for all basis candidate functions corresponding to coalescing Greville sites. In order to guarantee that the spline functions are also continuously differentiable in the interior of Ω, further coplanarity constraints on the coefficients are necessary, however [DGN05]. When using the Schoenberg operator to approximate a given function, the values of this function at the Greville sites are used as coefficients, and thus, basis candidate functions with identical corresponding Greville sites are assigned the same coefficient automatically. On the contrary, the additional coplanarity conditions reduce the approximation quality as one cannot just use the values at the Greville sites as coefficients [DGN05].

8.2.3 Computing Delaunay Configurations

In the previous subsection, we considered DCB-splines with respect to finite knot sets. However, "finite" could still be too large if the involved algorithms are not efficient enough. An important task when constructing DCB-splines is to find all Delaunay configurations of a given degree with respect to some finite knot set $X \subseteq \mathbb{R}^d$, $d \in \mathbb{N}_+$, in general Delaunay position. Let $N := |X|$ denote the number of knots. A naive approach would be to count the knots in each circumcircle spanned by any collection

of $d+1$ knots. This would yield an overall time complexity of $\mathcal{O}(N^{d+2})$, which is prohibitive for large knot sets even for $d=2$. However, in the bivariate case, there are two approaches towards an efficient computation of Delaunay configurations, both having an expected time complexity in $\mathcal{O}(N \log N)$. In the following, we will recall both approaches briefly.

An algorithm originally designed to enumerate all suitable triangles for *order-m Delaunay triangulations* is due to [GHK02; SK09] and can be adapted for the computation of Delaunay configurations [Han+08]. The algorithm can be split into two stages:

1. *Enumerating suitable edges:* The first stage computes a collection of certain pairs of knots as input for the second stage. According to [GHK02], these *m-OD edges* have a one-to-one correspondence to the Voronoi diagram of order $m+1$: Two knots $x, x' \in X$ constitute an m-OD edge if and only if there are $Y, Y' \subseteq X$ with $|Y| = |Y'| = m+1$ such that $x \in Y$, $x' \in Y'$, and the Voronoi regions with respect to Y and Y' are adjacent. For the computation of the Voronoi diagram of order $m+1$, [GHK02] use an algorithm which is due to [Ram99] and has an expected time complexity in $\mathcal{O}(Nm^2 + N \log N)$. The number of m-OD edges is in $\mathcal{O}(Nm)$ [GHK02].

2. *Finding Delaunay configurations for each edge:* The following procedure is applied to each of the m-OD edges found in the first stage of the algorithm and is an adapted version of the approach sketched in [SK09]. Consider the hyperplane spanned by the two knots $x, x' \in X$ constituting the m-OD edge that is currently under consideration. In both half spaces generated by this hyperplane, we enumerate the $m+1$ knots that are closest to x and x' with respect to an appropriate order of the points (which in fact is equivalent to the strict total order $\prec$ that we have introduced in Lemma 6.15) and sort these knots according to this order. This can be done with a time complexity of $\mathcal{O}(m \log m)$. The result is two sorted lists of knots, which, together with x and x', are the only knots potentially involved in Delaunay configurations featuring x and x' as boundary knots. As the lists of knots are sorted, the number of knots inside each circumcircle can be computed in $\mathcal{O}(m)$ time complexity, as described in [SK09]. Since the number of m-OD edges is in $\mathcal{O}(Nm)$, this yields a total time complexity $\mathcal{O}(Nm^2 \log m)$ for the second stage.

Hence, the expected total time complexity of the algorithm presented in [GHK02; SK09] is in $\mathcal{O}(Nm^2 \log m + N \log N)$, which reduces to $\mathcal{O}(N \log N)$ when considering m as constant.

The second approach has been proposed in [DGN05] specifically for the computation of Delaunay configurations of degree two, i.e., $m = 2$. The algorithm starts with a Delaunay triangulation of the knot set, which can be computed in $\mathcal{O}(N \log N)$ time complexity. For each knot $x \in X$, its *cell* is defined as the region covered by the Delaunay triangles that have x as a vertex. The cell of each knot, which is not necessarily convex, is then triangulated using a *constrained Delaunay triangulation*. Each of the triangles determines the boundary knots of a Delaunay configuration of degree one with x as interior knot. According to [DGN05], the time complexity for the computation of all Delaunay configurations of degree one from the given Delaunay triangulation is in $\mathcal{O}(N)$. In a similar way, the configurations of degree one can then be used to compute all configurations of degree two. For proofs and details of the algorithm, [DGN05] refer to a manuscript, which, to the best of our knowledge, has not been published. The time complexity of the whole algorithm is in $\mathcal{O}(N \log N)$, which is equivalent to the approach by [GHK02; SK09] in the case of a constant m.

8.3 Future Research Topics

There are clearly many open questions regarding DCB-splines. We close the thesis with some ideas for potential future research topics, which is by far not exhaustive.

As we have proved in Example 7.8, nonpooled DCB-splines are not a solution to the Fundamental Problem due to the potential linear dependence of basis candidate functions. Therefore, future research should focus on the pooled variant. Although it has been stated in [Nea01b] that the pooled basis candidate functions are linearly independent, a rigorous proof of this fact would be desirable. Additionally, an upper bound for the absolute coefficient values dependent on the norm of the spline function with these coefficients would ensure that the basis candidate for pooled DCB-splines is well-conditioned.

In this thesis, we formulated a necessary criterion for the knot insertion property to hold true for one particular inserted knot. We could show that this criterion is also sufficient in the bivariate, nonpooled case for degrees zero and one. A desirable generalization of this result to arbitrary degrees would confirm our conjecture that the criterion is sufficient for more general cases as well.

In general, it would be beneficial to gain a better understanding of the interactions between Delaunay configurations. Possibly, some of the combinatorial results on this topic, for example in [LS07b], [Sch19], and [Bar+22], could be employed for that

purpose. In particular, a thorough understanding of the pooling of simplex splines as basis candidate functions for pooled DCB-splines would be advantageous.

The multivariate Schoenberg operator defined in this thesis exhibits linear exactness and, as a consequence, provides a quadratic decrease of the approximation error as the knot set becomes denser. It can be expected that an operator with an exactness of degree $m \in \mathbb{N}_+$, i.e., all polynomials of degree at most m are invariant under the operator, would yield an approximation order of $m + 1$ [Boo82, p. 68]. Hence, the formulation of such operators would allow a better approximation of sufficiently smooth functions in terms of DCB-splines.

In addition to these theoretical questions, future research could also examine DCB-splines in practical applications. To that end, the development of an actual software framework for DCB-splines would be of interest. During such an endeavor, further questions probably arise in addition to the ones already addressed in the previous section. One of them could concern the efficient evaluation of pooled basis candidate functions, for which *"there is no associated recurrence relation relating these functions to basis [candidate] functions of lower degree"* [CLR13] so far. Despite these challenges, a framework facilitating a relatively easy usage of these splines would lower the hurdles to actually use DCB-splines in practical applications and would spark further interest in this spline space. After all, de Boor considers Neamtu's DCB-splines as *"the most convincing solution"* [Boo09] for the construction of a multivariate spline space employing simplex splines.

Bibliography

[AKL13] Franz Aurenhammer, Rolf Klein, and Der-Tsai Lee. *Voronoi Diagrams and Delaunay Triangulations*. Singapore: World Scientific Publishing, 2013 (cit. on pp. 71–75).

[Bar+22] Hélène Barucq, Henri Calandra, Julien Diaz, and Stefano Frambati. "Polynomial-Reproducing Spline Spaces From Fine Zonotopal Tilings". In: *Journal of Computational and Applied Mathematics* 402 (Mar. 2022) (cit. on pp. 95, 213).

[BT97] Dimitris Bertsimas and John N. Tsitsiklis. *Introduction to Linear Optimization*. Belmont, Massachusetts: Athena Scientific, 1997 (cit. on p. 140).

[Boe80] Wolfgang Boehm. "Inserting New Knots Into B-Spline Curves". In: *Computer-Aided Design* 12.4 (1980), pp. 199–201 (cit. on p. 30).

[BHS94] Wolfgang Boehm, Josef Hoschek, and Hans-Peter Seidel. "Mathematical Aspects of Computer Aided Geometric Design". In: *Duration and Change. Fifty Years at Oberwolfach*. Ed. by Michael Artin, Hanspeter Kraft, and Reinhold Remmert. Berlin, Heidelberg: Springer, 1994, pp. 106–138 (cit. on p. 3).

[Boo01] Carl de Boor. *A Practical Guide to Splines*. Revised Edition. New York: Springer, 2001 (cit. on pp. 9, 11–25, 28–31, 33, 93).

[Boo05] Carl de Boor. "Divided Differences". In: *Surveys in Approximation Theory* 1 (2005). Online article at `https://sat.net.technion.ac.il/2-3-2/`, pp. 46–69 (cit. on p. 40).

[Boo93] Carl de Boor. "Multivariate Piecewise Polynomials". In: *Acta Numerica* 2 (1993), pp. 65–109 (cit. on p. 94).

[Boo76] Carl de Boor. "Splines as Linear Combinations of B-Splines. A Survey". In: *Approximation Theory II*. Proceedings of an International Symposium Conducted by The University of Texas at Austin, Texas, January 18–21, 1976. Ed. by G. G. Lorentz, C. K. Chui, and L. L. Schumaker. New York: Academic Press, 1976, pp. 1–47 (cit. on pp. 40, 42, 44, 57, 58).

[Boo09] Carl de Boor. "The Way Things Were in Multivariate Splines: A Personal View". In: *Multiscale, Nonlinear and Adaptive Approximation*. Ed. by Ronald DeVore and Angela Kunoth. Berlin, Heidelberg: Springer, 2009, pp. 19–37 (cit. on p. 214).

[Boo82] Carl de Boor. "Topics in Multivariate Approximation Theory". In: *Topics in Numerical Analysis. Proceedings of the S.E.R.C. Summer School, Lancaster, July 19–August 21, 1981*. Ed. by P. R. Turner. Lecture Notes in Mathematics. Berlin, Heidelberg: Springer, 1982, pp. 39–78 (cit. on pp. 58–61, 199, 201, 214).

[BD83] Carl de Boor and Ronald DeVore. “Approximation by Smooth Multivariate Splines”. In: *Transactions of the American Mathematical Society* 276.2 (Apr. 1983), pp. 775–788 (cit. on p. 94).

[BH82a] Carl de Boor and Klaus Höllig. “B-Splines from Parallelepipeds”. In: *Journal d’Analyse Mathématique* 42 (Dec. 1982), pp. 99–115 (cit. on p. 94).

[BH82b] Carl de Boor and Klaus Höllig. “Recurrence Relations for Multivariate B-Splines”. In: *Proceedings of the American Mathematical Society*. Ed. by Thomas H. Brylawski et al. Vol. 85. 3. Providence, Rhode Island, July 1982, pp. 397–400 (cit. on pp. 45, 94).

[BHR93] Carl de Boor, Klaus Höllig, and Sherman Riemenschneider. *Box Splines*. Applied Mathematical Sciences. New York: Springer, 1993 (cit. on p. 94).

[Brø83] Arne Brøndsted. *An Introduction to Convex Polytopes*. Graduate Texts in Mathematics. New York: Springer, 1983 (cit. on p. 123).

[Cao+19] Juan Cao, Zhonggui Chen, Xiaodong Wei, and Yongjie Jessica Zhang. “A Finite Element Framework Based on Bivariate Simplex Splines on Triangle Configurations”. In: *Computer Methods in Applied Mechanics and Engineering* 357 (Dec. 2019) (cit. on p. 88).

[Cao+12] Juan Cao, Xin Li, Zhonggui Chen, and Hong Qin. “Spherical DCB-Spline Surfaces With Hierarchical and Adaptive Knot Insertion”. In: *IEEE Transactions on Visualization and Computer Graphics* 18.8 (Aug. 2012), pp. 1290–1303 (cit. on pp. 88, 91).

[Cao+09] Juan Cao, Xin Li, Guozhao Wang, and Hong Qin. “Surface Reconstruction Using Bivariate Simplex Splines on Delaunay Configurations”. In: *Computers & Graphics* 33.3 (June 2009), pp. 341–350 (cit. on pp. 88, 91).

[CT66] Ray W. Clough and James L. Tocher. “Finite Element Stiffness Matrices for Analysis of Plate Bending”. In: *Matrix Methods in Structural Mechanics*. Ed. by J. S. Przemieniecki et al. Air Force Flight Dynamics Laboratory. Nov. 1966, pp. 515–545 (cit. on p. 95).

[CLR13] Elaine Cohen, Tom Lyche, and Richard F. Riesenfeld. “A B-Spline-Like Basis for the Powell-Sabin 12-Split Based on Simplex Splines”. In: *Mathematics of Computation* 82.283 (July 2013), pp. 1667–1707 (cit. on pp. 90, 95, 214).

[CHB09] J. Austin Cottrell, Thomas J. R. Hughes, and Yuri Bazilevs. *Isogeometric Analysis. Toward Integration of CAD and FEA*. Chichester: John Wiley & Sons, 2009 (cit. on p. 93).

[CS66] H. B. Curry and I. J. Schoenberg. “On Pólya Frequency Functions IV: The Fundamental Spline Functions and their Limits”. In: *Journal d’Analyse Mathématique* 17 (Dec. 1966), pp. 71–107 (cit. on pp. 20, 39).

[Dah81] Wolfgang Dahmen. “Approximation by Linear Combinations of Multivariate B-Splines”. In: *Journal of Approximation Theory* 31.4 (Apr. 1981), pp. 299–324 (cit. on p. 58).

[Dah80] Wolfgang Dahmen. “On Multivariate B-Splines”. In: *SIAM Journal on Numerical Analysis* 17.2 (1980), pp. 179–191 (cit. on p. 45).

[Dah79] Wolfgang Dahmen. “Polynomials as Linear Combinations of Multivariate B-Splines”. In: *Mathematische Zeitschrift* 169.1 (Feb. 1979), pp. 93–98 (cit. on p. 58).

[DM82] Wolfgang Dahmen and Charles A. Micchelli. “On the Linear Independence of Multivariate B-Splines, I. Triangulations of Simploids”. In: *SIAM Journal on Numerical Analysis* 19.5 (1982), pp. 993–1012 (cit. on pp. 58–60).

[DM85] Wolfgang Dahmen and Charles A. Micchelli. “On the Local Linear Independence of Translates of a Box Spline”. In: *Studia Mathematica* 82 (1985), pp. 243–263 (cit. on p. 206).

[DMS92] Wolfgang Dahmen, Charles A. Micchelli, and Hans-Peter Seidel. “Blossoming Begets B-Spline Bases Built Better by B-Patches”. In: *Mathematics of Computation* 59.199 (July 1992), pp. 97–115 (cit. on pp. 56, 62–64, 66–68, 197, 199).

[Del34] Boris N. Delone. “Sur la Sphère Vide. A la mémoire de Georges Voronoï”. In: *Bulletin de l’Académie des Sciences de l’URSS*. Classe des Sciences Mathématiques et Naturelles 6 (1934), pp. 793–800 (cit. on p. 74).

[DGN05] Benjamin Dembart, Daniel Gonsor, and Marian Neamtu. “Bivariate Quadratic B-splines Used as Basis Functions for Collocation”. In: *Mathematics for Industry: Challenges and Frontiers. A Process View: Practice and Theory*. Proceedings of the SIAM Conference on Mathematics for Industry: Challenges and Frontiers, Toronto, Ontario, October 13–15, 2003. Ed. by David R. Ferguson and Thomas J. Peters. Philadelphia, Pennsylvania: Society for Industrial and Applied Mathematics, 2005, pp. 178–198 (cit. on pp. 91, 195–197, 210, 211, 213).

[ES96] Herbert Edelsbrunner and Nimish R Shah. “Incremental Topological Flipping Works for Regular Triangulations”. In: *Algorithmica* 15.3 (Mar. 1996), pp. 223–241 (cit. on p. 74).

[GL81] T. N. T. Goodman and S. L. Lee. “Spline Approximation Operators of Bernstein-Schoenberg Type in One and Two Variables”. In: *Journal of Approximation Theory* 33.3 (Nov. 1981), pp. 248–263 (cit. on p. 197).

[GKP89] Ronald L. Graham, Donald E. Knuth, and Oren Patashnik. *Concrete Mathematics. A Foundation for Computer Science*. 2nd ed. Addison-Wesley, 1989 (cit. on p. 155).

[Gra87] Thomas A. Grandine. “The Computational Cost of Simplex Spline Functions”. In: *SIAM Journal on Numerical Analysis* 24.4 (1987), pp. 887–890 (cit. on p. 209).

[Gra88] Thomas A. Grandine. “The Stable Evaluation of Multivariate Simplex Splines”. In: *Mathematics of Computation* 50.181 (Jan. 1988), pp. 197–205 (cit. on p. 209).

[GHK02] Joachim Gudmundsson, Mikael Hammar, and Marc van Kreveld. “Higher Order Delaunay Triangulations”. In: *Computational Geometry* 23.1 (July 2002), pp. 85–98 (cit. on pp. 91, 212, 213).

[Hak82] Hakop Hakopian. “Multivariate Spline Functions, B-Spline Basis and Polynomial Interpolations”. In: *SIAM Journal on Numerical Analysis* 19.3 (1982), pp. 510–517 (cit. on pp. 45, 147, 150, 210).

[Han+08] Michael Sass Hansen, Rasmus Larsen, Ben Glocker, and Nassir Navab. “Adaptive Parametrization of Multivariate B-Splines for Image Registration”. In: *2008 IEEE Conference on Computer Vision and Pattern Recognition*. IEEE. 2008, pp. 1–8 (cit. on pp. 91, 92, 212).

[Höl81] Klaus Höllig. “A Remark on Multivariate B-Splines”. In: *Journal of Approximation Theory* 33.2 (Oct. 1981), pp. 119–125 (cit. on p. 45).

[Höl03] Klaus Höllig. *Finite Element Methods With B-Splines*. Frontiers in Applied Mathematics. Philadelphia, Pennsylvania: Society for Industrial and Applied Mathematics, 2003 (cit. on p. 3).

[Höl82] Klaus Höllig. “Multivariate Splines”. In: *SIAM Journal on Numerical Analysis* 19.5 (1982), pp. 1013–1031 (cit. on pp. 59, 60).

[Höl86] Klaus Höllig. “Multivariate Splines”. In: *Approximation Theory*. Proceedings of Symposia in Applied Mathematics. Ed. by Carl de Boor. Vol. 36. Providence, Rhode Island: American Mathematical Society, 1986, pp. 103–127 (cit. on pp. 94, 209).

[Huß99] Markus Hußmann. “Ein Triangulierungsverfahren zur Approximation mit Dahmen-Micchelli-Seidel-Splines”. PhD thesis. Gerhard-Mercator-Universität Gesamthochschule Duisburg, 1999 (cit. on p. 57).

[IK94] Eugene Isaacson and Herbert Bishop Keller. *Analysis of Numerical Methods*. New York: Dover Publications, 1994 (cit. on p. 9).

[Itô93] Kiyosi Itô. *Encyclopedic Dictionary of Mathematics*. 2nd ed. Vol. 1. Cambridge, Massachusetts: MIT press, 1993 (cit. on p. 109).

[LS07a] Ming-Jun Lai and Larry L. Schumaker. *Spline Functions on Triangulations*. Encyclopedia of Mathematics and its Applications. Cambrige: Cambridge University Press, 2007 (cit. on pp. 34, 37, 95).

[LS80] Der-Tsai Lee and Bruce J. Schachter. “Two Algorithms for Constructing a Delaunay Triangulation”. In: *International Journal of Computer & Information Sciences* 9.3 (1980), pp. 219–242 (cit. on p. 74).

[Liu08] Yuanxin Liu. “Computations of Delaunay and Higher Order Triangulations, With Applications to Splines”. PhD thesis. University of North Carolina at Chapel Hill, 2008 (cit. on pp. 91, 94).

[LS07b] Yuanxin Liu and Jack Snoeyink. “Quadratic and Cubic B-Splines by Generalizing Higher-Order Voronoi Diagrams”. In: *Proceedings of the Twenty-Third Annual Symposium on Computational Geometry*. New York: Association for Computing Machinery, June 2007, pp. 150–157 (cit. on pp. 91, 94, 213).

[Mar70] Martin J. Marsden. “An Identity for Spline Functions With Applications to Variation Diminishing Spline Approximation”. In: *Journal of Approximation Theory* 3.1 (Mar. 1970), pp. 7–49 (cit. on p. 25).

[MS88] Martin J. Marsden and Isaac J. Schoenberg. “On Variation Diminishing Spline Approximation Methods”. In: *I. J. Schoenberg Selected Papers*. Ed. by Carl de Boor. Contemporary Mathematicians. Boston, Massachusetts: Birkhäuser, 1988, pp. 247–268 (cit. on p. 27).

[Mic80] Charles A. Micchelli. “A Constructive Approach to Kergin Interpolation in $\mathbb{R}^k$: Multivariate B-Splines and Lagrange Interpolation”. In: *The Rocky Mountain Journal of Mathematics* 10.3 (1980), pp. 485–497 (cit. on pp. 40, 42, 44–47, 154, 156).

[Mic95] Charles A. Micchelli. *Mathematical Aspects of Geometric Modeling*. Philadelphia, Pennsylvania: Society for Industrial and Applied Mathematics, 1995 (cit. on pp. 40, 41, 43, 44, 154).

[Mic79] Charles A. Micchelli. “On a Numerically Efficient Method for Computing Multivariate B-Splines”. In: *Multivariate Approximation Theory*. Proceedings of the Conference held at the Mathematical Research Institute at Oberwolfach Black Forest, February 4–10, 1979. Ed. by Walter Schempp and Karl Zeller. Vol. 51. ISNM International Series of Numerical Mathematics. Basel: Birkhäuser, 1979 (cit. on pp. 36, 39–42, 44–48, 209).

[Nea01a] Marian Neamtu. “Bivariate Simplex B-Splines: A New Paradigm”. In: *Proceedings of the Spring Conference on Computer Graphics, Budmerice, Slovakia, April 25–28, 2001*. IEEE. 2001, pp. 71–78 (cit. on pp. 3, 42, 43, 54, 70, 74, 77, 79, 91).

[Nea07] Marian Neamtu. “Delaunay Configurations and Multivariate Splines: A Generalization of a Result of B. N. Delaunay”. In: *Transactions of the American Mathematical Society* 359.7 (July 2007), pp. 2993–3004 (cit. on pp. 81–84, 89, 91, 98, 154, 168).

[Nea01b] Marian Neamtu. “What Is the Natural Generalization of Univariate Splines to Higher Dimensions?” In: *Mathematical Methods for Curves and Surfaces: Oslo 2000*. Ed. by Tom Lyche and Larry L. Schumaker. Nashville, Tennessee: Vanderbilt University Press, Jan. 2001, pp. 355–392 (cit. on pp. 3–5, 54, 56, 58, 59, 64–66, 69, 70, 72, 76, 78–91, 95, 98, 204, 213).

[PS77] Michael J. D. Powell and Malcolm A. Sabin. “Piecewise Quadratic Approximations on Triangles”. In: *ACM Transactions on Mathematical Software* 3.4 (Dec. 1977), pp. 316–325 (cit. on p. 95).

[PBP02] Hartmut Prautzsch, Wolfgang Boehm, and Marco Paluszny. *Bézier and B-Spline Techniques*. Mathematics and Visualization. Berlin, Heidelberg: Springer, 2002 (cit. on pp. 154, 155).

[PS85] Franco P. Preparata and Michael Ian Shamos. *Computational Geometry. An Introduction*. Texts and Monographs in Computer Science. New York: Springer, 1985 (cit. on p. 74).

[Ram99] Edgar A. Ramos. “On Range Reporting, Ray Shooting and K-Level Construction”. In: *SCG ’99: Proceedings of the Fifteenth Annual Symposium on Computational Geometry, Miami Beach, Florida, June 13–16, 1999*. New York: Association for Computing Machinery, June 1999, pp. 390–399 (cit. on p. 212).

[Ram87] Lyle Ramshaw. *Blossoming: A Connect-the-Dots Approach to Splines*. Tech. rep. Palo Alto, California: Digital Equipment Corporation, Systems Research Center, June 1987 (cit. on pp. 25, 27).

[Ram89] Lyle Ramshaw. "Blossoms Are Polar Forms". In: *Computer Aided Geometric Design* 6.4 (Nov. 1989), pp. 323–358 (cit. on pp. 25, 26).

[Roc70] Ralph Tyrell Rockafellar. *Convex Analysis*. Princeton Mathematical Series. Princeton, New Jersey: Princeton University Press, 1970 (cit. on p. 123).

[Run01] Carl Runge. "Über Empirische Funktionen und die Interpolation Zwischen Äquidistanten Ordinaten". In: *Zeitschrift für Mathematik und Physik* 46 (1901), pp. 224–243 (cit. on p. 9).

[Sab89] Malcolm Sabin. "Open Questions in the Application of Multivariate B-Splines". In: *Mathematical Methods in Computer Aided Geometric Design*. Ed. by Tom Lyche and Larry L. Schumaker. San Diego, California: Academic Press Professional, June 1989, pp. 529–537 (cit. on p. 78).

[Sau95] Thomas Sauer. "Multivariate B-Splines With (Almost) Arbitrary Knots". In: *Approximation Theory VIII - Vol. 1. Approximation and Interpolation*. College Station, Texas, January 8–12, 1995. Ed. by Charles K. Chui and Larry L. Schumaker. Approximations and Decompositions - Vol. 6. Singapore: World Scientific Publishing, 1995, pp. 477–484 (cit. on p. 70).

[Sau12] Tomas Sauer. *Splinekurven und -flächen in Theorie und Anwendung*. Lecture Notes, University of Passau, `https://www.fim.uni-passau.de/digitale-bildverarbeitung/lehre/` (last accessed on March 20, 2022). Mar. 2012 (cit. on p. 29).

[Sch19] Dominique Schmitt. "Bivariate B-Splines From Convex Pseudo-Circle Configurations". In: *Fundamentals of Computation Theory*. 22nd International Symposium, FCT 2019, Copenhagen, Denmark, August 12-14, 2019, Proceedings. Ed. by Leszek Antoni Gąsieniec, Jesper Jansson, and Christos Levcopoulos. Lecture Notes in Computer Science. Cham: Springer, 2019, pp. 335–349 (cit. on pp. 94, 213).

[Sch07] Larry L. Schumaker. *Spline Functions. Basic Theory*. 3rd ed. Cambridge Mathematical Library. Cambridge: Cambridge University Press, 2007 (cit. on pp. 1, 2, 9, 10, 17, 31, 92, 93).

[Sei92a] Hans-Peter Seidel. "Polar Forms and Triangular B-Spline Surfaces". In: *Computing in Euclidean Geometry*. Ed. by Ding-Zhu Du and Frank Hwang. Vol. 1. Lecture Notes Series on Computing. Singapore: World Scientific Publishing, 1992, pp. 235–286 (cit. on pp. 64, 67, 69, 209).

[Sei92b] Hans-Peter Seidel. "Representing Piecewise Polynomials as Linear Combinations of Multivariate B-Splines". In: *Mathematical Methods in Computer Aided Geometric Design II*. Ed. by Tom Lyche and Larry L. Schumaker. San Diego, California: Academic Press, 1992, pp. 559–566 (cit. on p. 69).

[Sei91] Hans-Peter Seidel. “Symmetric Recursive Algorithms for Surfaces: B-Patches and the de Boor Algorithm for Polynomials Over Triangles”. In: *Constructive Approximation* 7.1 (Dec. 1991), pp. 257–279 (cit. on p. 62).

[SH75] Michael Ian Shamos and Dan Hoey. “Closest-Point Problems”. In: *16th Annual Symposium on Foundations of Computer Science*. IEEE. 1975, pp. 151–162 (cit. on p. 77).

[Sil09] Rodrigo Ignacio Silveira. “Optimization of Polyhedral Terrains”. PhD thesis. Utrecht University, 2009 (cit. on p. 92).

[SK09] Rodrigo Ignacio Silveira and Marc van Kreveld. “Optimal Higher Order Delaunay Triangulations of Polygons”. In: *Computational Geometry: Theory and Applications* 42.8 (2009). Special Issue on the 23rd European Workshop on Computational Geometry, pp. 803–813 (cit. on pp. 92, 159, 212, 213).

[Spe+12] Hendrik Speleers, Carla Manni, Francesca Pelosi, and M. Lucia Sampoli. “Isogeometric Analysis With Powell–Sabin Splines for Advection–Diffusion–Reaction Problems”. In: *Computer Methods in Applied Mechanics and Engineering* 221-222 (May 2012), pp. 132–148 (cit. on p. 95).

[Ste06] Karl-Georg Steffens. *The History of Approximation Theory. From Euler to Bernstein*. Boston, Massachusetts: Birkhäuser, 2006 (cit. on p. 1).

[Tim06] Steffen Timmann. *Repetitorium der Analysis. Teil 1*. 3rd ed. Springe: Binomi, 2006 (cit. on p. 9).

[Zha+17] Yuhua Zhang, Juan Cao, Zhonggui Chen, and Xiaoming Zeng. “Surface Reconstruction Using Simplex Splines on Feature-Sensitive Configurations”. In: *Computer Aided Geometric Design* 50 (Jan. 2017), pp. 14–28 (cit. on pp. 88, 94).

[ZZZ16] Jochen Ziegenbalg, Oliver Ziegenbalg, and Bernd Ziegenbalg. *Algorithmen von Hammurapi bis Gödel. Mit Beispielen aus den Computeralgebrasystemen Mathematica und Maxima*. 4th ed. Wiesbaden: Springer, 2016 (cit. on p. 1).